

NUREG/CR-5469
MEA-2364

Irradiation-Anneal-Reirradiation (IAR) Studies of Prototypic Reactor Vessel Weldments

Prepared by J. R. Hawthorne

Materials Engineering Associates, Inc.

Prepared for
U.S. Nuclear Regulatory Commission

8912050374 891130
PDR NUREG
CR-5469 R PDR

AVAILABILITY NOTICE

Availability of Reference Materials Cited in NRC Publications

Most documents cited in NRC publications will be available from one of the following sources:

1. The NRC Public Document Room, 2120 L Street, NW, Lower Level, Washington, DC 20555
2. The Superintendent of Documents, U.S. Government Printing Office, P.O. Box 37082, Washington, DC 20013-7082
3. The National Technical Information Service, Springfield, VA 22161

Although the listing that follows represents the majority of documents cited in NRC publications, it is not intended to be exhaustive.

Referenced documents available for inspection and copying for a fee from the NRC Public Document Room include NRC correspondence and internal NRC memoranda; NRC Office of Inspection and Enforcement bulletins, circulars, information notices, inspection and investigation notices; Licensee Event Reports; vendor reports and correspondence; Commission papers; and applicant and licensee documents and correspondence.

The following documents in the NUREG series are available for purchase from the GPO Sales Program: formal NRC staff and contractor reports, NRC-sponsored conference proceedings, and NRC booklets and brochures. Also available are Regulatory Guides, NRC regulations in the *Code of Federal Regulations*, and *Nuclear Regulatory Commission Issuances*.

Documents available from the National Technical Information Service include NUREG series reports and technical reports prepared by other federal agencies and reports prepared by the Atomic Energy Commission, forerunner agency to the Nuclear Regulatory Commission.

Documents available from public and special technical libraries include all open literature items, such as books, journal and periodical articles, and transactions. *Federal Register* notices, federal and state legislation, and congressional reports can usually be obtained from these libraries.

Documents such as theses, dissertations, foreign reports and translations, and non-NRC conference proceedings are available for purchase from the organization sponsoring the publication cited.

Single copies of NRC draft reports are available free, to the extent of supply, upon written request to the Office of Information Resources Management, Distribution Section, U.S. Nuclear Regulatory Commission, Washington, DC 20555.

Copies of industry codes and standards used in a substantive manner in the NRC regulatory process are maintained at the NRC Library, 7920 Norfolk Avenue, Bethesda, Maryland, and are available there for reference use by the public. Codes and standards are usually copyrighted and may be purchased from the originating organization or, if they are American National Standards, from the American National Standards Institute, 1430 Broadway, New York, NY 10018.

DISCLAIMER NOTICE

This report was prepared as an account of work sponsored by an agency of the United States Government. Neither the United States Government nor any agency thereof, or any of their employees, makes any warranty, expressed or implied, or assumes any legal liability or responsibility for any third party's use, or the results of such use, of any information, apparatus, product or process disclosed in this report, or represents that its use by such third party would not infringe privately owned rights.

**NUREG/CR-5469
MEA-2364
RF, R5**

Irradiation-Anneal-Reirradiation (IAR) Studies of Prototypic Reactor Vessel Weldments

**Manuscript Completed: October 1989
Date Published: November 1989**

**Prepared by
J. R. Hawthorne**

**Materials Engineering Associates, Inc.
9700-B Martin Luther King, Jr. Highway
Lanham, MD 20706-1837**

**Prepared for
Division of Engineering
Office of Nuclear Regulatory Research
U.S. Nuclear Regulatory Commission
Washington, DC 20555
NRC FIN B8900**

ABSTRACT

The usefulness of intermediate annealing to periodically mitigate the deleterious effects of nuclear radiation on reactor pressure vessel steels is explored. Test materials are intermediate and high copper content weld deposits made commercially. Irradiation and reirradiation exposures were at 288°C. Annealing-induced properties recovery and resistance to reembrittlement by irradiation are qualified for 454°C and 399°C heat treatments and a total fluence of $2.7 \times 10^{19} n/cm^2$.

Tendencies toward a saturation of radiation embrittlement were observed in annealed material. With 454°C annealing, embrittlement levels were lower than those observed after irradiation to $1.5 \times 10^{19} n/cm^2$ without intermediate annealing. The method shows high promise for radiation-sensitive pressure vessel steels for increasing their fracture-safe service lifetimes.

CONTENTS

	<u>Page</u>
ABSTRACT.....	iii
LIST OF FIGURES.....	vi
LIST OF TABLES.....	viii
FOREWORD.....	ix
ACKNOWLEDGEMENT.....	xiii
1. INTRODUCTION.....	1
2. MATERIALS.....	2
3. MATERIAL IRRADIATION.....	3
4. IRRADIATION MATRIX.....	16
5. NOTCH DUCTILITY TEST RESULTS.....	16
5.1 As-Irradiated (I) Condition.....	21
5.2 Irradiation + Annealed (IA) Condition.....	21
5.3 Irradiation-Anneal-Reirradiation (IAR) Conditions.....	23
5.3.1 IAR Condition 1 (IAR ₁).....	23
5.3.2 IAR Condition 2 (IAR ₂).....	23
6. TENSION TEST RESULTS.....	38
7. DISCUSSION.....	38
8. CONCLUSIONS.....	42
REFERENCES.....	43
Appendix A Fabrication of Weldments: Materials and Procedures.....	47
Appendix B Reactor Operations History for Irradiation Assemblies UBR-62, UBR-70, UBR-71, and UBR-72.....	83
Appendix C Neutron Dosimetry Determinations: Irradiation Assemblies UBR-62, UBR-70, UBR-71, UBR-72.....	89
Appendix D Tabulations of Charpy-V Notch Ductility Test Results.....	106
Appendix E Computer Curve Fittings of Charpy-V Test Results, (Specimen Energy Absorption vs. Temperature).....	145

LIST OF FIGURES

<u>Figure</u>	<u>Page</u>
1 MEA irradiation facilities in the UBR Reactor.....	5
2 Design of Charpy V-Notch (C_V) test specimen.....	6
3 Design of threaded-end C_V -size tension test specimen.....	7
4 Placement of C_V and tension test specimens in Irradiation Assembly UBR-62.....	8
5 Placement of C_V and tension test specimens in Irradiation Assembly UBR-70.....	9
6 Placement of C_V and tension test specimens in Irradiation Assembly UBR-71.....	10
7 Placement of C_V and tension test specimens in Irradiation Assembly UBR-72.....	11
8 Irradiation Assembly UBR-62 showing thermocouple placements.....	12
9 Irradiation Assembly UBR-70 showing thermocouple placements.....	13
10 Irradiation Assembly UBR-71 showing thermocouple placements.....	14
11 Irradiation Assembly UBR-72 showing thermocouple placements.....	15
12 Objectives for Phase 1 Investigations (I and IA conditions).....	17
13 Objectives for Phase 2 Investigations (two IAR fluence conditions).....	17
14 Summary of notch ductility changes observed after irradiation and after postirradiation annealing.....	22
15 Notch ductility changes observed after reirradiation to $1.8 \times 10^{19} \text{ n/cm}^2$ vs. first exposure cycle.....	24
16 Notch ductility changes (total) observed after reirradiation to $1.8 \times 10^{19} \text{ n/cm}^2$ vs. first exposure cycle.....	25
17 C_V notch ductility of Weld W8A after reirradiation.....	26
18 C_V notch ductility of Weld W9A after reirradiation.....	27
19 C_V notch ductility of Weld WW7 after reirradiation.....	28
20 C_V notch ductility of Weld WW4 after reirradiation.....	29

21	Notch ductility changes observed after reirradiation to 2.7×10^{19} n/cm ² vs. first exposure cycle.....	30
22	Notch ductility changes (total) observed after reirradiation to a fluence of 2.7×10^{19} n/cm ² vs. first exposure cycle.....	31
23	Experimental data for IAR Condition 1 and IAR condition 2 of Weld W8A.....	32
24	Experimental data for IAR Condition 1 and IAR condition 2 of Weld W9A.....	33
25	Experimental data for IAR Condition 1 and IAR condition 2 of Weld WW7.....	34
26	Experimental data for IAR Condition 1 and IAR condition 2 of Weld WW4.....	35
27	Notch ductility changes by the second exposure cycle vs. changes observed for virgin material at a matching fluence.....	37

LIST OF TABLES

<u>Table</u>		<u>Page</u>
1	Submerged-Arc Weld Deposit Materials.....	2
2	Compositions of Submerged-Arc Weld Deposits.....	4
3	Exposure Histories of Irradiation Assmeblies.....	18
4	Charpy-V Notch Ductility of Welds in I-, IA-, and IAR conditions.....	19
5	Tensile Strengths of Welds in I-, IA-, and IAR- conditions.....	39

FOREWORD

The work reported here was performed at Materials Engineering Associates (MEA) under the program, Structural Integrity of Water Reactor Pressure Boundary Components, F. J. Loss, Program Manager. The program is sponsored by the Office of Nuclear Regulatory Research of the U. S. Nuclear Regulatory Commission (NRC). The technical monitor for the NRC is Alfred Taboada.

Prior reports under the current contract are listed below:

1. J. R. Hawthorne, "Significance of Nickel and Copper Content to Radiation Sensitivity and Postirradiation Heat Treatment Recovery of Reactor Vessel Steels," USNRC Report NUREG/CR-2948, Nov. 1982.
2. "Structural Integrity of Water Reactor Pressure Boundary Components, Annual Report for 1982," F. J. Loss, Ed., USNRC Report NUREG/CR-3228, Vol. 1, Apr. 1983.
3. J. R. Hawthorne, "Exploratory Assessment of Postirradiation Heat Treatment Variables in Notch Ductility Recovery of A 533-B Steel," USNRC Report NUREG/CR-3229, Apr. 1983.
4. W. H. Cullen, K. Torronen, and M. Kemppainen, "Effects of Temperature on Fatigue Crack Growth of A 508-2 Steel in LWR Environment," USNRC Report NUREG/CR-3230, Apr. 1983.
5. "Proceedings of the International Atomic Energy Agency Specialists' Meeting on Subcritical Crack Growth," Vols. 1 and 2, W. H. Cullen, Ed., USNRC Conference Proceeding NUREG/CP-0044, May 1983.
6. W. H. Cullen, "Fatigue Crack Growth Rates of A 508-2 Steel in Pressurized, High-Temperature Water," USNRC Report NUREG/CR-3294, June 1983.
7. J. R. Hawthorne, B. H. Menke, and A. L. Hiser, "Light Water Reactor Pressure Vessel Surveillance Dosimetry Improvement Program: Notch Ductility and Fracture Toughness Degradation of A 302-B and A 533-B Reference Plates from PSF Simulated Surveillance and Through-Wall Irradiation Capsules," USNRC Report NUREG/CR-3295, Vol. 1, Apr. 1984.
8. J. R. Hawthorne and B. H. Menke, "Light Water Reactor Pressure Vessel Surveillance Dosimetry Improvement Program: Postirradiation Notch Ductility and Tensile Strength Determinations for PSF Simulated Surveillance and Through-Wall Specimen Capsules," USNRC Report NUREG/CR-3295, Vol. 2, Apr. 1984.
9. A. L. Hiser and F. J. Loss, "Alternative Procedures for J-R Curve Determination," USNRC Report NUREG/CR-3402, July 1983.
10. A. L. Hiser, F. J. Loss, and B. H. Menke, "J-R Curve Characterization of Irradiated Low Upper Shelf Welds," USNRC Report NUREG/CR-3506, Apr. 1984.

11. W. H. Cullen, R. E. Taylor, K. Torronen, and M. Kemppainen, "The Temperature Dependence of Fatigue Crack Growth Rates of A 351 CF8A Cast Stainless Steel in LWR Environment," USNRC Report NUREG/CR-3546, Apr. 1984.
12. "Structural Integrity of Light Water Reactor Pressure Boundary Components -- Four-Year Plan 1984-1988," F. J. Loss, Ed., USNRC Report NUREG/CR-3788, Sep. 1984.
13. W. H. Cullen and A. L. Hiser, "Behavior of Subcritical and Slow-Stable Crack Growth Following a Postirradiation Thermal Anneal Cycle," USNRC Report NUREG/CR-3833, Aug. 1984.
14. "Structural Integrity of Water Reactor Pressure Boundary Components: Annual Report for 1983," F. J. Loss, Ed., USNRC Report NUREG/CR-3228, Vol. 2, Sept. 1984.
15. W. H. Cullen, "Fatigue Crack Growth Rates of Low-Carbon and Stainless Piping Steels in PWR Environment," USNRC Report NUREG/CR-3945, Feb. 1985.
16. W. H. Cullen, M. Kemppainen, H. Hanninen, and K. Torronen, "The Effects of Sulfur Chemistry and Flow Rate on Fatigue Crack Growth Rates in LWR Environments," USNRC Report NUREG/CR-4121, Feb. 1985.
17. "Structural Integrity of Water Reactor Pressure Boundary Components: Annual Report for 1984," F. J. Loss, Ed., USNRC Report NUREG/CR-3228, Vol. 3, June 1985.
18. A. L. Hiser, "Correlation of C_v and K_{Ic}/K_{Jc} Transition Temperature Increases Due to Irradiation," USNRC Report NUREG/CR-4395, Nov. 1985.
19. W. H. Cullen, G. Gabetta, and H. Hanninen, "A Review of the Models and Mechanisms For Environmentally-Assisted Crack Growth of Pressure Vessel and Piping Steels in PWR Environments," USNRC Report NUREG/CR-4422, Dec. 1985.
20. "Proceedings of the Second International Atomic Energy Agency Specialists' Meeting on Subcritical Crack Growth," W. H. Cullen, Ed., USNRC Conference Proceeding NUREG/CP-0067, Vols. 1 and 2, Apr. 1986.
21. J. R. Hawthorne, "Exploratory Studies of Element Interactions and Composition Dependencies in Radiation Sensitivity Development," USNRC Report NUREG/CR-4437, Nov. 1985.
22. R. B. Stonesifer and E. F. Rybicki, "Development of Models for Warm Prestressing," USNRC Report NUREG/CR-4491, Jan. 1987.
23. E. F. Rybicki and R. B. Stonesifer, "Computational Model for Residual Stresses in a Clad Plate and Clad Fracture Specimens," USNRC Report NUREG/CR-4635, Oct. 1986.
24. D. E. McCabe, "Plan for Experimental Characterization of Clad Vessel Steel After Irradiation," USNRC Report NUREG/CR-4636, Oct. 1986.

25. E. F. Rybicki, J. R. Shadley, and A. S. Sandhu, "Experimental Evaluation of Residual Stresses in a Weld Clad Plate and Clad Test Specimens," USNRC Report NUREG/CR-4646, Oct. 1986.
26. "Structural Integrity of Water Reactor Pressure Boundary Components: Annual Report for 1985," F. J. Loss, Ed., USNRC Report NUREG/CR-3228, Vol. 4, June 1986.
27. G. Gabetta and W. H. Cullen, "Application of a Two-Mechanism Model for Environmentally-Assisted Crack Growth," USNRC Report NUREG/CR-4723, Oct. 1986.
28. W. H. Cullen, "Fatigue Crack Growth Rates in Pressure Vessel and Piping Steels in LWR Environments," USNRC Report NUREG/CR-4724, Mar. 1987.
29. W. H. Cullen and M. R. Jolles, "Fatigue Crack Growth of Part-Through Cracks in Pressure Vessel and Piping Steels: Air Environment Results," USNRC Report NUREG/CR-4828, Oct. 1988.
30. D. E. McCabe, "Fracture Evaluation of Surface Cracks Embedded in Reactor Vessel Cladding: Unirradiated Bend Specimen Results," USNRC Report NUREG/CR-4841, May 1987.
31. H. Hanninen, M. Vulli, and W. H. Cullen, "Surface Spectroscopy of Pressure Vessel Steel Fatigue Fracture Surface Films Formed in PWR Environments," USNRC Report NUREG/CR-4863, July 1987.
32. A. L. Hiser and G. M. Callahan, "A User's Guide to the NRC's Piping Fracture Mechanics Data Base (PIFRAC)," USNRC Report NUREG/CR-4894, May 1987.
33. "Proceedings of the Second CSNI Workshop on Ductile Fracture Test Methods (Paris, France, April 17-19, 1985)," F. J. Loss, Ed., USNRC Conference Proceeding NUREG/CP-0064, Aug. 1988.
34. W. H. Cullen and D. Broek, "The Effects of Variable Amplitude Loading on A 533-B Steel in High-Temperature Air and Reactor Water Environments," USNRC Report NUREG/CR-4929, Apr. 1989.
35. "Structural Integrity of Water Reactor Pressure Boundary Components: Annual Report for 1986," F. J. Loss, Ed., USNRC Report NUREG/CR-3228, Vol. 5, July 1987.
36. F. Ebrahimi et al., "Development of a Mechanistic Understanding of Radiation Embrittlement in Reactor Pressure Vessel Steels: Final Report," USNRC Report NUREG/CR-5063, Jan. 1988.
37. J. B. Terrell, "Fatigue Life Characterization of Smooth and Notched Piping Steel Specimens in 288°C Air Environments," USNRC Report NUREG/CR-5013, May 1988.
38. A. L. Hiser, "Tensile and J-R Curve Characterization of Thermally Aged Cast Stainless Steels," USNRC Report NUREG/CR-5024, Sept. 1988

39. J. B. Terrell, "Fatigue Strength of Smooth and Notched Specimens of ASME SA 106-B Steel in PWR Environments," USNRC Report NUREG/CR-5136, Sept. 1988.
40. D. E. McCabe, "Fracture Evaluation of Surface Cracks Embedded in Reactor Vessel Cladding: Material Property Evaluations" USNRC NUREG/CR-5207, Sept. 1988.
41. J. R. Hawthorne and A. L. Hiser, "Experimental Assessments of Gundremmingen RPV Archive Material for Fluence Rate Effects Studies," USNRC Report NUREG/CR-5201, Oct., 1988.
42. J. B. Terrell, "Fatigue Strength of ASME SA 106-B Welded Steel Pipes in 288°C Air Environments," USNRC Report NUREG/CR-5195, Dec. 1988.
43. A. L. Hiser, "Post-Irradiation Fracture Toughness Characterization of Four Lab-Melt Plates," USNRC Report NUREG/CR-5216 Rev. 1, Jun. 1989.
44. R. B. Stonesifer, E. F. Rybicki and D. E. McCabe, "Warm Prestress Modeling: Comparison of Models and Experimental Results," USNRC Report NUREG/CR-5208, Apr. 1989.
45. A. L. Hiser and J. B. Terrell, "Size Effects on J-R Curves for A 302-B Plate," USNRC Report NUREG/CR-5265, Jan. 1989.
46. D. E. McCabe, "Fracture Evaluation of Surface Cracks Embedded in Reactor Vessel Cladding," USNRC Report NUREG/CR-5326, March 1989.
47. J.R. Hawthorne, "An Exploratory Study of Element Interactions and Composition Dependencies in Radiation Sensitivity Development: Final Report," USNRC Report NUREG/CR-5357, April 1989.
48. J.R. Hawthorne, "Steel Impurity Element Effects on Post Irradiation Properties Recovery By Annealing: Final Report," USNRC Report NUREG/CR - 5388, August 1989.

ACKNOWLEDGEMENT

This investigation was sponsored by the USNRC Office of Nuclear Regulatory Research; the continuing support of his agency is appreciated.

The author thanks M. Vagins and C. Z. Serpan of the NRC (Materials Engineering Branch) for their helpful suggestions and advice during the conduct of the investigations. He also expresses appreciation for the individual contributions of K. C. Miller, A. L. Hiser, W. E. Hagel, G. L. Lohr, H. Sanders, E. D'Ambrosio, C. Miller and D. Schaffer to the experimental phase of the studies. The assistance of G. Carlson in the preparation of graphics for the report is also acknowledged. The assistance of J. W. Rogers of EG&G Idaho, Inc. in neutron dosimetry analyses is appreciated with gratitude.

1. INTRODUCTION

In the United States (US), the steels and weld deposits forming reactor pressure vessels are required by law to exhibit a certain minimum fracture resistance throughout vessel life. For example, the Charpy-V (C_V) upper shelf level of vessel materials must be at least 68 J (50 ft-lb) for unrestricted vessel operation. Minimum requirements are set forth in the US Code of Federal Regulations (Title 10, Part 50) and the American Society of Mechanical Engineers (ASME) Boiler And Pressure Vessel Code. For those cases where properties could be reduced by radiation service to below minimum values, postirradiation heat treatment for the restoration of vessel safety margins is one option available for continuation of vessel operations [1].

Postirradiation heat treatment has been shown effective in mitigating radiation-induced embrittlement in low alloy steels and welds such as those forming early production (pre-1972) reactor pressure vessels [2,3]. The method has been applied successfully to the vessels of two light-water-cooled and moderated power reactors (the US Army SM-1A and the Belgian BR-3 reactors) whose rate of embrittlement accrual exceeded initial estimates [4,5]. The service temperatures of these vessels (224°C and 260°C , respectively), however, were significantly lower than the nominal service temperature (288°C) of large commercial power reactor vessels. Prior irradiation temperature is known to be a factor influencing annealing recovery [2]. That is, the extent of notch ductility changes by a given postirradiation heat treatment generally is smaller with a higher irradiation temperature in the range of about 200°C to 320°C .

Embrittlement by irradiation typically is judged by the degradation of C_V notch ductility, that is, the elevation of the C_V 41-J transition temperature and the reduction in the C_V upper shelf energy level. The amount of improvement in properties through heat treatment (annealing) is dependent not only on the prior irradiation exposure (irradiation temperature and neutron fluence) but also on the temperature and duration of the heat treatment applied. Studies to date have focused largely on 399°C annealing. Originally, this temperature was judged to be an upper limit for annealing for most vessels. A more recent MEA survey of reactor vessel fabricators and system suppliers found that annealing at a higher temperature is now considered possible for many vessels. Two vendors stated that temperatures in excess of 427°C are practical for a "dry" anneal, that is, with reactor internals and coolant removed. Annealing at 454°C appears feasible for many plants constructed to date. Vessel design temperatures typically are 343°C . Design aspects of some systems may prevent annealing at 454°C because the temperature limit is governed in part by the thermal behavior of piping, supports and the biological shielding in addition to the thermal considerations for the vessel Ref. [6, 7].

Exploratory studies of 454°C annealing by MEA and others have indicated that, in addition to the possibility for a higher percentage recovery in properties, material resistance to reirradiation

embrittlement may be significantly different from that following 399°C annealing. Certain data also suggest that a radiation embrittlement saturation may occur upon reirradiation and that the saturation level may be lower than the embrittlement level before the postirradiation anneal [3,9,10]. One known complication is the variability of steels (and welds) in their response to 454°C and 399°C annealing after irradiation [11].

The present study of irradiation-annealing (IA) and irradiation-anneal-reirradiation (IAR) behavior was mounted for the US Nuclear Regulatory Commission (USNRC) in 1984 to help resolve three issues: firstly, the extent of differences between (and the variability of) 454°C vs. 399°C annealing recovery for submerged-arc (S/A) weld metals typical of early US vessel fabrication; secondly, re-embrittlement trends and rates following 454°C vs. 399°C annealing; and thirdly, the significance of weld metal type and fabrication history to the recovery obtainable and to reirradiation embrittlement susceptibility. The research test matrix was formulated to test critically the existence and nature of radiation embrittlement saturation. Obviously, strong embrittlement saturation tendencies with IAR treatments, if confirmed for high radiation sensitivity steels, could have a major impact on future reactor vessel annealing decisions and goals by the industry.

2. MATERIALS

The focus of the investigation on weld deposit materials reflects the US primary interest in this component for reactor vessels. Thick section welds encompassing the four generic types found in early reactor vessels were obtained. The welds are identified by MEA code number, composition and welding materials in Table 1. Nickel contents and welding flux types depict the range of these variables found in early vessel welds. Each weld has a high or an intermediate copper content synonymous with high radiation sensitivity. High copper content welds are found in several US reactors built before 1972; the high content is a direct result of using copper-coated filler wire. This type of wire was abandoned when the detrimental effect of copper on the radiation resistance of steel became known [12].

Table 1 Submerged-Arc Weld Deposit Materials

Weld No.	MEA Code	Nominal Composition (wt-%)		Welding Filler	Welding Flux
		Cu	Ni		
1	W8A	0.39	0.65	MnMoNi	Linde 80
2	W9A	0.39	0.65	MnMoNi	Linde 0091
3	WW4	0.15	0.65	MnMoNi	Linde 124
4	WW7	0.35	0.11	MnMo	Linde 80

The four welds were commercially fabricated. Three of the four were produced with copper-coated weld filler wire. The remaining weld (high copper, low nickel content) was fabricated by welding with a low copper, low nickel filler wire coupled with a cold wire feed of high purity copper to obtain the desired copper content in the deposit. This special method of fabrication was necessary since prototypic welding wire (copper-coated, low nickel content) is no longer available commercially in the US. The weldment fabricator (Combustion Engineering Inc.) used the special method previously developed and employed for making prototypic high copper content welds for the Electric Power Research Institute (EPRI) for radiation effects studies [13,14]. Weld deposit compositions are given in Table 2 along with information on postweld stress relief heat treatments. Fabrication details and other information for the four weldments are given in Appendix A.

It will be noted that Welds W8A and W9A were intentionally produced with the same lot of welding wire but with different welding flux types (Linde 80 or Linde 0091). Accordingly, the significance of this welding variable could be assessed directly.

3. MATERIAL IRRADIATION

Test specimens were irradiated in the light-water-cooled and moderated, 2MW pool-type reactor known as the UBR located in the Buffalo Materials Research Center (BMRC) at Buffalo, New York. The experiment irradiation facilities employed are within the fuel lattice (Fig. 1); both B-4 and C-2 facilities were used. Fuel enrichment of the UBR is about 6 percent. Neutron spectrum conditions in the two facilities have been established [15,16,17].

Specimen types included full size C_v specimens (ASTM Type A) for notch ductility determinations and 5.74-mm gage diameter tension test specimens for tensile properties determinations. (See Fig. 2 and 3.) Specimens were irradiated in temperature-controlled capsules at 288°C (target); thermocouples welded to specimen midsections were used for temperature monitoring and control. Individual specimens were placed within the specimen arrays of the irradiation capsules as shown in Fig. 4 to 7; thermocouple placements are illustrated in Fig. 8 to 11. At full reactor power, temperature differences were less than $\pm 10^\circ\text{C}$.

The annealing of specimens between irradiation cycles (cycle 1 and 2) was performed in a special underwater furnace. The entire irradiation assembly was inserted in the furnace. Thermocouples attached to the specimens again provided electrical signals for temperature control. Specimen temperatures typically were within $\pm 7^\circ\text{C}$ of the target heat treatment temperature. Postirradiation annealing for IA-condition evaluations was accomplished in the hot cell using a recirculating air furnace. Specimen temperatures were held within 3°C of the target temperature in this case.

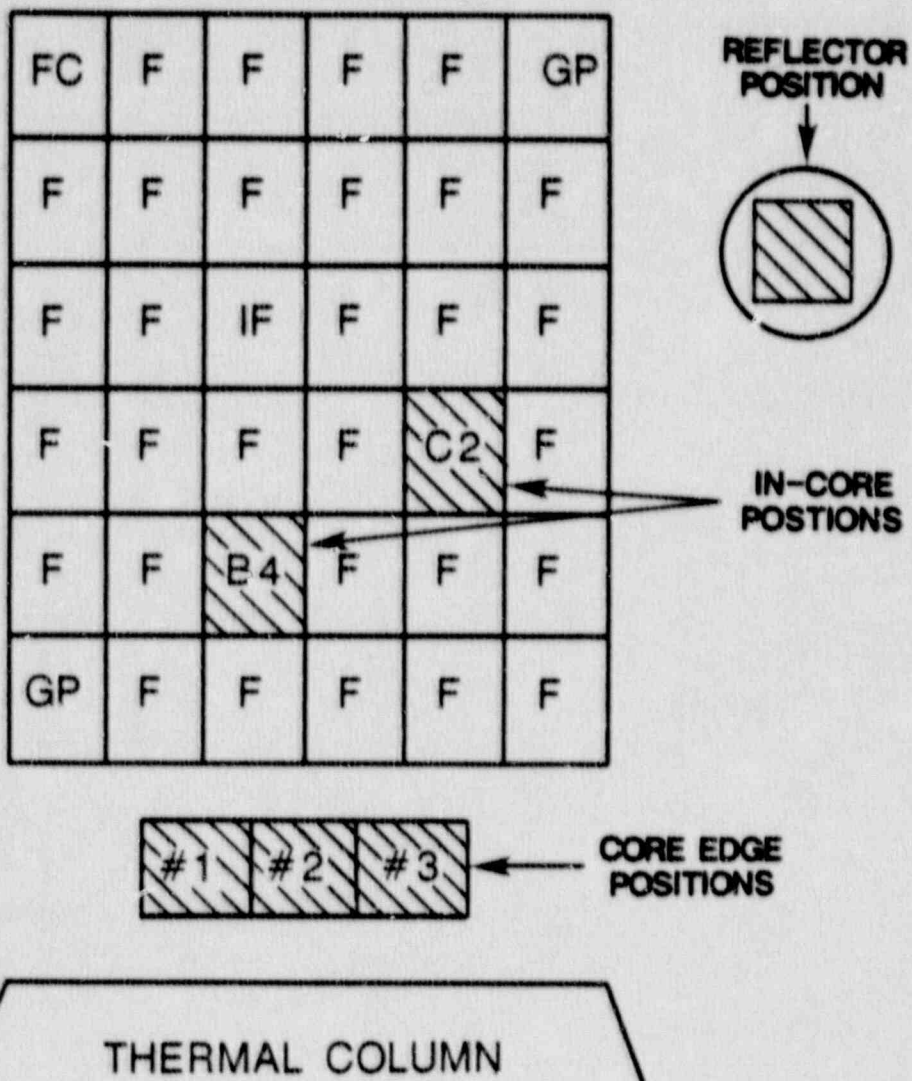
(text continues on page 16)

Table 2 Compositions of Submerged-Arc Weld Deposits

Weld	Chemical Composition (Wt-%)							Heat Treatment		
	C	Mn	Si	P	S	Ni	Cr			
Weld W8A (Linde 80 φ)	0.079(min) ^a	1.27	0.71	0.010	0.012	0.55	0.10	0.42	0.37	0.002
	0.096(max)	1.36	0.79	0.017	0.019	0.68	0.13	0.50	0.42	0.004
Weld W9A (Linde 0091 φ)	0.19(min)	1.21	0.23	0.008	0.005	0.64	0.10	0.49	0.35	0.003
	0.19(max)	1.27	0.23	0.012	0.010	0.77	0.11	0.50	0.43	0.004
Weld WW7 (Linde 80 φ)	0.08	1.56	0.60	0.013	0.008	0.10	0.12	0.54	0.35	0.002
	0.08	1.38	0.49	0.013	0.018	0.65	0.13	0.44	0.16	0.004
Weld WW4 (Linde 124 φ)									2 ^b	

^a Range (min/max) observed, multiple test locations in 1.83-m long weld seam^b (1) 621°C ± 14°C for 24 h
(2) 607°C ± 14°C for 50 h

**SUNY - BUFFALO
'PULSTAR' REACTOR**



FC - FISSION CHAMBER
 F - FUEL
 GP - GRID PLUG
 IF - ISOTOPE FACILITY

Fig. 1 MEA irradiation facilities in the UBR Reactor.

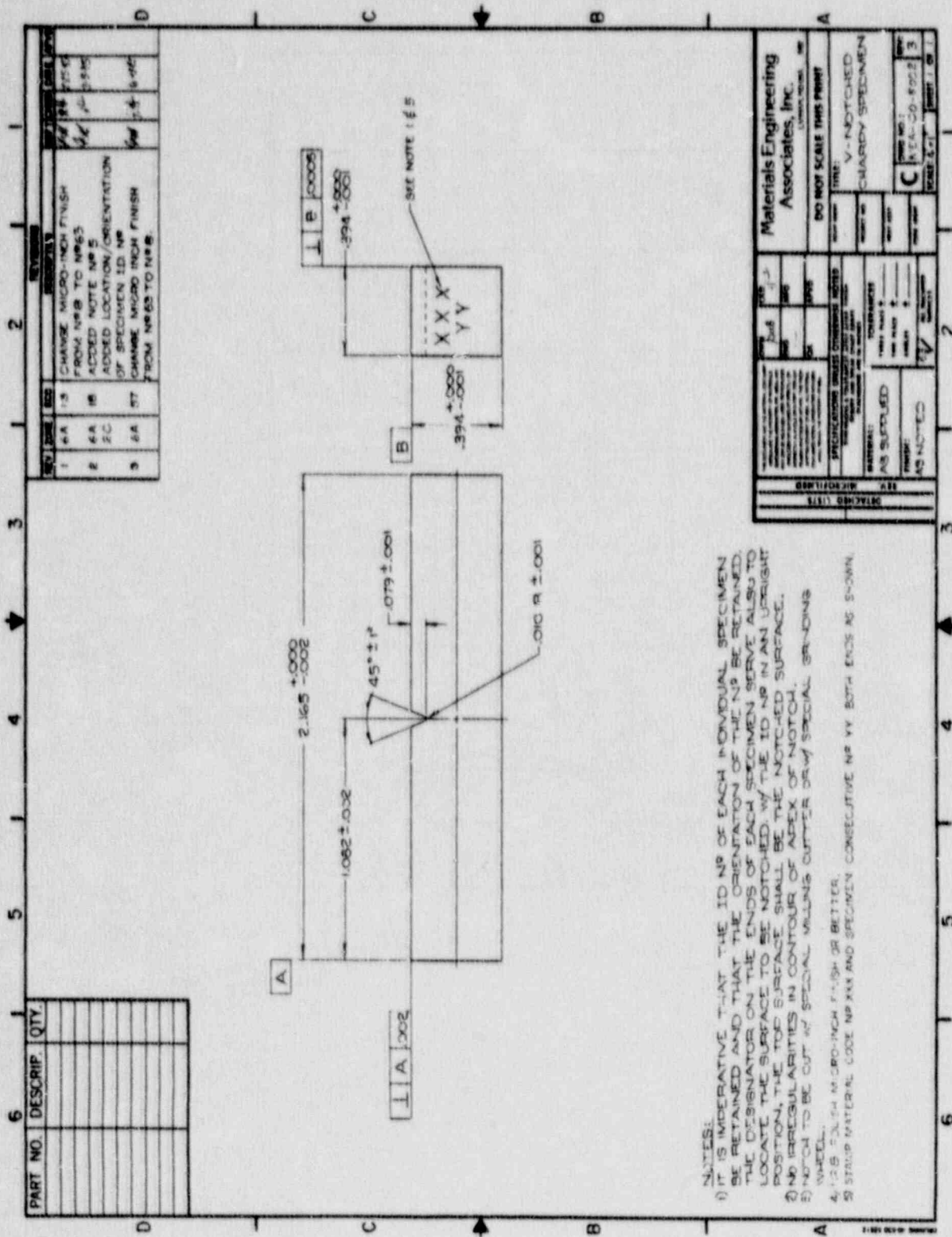


Fig. 2 Design of Charpy V-notch (C_V) test specimen.

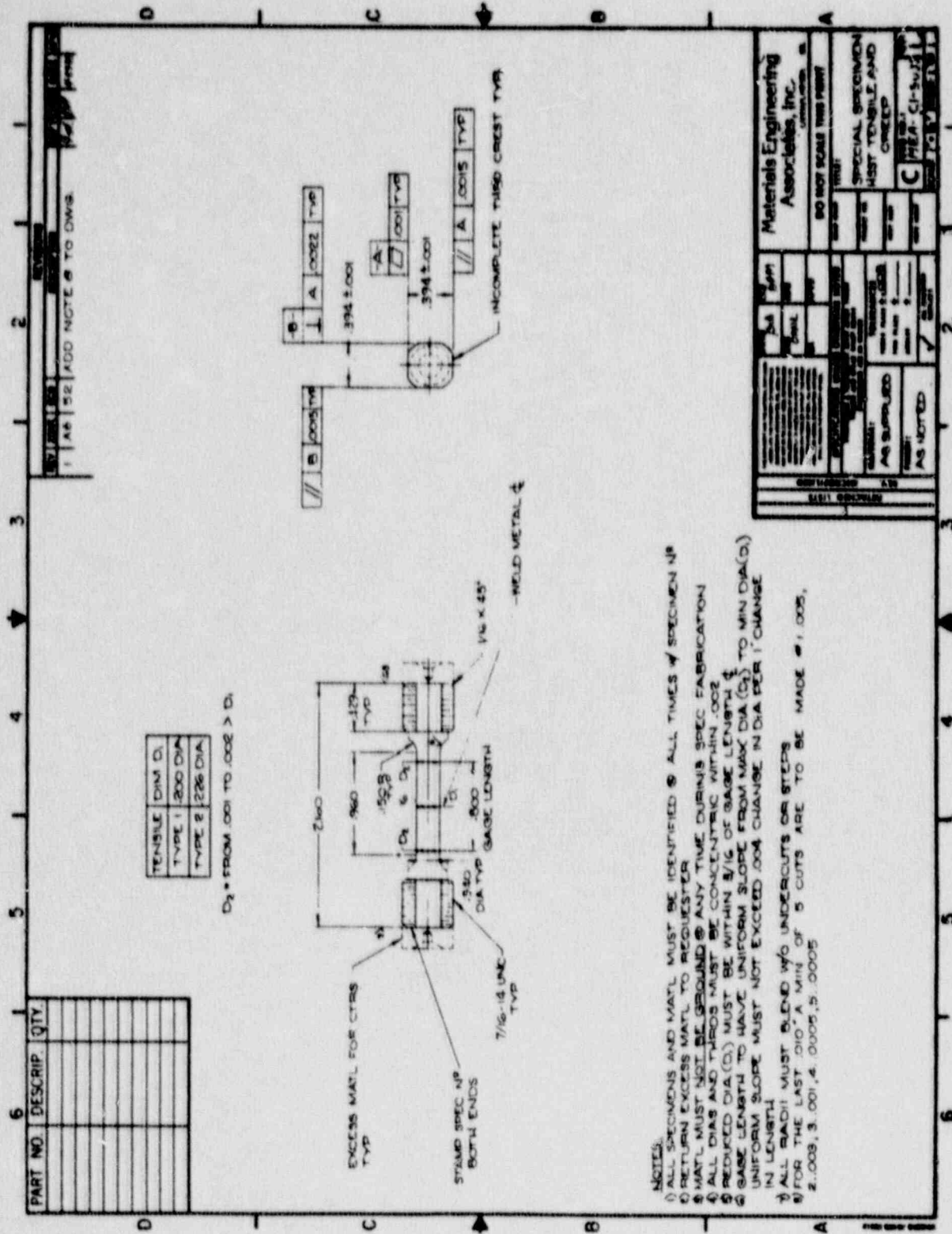


Fig. 3 Design of threaded-end, C_v-size tension test specimen. The Type 2 Design was used.

UBR-62**A-CAPSULE**

W8A	W8A	WW7		
457	375	16		
W8A	WW7	W8A	WW7	
465	60	460	41	
WW7	W8A	WW7	W8A	
61	463	42	498	
W8A	WW7	W8A	WW7	
467	43	500	62	
WW7	W4	WW7	W8A	
44	37	63	494	
WW7	WW7	WW7	WW7	
64	37	28	45	
WW7	W8A	W8A	WW7	
48	485	481	59	
W8A	WW7	W4	WW7	
458	54	87	47	
WW7	W8A	WW7	W8A	
55	462	48	464	
W8A	WW7	W8A	WW7	
493	49	466	56	
WW7	W8A	WW7	W8A	
50	468	57	496	
W8A	WW7	W8A	WW7	
499	58	501	51	

Total Fluence, $n/cm^2 \times 10^{18}$
(Fe Dosimetry)

← Fe 1.34

← Fe 1.37

← Fe 1.42

← ^{238}U (1.50)

← Fe 1.50

← Fe 1.53

← Fe 1.60

B-CAPSULE

W8A	W8A	W4	W8A	W4
386	380	144	V30	109
W4	W4	W8A	W4	W8A
169	148	420	115	419
W8A	W8A	W4	W8A	W4
410	414	142	416	112
W4	W4	W4	W8A	W8A
171	167	87	471	385
W8A	W8A	W8A	W8A	W8A
395	504	485	127	502
W8A	W4	W8A	W8A	W4
518	147	382	503	110
W4	W8A	W4	W8A	W8A
168	388	145	522	386
W8A	W8A	W8A	W4	W4
412	417	88	141	114
W4	W8A	W4	W8A	W8A
170	383	165	381	415
W8A	W4	W8A	W4	W4
409	166	351	143	116
W4	W8A	W4	W8A	W8A
172	394	146	418	V24

← Fe 1.55

← Fe 1.47

← ^{238}U (1.52)

← Fe 1.43

← Fe 1.38

← Fe 1.35

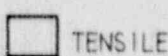
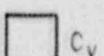


Fig. 4 Placement of C_v and tension test specimens in Irradiation Assembly UBR-62. (Capsules A and B; elevation view). Average neutron fluence values at various locations, based on iron dosimetry, are shown. Determinations, based on ^{238}U dosimetry, are also listed.

UBR-70

A-CAPSULE

W8A	WW7	W4	W8A
371	73	81	433
WW7	W4	W8A	W8A
75	148	438	361
W4	W8A	W8A	WW7
156	440	384	66
W8A	W8A	WW7	W4
443	368	70	85
W8A	W8A	W8A	W8A
372	87	472	434
WW7	W4	WW7	W4
77	89	89	86
W4	W8A	W8A	WW7
159	441	368	67
W8A	W8A	WW7	W4
444	368	71	88
W8A	WW7	W4	W8A
V18	74	82	438
WW7	W4	W8A	W8A
78	153	439	362
W4	W8A	W8A	WW7
162	442	367	68
W8A	W8A	WW7	W4
517	370	72	80

Total Fluence, $n/cm^2 \times 10^{18}$

(Fe Dosimetry)

← Fe 1.63
 ← Fe 1.68
 ← Fe 1.77
 ← (238U) (1.74)
 ← Fe 1.86
 ← Fe 1.88
 ← Fe 1.86

B-CAPSULE

W9A	WW7	W8A	W4	W8A
383	85	380	86	445
W8A	WW7	W4	W8A	W8A
455	86	151	450	373
WW7	W4	W8A	W8A	WW7
90	163	452	378	79
W4	WW7	W8A	W4	W4
161	89	381	113	93
W8A	W8A	WW7	W4	W8A
456	454	83	98	448
W8A	WW7	W4	W8A	W8A
384	87	154	451	374
WW7	W8A	WW7	W8A	WW7
91	152	381	379	80
W4	W8A	W4	WW7	W4
157	111	103	82	94
W8A	W8A	WW7	W4	W8A
520	382	84	98	448
W8A	WW7	W8A	W4	W8A
V21	88	453	100	378
WW7	W8A	W8A	WW7	W8A
20	23	47	24	34

← Fe 1.98
 ← Fe 1.91
 ← Fe 1.79
 ← Fe 1.76
 ← Fe 1.68



C_v



TENSILE

Fig. 5 Placement of C_v and tension test specimens in Irradiation Assembly UBR-70. (Capsules A and B; elevation view). Total neutron fluence values at various locations are shown in this figure and Fig. 6.

UBR-71

A-CAPSULE

W8A	WW7	W4	W8A
407	88	139	488
WW7	W4	W8A	W8A
101	152	474	387
W4	W8A	W8A	WW7
6	476	400	92
W8A	W8A	WW7	W4
478	404	98	101
W8A	W8A	W8A	W8A
408	477	450	470
WW7	W4	WW7	W4
103	129	84	102
W4	W8A	W8A	WW7
13	477	402	93
W8A	W8A	WW7	W4
480	405	87	104
W8A	WW7	W4	W8A
V27	100	108	475
WW7	W4	W8A	W8A
104	158	472	388
W4	W8A	W8A	WW7
164	478	403	95
W8A	W8A	WW7	W4
523	406	98	138

Total Fluence, $n/cm^2 \times 10^{18}$
(Fe Dosimetry)

← Fe 2.34
← Fe 2.44
← Fe 2.55
← (^{238}U) (2.57)
← Fe 2.68
← Fe 2.77
← Fe 2.88

B-CAPSULE

W8A	WW7	W8A	W4	W8A
431	111	428	128	481
W8A	WW7	W4	W8A	W8A
481	112	150	486	421
WW7	W4	W8A	W8A	WW7
116	160	488	426	105
W4	WW7	W8A	W4	W4
26	115	429	111	125
W8A	W8A	WW7	W4	W8A
492	480	109	130	482
W8A	WW7	W4	W8A	W8A
432	113	155	487	422
WW7	W8A	WW7	W8A	WW7
117	183	107	427	106
W4	W8A	W4	WW7	W4
37	401	105	108	126
W8A	W8A	WW7	W4	W8A
524	430	110	131	484
W8A	WW7	W8A	W4	W8A
V33	114	488	132	424
WW7	W8A	W8A	WW7	W8A
26	155	48	22	35

← Fe 2.95
← Fe 2.81
← Fe 2.73
← (^{238}U) (2.80)
← Fe 2.64
← Fe 2.54



C_v



TENSILE

Fig. 6 Placement of C_v and tension test specimens in Irradiation Assembly UBR-71. (Capsules A and B; elevation view).

UBR-72

A-CAPSULE

W8A	WW7	W4	W8A
359	125	107	505
WW7	W4	W8A	W8A
127	18	510	349
W4	W8A	W8A	WW7
50	512	352	118
W8A	W8A	WW7	W4
515	356	122	133
W8A	W8A	W8A	W8A
360	425	509	506
WW7	W4	W4	W4
129	85	120	134
W4	W8A	W8A	WW7
52	513	354	118
W8A	W8A	WW7	W4
516	357	123	136
W8A	WW7	W4	W8A
V15	126	140	508
WW7	W4	W8A	W8A
130	38	511	350
W4	W8A	W8A	WW7
65	514	355	121
W8A	W8A	WW7	W4
527	358	124	108

Total Fluence, $n/cm^2 \times 10^{18}$
(Fe Dosimetry)

→ Fe 1.07
→ Fe 1.06
→ Fe 1.07
→ (238U) 1.04
→ Fe 1.06
→ Fe 1.06
→ Fe 1.07

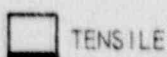
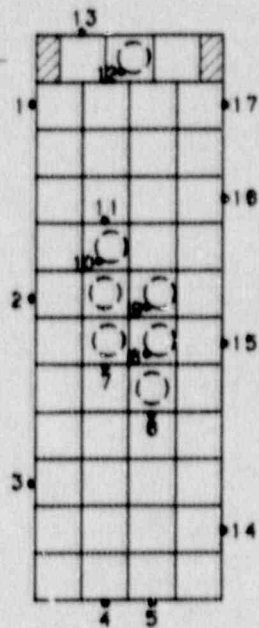


Fig. 7 Placement of C_V and tension test specimens in Irradiation Assembly UBR-72. (Capsule A; elevation view). Average neutron fluence values at various locations are also shown.

UBR-62

A-CAPSULE



B-CAPSULE

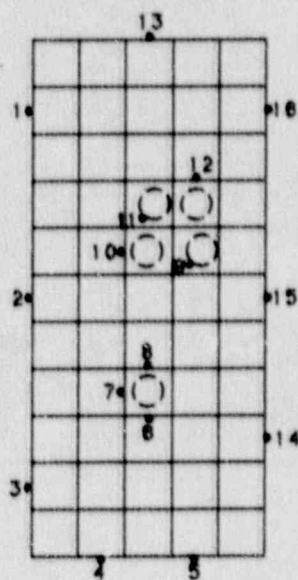
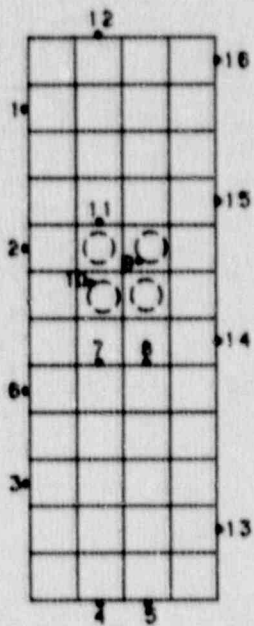


Fig. 8 Irradiation Assembly UBR-62 showing thermocouple placements in the specimen arrays.

UBR - 70

A-CAPSULE



B-CAPSULE

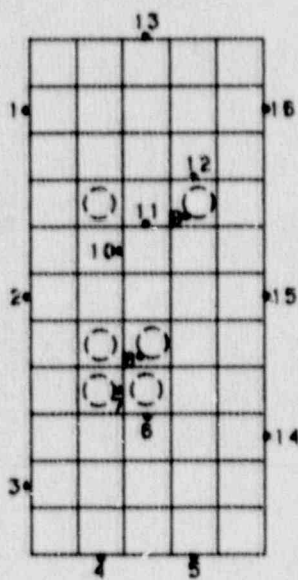
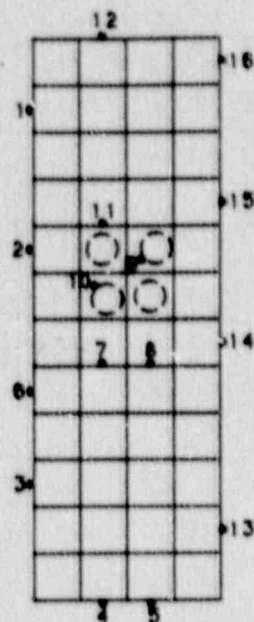


Fig. 9 Irradiation Assembly UBR-70 showing thermocouple placements in the specimen arrays.

UBR-71

A-CAPSULE



B-CAPSULE

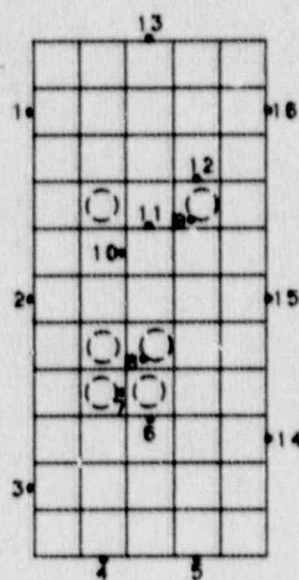


Fig. 10 Irradiation Assembly UBR-71 showing thermocouple placements in the specimen arrays.

UBR-72

A-CAPSULE

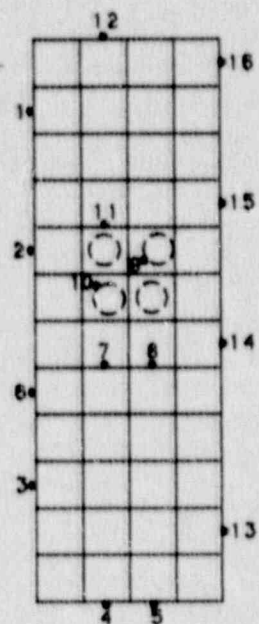


Fig. 11 Irradiation Assembly UBR-72 showing thermocouple placements in the specimen array.

Neutron fluences (n/cm^2 , $E < 1$ MeV) received by the specimens were determined from iron and nickel dosimeter wires placed in the V-notches of the C_v specimens and from ^{238}U dosimeter capsules placed within the specimen arrays (see Figs. 4 to 7). Neutron spectrum calculations indicate that the calculated spectrum fluence, Φ^{cs} ($E > 1$ MeV), is 1.43 times the fission spectrum fluence, Φ^{fs} . The exposure equivalent in terms of displacements per atom (dpa, $E > 1$ MeV) is $1.62 \times 10^{-21} \Phi^{cs}$. The average neutron fluence rate, $n/cm^2 \cdot s^{-1}$ is on the order of 8.5×10^{12} , $E > 1$ MeV. Thermal neutron fluences were determined from cobalt-aluminum and silver-aluminum dosimeter wires located in the C_v specimen notches.

4. IRRADIATION MATRIX

Figures 12 and 13 illustrate schematically the research questions addressed by the planned group of experiments. The target first cycle fluence was $1.2 \times 10^{19} n/cm^2$, $E < 1$ MeV; the target reirradiation fluence was $0.3 \times 10^{19} n/cm^2$ or $0.7 \times 10^{19} n/cm^2$. As the irradiation program progressed, a matrix modification increased the higher of the two target reirradiation fluences to $1 \times 10^{19} n/cm^2$ for reasons discussed below. The irradiation matrix also called for the irradiation of virgin material to a fluence matching this value for an assessment, based on 1:1 comparisons, of the embrittlement sensitivity of heat-treated (annealed) vs. non-heat-treated material. A total of 7 irradiation assemblies was required. The I and IAR treatments of the assemblies are indicated in Table 3; the detailed reactor operations history of each capsule is given in Appendix B.

Neutron fluences reported herein carry uncertainties, based on counting and assumed cross section components, of $\pm 8\%$, $\pm 7\%$ and $\pm 5\%$ for the Fe, Ni and ^{238}U dosimeters, respectively, at the 1σ confidence level. Fission spectrum averaged cross section values for neutrons having energies greater than 1 MeV are assumed to be 115.2, 156.8, and 441 millibarns for the three dosimeter types, respectively. Dosimetry postirradiation measurements and analyses were performed by EG&G Idaho, Inc. (J. W. Rogers) for MEA under contract; Appendix C lists the average neutron fluence rate determinations from the dosimeters.

5. NOTCH DUCTILITY TEST RESULTS

Observations on notch ductility for the I, IA and IAR conditions are summarized in Table 4. Individual C_v test results are tabulated in Appendix D.

The analysis and discussion of C_v data trends given below are based on visual best-fits to the data. Computer curve-fits of the data and the values of curve-fit parameters are provided in Appendix E. Comparisons of the hand-drawn vs. computer-fit curves in general show good agreement in the independent 41-J transition temperature determination (see Table 1 of Appendix E).

(text continues on page 21)

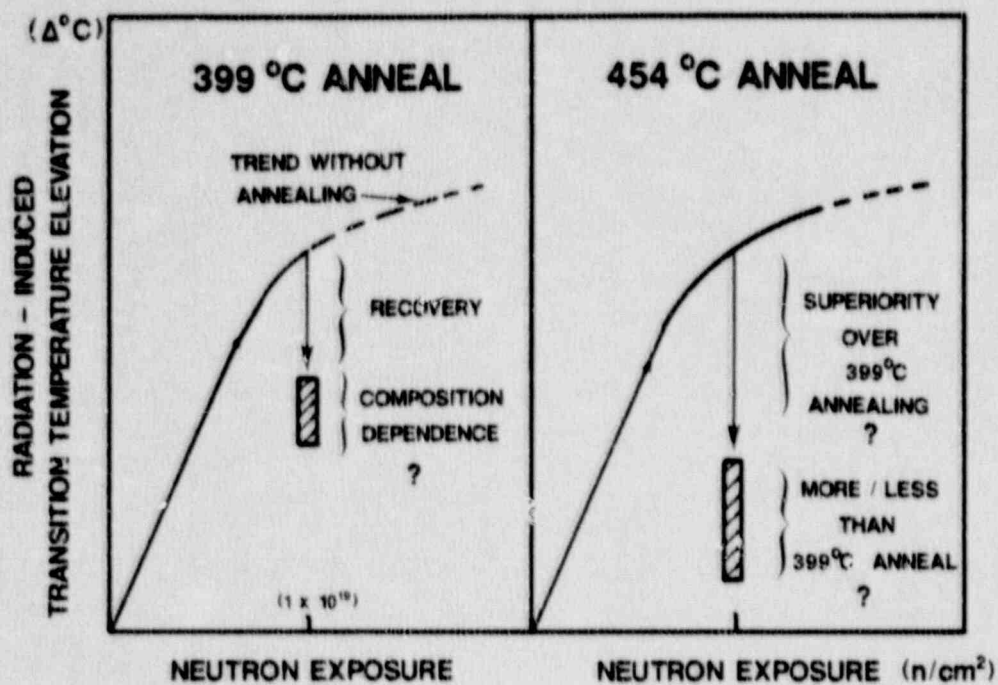


Fig. 12 Objectives for Phase 1 Investigations (I and IA conditions).

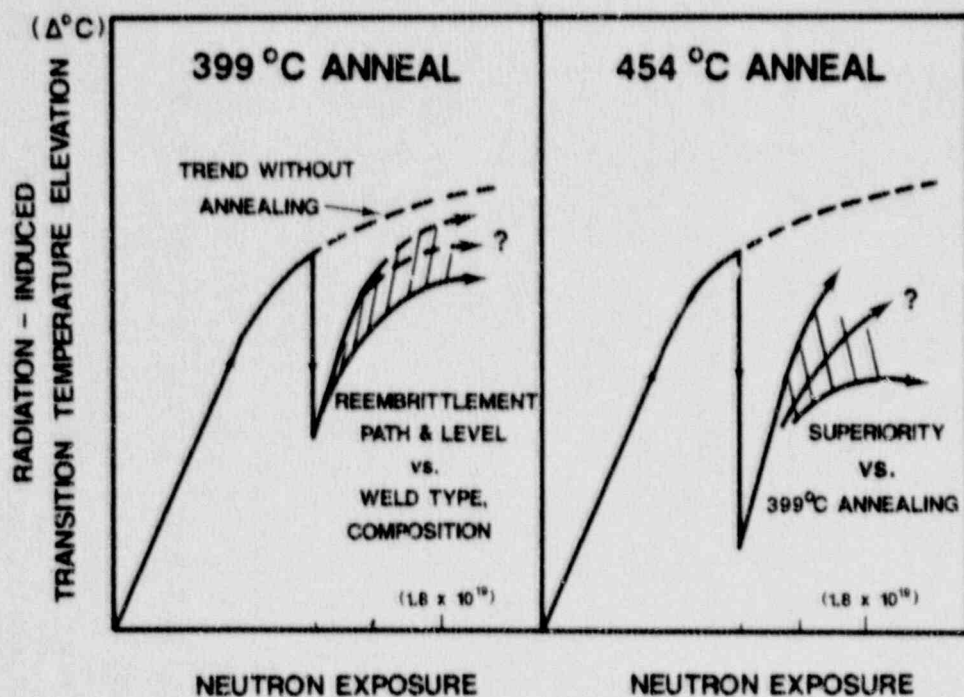


Fig. 13 Objectives for Phase 2 Investigations (two IAR fluence conditions).

Table 3 Exposures Histories of Irradiation Assemblies

Irradiation Assembly	First Cycle Irradiation Fluence ^c (x10 ¹⁹)	Duration ^d (hours)	Intermediate Anneal ^a (°C)	Second Cycle Irradiation Fluence ^c (x10 ¹⁹)	Duration ^d (hours)	Total Fluence (x10 ¹⁹)	Postirradiation Test Conditions ^b
1 (UBR-62A,B) ^e	1.44 ^f	447	--	-	1.44	1	IA(399°C) and IA(454°C)
2 (UBR-72A)	1.06 ^g	318	--	-	1.06	1	
3 (UBR-70A)	1.42	423	399	0.37 ^h	111	1.80	IAR (399°C)
4 (UBR-70B)	1.42	423	454	0.37	111	1.80	IAR (454°C)
5 (UBR-71A)	1.52	449	399	1.09 ⁱ	322	2.61	IAR (399°C)
6 (UBR-71B)	1.57	449	454	1.12	322	2.69	IAR (454°C)

^a 168-hour heat treatment^b I = as-irradiated; IA = irradiated + annealed; IAR = reirradiated^c Calculated spectrum fluence, n/cm² E > 1 MeV^d Exposure time at full reactor power^e MEA irradiation assembly number^f Irradiation Test I₁^g Irradiation Test I₂^h Reirradiation Condition 1ⁱ Reirradiation Condition 2

Table 4 Charpy-V Notch Ductility of Welds in Irradiated, Annealed and Reirradiated Conditions

Weld	Test Condition	C _V 41-J Transition Temperature						C _V Upper Shelf Energy					
		Initial		Final		Change		Initial		Final		Change	
		(°C)	(°F)	(°C)	(°F)	(Δ°C)	(Δ°F)	(J)	(ft-lb)	(J)	(ft-lb)	(ΔJ)	(Δft-lb)
W8A	I ₂	-23	-10	91	195	114	205	79	58	53	39	26	19
	I ₁	-23	-10	96	205	119	215	79	58	52	38	27	20
	IA(399)	96	205	54	130	42	75	52	38	~79	~58	27	20
	IA(454)	96	205	13	55	83	150	52	38	87	64	>27	>20
	IAR ₁ (399)	54	130	93	200	39	70	~79	~58	60	44	19	14
	IAR ₂ (399)	54	130	~93	~200	~39	~70	~79	~58	58	43	21	15
	IAR ₁ (454)	13	55	35	95	22	40	87	64	75	55	12	9
	IAR ₂ (454)	13	55	41	105	28	50	87	64	76	56	11	8
W9A	I ₂	-62	-80	27	80	89	160	156	115	117	86	39	29
	I ₁	-62	-80	27	80	89	160	156	115	114	84	42	31
	IA(399)	27	80	-21	-5	48	85	114	84	~145	~107	31	23
	IA(454)	27	80	-29	-20	56	100	114	84	~165	~122	>42	>31
	IAR ₁ (399)	-21	-5	10	50	31	55	~145	~107	118	87	27	20
	IAR ₂ (399)	-21	-5	18	65	39	70	~145	~107	117	86	28	21
	IAR ₁ (454)	-29	-20	-23	-10	<10	10	~165	~122	153	113	12	9
	IAR ₂ (454)	-29	-20	-21	-5	<10	15	~165	~122	~153	~113	~12	~9

Table 4 Charpy-V Notch Ductility of Welds in Irradiated, Annealed and Reirradiated Conditions (cont'd)

Weld	Test Condition	C _V 41-J Transition Temperature						C _V Upper Shelf Energy					
		Initial		Final		Change		Initial		Final		Change	
		(°C)	(°F)	(°C)	(°F)	(Δ°C)	(Δ°F)	(J)	(ft-lb)	(J)	(ft-lb)	(ΔJ)	(Δft-lb)
20 WW7	I ₂	-15	5	60	140	75	135	84	62	68	50	16	12
	I ₁	-15	5	66	150	81	145	84	62	60	44	24	18
	IA(399)	66	150	21	70	45	80	60	44	85	63	>24	>18
	IA(454)	66	150	7	45	59	105	60	44	103	76	>24	>18
	IAR ₁ (399)	21	70	54	130	33	50	85	63	68	50	17	13
	IAR ₂ (399)	21	70	60	140	39	70	85	63	74	55	11	8
	IAR ₁ (454)	7	45	27	80	20	35	103	76	84	62	19	14
	IAR ₂ (454)	7	45	38	100	31	55	103	76	~86	~63	17	13
WW4	I ₂	-37	-35	4	40	41	75	129	95	108	80	21	15
	I ₁	-37	-35	13	55	50	90	129	95	106	78	23	17
	IA(399)	13	55	-34	-30	47	85	106	78	142	105	>23	>17
	IA(454)	13	55	-34	-30	47	85	106	78	148	~109	>23	>17
	IAR ₁ (399)	-34	-30	2	35	36	65	143	105	117	86	26	19
	IAR ₂ (399)	-34	-30	16	60	50	90	143	105	111	82	32	23
	IAR ₁ (454)	-34	-30	-7	20	27	50	~148	~109	129	95	19	14
	IAR ₂ (454)	-34	-30	16	60	50	90	~148	~109	~129	~95	~19	~14

5.1 As-Irradiated (I) Condition

The welds exhibited a range of radiation embrittlement sensitivities. Increases in C_v 41-J temperatures are illustrated in Figure 14.

As expected, a high sensitivity to embrittlement was induced by a high copper content. A high copper content coupled with a high nickel content, represented by Welds W8A and W9A, proved particularly detrimental to radiation embrittlement resistance. A 50 percent higher 41-J transition temperature elevation was found for the high nickel content Weld W8A compared to the low nickel content Weld WW7 having the same welding flux type. The effect of different welding fluxes can be discerned from the data for Weld W8A vs. Weld W9A. Flux type, in part, governs the as-deposited weld metal composition (see Table 2) which, in turn, has a direct effect on radiation embrittlement resistance.

In terms of observed embrittlement by irradiation, the two, independent I-condition tests were found to be in good agreement. A fluence of $1.1 \times 10^{19} \text{ n/cm}^2$ (Irradiation Test I₂) produced a slightly smaller 41-J transition temperature elevation than a fluence of $1.4 \times 10^{19} \text{ n/cm}^2$ (Irradiation Test I₁) for three welds. The two exposures produced essentially the same embrittlement in Weld W9A. Large differences due to fluence level were not expected for this fluence range.

5.2 Irradiation + Annealed (IA) Condition

The recoveries in 41-J transition temperature by 454°C and 399°C postirradiation heat treatments also are illustrated in Figure 14. The residual embrittlement after the anneal is depicted by the height of the bar; percentage recovery was computed as: [transition temperature reduction (deg. C) divided by the original radiation-induced elevation (deg. C)] x 100.

A key determination from these data is that C_v 41-J transition temperature recovery may or may not be significantly greater with a 454°C anneal compared to a 399°C anneal. Notice that the recovery appears roughly independent of the annealing temperature for Welds W9A and WW4 but not Welds WW7 or W8A. It can be speculated that this division of behavior is due to welding flux type. The former were produced with welding fluxes (Linde 0091 and 124) normally associated with a "high" preirradiation C_v upper shelf level; the latter were produced with a welding flux (Linde 80) normally resulting in a "low" C_v upper shelf energy level. A high C_v upper shelf level is considered to be one in excess of 135 J (100 ft-lb); the energy absorption range for the low C_v upper shelf welds is about 80 J to 115 J (60 to 85 ft-lb).

Referring to 399°C annealing effectiveness, full transition temperature recovery was obtained with Weld WW4 but only partial recovery was obtained for the remaining materials. This is believed to be a direct consequence of their respective copper contents.

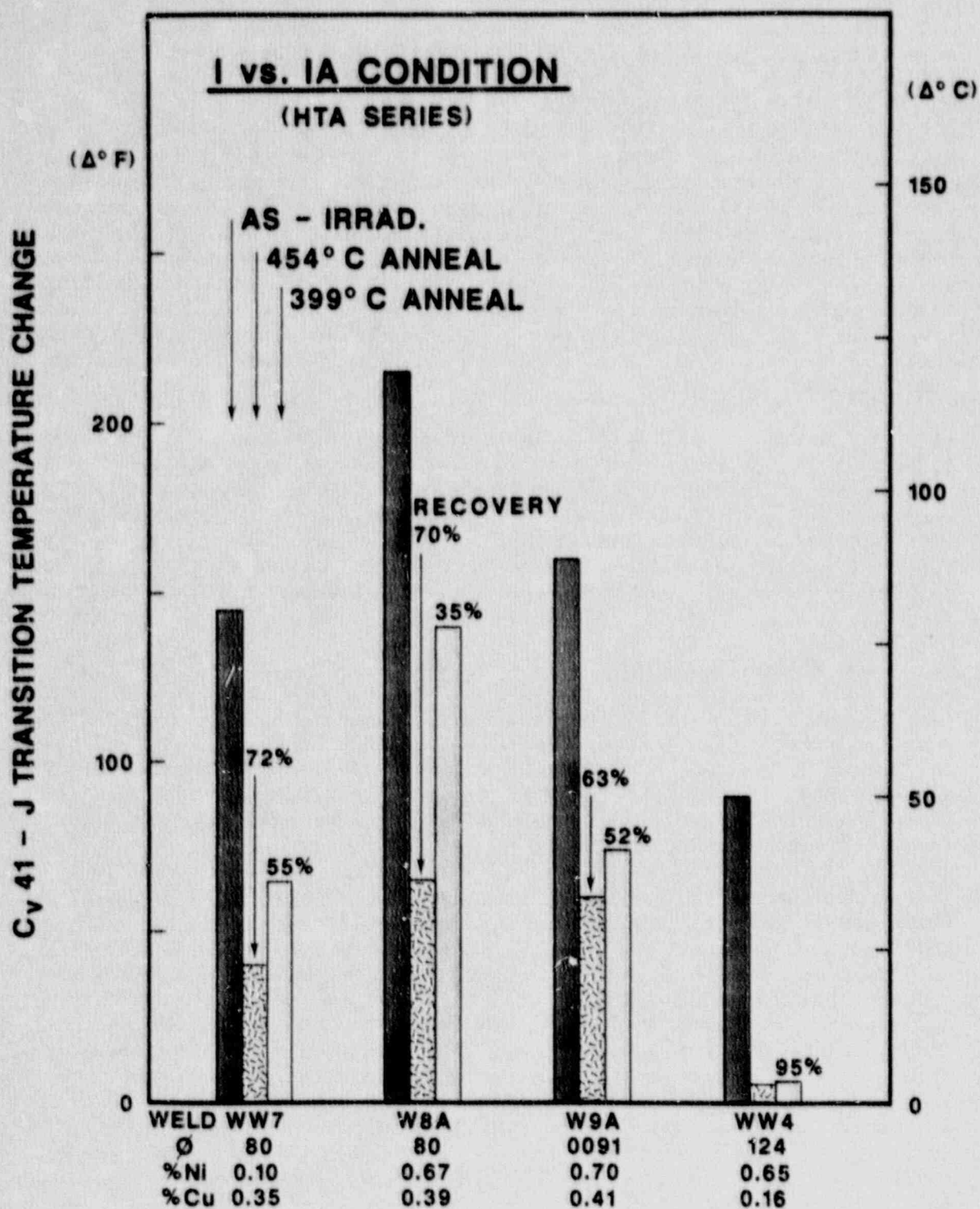


Fig. 14 Summary of notch ductility changes observed for Welds W8A, W9A, WW4 and WW7 after irradiation and after postirradiation annealing at 454°C or 399°C (UBR-62).

Studies of composition effects on annealing, using A 533-B plate materials from split laboratory melts, have shown that copper content is one key factor governing residual embrittlement level after an anneal [18]. Phosphorus content, on the other hand, is not.

5.3 Irradiation-Anneal-Reirradiation (IAR) Conditions

5.3.1 IAR Condition 1 (IAR₁)

Figures 15 and 16 illustrate the amount of reembrittlement produced by a second cycle of neutron exposure of 0.4×10^{19} n/cm². The total fluence (cycles 1 and 2) was 1.8×10^{19} n/cm².

Two general observations are made. Firstly (Fig. 15), the extent of embrittling or 41-J transition temperature change by the second cycle exposure (IAR-condition) is much less than that produced by the first exposure cycle (I-condition). This observation applies for 454°C and 399°C intermediate annealing. Secondly and more importantly, the extent of reembrittlement by a fluence of 0.4×10^{19} n/cm² after a 454°C intermediate anneal is less than that after a 399°C intermediate anneal. (In view of this, the target reirradiation fluence for IAR Condition 2 (below) was increased to 1.1×10^{19} n/cm² to test this trend more closely.)

In Figure 16, the results clearly show a benefit of IAR procedures with 454°C intermediate annealing. The benefit is less dramatic for 399°C annealing conditions; however, the fluence difference, that is, 0.4×10^{19} n/cm², between the IAR-condition data and the I-condition data must not be overlooked. This adds significance to the indicated transition temperature benefit by the lower temperature anneal. Another conclusion from the IAR-condition (399°C anneal) data is that the material reembrittles at a relatively-rapid rate. Notice that the 41-J transition temperature is returned to near the pre-anneal level by a second cycle fluence of only 0.4×10^{19} n/cm². For some reactor vessels, this may correspond to only a few fuel cycles.

Figures 17 to 20 provide the actual notch ductility trend curves from which Figures 15 and 16 were constructed.

5.3.2 IAR Condition 2 (IAR₂)

Figures 21 and 22 illustrate the reembrittlement produced by a second cycle fluence of 1.1×10^{19} n/cm². The total fluence (cycles 1 + 2) for this IAR condition is 2.7×10^{19} n/cm². Again, the I-condition shown in the figures represents a fluence of 1.4×10^{19} n/cm² or only 52 percent of the IAR₂ fluence.

Referring to Figure 21, it is immediately apparent that the increase in reirradiation fluence from 0.4×10^{19} (IAR Condition 1) to 1.1×10^{19} n/cm² (IAR Condition 2) produced only a small, additional increase in transition temperature for the high copper content Welds WW7, W8A and W9A. The small increases are viewed as indications of a possible trend toward radiation embrittlement saturation. Relative

(text continues on page 36)

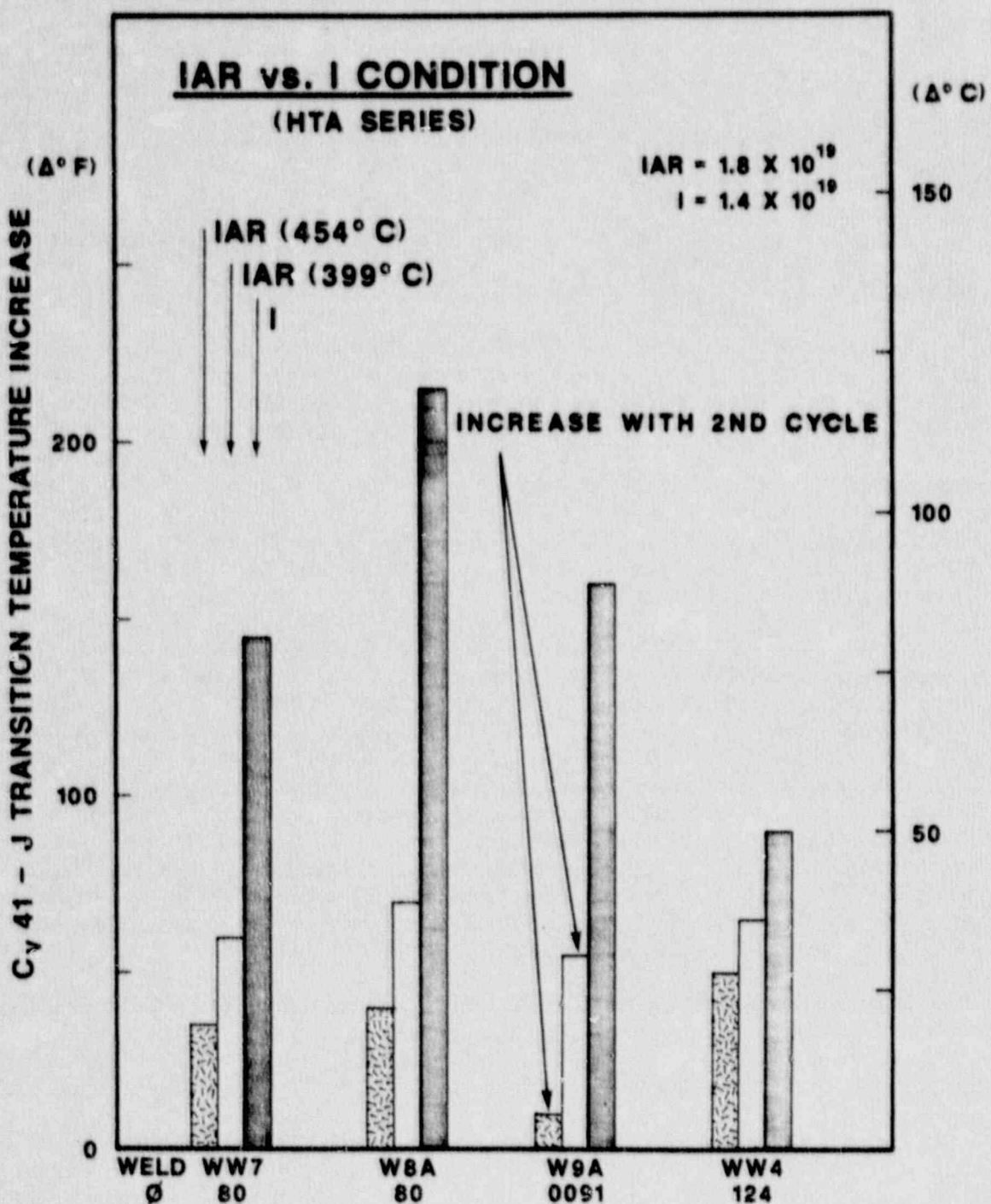


Fig. 15 Notch ductility changes observed after reirradiation to $1.8 \times 10^{19} \text{ n/cm}^2$ following a 454°C or 399°C intermediate anneal vs. first exposure cycle. The left-hand and center bars indicate the increase in transition temperature by the second exposure cycle only.

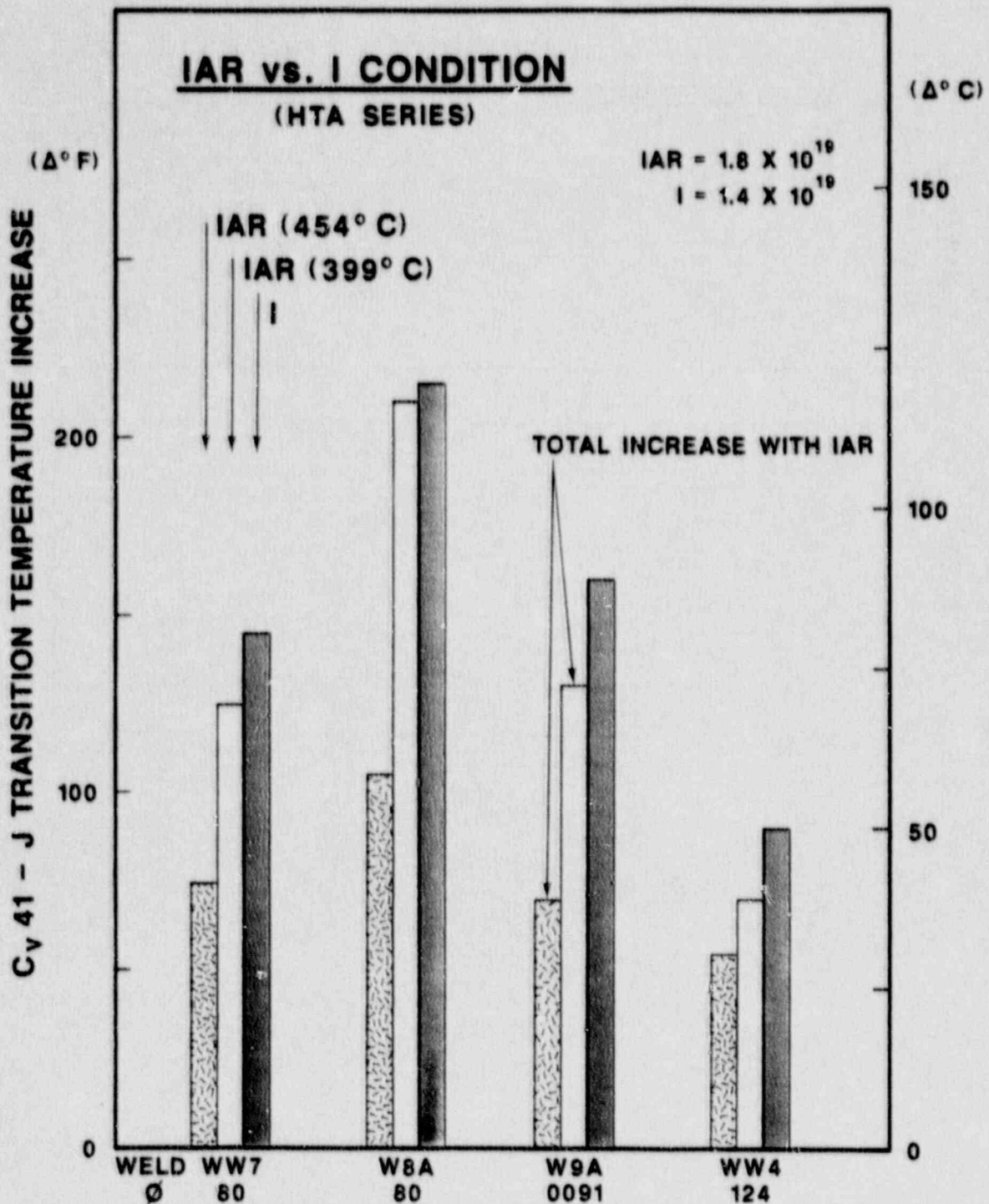


Fig. 16 Notch ductility changes (total) observed after reirradiation to $1.8 \times 10^{19} \text{ n/cm}^2$ following a 454°C or 399°C intermediate anneal vs. first exposure cycle. The left-hand and center bars indicate the total transition temperature elevation with the IAR treatment.

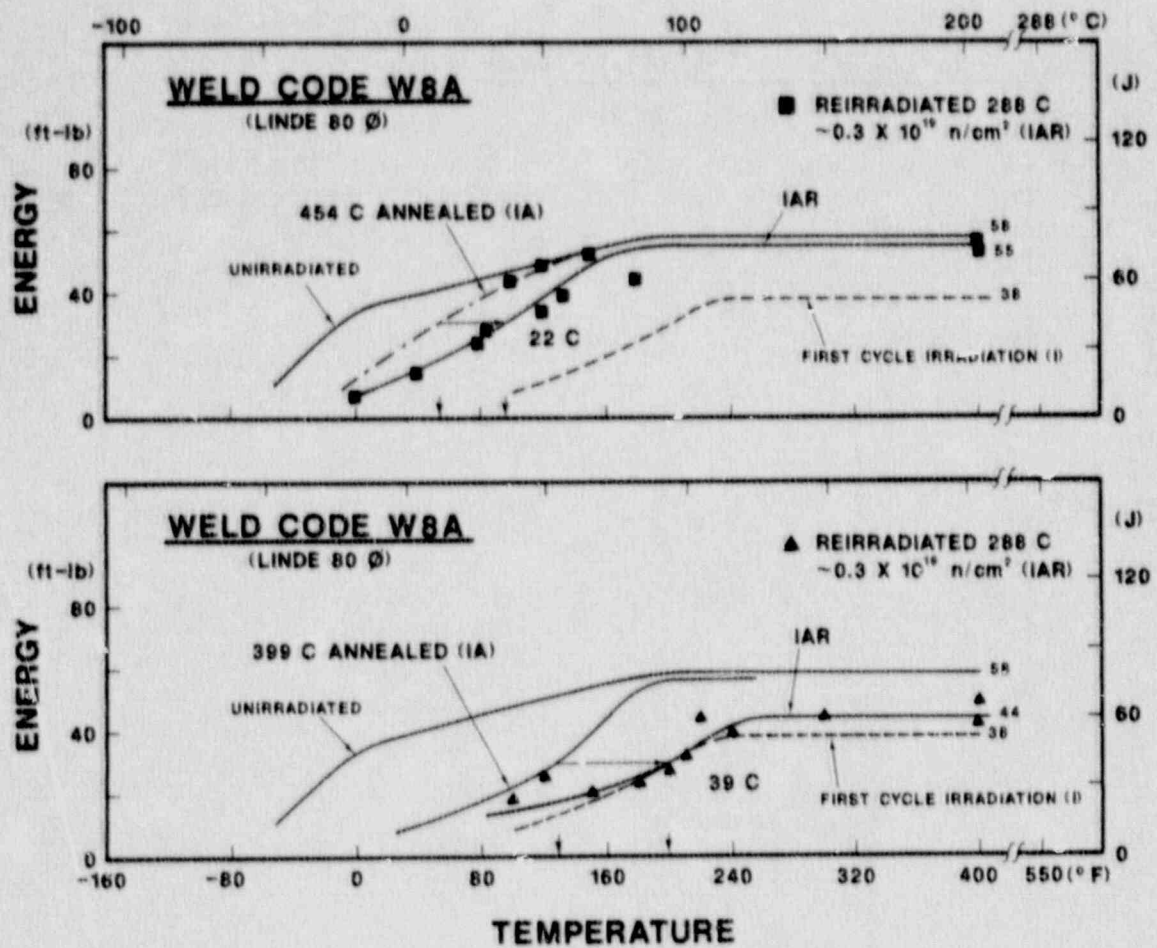


Fig. 17 C_V notch ductility of Weld W8A after reirradiation following a 454°C intermediate anneal (upper graph) and after reirradiation following a 399°C intermediate anneal (lower graph). Trend lines for the I-condition and IA-condition are also shown in this figure and in Fig. 18, 19 and 20.

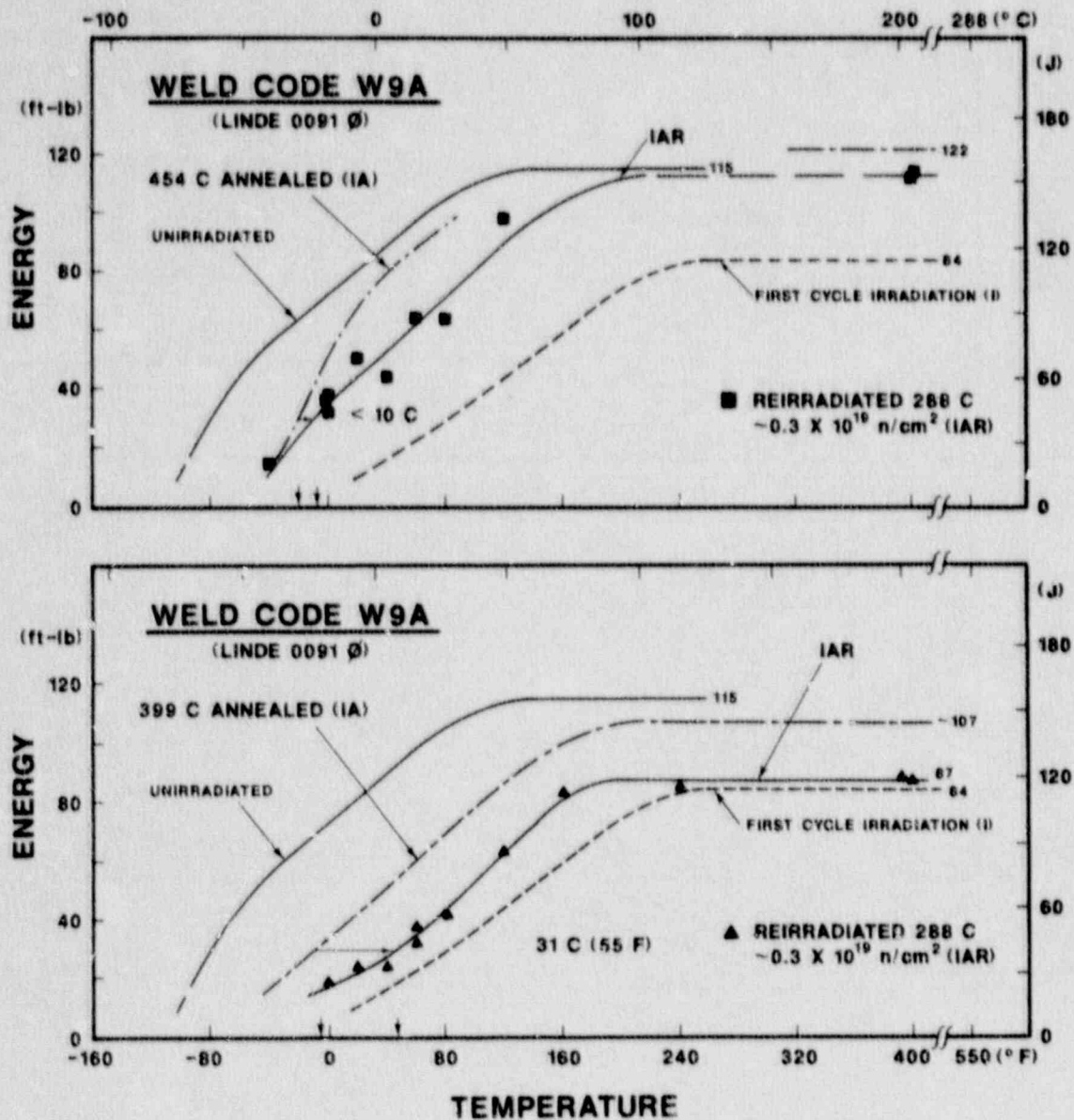


Fig. 18 C_V notch ductility of Weld W9A after reirradiation following a 454°C or 399°C intermediate anneal.

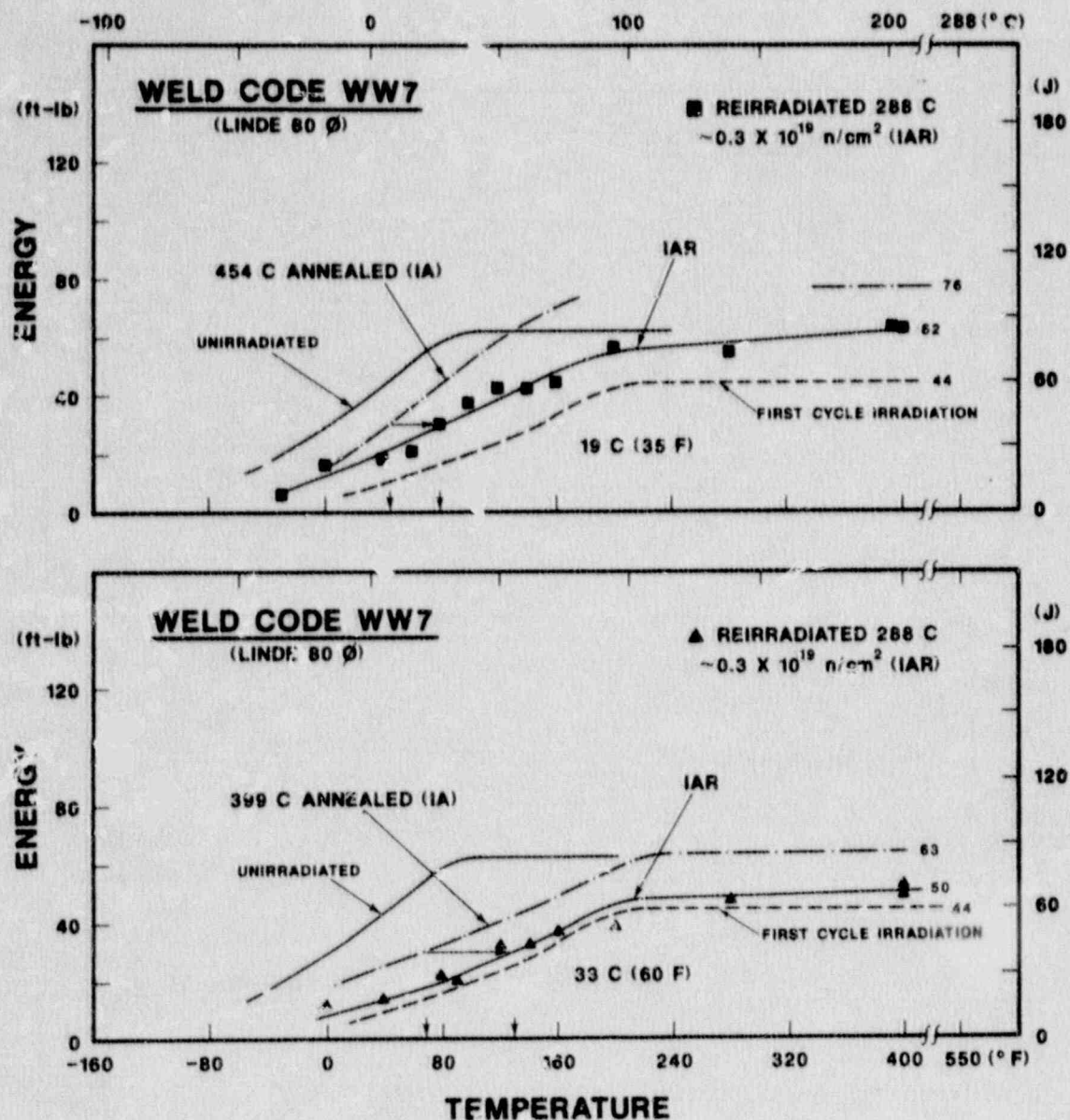


Fig. 19 C_V notch ductility of Weld WW7 after reirradiation following a 454°C or 399°C intermediate anneal.

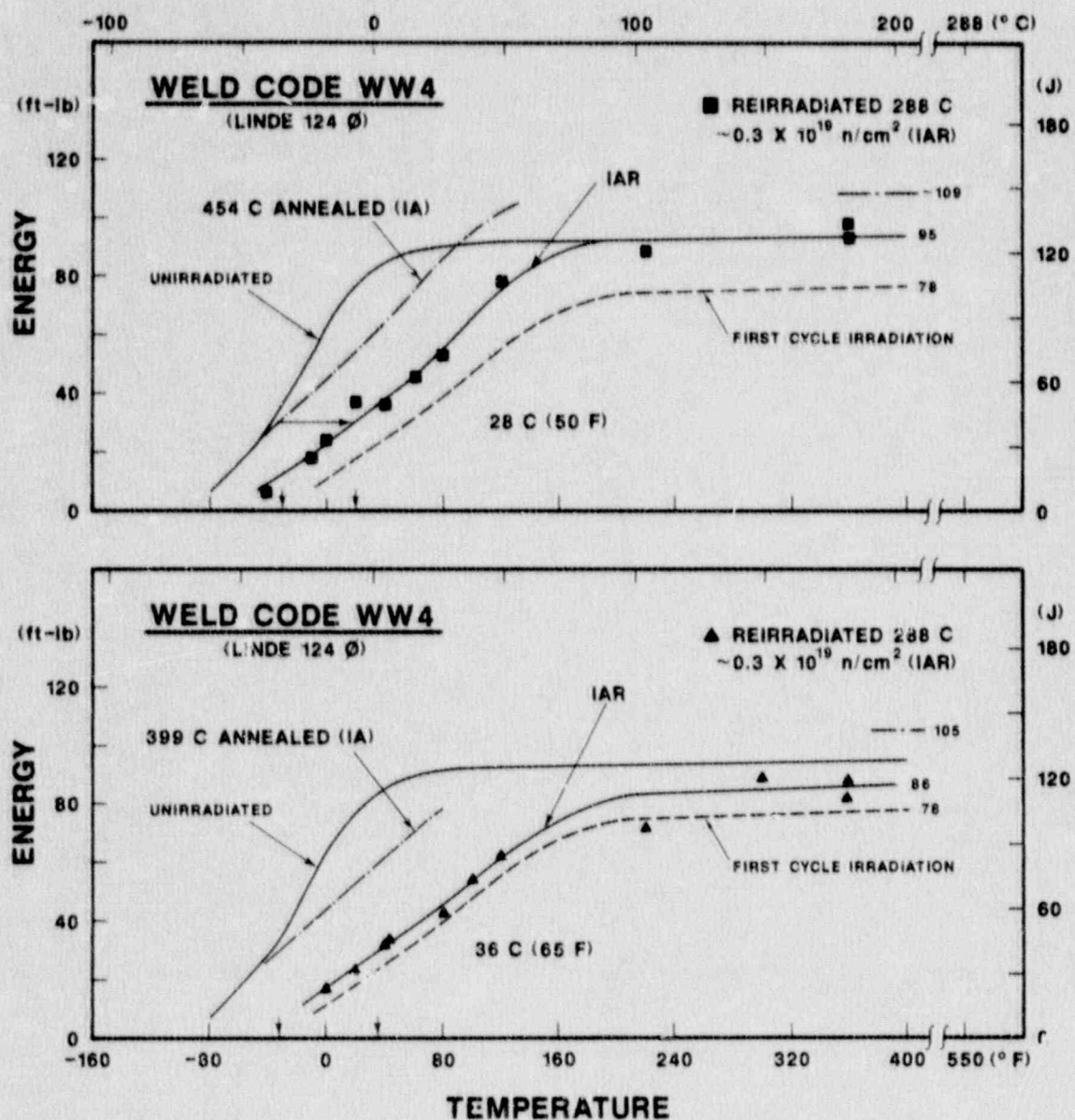


Fig. 20 C_V notch ductility of Weld WW4 after reirradiation following a 454°C or 399°C intermediate anneal.

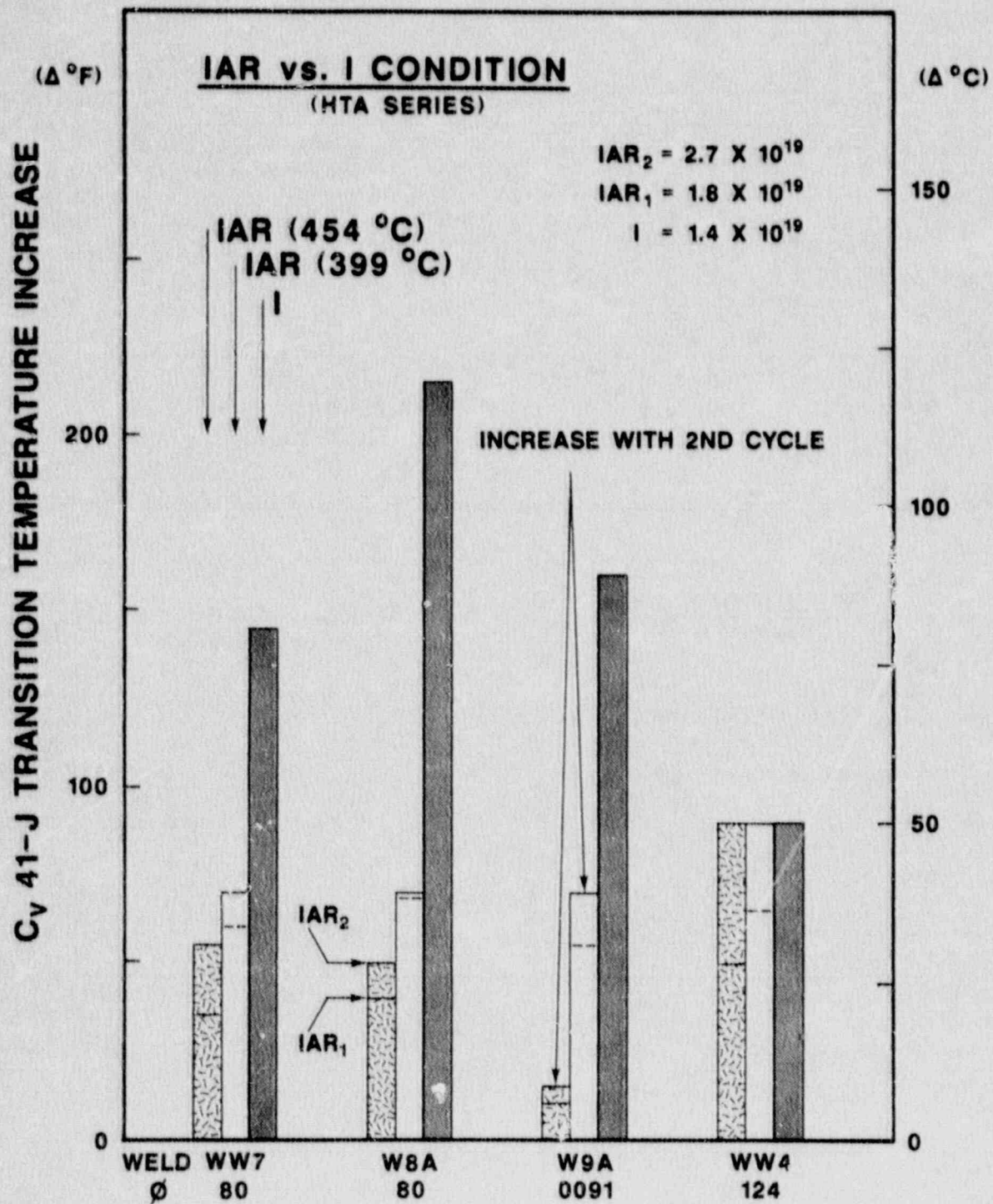


Fig. 21 Notch ductility changes observed after reirradiation to $2.7 \times 10^{19} \text{ n/cm}^2$ vs. first exposure cycle. The left-hand and center bars indicate the increase in transition temperature by the second exposure cycle only.

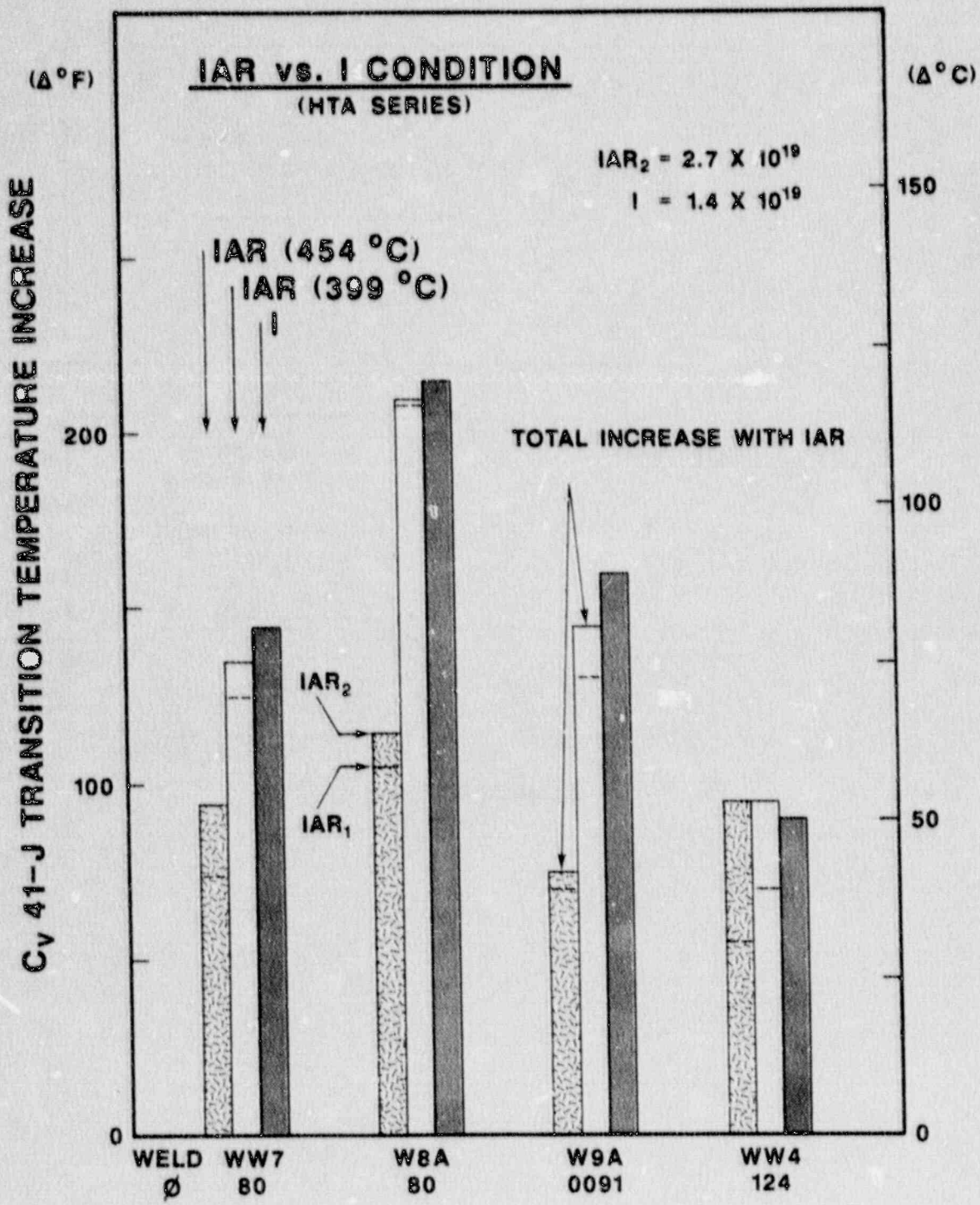


Fig. 22 Notch ductility changes (total) observed after reirradiation to a fluence of $2.7 \times 10^{19} \text{ n/cm}^2$ (IAR_2) or $1.8 \times 10^{19} \text{ n/cm}^2$ (IAR_1) vs. first exposure cycle. The left-hand and center bars indicate the total transition temperature elevation with the IAR treatment.

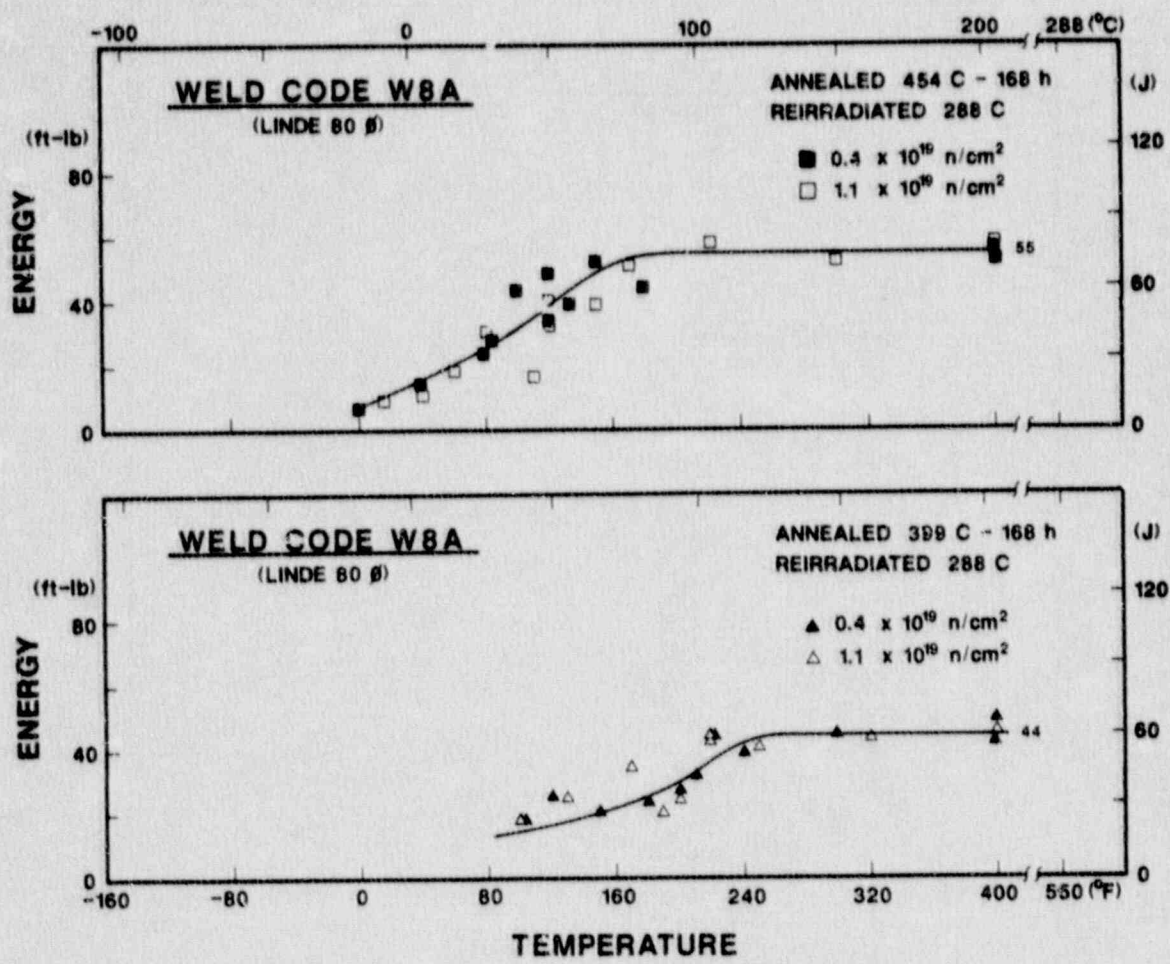


Fig. 23 Experimental data for IAR Condition 1 and IAR Condition 2 of Weld W8A. Trend lines in this figure (and in Figures 24, 25, and 26) describe average IAR Condition 1 properties.

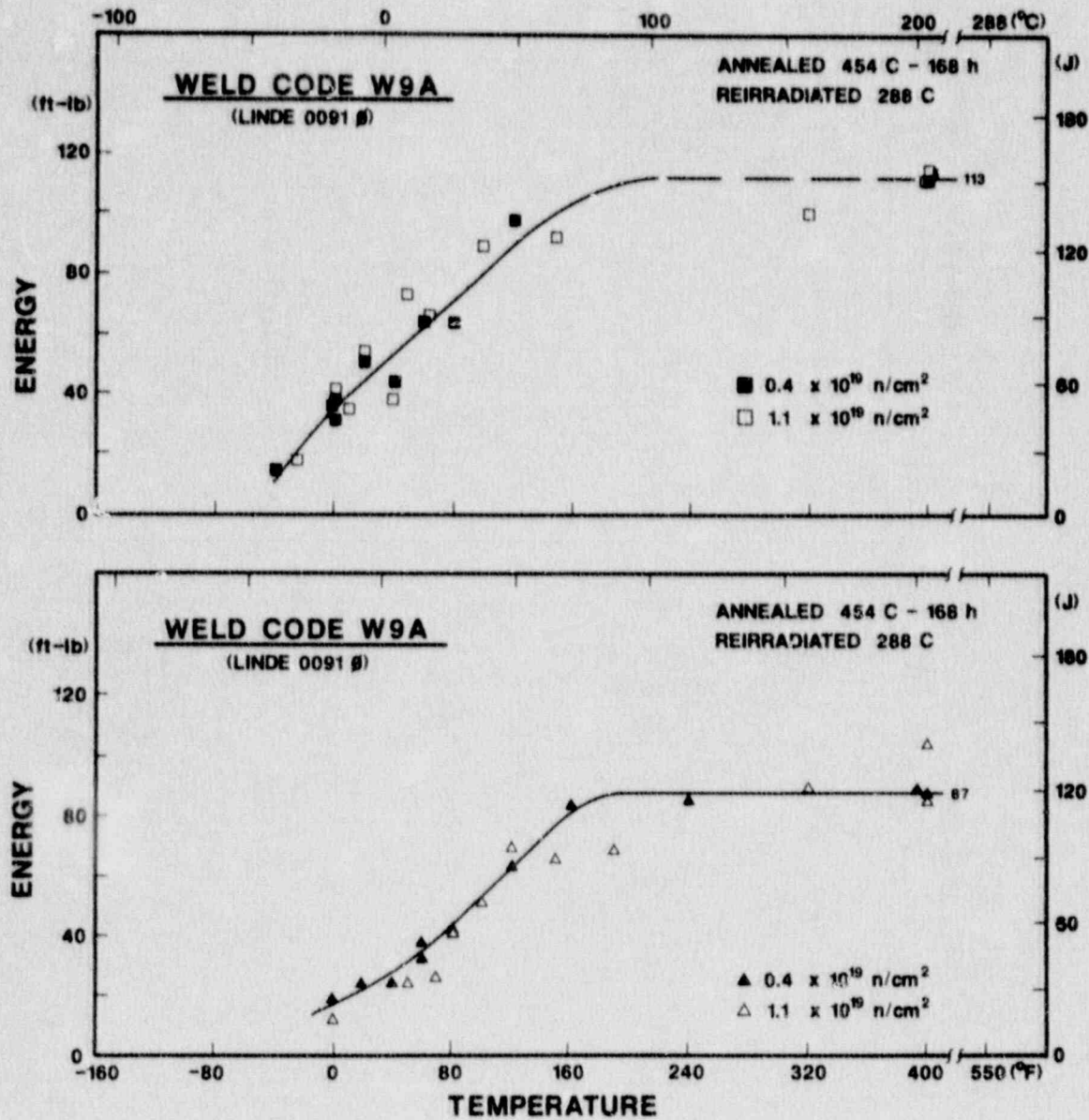


Fig. 24 Experimental test data for IAR Condition 1 and IAR Condition 2 of Weld W9A.

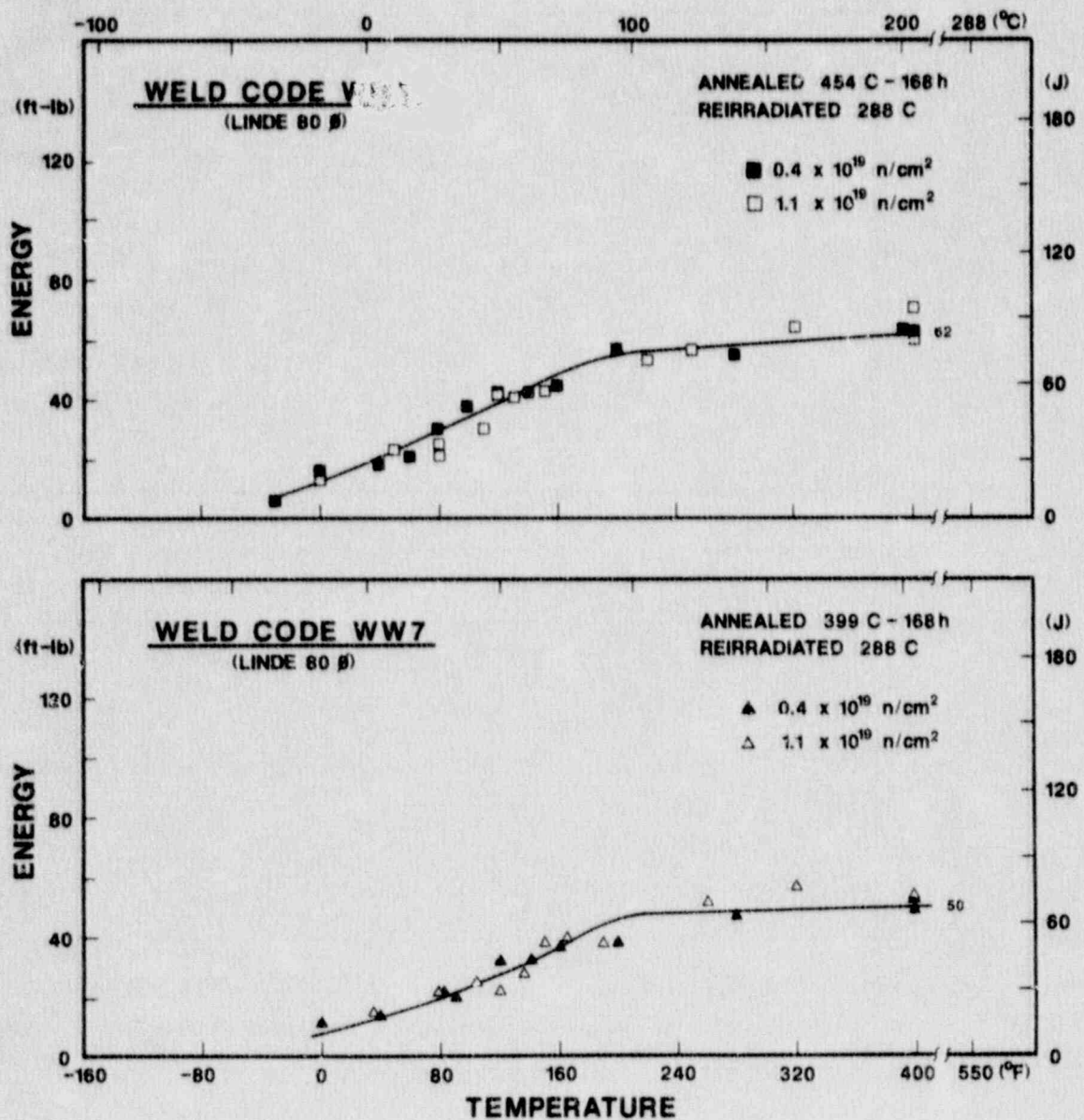


Fig. 25 Experimental test data for IAR Condition 1 and IAR Condition 2 of Weld WW7.

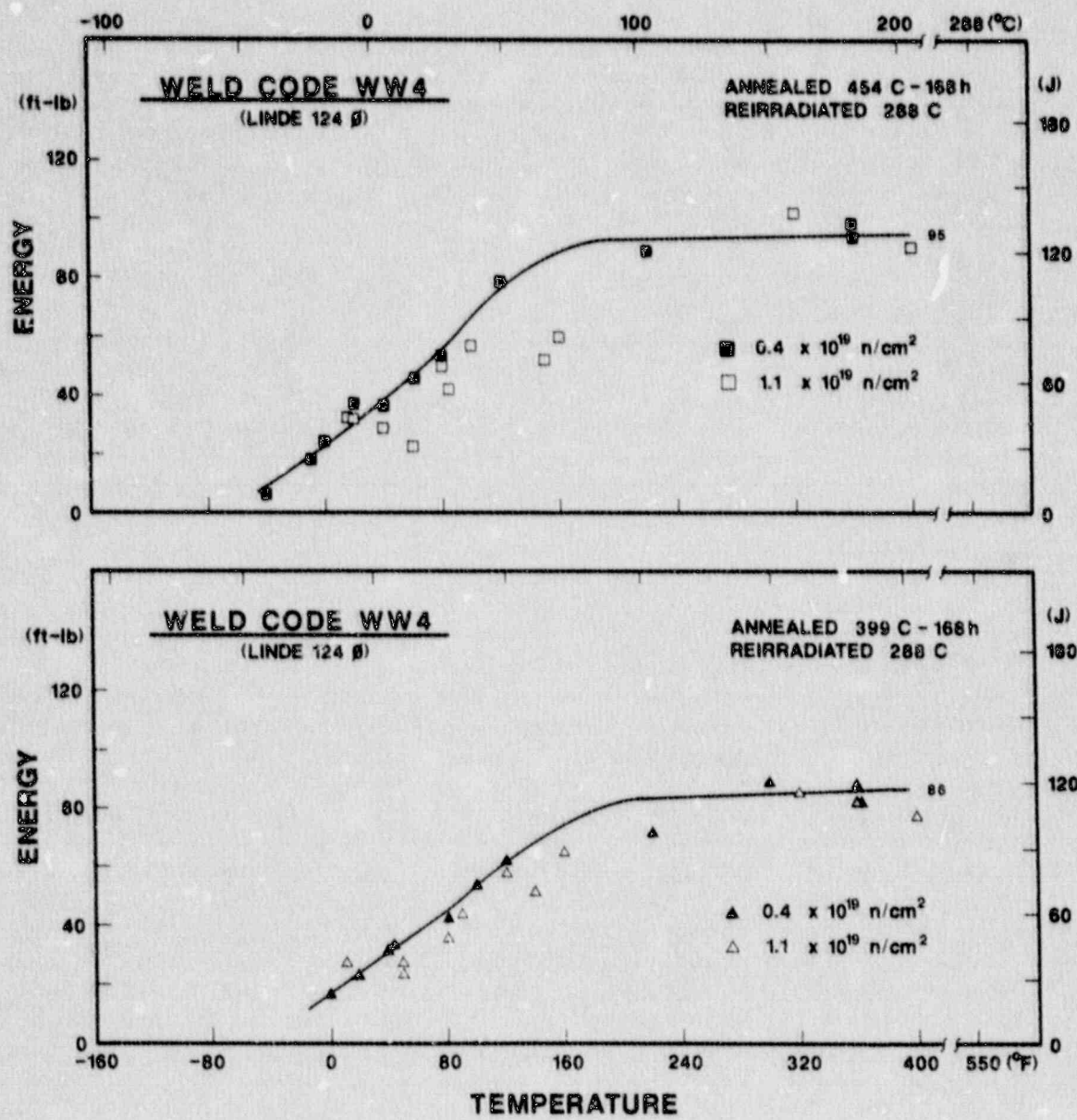


Fig. 26 Experimental test data for IAR Condition 1 and IAR Condition 2 of Weld WW4.

differences in notch ductility between the two IAR conditions are illustrated further in Figures 23 through 26 (compare open symbols vs. filled symbols).

The reembrittlement of the three high copper content welds by the second cycle fluence of $1.1 \times 10^{19} \text{ n/cm}^2$ is less than 50 percent of that observed for an equivalent exposure of virgin material as illustrated in Figure 27. Accordingly, the driving force toward embrittling is less in heat-treated material. The significance of this observation to probable radiation effects mechanisms is discussed in a latter section.

In Figure 22, the total transition temperature elevation with IAR (399°C intermediate annealing) is slightly less than that determined for the first cycle exposure (I₁-Condition). Nonetheless, a significant benefit of the IAR procedure is suggested because of the relative difference in the total fluences. The total transition temperature elevation with IAR (454°C intermediate annealing) is markedly less than that for the first cycle exposure condition (by 30 to 50 percent). Coupled with the material indications of embrittling saturation with IAR, the results do have high significance to further reactor vessel annealing decisions.

Of further interest (Fig. 27), the reembrittlements of the three high copper welds by the second exposure cycle after 399°C intermediate annealing (IAR Condition 2) are identical ($\Delta 39^\circ\text{C}$, $\Delta 70^\circ\text{F}$). For 454°C intermediate annealing, the reembrittlements of the Linde 80 welds (high and low nickel versions) were the same but differ from that of the Linde 0091 weld.

The IAR data for the intermediate copper, high nickel weld (WW4) describe annealing recovery and reembrittlement behavior patterns unlike those of the high copper welds. Full recovery was obtained with both annealing treatments. A comparison of embrittlement produced by the second exposure cycle (IAR Condition 2) vs. that produced in virgin material with a fluence of $1.1 \times 10^{19} \text{ n/cm}^2$ indicates about equal radiation sensitivities (Fig. 27). Unlike the high copper welds, the reembrittlement sensitivity of this weld is relatively independent of the annealing temperature. Its propensity to reirradiation embrittlement after 454°C annealing is somewhat greater than that of the remaining welds. The total transition temperature increase (exposure cycles 1 + 2) was less than that of the high copper welds in the case of 399°C intermediate annealing but was equal to or more than that for the high copper welds for 454°C intermediate annealing. Thus, the pattern of IAR behavior is shown material dependent. Recalling an earlier 288°C irradiation test of Weld WW4 [13], a fluence of $2.2 \times 10^{19} \text{ n/cm}^2$ produced a transition temperature elevation of 97°C (175°F). Thus, the transition temperature elevation of 50°C (90°F) found for IAR-treated material with a fluence of $2.7 \times 10^{19} \text{ n/cm}^2$ still denotes a significant benefit of IAR procedures.

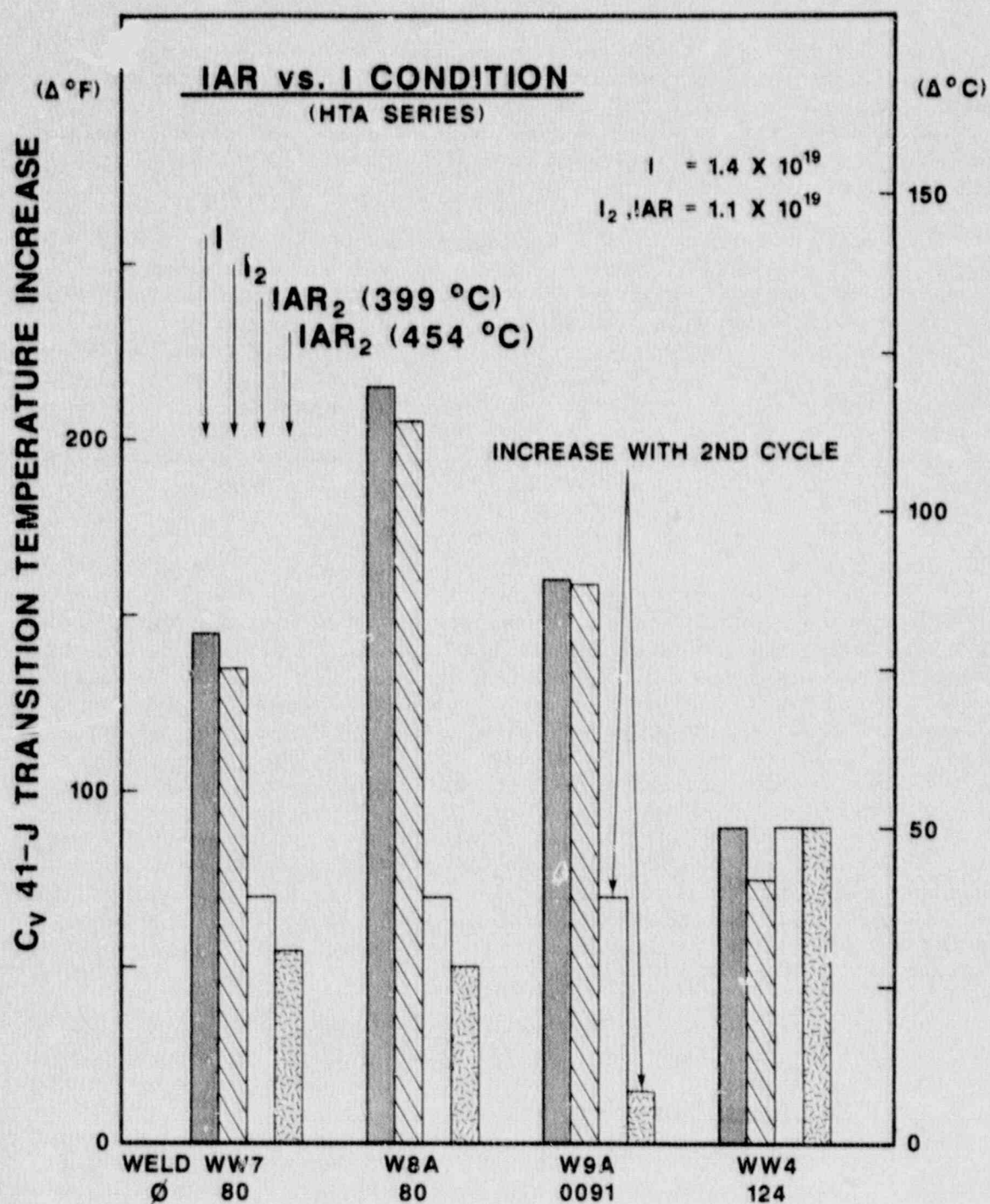


Fig. 27 Notch ductility changes produced by the second exposure cycle vs. changes observed for virgin material at a matching fluence of $1.1 \times 10^{19} \text{ n/cm}^2$. I-condition data for a slightly higher fluence are also shown.

6. TENSION TEST RESULTS

The tension test results are summarized in Table 5. Unirradiated (U) condition strength values are the average of duplicate tests in each case. In general, the changes in yield strength agree with the C_v notch ductility determinations with respect to indications of variable radiation embrittlement sensitivity and variable annealing recovery among the materials.

A superior benefit of 454°C annealing compared to that of 399°C annealing is evident in both IA-condition and IAR-condition results. Referring to the IAR Condition 2 data, the yield strength of each high copper content weld for the 399°C intermediate annealing case is within 5 percent of the yield strength of the I_2 condition. However, with 454°C intermediate annealing, the yield strengths of the welds are no more than 91 percent of the corresponding I_2 condition values. This is not the case for the Weld WW4. Here, the IAR Condition 2 yield strength changes for 454°C and 399°C intermediate annealing cases are about equal to the I_2 Condition strength elevation.

7. DISCUSSION

The experimental results obtained by the investigation, when applied to the experimental issues outlined at the beginning of this report, describe a complex picture for IA- and IAR-behavior. Several metallurgical variables appear to be contributing to each. Subtle effects of welding flux type are also indicated. Tests of additional welds are in order to see if the behavior categories suggested by the present set of data are appropriate to all RPV weldments.

For most but not all of the weldments, a significant difference was observed in 454°C vs. 399°C annealing recovery and in reirradiation embrittlement sensitivity. Because the specimens of the welds were commingled in each assembly, observed behavior differences cannot be attributed to some "variation" in experimental procedure or individual irradiation history.

One interesting aspect is the general difference in the benefits of IAR (454°C annealing) vs. IAR (399°C annealing) procedures found for the high copper content welds vs. the intermediate copper content weld. With the former, a pronounced difference with annealing temperatures of 454°C vs. 399°C was evident for both IAR₁ and IAR₂ Conditions. This is not the case for the intermediate copper weld. This would support arguments for two mechanisms of properties recovery by intermediate annealing.

Referring to the process of radiation damage, it is well recognized that copper causes an enhancement of steel sensitivity to radiation-induced embrittlement at typical RPV service temperatures, and secondly, that nickel (in amounts up to about 0.9 percent), while not contributing independently to radiation damage, causes a

Table 5 Tensile Strengths of Welds in Irradiated, Annealed and Reirradiated Conditions

Weld	Test Condition	Yield Strength				Ultimate Tensile Strength			
		Final		Change		Final		Change	
		(MPa)	(ksi)	(ΔMPa)	(Δksi)	(MPa)	(ksi)	(ΔMPa)	(Δksi)
(Linde 80 φ)	U ^a	498	72.2	-	-	617	89.5	-	-
	I ₂	625	90.6	127	18.4	721	104.6	104	15.1
	IA(399)	568	82.4	57	8.2	678	98.3	43	6.3
	IA(454)	521	75.5	104	15.1	638	92.1	83	12.5
	IAR ₁ (399)	596	86.5	28 ^b (98) ^c	4.1 ^b (14.3) ^c	705	102.3	27 (88)	4.0 (12.8)
	IAR ₂ (399)	623	90.3	55 (125)	7.9 (18.1)	719	104.3	41 (102)	6.0 (14.8)
	IAR ₁ (454)	532	77.2	11 (34)	1.7 (5.0)	649	94.1	14 (32)	2.0 (4.6)
	IAR ₂ (454)	558	80.9	37 (60)	5.4 (8.7)	660	95.7	25 (43)	3.6 (6.2)
(Linde 0091 φ)	U ^a	574	83.3	-	-	656	95.2	-	-
	I ₂	704	102.1	130	18.8	771	111.8	115	16.6
	IA(399)	644	93.4	60	8.7	728	105.6	43	6.2
	IA(454)	581	84.3	123	17.8	681	98.7	90	13.1
	IAR ₁ (399)	665	96.5	21 (91)	3.1 (13.2)	753	109.2	25 (97)	3.6 (14.0)
	IAR ₂ (399)	666	96.6	22 (92)	3.2 (13.3)	756	109.6	26 (99)	4.0 (14.4)
	IAR ₁ (454)	597	86.6	16 (23)	2.3 (3.3)	696	101.0	15 (40)	2.3 (5.8)
	IAR ₂ (454)	613	88.9	32 (39)	4.6 (5.6)	705	102.3	25 (49)	3.5 (7.1)

Table 5 Tensile Strengths of Welds in Irradiated, Annealed and Reirradiated Conditions (cont'd)

Weld	Test	Yield Strength				Ultimate Tensile Strength			
		Condition	Final	Change		Final	Change		
			(MPa)	(ksi)	(ΔMPa)	(Δksi)	(MPa)	(ksi)	(ΔMPa)
WN7 (Linde 80 φ)	U ^a	509	73.8	-	-	612	88.8	-	-
	I ₂	617	89.5	108	15.7	710	103.0	99	14.2
	IA(399)	578	83.8	39	5.7	679	98.5	31	4.5
	IA(454)	531	77.0	86	12.5	639	92.7	71	10.3
	IAR ₁ (399)	603	87.4	25	3.6	698	101.2	19	2.7
	IAR ₂ (399)	60%	87.6	26	3.8	701	101.6	21	3.1
				(95)	(13.8)			(88)	(12.8)
	IAR ₁ (454) ^a	556	80.6	25	3.6	656	95.2	17	2.5
	IAR ₂ (454) ^a	562	81.5	31	4.5	663	96.1	23	3.4
				(53)	(7.7)			(50)	(7.3)
WW4 (Linde 124 φ)	U ^a	479	69.5	-	-	592	85.8	-	-
	I ₂	527	76.5	48	7.0	630	91.4	38	5.6
	IA(399) ^a	480	70.0	47	6.5	593	86.0	37	5.4
	IA(454) ^a	461	66.8	66	9.7	578	83.8	52	7.6
	IAR ₁ (399)	532	77.1	52	7.1	632	91.7	39	5.7
	IAR ₂ (399)	543	78.7	60	8.7	643	93.2	50	7.2
				(63)	(9.2)			(51)	(7.4)
	IAR ₁ (454) ^a	505	73.3	44	6.5	608	88.1	30	4.3
	IAR ₂ (454) ^a	523	75.9	63	9.1	523	90.3	45	6.5
				(44)	(6.4)			(31)	(4.5)

^a Average of duplicate tests^b Increase by second exposure cycle^c Total increase over U-condition

reinforcement of the copper content contribution to radiation sensitivity. Interactions between other alloying elements (Mn, Mo) and copper impurities have also been demonstrated experimentally by MEA [19]. When the copper content is low, a significant detrimental influence of phosphorus on radiation resistance at 288°C can also be expected. The level of the phosphorus contribution is inversely dependent on the level of copper content [19].

Mechanistically, it is generally accepted that a radiation-induced copper precipitation is responsible for the observed elevation of embrittlement sensitivity in plate and weld materials. Studies by a joint MEA-Oak Ridge National Laboratory-University of Florida undertaking have established that a precipitation and hardening mechanism likewise is responsible for the phosphorus contribution [20,21]. Small Angle Neutron Scattering (SANS) tests have helped reveal further that the "copper precipitate" is in fact a copper-rich precipitate also containing the elements manganese and nickel in significant proportions [22]. Whether or not the chemistry of the copper-rich precipitates is a fixed stoichiometric ratio or conversely, varies in proportion to weld metal composition, has yet to be determined.

The two mechanisms of properties recovery which appear to be operating are (1) the overaging of the copper-rich precipitate (Ostwald ripening) and (2) re-solution of copper. The overaging of precipitates has been observed in SANS [22]; the potential for dissolution is under investigation. If assumed to be proceeding jointly during heat treatment, the two mechanisms could explain the IAR trends and material variability observed here. In the case of the high copper welds, the overaging mechanism would be predominant and the growth of precipitates would occur more rapidly at 454°C than 399°C. In turn, the ripening process would effectively remove copper from taking part in the reembrittlement process upon reirradiation. Reembrittlement sensitivity would be expected to be less with the 454°C intermediate anneal. In the case of the intermediate copper (0.16% Cu) weld, the amount of copper tied up by precipitation would be much less. Dissolution could account for the observed cycling of embrittlement between two levels (the irradiation or reirradiation level vs. the annealed level) for the fluence increment of about $1 \times 10^{19} \text{ n/cm}^2$, independent of the anneal temperature. That is, the driving force for reembrittlement of annealed material remains as great as that for the embrittlement of virgin material. A key to this behavior is the essentially full notch ductility recovery obtained with the intermediate anneal. A significant benefit of IAR procedures, nonetheless, is described for intermediate copper content material compared to material irradiated without annealing as shown by the Weld WW4.

8. CONCLUSIONS

- IAR procedures can be very effective for controlling total radiation-induced property changes of weld deposits in 288°C pressure vessel service. The data for two IAR fluence conditions suggest a trend toward radiation embrittlement saturation at a level lower than the embrittlement level reached prior to annealing.
- A 454°C-168 hour intermediate anneal is much more effective than a 399°C-1f8 hour intermediate anneal, in terms of residual embrittlement after the anneal and in terms of sensitivity to reembrittlement by reirradiation, for welds having a high copper content but not for welds having an intermediate copper content.
- Large differences in notch ductility and yield strength recovery by postirradiation annealing are evident among the welds investigated and can be attributed to copper content, nickel content and composition differences traceable to welding flux types.
- Two mechanisms appear to be responsible for properties recovery by annealing and subsequent reirradiation behavior: overaging of the copper-rich precipitates and dissolution of copper.

REFERENCES

1. "Fracture Toughness Requirements for Light-Water Nuclear Power Reactors," Appendix G, Federal Register, Rules and Regulations, Vol. 48 (104), May 27, 1983, pp. 24008-24011.
2. Hawthorne, J. R., "Survey of Postirradiation Heat Treatment as a Means to Mitigate Radiation Embrittlement of Reactor Vessel Steels," Proceedings of the IAEA Specialists' Meeting on Analysis of Behavior of Advanced Reactor Pressure Vessel Steels Under Neutron Irradiation, International Atomic Energy Agency, Vienna, Austria, 1-2 March, 1979.
3. U. S. Nuclear Regulatory Commission Research Information Letter No. 76, "Annealing of Irradiated Reactor Pressure Vessels", December 28, 1979.
4. Potapovs, U., Knighton, G. W. and Denton, A. S., "Critique of In-Place Annealing of SM-1A Nuclear Reactor Vessel," Nuclear Engineering Design, Vol. 8, 1968, pp. 39-57.
5. Fabry, A., et al., "Annealing of the BR3 Reactor Pressure Vessel," in Proceedings of the U. S. Nuclear Regulatory Commission Twelfth Water Reactor Safety Research Information Meeting, Oct. 22-26, 1984, USNRC Conference Proceeding NUREG/CP-0058, Vol. 4, 1984.
6. Server, W.L., "In-Place Thermal Annealing of Nuclear Reactor Pressure Vessels," USNRC, Report NUREG/CR-4212, April 1985.
7. Rishel, R.D., "Development of Generic Procedures for Thermal Annealing an Embrittled Reactor Vessel Using a Dry Anneal Method," EPRI RP 1021-1, Topical Report Electric Power Research Institute, March 1982.
8. Hawthorne, J. R., Watson, H. E. and Loss, F. J., "Experimental Investigation of Multicycle Irradiation and Annealing Effects on Notch Ductility of A 533-B Weld Deposits," Effects of Radiation on Materials: Tenth Conference, ASTM STP 725. D. Kramer, H. R. Brager, and J. S. Perrin, Eds., Am. Soc. for Testing and Materials, 1981, pp. 63-75.
9. Loss, F. J., Menke, B. H., Gray, R. A., Jr., Hawthorne, J. R. and Watson, H. E., "J-R Curve Characterization of A 533-B Weld Metal with Irradiation and Postirradiation Annealing," Effects of Radiation on Materials: Tenth Conference, ASTM STP 725. D. Kramer, H. R. Brager and J. S. Perrin, Eds. Am. Soc. for Testing and Materials, 1981, pp. 76-91.

10. Lott, R. G., Mager, T. R., Shogan, R. P., and Yanichko, S. E., "Annealing and Reirradiation Response of Irradiated Pressure Vessel Steels," Radiation Embrittlement of Nuclear Reactor Pressure Vessel Steels: An International Review, ASTM STP 909, L. E. Steele, Ed., Am. Soc. for Testing and Materials, 1986, pp. 242-259.
11. Hawthorne, J. R., "Significance of Nickel and Copper Content to Radiation Sensitivity and Postirradiation Heat Treatment Recovery of Reactor Vessel Steels," Effects of Radiation on Materials, ASTM STP 782, Am. Soc. for Testing and Materials, 1982, pp. 375-391.
12. Hawthorne, J. R., Koziol, J. J. and Groeschel, R. C., "Evaluation of Commercial Production A 533-B Plates and Weld Deposits Tailored for Improved Radiation Resistance," Properties of Reactor Structural Alloys After Neutron or Particle Irradiation, ASTM STP 570, Am. Soc. for Testing and Materials, 1975, pp. 83-102.
13. "Evaluation and Prediction of Neutron Embrittlement in Reactor Pressure Vessel Materials," EPRI NP-2782, Research Project 886-2, Final Report, J. R. Hawthorne, Ed., Electric Power Research Institute, Dec. 1982.
14. "Feasibility and Methodology for Thermal Annealing an Embrittled Reactor Vessel," EPRI NP-2712, Vol. 2, Research Project 1021-1, Final Report, T. R. Mager, Ed., Electric Power Research Institute, Nov. 1982.
15. Lippincott, E. P., "Buffalo Light Water Reactor Calculation," Letter Communication Serial No. 7754977, Harford Engineering Development Laboratory, Richland, WA to J.R. Hawthorne dated November 16, 1977.
16. Lippincott, E. P., Kellogg, L. S., Matsumoto, W. Y., McElroy, W. N., and Baldwin, C. A., "Evaluation of Neutron Exposure Conditions for the Buffalo Reactor," Proc. 5th International ASTM-Euratom Symposium on Reactor Dosimetry, Geesthacht, Federal Republic of Germany, Sept. 24-28, 1984
17. G. Prillinger, E.D. McGarry, and J.R. Hawthorne, "Neutron Spectrum Calculations for Ex-Core Irradiation Experiments at the Buffalo Reactor," presented at the ASTM Fourteenth International Symposium on Effects of Radiation on Material, Andover, MA, June 1988.
18. Hawthorne, J. R., "Steel Impurity Element Effects on Postirradiation Properties Recovery By Annealing," Influence of Radiation on Material Properties: 13th International Symposium (Part II), ASTM STP 956, F. A. Garner, C. H. Henager and N. Igata, Eds., Am. Soc. for Testing and Materials, 1987, pp. 461-479.

19. Hawthorne, J. R., An Exploratory Study of Element Interactions and Composition Dependencies in Radiation Sensitivity Development: Final Report, USNRC, Report NUREG/CR-5357, April 1989.
20. Hawthorne, J. R., "Mechanisms of Irradiation Damage for Reactor Vessel Steels, in Structural Integrity of Water Reactor Pressure Boundary Components, Annual Report for 1986, F. J. Loss, Ed., USNRC, Report, NUREG/CR-3228, Vol. 5, July 1987, pp. 183-189.
21. Miller, M. K., Hoelzer, D. T., Ebrahimi, F., Hawthorne, J. R., and Burke, M. G., "Microstructural Characterization of Irradiated Fe-Cu-P Model Steels," Proc. 3rd International Symposium on Environmental Degradation of Materials in Nuclear Power Systems -Water Reactors," Traverse City, MI, Aug. 30 - Sept. 3, 1987, The Metallurgical Society, Inc., 1988, pp. 133-140.
22. Beaven, P. A., Frisius, F., Kampmann, R., Wagner, R., and Hawthorne, J. R., "SANS Investigation of Irradiated A 533-B Steels Doped with Phosphorus," in Radiation Embrittlement of Nuclear Reactor Pressure Vessel Steels: An International Review, 3rd Volume, L.E. Steele, Ed., American Society for Testing and Materials, ASTM STP 1011, 1989, pp. 243-256.

APPENDIX A

Fabrication of Weldments: Materials and Procedures

Fabrication of Weldments W8A and W9A

1. General

The weldments were produced commercially by Lukens Steel Company under contract. The welds were made using buyer-supplied 210-mm (8.25-in.) thick A 533 Grade B Class 1 plate and contractor-supplied welding fluxes and filler wire. The filler wire was copper-coated by other subcontractors to the buyer (see Section 4, below). The purchase specifications for the plate are given in Attachment 1; the mill test report is given as Attachment 2. The purchase specifications for the set of Linde 80 welds which included Weld W8A are given in Attachment 3; the same specifications except for welding flux type were used for the Linde 0091 Weld, W9A.

The same lot of weld filler wire was used for both welds. The wire was made from Steel Melt 3P8393. The filler wire composition before copper coating as determined by Airco Welding Products is given in Attachment 4. The weld joint design is shown in Figure A-1.

2. Fabrication of Weld W8A

The Lukens Steel Company report documenting fabrication details for Weld W8A is given as Attachment 5. No particular problems were encountered in the production of this weld.

The post welding stress relief anneal (SRA) of 621°C (1150°F) for 24 hours was performed by the buyer after weld receipt, using a recirculating air furnace. Workpiece temperatures were monitored using chromel-alumel thermocouples attached to the weldment at several locations. Cooling rates after the SRA were less than 6°C (100°F) hour.

3. Fabrication of Weld W9A

The Lukens Steel Company report documenting fabrication details for Weld W9A is given as Attachment 6. No particular problems were encountered in the production of this weld.

The post welding SRA of 621°C (1150°F) for 24 hours was performed by the buyer after weld receipt using the same furnace and procedures employed for Weld W8A (above).

4. Special Note on Copper Coating of Filler Wire

Copper-coated Hi Mn-Mo-Ni filler wire was no longer available at the time this project commenced. The acquisition of wire that was prototypic of the copper-coated wire used in early vessel construction proved very difficult and time-consuming.

The first subcontractor, Airco Welding Products, resurrected equipment from storage and after considerable effort, was only able to provide one-half of the total wire lot in an acceptable coated condition. The remainder of the wire lot either did not have the required coating thickness or had a poorly adherent coating which easily flaked off in the welder wire feed apparatus.

The second subcontractor, Techalloy Maryland, Inc. reprocessed the remainder of the wire successfully but with difficulties stemming from two sources. One difficulty was the attainment of sufficient coating thickness without a flaking propensity. The second difficulty was the ready determination of "as-deposited" copper content without production of an actual weld. Trial weld pads provided inconsistent copper content results; the production of "button melts" for spectrographic determinations gave highly misleading results. In the case of the latter, it was subsequently determined that the cross sections of the melts were highly inhomogeneous with regard to copper content. Ultimately, the problem of copper content determinations for the clad wire was solved by resorting to wet chemistry determinations. Each coil produced was checked at the start-end and at the finish-end. Because of the extreme difficulties encountered in the production of copper-clad wire yielding uniform as-deposited copper contents in the range of 0.30% Cu or higher, it is recommended for any future efforts of this type, that close attention be given to all details in the production of such wire and its usage.

BASE PLATE PURCHASE SPECIFICATIONS

1. Melt/Chemical Composition

Lukens Steel Company Melt No. D-2819 representing electric furnace, vacuum degassed melting practice will be the source melt for the ASTM A 533 Grade B plates. The copper content will be in the range of 0.20% to 0.26% Cu; the nickel content will be in the range of 0.60% to 0.65% Ni.

2. Dimensions of Plate Sections

Thickness: 210-mm (8.25-in.)
Width: 406-mm (16-in.)
Length: 1829-mm (72-in.)^a

^a Length direction to be parallel to primary plate rolling direction.

3. Heat Treatment

The as-rolled plate will be heat treated by water quenching and tempering using Lukens procedures for A 533-B Class 1 plate. For the austenitizing treatment and the tempering treatment, the plate will be held at temperature for a minimum of 0.5 hour per inch of thickness.

4. Mechanical Property Tests

Tensile tests will be conducted to verify A 533-B Class 1 strength properties. A drop weight NDT temperature of -1°C (30°F) will be guaranteed.

5. Non-destructive Tests

Ultrasonic examinations will be conducted to determine if the plate is sonically sound and in compliance with ASME Paragraph NB 2532-1.

6. Stress Relief Anneal

Test specimens (only) will be stress relief annealed for 40 hours at 621°C (1150°F) \pm 14°C (25°F) prior to testing.

7. Report

One (1) certified copy of reports from destructive and non-destructive test examinations and the verification of the source of the plate (melt number) is required.

PURCHASER:

LUKENS STEEL COMPANY

COATESVILLE, PA. 19320

TEST CERTIFICATE

DATE: 5-15-79
CONSIGNEE:

FILE NO. 3195-01-01

MILL ORDER NO.	CUSTOMER P.O.	MP
66743 1	10-20-78	61179 BT 5/1

THIS MATERIAL HAS BEEN MANUFACTURED AND TESTED IN ACCORDANCE WITH PURCHASE ORDER REQUIREMENTS AND SPECIFICATION(S).

A-533-76 CL.1 TYPE-B

BEND TEST

HOMOGENEITY TEST

CHEMICAL ANALYSIS

MELT NO.	C	MN	P	S	CU	SI	Ni	Cr	MO	V	Ti	XAK	XXX		BASIC PROCESS
D2819	.22	1.40	.010	.008	.20	.19	.63		.54			VIP STEEL			ELEC.

PHYSICAL PROPERTIES

MELT NO.	SLAB. NO.	TENS PSI X100	TENS PSI X100	% REDG. IN 2"	% R.A.	BHN	IMPACTS	DESCRIPTION
D2819	6	701	940	24				8-1/4" X 12 X 18
		782	970	22				
LONG. N.D.T.	DROP WEIGHT TESTS IS +20°F. OR BELOW.				TESTS PER E208(SIZE P3)	0 +30°F.	EXHIBIT NO BREAK.	

PLATE AND TESTS HEATED 1625°F./1675°F. HELD 1/2 HR. PER INCH MIN. AND WATER QUENCHED, THEN TEMPERED 1220°F. HELD 1/2 HR. PER INCH MIN. AND WATER QUENCHED.

TESTS STRESS RELIEVED BY HEATING TO 1100°F./1175°F. HELD 40 HRS. AND FURNACE COOLED TO 600°F.

We hereby certify the above information is correct.

SUPERVISOR SIGNATURE

H. A. Kline

Attachment No. 3

WELDMENT PURCHASE SPECIFICATIONS

1. Submerged Arc Weld Using Linde 80 Welding Flux

Electrode diameter : 3.18-mm (1/8-in.)

Welding flux type : Linde 80 (20x200, Baked) (one lot only)

Welding process : Submerged arc using single electrode

Filler type : High Mn-Mo-Ni (one melt only)

Electrode connection : AC

Welding voltage : 30-35V, AC

Welding current : 500-575A

Travel speed : 254-305 mm ppm (10-12 ipm)

Heat input : 80 Kilojoules/in. (minimum)
95 Kilojoules/in. (maximum)

Weld joint : Offset double vee, 134-mm 5.25-in.) deep
from one side and with 5 deg. bevel and
25.4-mm (1-in) minimum gap by mild steel
spacer. Spacer to be back gouged and
refilled with weld metal.

Weld joint gap : 25.4-mm (1-in.) minimum

Weld configuration : Full thickness weld; weld crowns will not
be removed by contractor.

Preheat temperature : 121°C (250°F) minimum, 205°C (400°F)
maximum, 149°C (300°F) aim

Interpass temperature : 121°C (250°F) minimum, 260°C (500°F)
maximum

Restraint : Full

Postweld stress relief : 538°C (1000°F) maximum for 4 h, followed
by slow cooling

Inspection : Radiograph to acceptance standards of
ASME Section III (NB 5320).

Weld deposit composition (wt-%)	Element	Minimum	Maximum	Aim
	Copper	0.31	0.39	0.35
	Nickel	0.60	0.80	0.70
Filler wire composition (wt-%)	Element	Minimum	Maximum	
	Carbon	0.14	0.19	
	Manganese	1.80	2.10	
	Phosphorus	-	0.010	
	Sulfur	-	0.015	
	Silicon	-	0.10	
	Nickel	0.60	0.85	
	Molybdenum	0.45	0.60	
Repairs	None allowed			
Documentation and report	Bead-by-bead record of welding conditions and materials will be furnished together with full descriptions of filler/flux qualifications.			

Attachment No. 4

Composition of Filler Wire for Fabricating Weld W8A and Weld W9A

(Before Copper Coating; Steel Melt 3P8393)

Element	Content (wt-%) ^a
Carbon	0.135
Manganese	1.98
Phosphorus	0.007
Sulfur	0.011
Silicon	0.053
Nickel	0.602
Chromium	0.110
Molybdenum	0.488
Tungsten	0.012
Niobium	0.000 ^b
Vanadium	0.000 ^b
Copper	0.044
Cobalt	0.013
Aluminum	0.007
Titanium	0.002
Zirconium	0.004
Tantalum	0.004
Tin	0.004
Boron	0.000 ^a

^a Determinations by Airco Welding Products (1981).

^b Content below detection limit.

Submerged-Arc Weld in 8-1/4" Gage,
A533 Grade B Class 1 Plate

Item 1- Base Plates #1 and #2

CONTRACT NO. N00173-79-C-0218

LUKENS STEEL COMPANY
Research Service Group
Coatesville, PA 19320
March, 1982

<u>INDEX</u>	<u>Page</u>
Purpose	1
Materials	2
Certificate of Acceptance (flux)	3,4
Weld Preparation	5
Weld Procedure	6
Bead-by-Bead Record	7
Post-Weld Heating	8
Preparation for Radiography	9
Eilt Evaluations	9
Radiography Interpretation	10

Materials

Buyer furnished the following base materials and wire for completion of the contract:

- (A) 12 pieces - A533-B Class 1

Approximately 8-1/4" x 15" x 72" with machined bevel on one edge. Problems occurred with the spacer-bar procedure, therefore the bevels were remachined at Lukens to an unbalanced double J preparation. This will be performed on each piece.

Pieces are numbered consecutively, #1 through #12 and each pair will follow in sequence regardless of type of flux employed.

- (B) 1/8" dia. copper-coated High Mn-Mo-Ni wire -

Approximately 3000 lbs. all from one heat. Since attempts by Techalloy Raco to rewind the wire from the wooden spools to 12" dia. - 60 lb. coils resulted in flaking-off of the copper-coating, a holder for the wooden spools was improvised. Some flaking of copper was also noted on the spooled wire.

- (C) Linde 80 and Linde 0091 fluxes will be used in the six weldments, three welds with each flux.

There were 3000 lbs. of each purchased by Lukens Steel Co. and each type was from the same lot and control. All fluxes were baked in pans at 800°F., held 1 hour, furnace-cooled to 300°F., then air-cooled to ambient temperature to minimize moisture content.

The Certificate of Acceptance Inspection forms are presented on the next two pages.

LINDE DIVISION
P.O. Box 747, Niagara Falls, New York 14302

Pg. 3

CERTIFICATE OF ACCEPTANCE INSPECTION

Shipped to: Lukens Steel Company
Central Stores
Coatesville, PA 19320

Shipper's No.: 024552 A
Quantity Shipped: 3,000 Lbs.
Date Shipped: 6/16/81

Your Order No.: 4543-P

REPORT OF TESTS OF GRADE 80 UNIONMELT WELDING COMPOSITION

Identification of Material Tested - Grade 80, Size 20x200,
Lot 0418, Control 8556.

This certifies that the Welding Composition Identified above has been tested
for conforming to specifications as follows:

Sizing: 20 Mesh Minus 200 Mesh

<u>1.7%</u>	<u>0.4%</u>
<u>5.0%</u>	<u>3.5%</u>

Uniformity: SiO₂ CaO Al₂O₃

<u>37.85%</u>	<u>20.96%</u>	<u>15.47%</u>
<u>32.4-39.6%</u>	<u>19.8-24.2%</u>	<u>12.4-18.6%</u>

Lower line gives specification limits - single values are maximum.

State of New York
County of Niagara

Sworn to before me this

17 day of June, 1981

Deborah L. Cooke

DEBORAH L. COOKE
Notary Public, State of N.Y., New York
Qualified in Niagara County
My Commission Expires March 31, 1982

83

Theresa
Consumables Quality - Electric Welding

UNION CARBIDE CORPORATION
LINDE DIVISION
P.O. Box 747, Niagara Falls, New York 14302

Pg. 4

CERTIFICATE OF ACCEPTANCE INSPECTION

Shipped to: Lukens Steel Company
Central Stores -
Coatesville, PA 19320

Shipper's No.: 024552 A
Quantity Shipped: 3,000 Lbs.
Date Shipped: 6/16/81

Your Order No.: 4543-P

REPORT OF TESTS OF GRADE 0091 UNIONMELT WELDING COMPOSITION

Identification of Material Tested - Grade 0091, Size 65x200,
Lot 0204, Control 3756.

This certifies that the Welding Composition identified above has been tested
for conforming to specifications as follows:

Sizing: 32 Mesh 48 Mesh Minus 200 Mesh

0.4% 24.2% 15.0%
5% 40% 10-20%

Uniformity: 810 - 640 - —

38.01% 44.40%
34-40% 43-49% —

Lower line gives specification limits - single values are maximum.

State of New York
County of Niagara

Sworn to before me this

17 day of June, 1981

Robert L. Cooke

ROBERT L. COOKE
100 Franklin Street, New York
Lived in Niagara County
, Commenced to practice March 30, 1983

M. Blawie
Consumables Quality - Electric Welding

Preparation for Welding

Base plates were grit-blasted prior to re-machining of the bevels. The pair of base plates to be used in each weldment were aligned on edge so the 1/2" lands would be aligned, making the fit-up of each weldment simpler and at the same time compensating for the slight out-of-flatness of the plates.

Two lifting lugs were welded to the long edge (72" dimension) of one plate of the pair to facilitate the turning-over of the weldment several times during the fabrication of the test.

Since the lugs were always kept at the back side of the test, the start end and finish end of the passes were reversed with each turn.

The start end and finish end, however, were standardized for orientation purposes as being those on the face side.

Run-out tabs were welded at start end and finish end on the deepest side (face side), six (6) passes deposited, then the weldment turned over, moved to cutting table, arc-air'd from root side to sound metal and ground, then set-up and aligned on welding table (root side up), and at this point the run-outs were welded at both ends of the weld test on the root side.

A 1/2" thick carbon steel plate was employed in the run-outs as an extension of the 1/2" land. Upon arc-airing of the root side, only a small distance (1/2" to 1") was arc-air'd in the 1/2" plate. This was reflected in the junction chemical analysis for copper and nickel in the run-outs due to dilution with the mild steel.

Welding ProcedureItem 1 - Base Plates 1 & 2 Linde 80 (Baked)

Preheat 300°F. - Interpass 325°F. - Heat Input 85,000 Joules/Inch

<u>Pass #</u>	<u>(AC)</u>	<u>Amps</u>	<u>Volts</u>	<u>Speed(ipm)</u>	<u>Start Copper and Spool No.</u>	<u>Wire Consumed (lbs.)</u>
1		500	33	16	.39	14
2		500	33	11		
3 to 6		500	34	12		
Turn - Arc-Air 1/2" deep - Grind						
7		500	34	16		
8		500	34	14		
9 to 14		500	34	12		
Turn						
15 to 22		500	34	12		
Turn						
23 to 33		500	34	12	.33	13 (thru pass #27) 53
Turn						
34 to 66		500	34	12	.44 .42 chk. 15 15	63 (thru pass #62)
Turn						
67 to 101		500	34	12	:37 :33 end 15 16	64 (thru pass #99)
102		500	34	16		
Turn						
103 to 140		500	34	12	.35 17	65 (thru pass #135) 8 (thru pass #140)
Total = 253 Lbs.						

1 Defect - Face side, pass #138, lack of fusion with bevel, 2-1/4" from start end - 7/8" long, approximately 1/8" deep.

Base Plates 1 and 2.
 Spool or Coil 14, 13, 15, 16, 17
 Wire Consumed 253 lbs.

Item 1
 Flux Linde 80

Ht. Input 85,000 J/m.

Sfe.	Cu	Ni	Cu	Ni
Start Run-out	* 1 .43	.69		
			140	145
			135	137
			130	135
			129	131
			127	128
			125	127
			121	123
			119	119
			115	116
			112	113
			109	110
			106	107
			105	106
			103	104
1/4L	* 3 .43	.69	64	65
			61	62
			58	59
			55	56
			52	53
	* 4 .40	.66	49	50
			46	47
			44	45
			42	43
			40	41
CL	* 5 .43	.68	37	38
			34	35
			32	33
			30	31
Junction	* 6 .41	.56	27	28
			24	25
			22	23
			20	21
			18	19
1/4L	* 7 .43	.68	15	16
			12	13
			10	11
			7	8
			5	6
			3	4
			1	2
			7	8
			10	11
			13	14
			16	17
			19	20
			22	23
			25	26
			28	29
			31	32
			34	35
			37	38
			40	41
			43	44
			46	47
			49	50
			52	53
			55	56
			58	59
			61	62
			64	65
			67	68
			70	71
			73	74
			76	77
			79	80
			82	83
			85	86
			88	89
			91	92
			94	95
			97	98
			100	101
Root Side	* 9 .40	.65	102	103

Post-Weld Heating

Upon completion of the welding, the weldment was draped with asbestos blankets and maintained at 375° F. for 24 hours. The heat was then turned off and the asbestos blanket was kept on the surface of the weldment which slowly cooled to ambient temperature (approx. 70° F.).

Run-Outs

Both start end and finish end (based on face side) run-outs were band-saw cut off and identified by stamping as follows: start, surface, root, and base plate numbers.

A 1/2" thick x 1-1/4" wide x full weld thickness section was saw-cut and ground in preparation for spectrographic checks of nickel and copper throughout the total weld metal, surface to surface, adjacent to the main weld.

The results of these analyses are contained in the bead-by-bead record.

The remainder of each identified run-out was sent to the attention of Mr. R. Hawthorne.

Preparation for Radiography

The two lifting lugs were removed by flame-cutting and the weldment was shipped to the Birdsboro Corporation for radiography per ASME Section V, Article 2, NB5000.

Upon completion, the films were sent to Lukens Steel Company for evaluation and interpretation by the Inspection personnel.

The weldment was held at Birdsboro until the evaluation of the films was determined to be of satisfactory quality. The weldment was then shipped.

The reinforcement varied from essentially none to 1/8" maximum on both the face and root sides.

Film Interpretation

The films were interpreted by Level II personnel. The non-fused area at the top surface (pass #138) was noted at Position V1-V2 and a small crack-like indication noted at Position V5-V6. A copy of the interpretation is presented on the next page.

The films were sent to Mr. Russ Hawthorne.

LUKENS STEEL COMPANY
RADIOGRAPHY INTERPRETATION

A - ACCEPTABLE
R - REJECTED
T - RETAKE

INTERPRETATION

Earlston L V II

Submerged-Arc Weld in 8-1/4" Gage
'A533 Grade B Class 1 Plate'

Item 2 - Base Plates #5 and #6

CONTRACT NO. N00173-79-C-0218

LUKENS STEEL COMPANY
Research Service Group
June, 1982

UNION CARBIDE CORPORATION
LINDE DIVISION
P.O. Box 747, Niagara Falls, New York 14302

CERTIFICATE OF ACCEPTANCE INSPECTION

Shipped to: Lukens Steel Company
Central Stores
Coatesville, PA 19320

Shipper's No.: 024552 A
Quantity Shipped: 3,000 Lbs.
Date Shipped: 6/16/81

Your Order No.: 4543-P

REPORT OF TESTS OF GRADE 0091 UNIONMELT WELDING COMPOSITION

Identification of Material Tested - Grade 0091, Size 65x200,
Lot 0204, Control 3756.

This certifies that the Welding Composition identified above has been tested
for conforming to specifications as follows:

Sizing: 32 Mesh 48 Mesh Minus 200 Mesh

<u>0.4%</u>	<u>24.2%</u>	<u>5.0%</u>
<u>5%</u>	<u>40%</u>	<u>10-20%</u>

Uniformity: SiO₂ CaO

<u>38.01%</u>	<u>44.40%</u>	<u> </u>
<u>34-40%</u>	<u>43-49%</u>	<u> </u>

Lower line gives specification limits - single values are maximum.

State of New York
County of Niagara

Sworn to before me this

17 day of June, 1981

Donald L. Cooke

DONALD L. COOKE
New York
State of New York
Accomplished March 30, 1983

M. Blaney
Consumables Quality - Electric Welding

Welding Procedure

Item 2 - Base Plates 5 & 6 - Linde 009' (Baked)

Preheat 300°F. - Interpass 325°F. - Heat Input 93,500 Joules/Inch

<u>Pass #</u>	(AC)		<u>Volts</u>	<u>Speed(ipm)</u>	<u>Copper</u>	<u>Spool #</u>	<u>Wire Consumed (lbs.)</u>
1	550	34		15	.34	10	
2 to 6	550	34		12			

Turn - Arc-Air - Grind - 7/16" deep

7	550	34	15
8 to 26	550	34	12

Turn

27 to 43	550	34	12	(thru pass 43) 59
----------	-----	----	----	----------------------

Turn

44 to 49	550	34	12	.39	11
----------	-----	----	----	-----	----

Turn

50 to 82	550	34	12
----------	-----	----	----

Turn

83 to 91	550	34	12	(thru pass 93) 69
92 & 93	550	34	10	

Total Wire = 128 Lbs.

Base Plates 5 and 6.

Spool or Coil 10 & 11

Wire Consumed 128 lbs.

Sub-size Item 2

Flux 0091

Ht. Input 93500 J/in

Sfe.

Cu .35
Ni .60

Start
Run-out

Cu .39
Ni .62

Finish
Run-out

* .36
.63

.36
.62

1/4L * .40
.65

.39
.62

* .36
.65

.38
.63

CL * .34
.58

.37
.61

Junction * .28
.26

.28
.44

1/4L * .39
.64

.37
.62

* .37
.61

.41
.64

Root Side * .40
.62

.41
.63

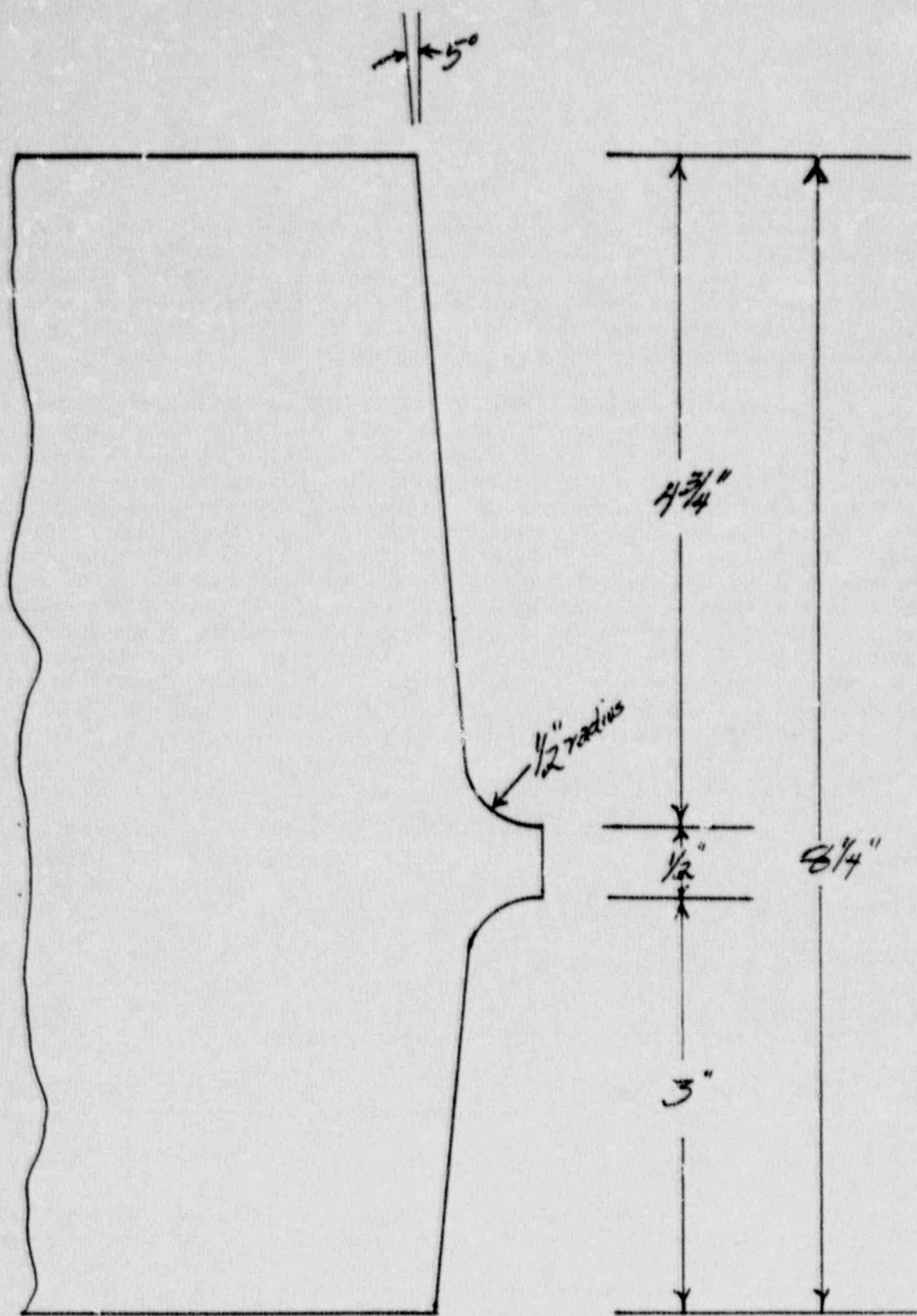


Fig. A-1 Weld joint design for Welds W8A and W9A

Fabrication of Weldment WW7

1. General

This weldment was produced commercially by Combustion Engineering, Inc. (CE) under contract. The weld was made using buyer-supplied 216-mm (8.5-in.) thick A 533-B Grade B Class 1 plate and contractor-supplied welding flux and filler wire. The mill test report for the plate is given as Attachment No. 7. The chemical compositions of the base plate, the filler wire and the weldments made for this project are indicated in Table A-1.

The filler wire was not copper-coated. The target copper content (0.35% Cu) for the weld deposit was obtained by using special welding equipment which can feed two filler wires simultaneously into the weld pool, in this case, a low nickel, low copper primary wire and a high purity copper auxiliary wire. Because the welding equipment had been idle at CE for several years beforehand and because new welding materials were involved, the contract called for a phased approach (Table A-2). Phase 1 showed a good uniformity of copper deposition along weld beads produced by the welding apparatus (see Fig. A-2) and that the filler wire feed rates produced a copper content approaching the target copper content value. Phase 2 demonstrated the capability of the equipment and welding materials to yield the proper copper content and required mechanical properties in a 76-mm (3-in.) thick trial weld deposit. The 1780-mm (70-in.) long main weldment fabricated in Phase 3, was found to fully satisfy the purchase specifications given as Attachment 8.

2. Fabrication of Trial Welds and Main Weld

A report by C.T. Ward, "Fabrication Records: A 533-B Weldments", Combustion Engineering Report MML-85-195, of 13 December 1985 contains full details of the welding program. Excerpts from this report are provided here for documentation of Weld WW7.

- Filler wire source melt: 5P2320.
- Welding flux: Linde 80, prebaked at 177°C (350°F) and held at temperature during the entire welding period.
- Heat input and arc conditions: 630A, 32V, 13 ipm travel speed, 93 kJ/in. travel speed. Arc conditions held constant for all weld passes.
- Set up: Single arc, 60 Hz alternating current.
- Preheating and Postheating: 149°C (300°F) minimum and 204°C (400°F) maximum preheat and interpass temperature. Temperature was measured and controlled directly on the surface of weld passes previously deposited. One postwelding heat treatment of 621°C (1150°F) \pm 6°C (10°F) for 24 hours with heating and cooling above 316°C (600°F) at 56°C (100°F)/hour maximum. The postwelding heat treatment was performed in a furnace equipped with fan recirculation. Temperatures were monitored with thermocouples placed over the length of the weld seam.

- Weld joint: Single Vee, zero bevel, root opening of 33.0-mm (1.3-in.) minimum.
- Weld passes: 17. total, where 3 side-by-side passes formed each weld layer.
- Inspection: No defects were detected by the various examinations, including radiography and magnetic particle testing.

LUKENS STEEL CO. COATESVILLE, PA. 19320

PHYSICAL TESTING RECORD - INSPECTORG 05-17-77

MILL ORDER # 8185-74564 1
 CUST. PURCHASE ORDER # .00173-77-C-0092
 SPECIF. A-533-74 CL. 1 TYPE-B

MELT	C	MN	P	S	CU	SI	NI	CR	MO	V	TI	B	AL	PE	ZR	CG	CB
A5401	.13	1.40	.005	.004		.25	.70		.57								

74

REQUIREMENTS - TEN. 80/100 YD. 50 MIN. ELG. 18% IN 2

MELT	SLAB	YD.	TEN.	ELG-	2"		TYPE	IMPACTS	FRA. APP	LAT. EXP. IN.	
					X R.A.	PEND					SHR
A5401	2	726	930	22				TV+20°F.	56-64-62	60-60-60	.051-.058-.055
		716	929	24							

DROP WEIGHT TRANSITION CURVE PER ESRN E208 (Size 2-3)

TEMP.	RESULTS
0°F.	No Break
-10°F.	No Break
-20°F.	No Break
-30°F.	No Break
-40°F.	Break

N.D.T. IS -40°F.
 REFERENCE TEMP. -40°F.

A533 CL1 Types A and		15-1		4+		5-11-77	
ITEM NO.	CHARGE	1/2	51K	104	997E	UM7d/	#13 8-1-77
QTY	GAUGE	104	104	104	53		
106173-77-C-0092		WHEELS		81250		SEARCH UNIT	
REPORTABLE INDICATIONS							
15	area	*	c	size	SCREEN LINE	TYPE OF SEARCH	
16	area	*	c	size	size	STATE POINTS	
17						TRANSDUCER	
18						TYPE OF PHONIC	
19						ECHO	
20						AMPLITUDE	
21						AMPLITUDE	
22						CALIBRATION	
23						COMBINING SW/W	
24						METHOD	
25						TYPE SURFACE	
26						C	
27						COND.	
28						CONE END	
29						CYL	
30						NO POINTS	
31						REMARKS	
32							
33							
34							
35							
36							
37							
38							
39							
40							
41							
42							
43							
44							
45							
46							
47							
48							
49							
50							
51							
52							
53							
54							
55							
56							
57							
58							
59							
60							
61							
62							
63							
64							
65							
66							
67							
68							
69							
70							
71							
72							
73							
74							
75							
76							
77							
78							
79							
80							
81							
82							
83							
84							
85							
86							
87							
88							
89							
90							
91							
92							
93							
94							
95							
96							
97							
98							
99							
100							
101							
102							
103							
104							
105							
106							
107							
108							
109							
110							
111							
112							
113							
114							
115							
116							
117							
118							
119							
120							
121							
122							
123							
124							
125							
126							
127							
128							
129							
130							
131							
132							
133							
134							
135							
136							
137							
138							
139							
140							
141							
142							
143							
144							
145							
146							
147							
148							
149							
150							
151							
152							
153							
154							
155							
156							
157							
158							
159							
160							
161							
162							
163							
164							
165							
166							
167							
168							
169							
170							
171							
172							
173							
174							
175							
176							
177							
178							
179							
180							
181							
182							
183							
184							
185							
186							
187							
188							
189							
190							
191							
192							
193							
194							
195							
196							
197							
198							
199							
200							
201							
202							
203							
204							
205							
206							
207							
208							
209							
210							
211							
212							
213							
214							
215							
216							
217							
218							
219							
220							
221							
222							
223							
224							
225							
226							
227							
228							
229							
230							
231							
232							
233							
234							
235							
236							
237							
238							
239							
240							
241							
242							
243							
244							
245							
246							
247							
248							
249							
250							
251							
252							
253							
254							
255							
256							
257							
258							
259							
260							
261							
262							
263							
264							
265							
266							
267							
268							
269							
270							
271							
272							
273							
274							
275							
276							
277							
278							
279							
280							
281							
282							
283							
284							
285							
286							
287							
288							
289							
290							

Table A-1 Chemical Compositions of Base Plate, Filler Wire,
76-mm Trial Weld, and 216-mm Main Weld (Code WW7)

	Chemical Composition (Wt %)				
	Base Plate (Trial Weld)	Base Plate (Main Weld)	Filler Wire ^a	Trial Weld ^b	Main Weld ^c
C	0.24	0.21	(0.22) ^d	0.15	0.08
Mn	1.44	1.40	(1.40)	2.08	1.53
Si	0.29	0.17	(0.19)	0.07	0.59
P	0.011	0.017	(0.010)	0.009	0.014
S	0.005	0.007	(0.008)	0.006	0.009
Ni	0.70	0.61	(0.63)	0.09	0.11
Cr	0.12	----	----	0.11	0.12
Mo	0.54	0.55	(0.54)	0.53	0.53
Cu	0.10	0.18	(0.20)	0.03	0.34
V	---- ^e	----	----	0.006	0.006
Sn	----	----	----	0.002	0.002
As	----	----	----	0.004	0.001 < 0.001
B	----	----	----	< 0.001	< 0.001 < 0.001

^a 4.76-mm dia. Heat No. 5P2320, Type 80S-2RC

^b 76.2-mm thick x .51-m long, single Vee joint

^c 216-mm thick, 1.78-m long, single Vee joint, average of 4 determinations through the thickness

^d Mill melt analysis

^e Not determined

Table A-2 Details of Three-Phase Approach to Fabrication of Weld

Phase	Action	Acceptance Criteria
1 Objective: Qualify proposed welding equipment.	Assemble, calibrate, test cold wire feed, welding apparatus. Prepare two-layer deep, bead-on-plate weld stringers using specified heat input and a cold wire feed rate for 0.35% Cu in the deposit. Analyze weld deposit (upper layer only) for % copper at eight predetermined points.	Weld deposit analyses show a uniform copper content ($\pm 0.02\%$ Cu) over the weld lengths.
2 Qualify cold wire feed rate; qualify filler wire flux combination for A 533-B Class 1.	Fabricate and postweld heat treat a 76.2-mm (3-in.) thick \times 0.51 m (20-in.) long trial weld. Test for tensile properties and Charpy-V notch ductility. Test for as-deposited chemical composition.	41-J transition temperature and C _U upper shelf energy are < -7°C (< 20°F) and > 81 J (> 60 ft-lb). Copper content is uniform and between 0.32% and 0.39% Cu.
3 Fabricate main weld seam.	Fabricate, heat treat, X-ray and chemically analyze the 216-mm (8.5-in.) thick \times 1.78-m (70-in.) long weld seam using welding parameters/conditions qualified in Phase 2.	Weldment was fabricated in full compliance with specifications, is reasonably free of defects; and represents good welding practices and workmanship.

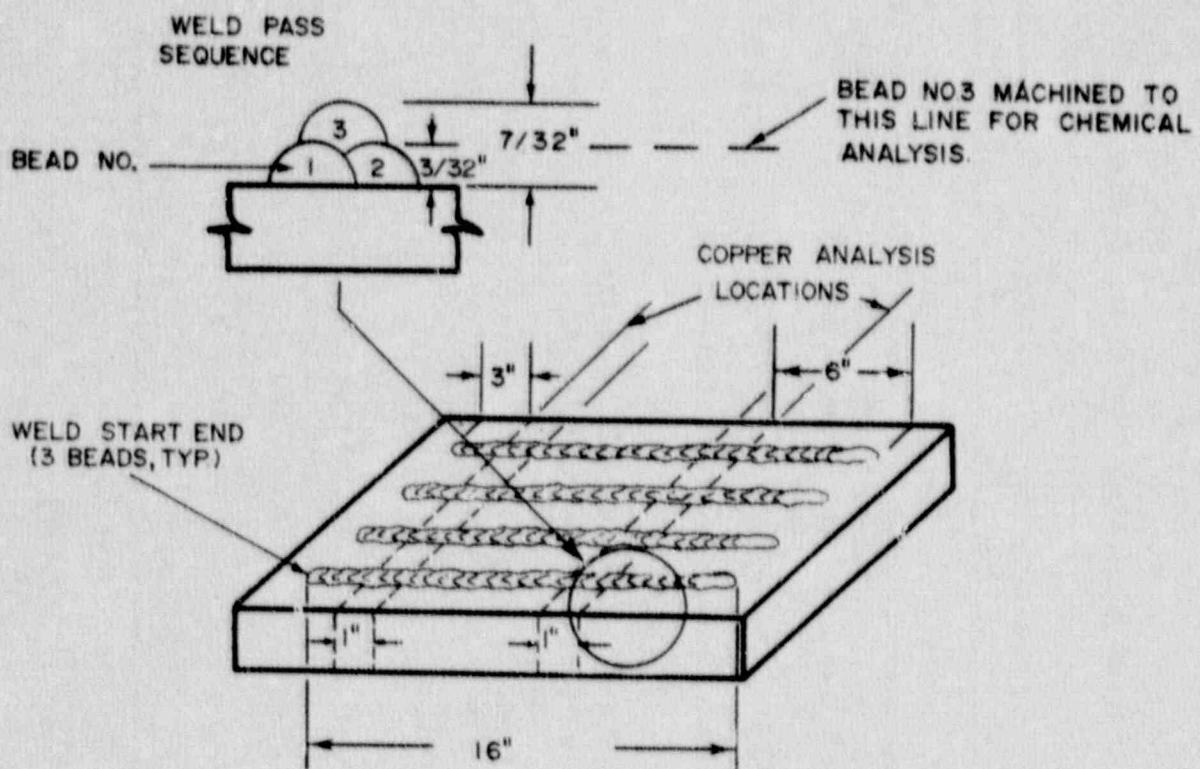


Fig. A-2

Phase 1 bead-on-plate weld tests for qualifying cold wire feed apparatus for producing a high copper content weld deposit. Analyses of bead no. 3 at the eight points shown, indicated copper contents of 0.33% or 0.34% Cu. (Note: in. \times 2.4 = mm)

SPECIFICATIONS WELD NO. 1

FINISHED SIZE : 8.5-in. thick x 70-in. weld (seam) length; finished weldment width will be approximately 41 in. Weldment length is exclusive of run-in/run-out end tabs.

BASE PLATE : A 533-B Class 1 steel (furnished by Buyer, complete with edge preparation).

ELECTRODE TYPE : The wire (provided by Seller) will be the high manganese molybdenum type (low nickel) used for welding A 533-B steel. The specific heat of wire used will be mutually agreed upon by Seller and Buyer. The filler wire to be used will have a nickel content of 0.09% Ni by a check analysis of the Seller.

ELECTRODE SIZE : 3/16-in. diameter

COLD WIRE FEED : High purity copper (provided by Seller; Seller chooses diameter)

WELDING FLUX : Linde 80 (size 20 x 200), (provided by Buyer, 370-lb total) baked (baking provided by Seller).

PROCESS : Single arc, AC, cold wire feed

SPEED : 10-13 ipm

VOLTAGE : 31.5-35

AMPERAGE : 500-650

JOULES/INCH : 85,000 (min) to 93,500 (max) (93,500 aim)

PREHEAT : 250°F (min) - 400°F (max) (300°F aim)

INTERPASS : 250°F (min) - 500°F (max)

JOINT : Single Vee, machined, straight-sided joint; root gap to be 1.312-in. (minimum). Each weld layer is to consist of three, nominally side-by-side weld passes. All required copper content determinations (main weld and 3-in. thick trial weld) will be on the vertical centerline of the weld deposit. Backing strip to be mild steel or low-alloy steel (provided by Seller). Backing strip will be removed after welding, the root area excavated by 0.5-in. deep (maximum) and examined by MT. Root area will not be back welded. End tab mold material to be mild steel or preferably A 533-B steel (provided by Seller).

RESTRAINT : Pieces being joined may be restrained by heavy clamps initially at the Seller's option; however, an initial preset will be the method used by the Seller to keep the weldment flat.

DEPOSIT CHEMISTRY: Range of copper content will be established during phase 2 (see Approach below). Nickel content should be as low as practical. Deposit chemistry will be consistent with that required for attainment of A 533-B Class 1 weld mechanical properties.

WELD DEPOSIT COMPOSITION DETERMINATION : For chemical analyses, the run-in/run out tabs will be removed from the weld seam (by sawing or equal) at the immediate juncture of the runoff and the base plate end. The sawed surfaces will then be made smooth after which four locations in the weld run-in/run-out tabs will be tested on the "sawed surface" for chemical composition. Analyses will be made for %C, %Mn, %Si, %P, %S, %Ni, %Mo, %Cu and %Cr at a minimum. Locations in the run-in tab (and in the run-out tab) are: 1.00, 3.2, 5.3, and 7.5 in. above the bottom surface of the base plate; measurements will be made on the vertical centerline of the weld joint. A 5/8-in. thick, full cross section slice of the weldment will also be saw cut at the mid-length of the weld seam for chemical analyses. The slice will be sent to the Buyer within two weeks after it has been removed from the weldment.

POSTWELD HEAT-TREATMENT : The weldment will be postweld heat-treated by furnace treating at $1150^{\circ}\text{F} \pm 25^{\circ}\text{F}$ for 24 hrs. Heat-up and cool-down will be at a rate not exceeding $100^{\circ}\text{F}/\text{hr}$ above 600°F . Air cooling is permissible once the workpiece has cooled to 600°F . Weldment length can be saw cut in half for heat-treatment at Seller option provided that mating edges of the halves are permanently marked for identification.

MONITORING OF HEAT-TREATMENT TEMPERATURES : A minimum of two (2) thermocouples will be attached to the weldment to monitor temperatures throughout the stress-relief anneal. A strip-chart temperature recorder will be used to record temperature indications from the thermocouples. The temperature charts will be made available to the Buyer for his review. Thermocouple locations on the workpiece (approximate) will be recorded and the workpiece orientation in the furnace (edge nearest the furnace door) will be identified for the Buyer.

POSTWELD INSPECTION : X-ray inspection of the weld seam will be performed after the stress-relief annealing operation. Radiography will be to acceptance standards of ASME Section V, NB5000 or current equal.

REPAIRS : None are allowed without Buyer's prior permission except for the following case:

If a short undercut (2-in. max in length) is observed, the Seller will record its location (depth and position along the weld seam length) and will repair the undercut on the spot. A maximum of three such repairs are allowed.

Defects observed in X-ray will not be repaired but will be marked on the weldment. Defects observed in X-ray also will be reported to MEA verbally and in writing before the weld is shipped to the Buyer.

- WELD CONFIGURATION : The weld deposit will be full thickness and will have a 1/8-in. thick (min) crown on the top surface.
- DOCUMENTATION : A detailed, bead-by-bead record of welding conditions for the weldment will be furnished to the Buyer. Documentation will include results from chemical analyses made on the weld run-in/run-out tabs, the results of X-ray analyses, and a confirmation by the Seller that heat treatment and other specifications, given here, were satisfied.
- APPROACH : A three-step approach will be followed in the determination of the necessary welding procedures, materials and control settings to help assure proper fabrication of the 8.5-in. thick x 70-in. long weld seam.

The three-step approach is detailed in the Attachment.

Fabrication of Weld WW4

1. General

This submerged arc weld was fabricated commercially by a reactor vessel fabricator. Details of weld fabrication procedures other than the welding flux type (Linde 124) and the postwelding heat treatment (607°C and 50 h) are not available. The weldment supplier has offered that the weldment is prototypic of some welds found in reactor vessels.

APPENDIX B

Reactor Operations History:
Irradiation Assemblies UBR-62, UBR-70, UBR-71 and UBR-72

EXPOSURE HISTORY

MEA UBR 62 A G E

EXPOSURE HISTORY

UBR 70 A,B -

DATE IN	TIME IN	DATE OUT	TIME OUT	EXPOSURE HOURS	SIGMA HOURS	CORE POSITION	NOTES
2-14-86		70 A,B	LOADED			B-4	6 3/8" Sp
2-17-86	1649	2-21-86	0900	88.18	88.18		
		70 A,B	ROTATED	180°			
2-23-86	1709	2-28-86	0800	110.85	199.03		T.C.
3-2-86	1658	3-3-86	1030	17.53	216.56		
3-3-86	1306	3-4-86	2224	33.30	249.86		
3-4-86	2314	3-5-86	1906	19.87	269.73		
3-5-86	1937	3-7-86	1241	41.07	310.86		
		70 A,B	ROTATED	180°			
3-9-86	1641	3-14-86	0900	112.32	423.12		
		70 A,B	OUT FOR ANSEAL				T.C.
3-21-86		70 A	INTO OVEN				
		70 B	INTO OVEN				
4-18-86		70 A,B	BACK IN	B-4			
-20-86	1700	4-23-86	0000	55.00	478.12		
		70 A,B	ROTATED	180°			

EXPOSURE HISTORY

UBR 70 -A,B

PAGE 2

EXPOSURE HISTORY:

MEA 71 A & B

EXPOSURE HISTORY

MLA UBR 72 A

APPENDIX C

**Neutron Dosimetry Determinations:
Irradiation Assemblies UBR-62, UBR-70, UBR-71, and UBR-72**

No. Rate Determinations
Be Spectro Assumption
For Series A and B)

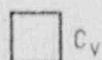
UBR-62

A-CAPSULE

238U	→	W8A W8A WW7 457 375 16	Fe, Ni
		W8A WW7 W8A WW7 465 60 160 41	Fe, CoAl
		WW7 W8A WW7 W8A 51 463 2 498	
		W8A WW7 W8A WW7 467 13 500 62	Fe, Ni
		WW7 W4 WW7 W8A 44 137 63 484	
		WW7 WW7 WW7 WW7 64 37 28 45	
		WW7 W8A W8A WW7 46 495 481 59	Fe, Ni
		W8A WW7 W4 WW7 458 54 97 47	
		WW7 W8A WW7 W8A 35 462 48 484	Fe, CoAl
		W8A WW7 W8A WW7 483 49 466 53	
		WW7 W8A WW7 W8A 50 468 57 486	Fe, Ni
		W8A WW7 W8A WW7 498 58 501 51	

B-CAPSULE

238U	→	W8A W8A W4 W8A W4 396 390 144 V30 109	Fe, CoAl, AgAl
		W4 W4 W8A W4 W8A 169 148 420 115 419	
		W8A W8A W4 W8A W4 410 416 42 416 112	
		W4 W4 W4 W8A W8A 171 167 87 17 385	Fe, Ni
		W8A W8A W8A W4 W8A 395 504 485 27 502	
		W8A W4 W8A W8A W4 518 147 392 503 110	
		W4 W8A W4 W8A W8A 168 388 145 522 386	Fe, Ni
		W8A W8A W8A W4 W4 412 417 389 141 114	
		W4 W8A W4 W8A W8A 170 393 165 391 415	Fe, CoAl, AgAl
		W8A W4 W8A W4 W4 409 166 351 143 116	
		W4 W8A W4 W8A W8A 172 384 146 418 V24	Fe, Ni



Cv



TENSILE

Fig. C-1

Irradiation Assembly UBR-62 showing neutron fluence-rate monitor locations.

Table C-1 Irradiation Assembly UBR-62 Capsule A Fluence-Rate Monitor Results (Ref.1)

Monitor/Segment ^a		Fluence Rate ^b × 10 ¹² (Average)	Monitor Location in Specimen Array
A1	(Fe)	5.81	
	(Ni)	5.80	Immediately above layer 1
A2	(Fe)	5.97	
	(AgCo)	3.02 ^c	Between layers 2 and 3
A3	(Fe)	6.18	
	(Ni)	6.18	Between layers 4 and 5
A4	(Fe)	6.51	
	(Ni)	6.61	Between layers 7 and 8
A5	(Fe)	6.65	
	(AgCo)	3.31 ^c	Between layers 9 and 10
A6	(Fe)	6.94	
	(Ni)	6.94	Between layers 11 and 12
Vial (2 ³⁸ U)		8.18 ^d (9.33) ^e	Between layers 6 and 7
	(Fe)	6.53	
	(Ni)	6.54	

^a See Figure C-1 for monitor locii. The Fe, Ni and 2³⁸U results are based on > 1 MeV fission spectrum-averaged cross sections of 115.2, 156.8 and 441 millibarns, respectively.

^b Fission spectrum assumption; n/cm²·s⁻¹ (E > 1 MeV) unless noted.

^c Thermal fluence rate corrected for epithermal neutron contributions based on ¹⁰⁹Ag and ⁵⁹Co reaction rates and their cross sections. Single determination value.

^d Determination from ¹³⁷Cs results (only).

^e Calculated spectrum value.

Table C-2 Irradiation Assembly UBR-62 Capsule B Fluence-Rate Monitor Results (Ref. 1)

Monitor/Segment ^a		Fluence Rate ^b x 10 ¹² (Average)	Monitor Location in Specimen Array
B1	(Fe) (AgCo)	6.74 3.00 ^c	Between layers 1 and 2
B2	(Fe) (Ni)	6.38 6.49	Between layers 3 and 4
B3	(Fe) (Ni)	6.20 6.34	Between layers 6 and 7
B4	(Fe) (AgCo)	6.01 2.74	Between layers 8 and 9
B5	(Fe) (Ni)	5.88 5.97	Between layers 10 and 11
Vial	(²³⁸ U) (Fe) (Ni)	8.29 ^d (9.45) ^e 6.51 6.47	Between layers 4 and 5

^a See Figure C-1 for monitor locii. The Fe, Ni and ²³⁸U results are based on > 1 MeV ²³⁸U fission spectrum-averaged cross sections of 115.2, 156.8 and 441 millibarns, respectively.

^b Fission spectrum assumption; n/cm²·s⁻¹ (E > 1 MeV) unless noted.

^c Thermal fluence rate corrected for epithermal neutron contributions based on ¹⁰⁹Ag and ⁵⁹Co reaction rates and their cross sections. Single determination value.

^d Determination from ¹³⁷Cs results (only).

^e Calculated spectrum value.

Neutron fluence-Rate Determinations

Based on Fission Spectrum Assumption

For Assembly UBR-70 (Capsules A and B)

UBR-70

A-CAPSULE

W8A	WW7	W4	W8A	Fe, Ni
371	73	81	433	
WW7	W4	W8A	W8A	Fe, CoAl
75	149	438	361	
W4	W8A	W8A	WW7	Fe, Ni
158	440	364	66	
W8A	W8A	WW7	W4	Fe, Ni
443	368	70	83	
W8A	W8A	W8A	W8A	Fe, Ni
372	387	473	434	
WW7	W4	WW7	W4	Fe, Ni
77	88	68	86	
W4	W8A	W8A	WW7	Fe, Ni
159	441	368	67	
W8A	W8A	WW7	W4	Fe, Ni
444	369	71	88	
W8A	WW7	W4	W8A	Fe, CoAl
V18	74	92	436	
WW7	W4	W8A	W8A	Fe, Ni
78	153	438	362	
W4	W8A	W8A	WW7	Fe, Ni
162	442	367	69	
W8A	W8A	WW7	W4	Fe, Ni
517	370	72	90	

B-CAPSULE

W8A	WW7	W8A	W4	W8A	Fe, CoAl
383	85	380	96	445	
W8A	WW7	W4	W8A	W8A	Fe, Ni
455	86	151	450	373	
WW7	W4	W8A	W8A	WW7	Fe, Ni
90	163	452	378	79	
W4	WW7	W8A	W4	W4	Fe, Ni
161	88	381	173	93	
W8A	W8A	WW7	W4	W8A	Fe, Ni
456	454	83	98	446	
W8A	WW7	W4	W8A	W8A	Fe, Ni
384	87	154	451	374	
WW7	W8A	WW7	W8A	WW7	Fe, Ni
91	169	81	379	80	
W4	W8A	W4	WW7	W4	Fe, CoAl
157	41	103	82	94	
W8A	W8A	WW7	W4	W8A	Fe, Ni
520	382	84	99	448	
W8A	WW7	W8A	W4	W8A	Fe, Ni
1/21	88	453	100	376	
WW7	W8A	W8A	WW7	W8A	Fe, Ni
20	23	47	24	34	

C_V

TENSILE

Fig. C-2 Irradiation Assembly UBR-70 showing neutron fluence-rate monitor locations.

Table C-3 Irradiation Assembly UBR-70 Capsule A Fluence Rate Monitor Results (Ref. 2)

Monitor/Segment ^a	Fluence Rate ^b $\times 10^{12}$ (Average)	Monitor Location in Specimen Array
A13 (Fe) (Ni)	5.93 5.96	Immediately above layer 1
A14 (Fe) (AgCo)	6.10 3.50 ^c	Between layers 2 and 3
A16 (Fe) (Ni)	6.42 6.48	Between layers 4 and 5
A15 (Fe) (Ni)	6.75 6.71	Between layers 7 and 8
A17 (Fe) (AgCo)	6.79 3.91 ^c	Between layers 9 and 10
A18 (Fe) (Ni)	7.13 7.14	Between layers 11 and 12
Vial (2 ³⁸ U) (Fe) (Ni)	7.93 ^d (9.04) ^e 6.41 6.33	Between layers 5 and 6

^a See Figure C-2 for monitor locii. The Fe, Ni and ^{238}U results are based on $> 1 \text{ MeV}$ ^{238}U fission spectrum-averaged cross sections of 115.2, 156.8 and 441 millibarns, respectively.

^b Fission spectrum assumption; $\text{n}/\text{cm}^2 \cdot \text{s}^{-1}$ ($E > 1 \text{ MeV}$) unless noted.

^c Thermal fluence rate corrected for epithermal neutron contributions based on ^{109}Ag and ^{59}Co reaction rates and their cross sections.

^d Average determination from ^{137}Cs , ^{103}Ru and ^{95}Zr results.

^e Calculated spectrum value.

Table C-4 Irradiation Assembly UER-70 Capsule B Fluence-Rate Monitor Results (Ref. 2)

Monitor/Segment ^a		Fluence Rate ^b x 10 ¹² (Average)	Monitor Location in Specimen Array
B20	(Fe) (AgCo)	7.18 3.38 ^c	Between layers 1 and 2
B21	(Fe) (Ni)	6.95 6.85	Between layers 3 and 4
B22	(Fe) (Ni)	6.51 6.71	Between layers 6 and 7
B22	(Fe) (AgCo)	6.38 2.92 ^c	Between layers 8 and 9
B24	(Fe) (Ni)	6.11 6.15	Between layers 10 and 11

^a See Figure C-2 for monitor locii. The Fe and Ni results are based on >1 MeV ^{238}U fission spectrum-averaged cross sections of 115.2 and 156.8 millibarns, respectively.

^b Fission spectrum assumption; $\text{n}/\text{cm}^2 \cdot \text{s}^{-1}$ ($E > 1 \text{ MeV}$) unless noted.

^c Thermal fluence rate corrected for epithermal neutron contributions based on ^{109}Ag and ^{59}Co reaction rates and their cross sections.

Neutron Fluence-Rate Determinations
Based on Fission Spectrum Assumption
For Assembly UBF-71 (Capsules A and B)

UBR-71

A-CAPSULE

$^{238}\text{U} \rightarrow$

W8	WW7	W4	W8A	
40	99	138	469	
WW7	W4	W8A	W8A	
101	152	47	387	
W4	W8A	W	WW7	
6	175	400	82	
W8A	W8A	WW7	W4	
479	404	86	101	
W8A	W8A	W8A	W8A	
408	405	152	470	
WW7	W4	WW7	W4	
103	129	84	102	
W4	W8A	W8A	WW7	
13	477	402	83	
W8A	W8A	WW7	W4	
480	405	97	104	
W8A	W7	W4	W8A	
V27	100	108	475	
WW7	W4	W8A	W8A	
104	158	472	388	
W4	W8A	W8A	WW7	
164	478	403	95	
W8A	W8A	WW7	W4	
523	406	98	138	

← Fe, Ni

← Fe, CoAl

← Fe, Ni

← Fe, Ni

← Fe, CoAl

← Fe, Ni

B-CAPSULE

$^{238}\text{U} \rightarrow$

W8A	WW7	W8A	W4	W8A
431	111	428	128	481
W8A	WW7	W4	W8A	W8A
491	112	150	486	421
WW7	W4	W8A	W8A	WW7
116	160	488	426	105
W4	WW7	W9A	W4	W4
26	115	429	11	125
W8A	W8A	WW7	W4	W8A
492	490	109	130	482
W8A	WW7	W4	W8A	W8A
432	113	155	487	422
WW7	W8A	WW7	W8A	WW7
117	123	12	427	106
W4	W8A	W4	WW7	W4
37	101	105	108	126
W8A	W8A	WW7	W4	W8A
524	430	110	131	484
W8A	WW7	W8A	W4	W9A
V33	114	489	132	424
WW7	W8A	W8A	WW7	W8A
26	155	48	22	35

← Fe, CoAl, AgAl

← Fe, Ni

← Fe, Ni

← Fe, CoAl

← Fe, Ni

Cv

TENSILE

Fig. C-3 Irradiation Assembly UBR-71 showing neutron fluence-rate monitor locations

Table C-5 Irradiation Assembly UBR-71 Capsule A Fluence-Rate Monitor Results (Ref. 3)

Monitor/Segment ^a		Fluence Rate ^b x 10 ¹² (Average)	Monitor Location in Specimen Array
A8	(Fe) (Ni)	5.90 5.62	Immediately above layer 1
A9	(Fe) (AgCo)	6.13 3.61 ^c	Between layers 2 and 3
A11	(Fe) (Ni)	6.42 6.18	Between layers 4 and 5
A10	(Fe) (Ni)	6.77 6.48	Between layers 7 and 8
A12	(Fe) (AgCo)	6.97 3.89 ^c	Between layers 9 and 10
A13	(Fe) (Ni)	7.26 7.00	Between layers 11 and 12
Vial	(²³⁸ U) (Fe) (Ni)	8.12 ^d (9.26) ^e 6.54 6.60	Between layers 5 and 6

^a See Figure C-3 for monitor locii. The Fe, Ni and ²³⁸U results are based on > 1 MeV ²³⁸U fission spectrum-averaged cross sections of 115.2, 156.8 and 441 millibarns, respectively.

^b Fission spectrum assumption; n/cm²·s⁻¹ (E > 1 MeV) unless noted.

^c Thermal fluence rate corrected for epithermal neutron contributions based on ¹⁰⁹Ag and ⁶⁹Co reaction rates and their cross sections.

^d Average determination from ¹³⁷Cs, ¹⁰⁸Ru and ⁹⁵Zr results.

^e Calculated spectrum value.

Table C-6 Irradiation Assembly UBR-71 Capsule B Fluence-Rate Monitor Results (Ref. 3)

Monitor/Segment ^a		Fluence Rate ^b $\times 10^{12}$ (Average)	Monitor Location in Specimen Array
B1	(Fe) (AgCo)	7.42 3.74 ^c	Between layers 1 and 2
B2	(Fe) (Ni)	7.07 6.90	Between layers 3 and 4
B3	(Fe) (Ni)	6.87 6.67	Between layers 6 and 7
B4	(Fe) (AgCo)	6.64 3.13 ^c	Between layers 8 and 9
B5	(Fe) (Ni)	6.40 6.27	Between layers 10 and 11
Vial (²³⁸ U)		6.83 ^d (10.07) ^e	Between layers 7 and 8
	(Fe)	6.83	
	(Ni)	6.74	

^a See Figure C-3 for monitor locii. The Fe, Ni and ²³⁸U results are based on > 1 MeV ²³⁸U fission spectrum-averaged cross sections of 115.2, 156.8 and 441 millibarns, respectively.

^b Fission spectrum assumption; n/cm²·s⁻¹ (E > 1 MeV) unless noted.

^c Thermal fluence rate corrected for epithermal neutron contributions based on ¹⁰⁸Ag and ⁵⁹Co reaction rates and their cross sections.

^d Average determination from ¹³⁷Cs, ¹⁰⁸Ru and ⁹⁵Zr results.

^e Calculated spectrum value.

Neutron Fluence-Rate Determinations
Based on Fission Spectrum Assumption
For Assembly UBR-72 (Capsule A)

UBR-72

A-CAPSULE

W8A	WW7	W4	W8A
359	125	107	505
WW7	W4	W8A	W8A
127	18	510	349
W4	W8A	W8A	WW7
50	512	352	118
W8A	W8A	WW7	W4
515	35	122	133
W8A	W9	W8A	W8A
360	425	509	506
WW7	W4	WW7	W4
129	85	120	134
W4	W8A	W8A	WW7
5	513	354	118
W8A	W8A	WW7	W4
516	357	123	136
W8A	WW7	W4	W8A
V15	126	140	508
WW7	W4	W8A	W9A
130	39	511	350
W4	W8A	W8A	WW7
65	514	355	121
W8A	W8A	WW7	W4
527	358	124	106

← Fe, Ni, Nb

← Fe, CoAl, AgAl

← Fe, Ni, Nb

← Fe, Ni

← Fe, CoAl

← Fe, Ni, Nb



C_v



TENSILE

Fig. C-4 Irradiation Assembly UBR-72 showing neutron fluence-rate monitor locations

Table C-7 Irradiation Assembly UBR-72 Capsule A Fluence-Rate Monitor Results (Ref. 4)

Monitor/Segment ^a	Fluence Rate ^b x 10 ¹² (Average)	Monitor Location in Specimen Array
A1 (Fe) (Ni)	6.51 6.42	Immediately above layer 1
A2 (Fe) (AgCo)	6.45 4.20 ^c	Between layers 2 and 3
A3 (Fe) (Ni)	6.54 6.46	Between layers 4 and 5
A5 (Fe) (Ni)	6.49 6.43	Between layers 7 and 8
A6 (Fe) (AgCo)	6.46 3.99 ^c	Between layers 9 and 10
A7 (Fe) (Ni)	6.52 6.48	Between layers 11 and 12
Vial (²³⁸ U) (Fe) (Ni)	7.96 ^d (9.07) ^e 6.60 6.65	Between layers 5 and 6

^a See Figure C-4 for monitor locii. The Fe, Ni and ²³⁸U results are based on > 1 MeV ²³⁸U fission spectrum-averaged cross sections of 115.2, 156.8 and 441 millibarns, respectively.

^b Fission spectrum assumption; r./cm²·s⁻¹ (E > 1 MeV) unless noted.

^c Thermal fluence rate corrected for epithermal neutron contributions based on ¹⁰⁹Ag and ⁵⁹Co reaction rates and their cross sections.

^d Average determination from ¹³⁷Cs, ¹⁰³Ru, ¹⁴⁰BaLa and ⁹⁶Zr results.

^e Calculated spectrum value.

References

1. J.W. Rogers, "Neutron Fluence Rates for MEA-UBR Experiments," Letter Report JVR-32-88, EG&G Idaho, Inc., Idaho Falls, ID, 16 August 1988.
2. J.W. Rogers, "Neutron Fluence Rates for MEA-UBR Experiments," Letter Report JWR-35-86, EG&G Idaho, Inc., Idaho Falls, ID, 25 November 1986.
3. J.W. Rogers, "Neutron Fluence Rates for MEA-UBR Experiments," Letter Report JWR-7-87, EG&G Idaho, Inc., Idaho Falls, ID, 10 September 1987.
4. J.W. Rogers, "Neutron Fluence Rates for MEA-UBR Experiments," Letter Report JWR-15-87, EG&G Idaho, Inc., Idaho Falls, ID, 26 May 1987.

APPENDIX D

Tabulations of Charpy-V Notch Ductility Test Results

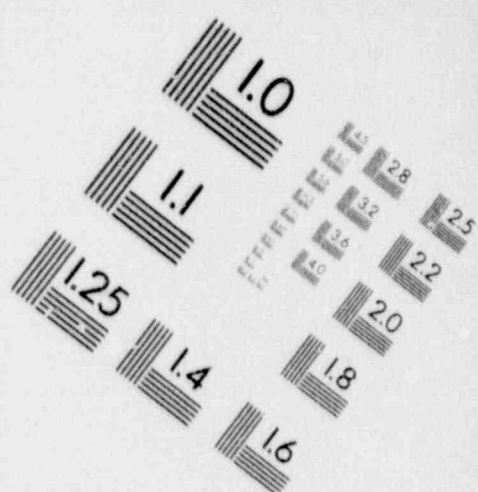
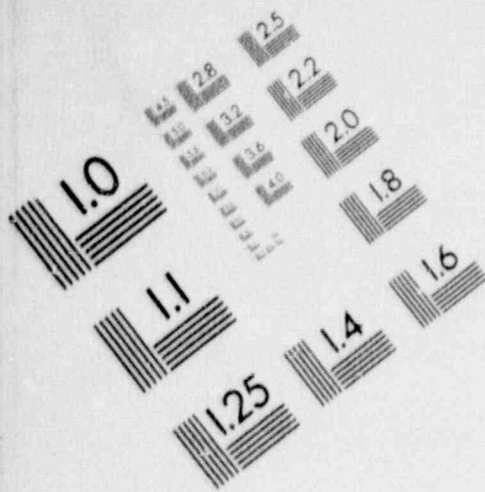
Charpy-V Data from Unirradiated Condition Tests

Code W8A (Unirradiated Condition)

No.	Specimen Number	Layer	Capsule	Test Temp.		Energy		Lat. Exp.		Shear (%)
				(°C)	(°F)	(J)	(ft-lb)	(mm)	(mils)	
1	4	4	---	-40	-40	19.0	14.0	0.33	13	5
2	11	11	---	-40	-40	24.4	18.0	0.43	17	5
3	30	6	---	-23	-10	35.3	26.0	(ND)	(ND)	----
4	5	5	---	-18	0	48.8	36.0	0.94	37	----
5	12	12	---	-18	0	43.4	32.0	0.79	31	20
6	23	11	---	4	40	28.5	21.0	(ND)	(ND)	----
7	18	6	---	4	40	52.9	39.0	(ND)	(ND)	----
8	10	10	---	27	80	40.7	30.0	0.74	29	35
9	3	3	---	27	80	56.9	42.0	1.09	43	45
10	6	6	---	49	120	70.5	52.0	1.27	50	80
11	1	1	---	49	120	63.7	47.0	1.19	47	60
12	9	9	---	93	200	75.9	56.0	1.47	58	100
13	2	2	---	93	200	81.3	60.0	1.55	61	100
14	15	3	---	204	400	78.6	58.0	1.68	56	100
15	22	10	---	204	400	78.6	58.0	1.52	60	100

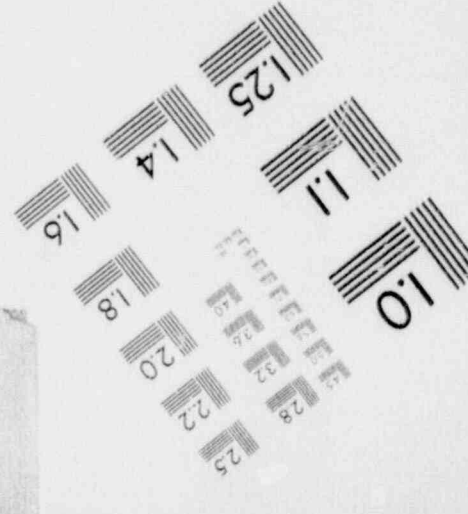
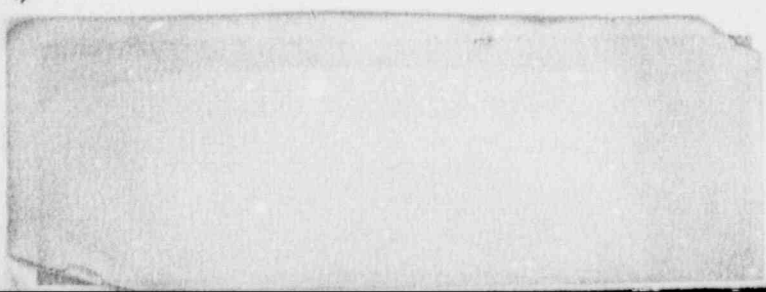
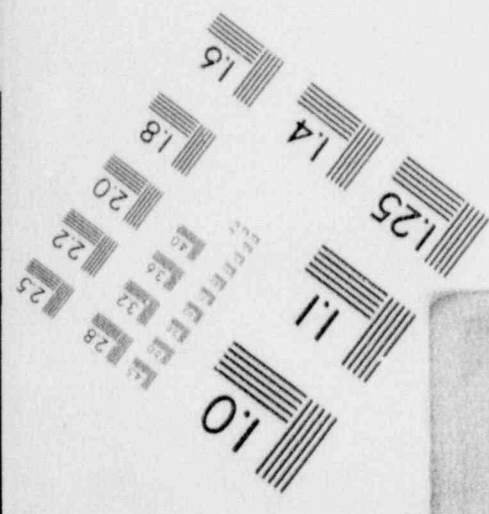
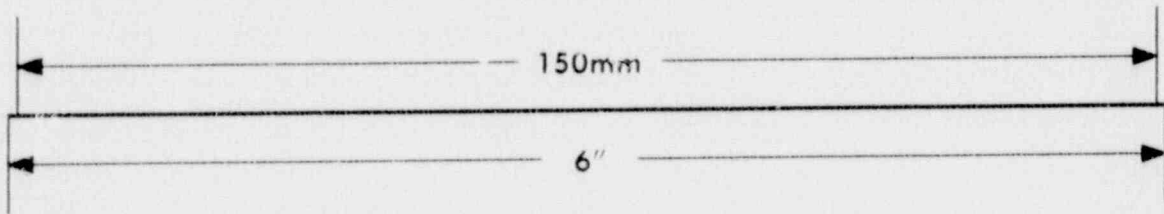
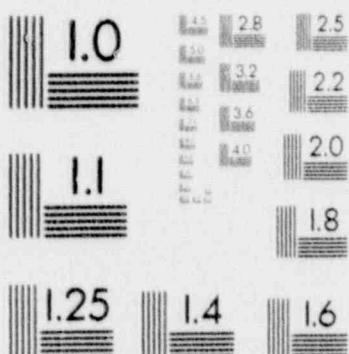
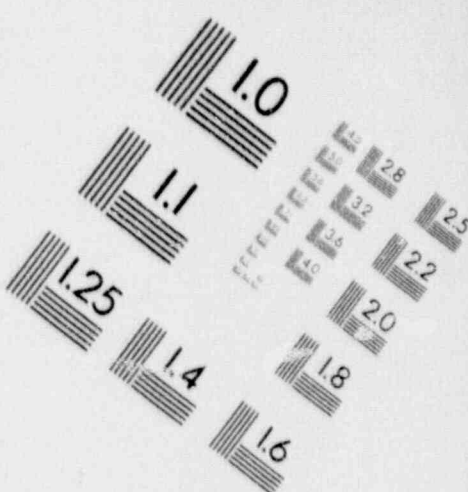
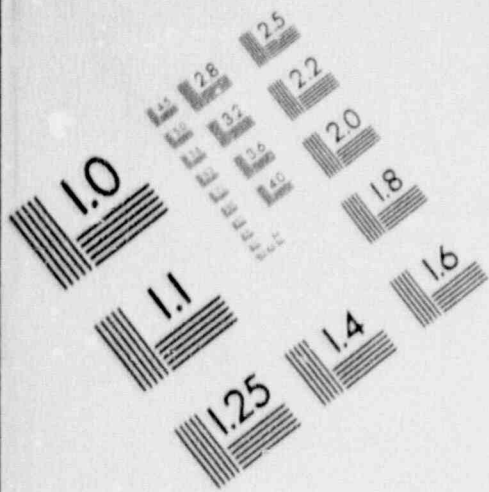
1

IMAGE EVALUATION TEST TARGET (MT-3)



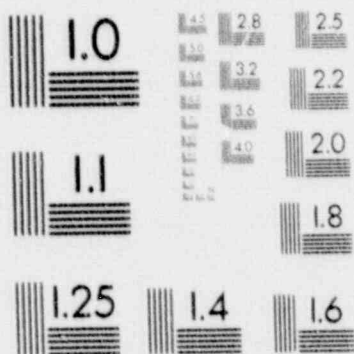
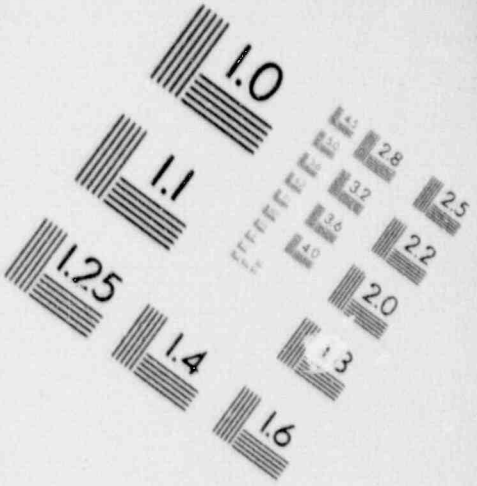
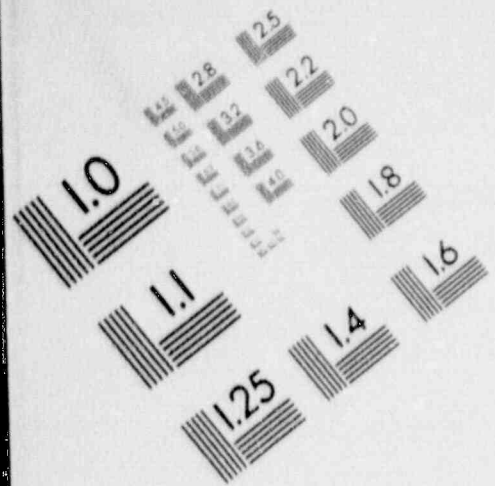
1

IMAGE EVALUATION TEST TARGET (MT-3)



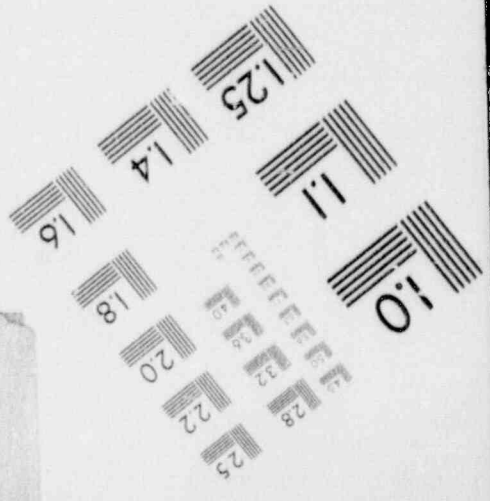
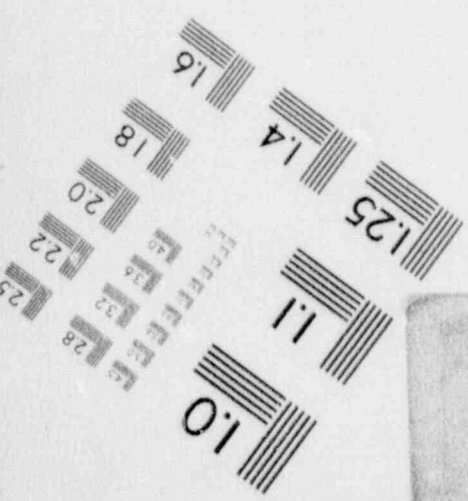
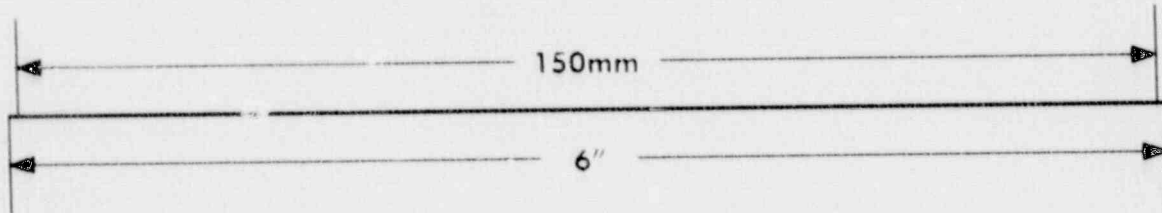
1

**IMAGE EVALUATION
TEST TARGET (MT-3)**



150mm

6 //



Code W9A (Unirradiated Condition)

No.	Specimen Number	Layer	Capsule	Test Temp.		Energy		Lat. Exp.		Shear (%)
				(°C)	(°F)	(J)	(ft-lb)	(mm)	(mils)	
1	5	5	---	-62	-80	39.3	29.0	0.71	28	20
2	15	3	---	-62	-80	38.0	28.0	0.64	25	10
3	3	3	---	-46	-50	71.9	53.0	1.09	43	50
4	19	7	---	-46	-50	67.8	50.0	1.07	42	20
5	18	7	---	24	75	138.2	96.0	1.85	73	95
6	27	3	---	24	75	149.1	110.0	1.96	77	99
7	6	6	---	71	160	154.6	114.0	2.18	86	100
8	16	4	---	204	400	169.5	125.0	2.21	87	100
9	29	5	---	204	400	169.5	125.0	2.21	87	100
10	35	11	---	204	400	168.1	124.0	2.16	85	100

Code WW4 (Unirradiated Condition)

No.	Specimen Number	Layer	Capsule	Test Temp.		Energy		Lat. Exp.		Shear (%)
				(°C)	(°F)	(J)	(ft-lb)	(mm)	(mils)	
1	20	8	---	-62	-80	9.5	7.0	0.23	9	----
2	1	1	---	-51	-60	23.0	17.0	0.43	17	----
3	33	9	---	-40	-40	46.1	34.0	0.75	30	----
4	66	6	---	-34	-30	55.6	41.0	0.94	37	----
5	49	6	---	-34	-30	55.6	41.0	0.94	37	----
6	62	2	---	-18	0	39.3	29.0	0.74	29	----
7	72	12	---	-18	0	89.5	66.0	1.40	55	----
8	40	4	---	-1	30	111.2	82.0	1.75	69	----
9	53	5	---	16	60	120.7	89.0	1.83	72	----
10	7	7	---	49	120	124.7	92.0	2.01	79	----
11	12	12	---	60	140	141.0	104.0	2.16	85	----
12	46	10	---	121	250	143.7	106.0	2.18	86	----
13	27	3	---	149	300	128.8	95.0	2.06	81	----
14	14	2	---	204	400	128.8	95.0	2.06	81	----
15	59	11	---	204	400	153.2	113.0	2.29	90	----

Code WW7 (Unirradiated Condition)

No.	Specimen Number	Layer	Capsule	Test Temp. (°C)	Test Temp. (°F)	Energy (J)	Energy (ft-lb)	Lat. Exp. (mm)	Lat. Exp. (mils)	Shear (%)
1	CE8	.75	---	-34	-30	31.2	23.0	(ND)	(ND)	<100
2	3	3	---	-18	0	39.3	29.0	0.76	30	34
3	11	11	---	-18	0	33.9	25.0	0.76	30	43
4	CE5	.25	---	-18	0	48.7	36.0	(ND)	(ND)	<100
5	CE4	.75	---	-18	0	48.7	36.0	(ND)	(ND)	<100
6	CE7	.25	---	4	40	61.0	45.0	(ND)	(ND)	<100
7	CE6	.75	---	4	40	59.7	44.0	(ND)	(ND)	<100
8	2	2	---	10	50	63.7	47.0	1.12	44	70
9	9	9	---	10	50	62.4	46.0	1.17	46	66
10	4	4	---	99	210	85.4	63.0	1.78	70	100
11	12	12	---	99	210	80.0	59.0	1.57	62	100
12	1	1	---	99	210	78.6	58.0	1.57	62	100
13	10	10	---	99	210	88.1	65.0	1.68	66	100
14	CE1	.75	---	100	212	89.5	66.0	(ND)	(ND)	100
15	CE2	.25	---	100	212	88.1	65.0	(ND)	(ND)	100
16	CE3	.25	---	100	212	88.1	65.0	(ND)	(ND)	100

Charpy-V Data from Thermally-Aged Condition Tests

Code WW4 (Thermally Aged 288 C - 2160h)

No.	Specimen Number	Layer	Capsule	Test Temp.		Energy		Lat. Exp.		Shear (%)
				(°C)	(°F)	(J)	(ft-lb)	(mm)	(mils)	
1	31	7	---	-46	-50	13.6	10.0	0.36	14	----
2	5	5	---	-34	-30	70.5	52.0	1.12	44	----
3	44	8	---	-34	-30	61.0	45.0	0.94	37	----
4	18	6	---	-23	-10	58.3	43.0	0.94	37	----
5	57	9	---	-7	20	89.5	66.0	1.30	51	----
6	61	1	---	-1	30	97.6	72.0	1.55	61	----
7	24	12	---	49	120	143.7	106.0	2.11	83	----
8	11	11	---	116	240	135.6	100.0	2.21	87	----
9	70	10	---	199	390	160.0	118.0	2.18	86	----
10	74	2	---	199	390	136.9	101.0	2.01	79	----

Charpy-V Data from Irradiation Assembly UBR-62

(As-Irradiated Condition and Postirradiation-Annealed Conditions)

Code W8A (UBR-62, Capsules A & B, As-Irradiated)

No.	Specimen Number	Layer	Capsule	Test Temp. (°C)	Test Temp. (°F)	Energy (J)	Energy (ft-lb)	Lat. Exp. (mm)	Lat. Exp. (mils)	Shear (%)
1	493	1	62A	49	120	16.3	12.0	0.23	9	<100
2	460	4	62A	57	135	21.7	16.0	0.33	13	<100
3	498	6	62A	71	160	32.5	24.0	0.61	24	<100
4	502	10	62B	82	180	25.8	19.0	0.48	19	<100
5	500	8	62A	93	200	42.0	31.0	0.74	29	<100
6	501	9	62A	107	225	47.5	35.0	0.76	30	<100
7	468	12	62A	138	280	52.9	39.0	0.94	37	97
8	518	2	62B	204	400	58.2	37.0	0.97	38	100

Code W8A (UBR-62, Capsules A & B, 399 C Annealed)

No.	Specimen Number	Layer	Capsule	Test Temp. (°C)	Test Temp. (°F)	Energy (J)	Energy (ft-lb)	Lat. Exp. (mm)	Lat. Exp. (mils)	Shear (%)
1	464	8	62A	27	80	35.3	26.0	(ND)	(ND)	<100
2	462	6	62A	49	120	66.4	49.0	1.17	46	<100
3	503	11	62B	60	140	48.8	36.0	0.84	33	<100
4	494	2	62A	71	160	51.5	38.0	1.07	42	<100
5	457	1	62A	138	280	74.6	55.0	1.32	52	100
6	499	7	62A	204	400	78.6	58.0	1.65	65	100

Code W8A (UBR-62, Capsules A & B, 454 C Annealed)

No.	Specimen Number	Layer	Capsule	Test Temp. (°C)	Test Temp. (°F)	Energy (J)	Energy (ft-lb)	Lat. Exp. (mm)	Lat. Exp. (mils)	Shear (%)
1	465	9	62A	-7	20	36.6	27.0	0.61	24	<100
2	496	4	62A	-1	30	20.3	15.0	0.43	17	<100
3	467	11	62A	21	70	46.1	34.0	0.86	34	<100
4	466	10	62A	21	70	38.0	28.0	0.69	27	<100
5	504	12	62B	32	90	61.0	45.0	1.04	41	<100
6	458	2	62A	54	130	62.4	46.0	1.09	43	<100
7	463	7	62A	204	400	92.2	68.0	1.57	62	100
8	522	6	62B	204	400	81.3	60.0	1.96	77	100

Code W9A (UBR-62, Capsule A, As-Irradiated)

No.	Specimen Number	Layer	Capsule	Test Temp. (°C)	Test Temp. (°F)	Energy (J)	Energy (ft-lb)	Lat. Exp. (mm)	Lat. Exp. (mils)	Shear (%)
1	391	7	62A	4	40	23.0	17.0	0.33	13	<100
2	419	11	62A	27	80	38.0	28.0	0.66	26	---
3	414	6	62A	38	100	61.0	45.0	0.84	33	<100
4	392	8	62A	49	120	73.2	54.0	1.12	44	<100
5	412	4	62A	71	160	77.3	57.0	1.24	49	<100
6	418	10	62A	82	180	78.6	58.0	1.24	49	<100
7	386	2	62A	138	280	100.3	74.0	1.60	63	<100
8	V30	9	62A	204	400	113.9	84.0	2.01	79	100

Code W9A (UBR-62, Capsule B, 399 C Annealed)

No.	Specimen Number	Layer	Capsule	Test Temp. (°C)	Test Temp. (°F)	Energy (J)	Energy (ft-lb)	Lat. Exp. (mm)	Lat. Exp. (mils)	Shear (%)
1	409	1	62B	-29	-20	36.6	27.0	0.53	21	<100
2	416	8	62B	-18	0	42.0	31.0	0.64	25	<100
3	395	11	62B	-7	20	62.4	46.0	0.91	36	<100
4	388	4	62B	27	80	92.2	68.0	1.32	52	<100
5	396	12	62B	182	360	136.9	101.0	1.88	74	100
6	V24	9	62B	204	400	160.0	118.0	2.21	87	98

Code W9A (UBR-62, Capsule B, 454 C Annealed)

No.	Specimen Number	Layer	Capsule	Test Temp. (°C)	Test Temp. (°F)	Energy (J)	Energy (ft-lb)	Lat. Exp. (mm)	Lat. Exp. (mils)	Shear (%)
1	385	1	62B	-29	-20	36.6	27.0	0.64	25	<100
2	417	9	62B	-23	-10	77.3	57.0	0.99	39	<100
3	410	2	62B	-21	-5	50.2	37.0	0.84	33	<100
4	415	7	62B	-12	10	84.1	62.0	1.24	49	---
5	394	10	62B	7	45	16.3	12.0	0.28	11	<100
6	393	9	62B	10	50	119.3	88.0	1.60	63	---
7	390	6	62B	21	70	116.6	86.0	1.63	64	<100
8	420	12	62B	204	400	155.9	115.0	2.18	86	100
9	351	3?	62B	204	400	174.9	129.0	2.21	87	100

Code WW7 (UBR-62, Capsule A, As-Irradiated)

No.	Specimen Number	Layer	Capsule	Test Temp.		Energy		Lat. Exp.		Shear (%)
				(°C)	(°F)	(J)	(ft-lb)	(mm)	(mils)	
1	58	6	62A	-1	30	10.8	8.0	0.20	8	<100
2	63	11	62A	27	80	27.1	20.0	0.48	19	<100
3	47	8	62A	49	120	28.5	21.0	0.53	21	<100
4	43	4	62A	63	145	40.7	30.0	0.74	29	<100
5	49	10	62A	71	160	47.5	35.0	0.81	32	<100
6	41	2	62A	82	180	44.7	33.0	0.84	33	<100
7	57	5	62A	138	280	58.3	43.0	1.02	40	97
8	61	9	62A	204	400	59.7	44.0	1.19	47	100

Code WW7 (UBR-62, Capsule A, 399 C Annealed)

No.	Specimen Number	Layer	Capsule	Test Temp.		Energy		Lat. Exp.		Shear (%)
				(°C)	(°F)	(J)	(ft-lb)	(mm)	(mils)	
1	42	3	62A	-4	25	32.5	24.0	0.48	19	<100
2	54	2	62A	13	55	36.6	27.0	0.53	21	<100
3	45	6	62A	21	70	40.7	30.0	0.66	26	<100
4	59	7	62A	43	110	51.5	38.0	0.79	31	<100
5	51	12	62A	71	160	65.1	48.0	1.12	44	<100
6	62	10	62A	138	280	84.1	62.0	1.57	62	100
7	55	3	62A	204	400	88.1	65.0	1.48	55	100

Code WW7 (UBR-62, Capsule A, 454 C Annealed)

No.	Specimen Number	Layer	Capsule	Test Temp.		Energy		Lat. Exp.		Shear (%)
				(°C)	(°F)	(J)	(ft-lb)	(mm)	(mils)	
1	46	7	62A	-12	10	21.7	16.0	0.43	17	<100
2	44	5	62A	4	40	28.5	21.0	0.58	23	<100
3	64	12	62A	4	40	47.5	35.0	0.76	30	<100
4	48	9	62A	13	55	51.5	38.0	0.84	33	<100
5	56	4	62A	21	70	59.7	44.0	0.89	35	<100
6	16	1	62A	32	90	56.9	42.0	0.97	38	<100
7	60	8	62A	204	400	107.1	79.0	1.42	56	100
8	50	11	62A	204	400	100.3	74.0	2.01	79	100

Code WW4 (UBR-62, Capsule B, As-Irradiated)

No.	Specimen Number	Layer	Capsule	Test Temp. (°C)	Test Temp. (°F)	Energy (J)	Energy (ft-lb)	Lat. Exp. (mm)	Lat. Exp. (mils)	Shear (%)
1	170	6	62B	-34	-30	46.1	34.0	0.76	30	<100
2	172	8	62B	-18	0	14.9	11.0	0.25	10	<100
3	169	5	62B	4	40	36.6	27.0	0.64	25	<100
4	142	2	62B	16	60	39.3	29.0	0.69	27	<100
5	171	7	62B	27	80	56.9	42.0	0.94	37	<100
6	168	4	62B	49	120	71.9	53.0	1.22	48	<100
7	109	1	62B	138	280	101.7	75.0	1.50	59	<100
8	143	3	62B	204	400	141.0	104.0	1.70	67	100

Code WW4 (UBR-62, Capsule B, 399 C Annealed)

No.	Specimen Number	Layer	Capsule	Test Temp. (°C)	Test Temp. (°F)	Energy (J)	Energy (ft-lb)	Lat. Exp. (mm)	Lat. Exp. (mils)	Shear (%)
1	116	6	62B	-34	-30	46.1	34.0	0.76	30	<100
2	145	5	62B	-18	0	61.0	45.0	0.99	39	<100
3	115	7	62B	-12	10	63.7	47.0	1.02	40	<100
4	110	2	62B	-7	20	46.1	34.0	(ND)	(ND)	<100
5	112	4	62B	16	60	86.8	64.0	1.42	56	<100
6	141	1	62B	204	400	142.4	105.0	1.91	75	100

Code WW4 (UBR-62, Capsule B, 454 C Annealed)

No.	Specimen Number	Layer	Capsule	Test Temp. (°C)	Test Temp. (°F)	Energy (J)	Energy (ft-lb)	Lat. Exp. (mm)	Lat. Exp. (mils)	Shear (%)
1	146	6	62B	-48	-55	24.4	18.0	0.41	16	<100
2	147	7	62B	-34	-30	46.1	34.0	0.66	26	<100
3	114	6	62B	-29	-20	47.5	35.0	0.74	29	<100
4	167	3	62B	-12	10	66.4	49.0	1.04	41	<100
5	148	8	62B	-1	30	75.9	56.0	1.17	46	<100
6	144	4	62B	21	70	112.5	83.0	1.65	65	----
7	165	1	62B	204	400	154.6	114.0	1.52	60	100
8	166	2	62B	204	400	141.0	104.0	1.70	67	100

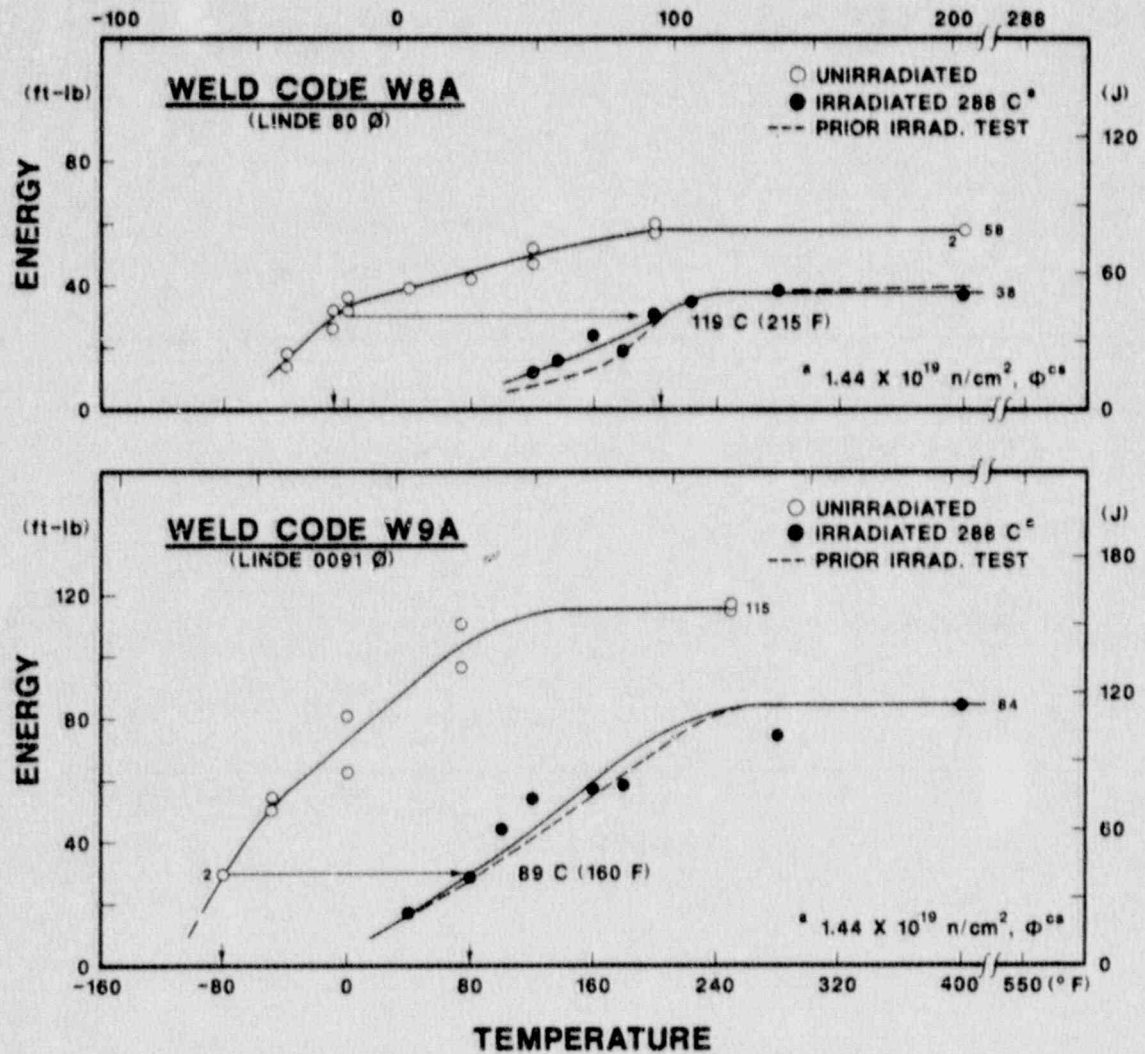


Fig. D-1 C_V notch ductility of Weld W8A and Weld W9A after irradiation to $1.44 \times 10^{19} \text{ n/cm}^2$ (UBR-62)

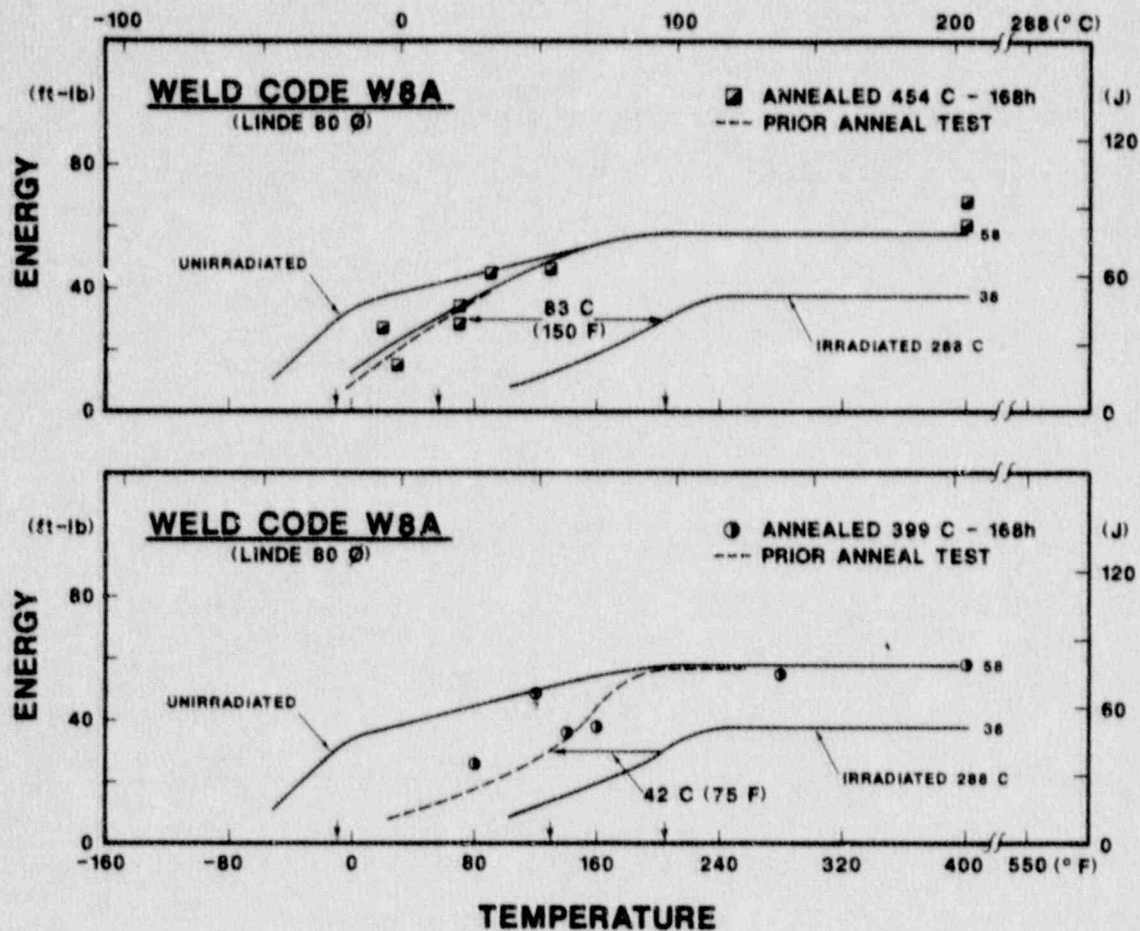


Fig. D-2 G_V notch ductility of Weld W8A after postirradiation annealing at 454°C or 399°C (UBR-62)

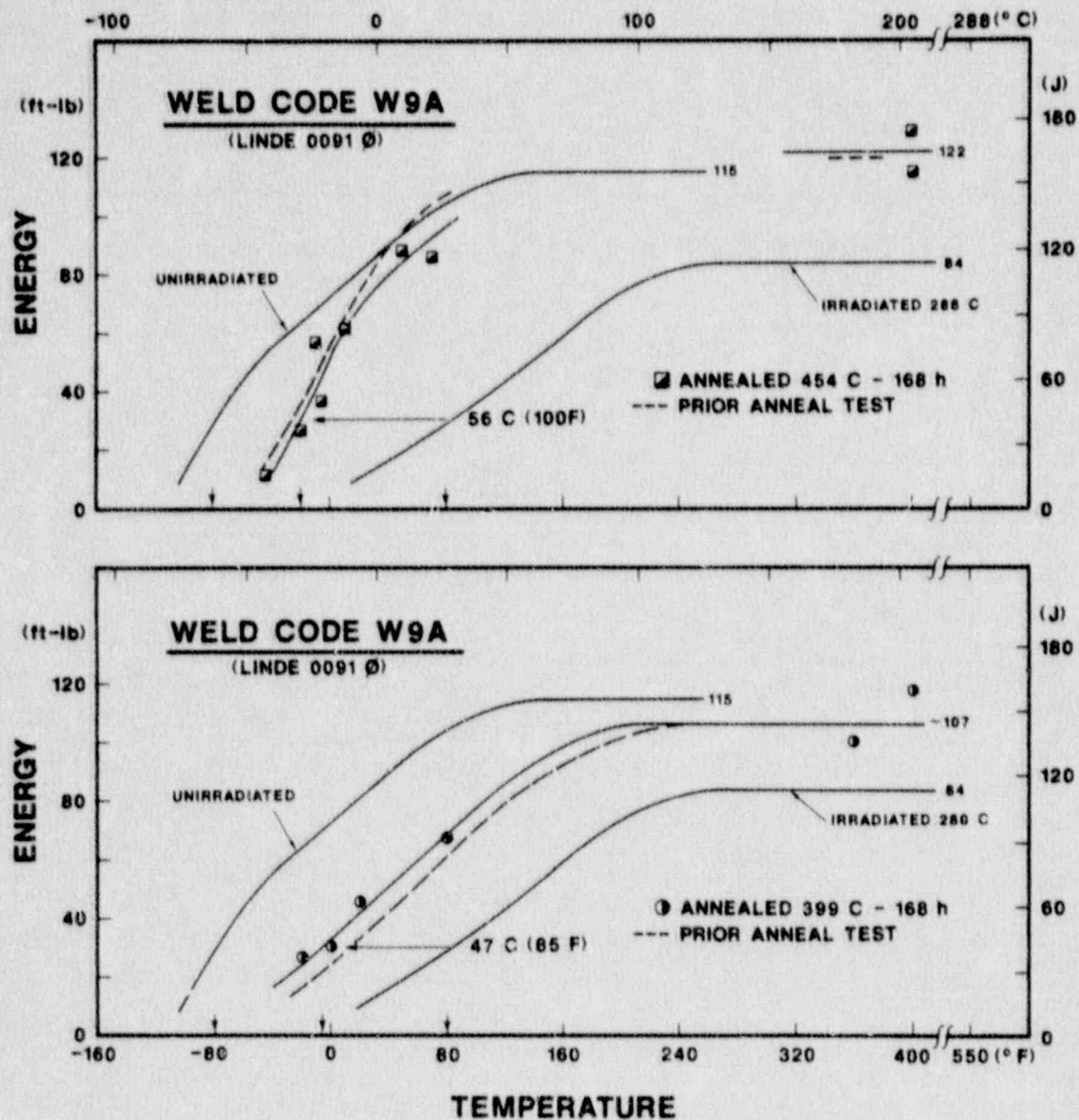


Fig. D-3 C_V notch ductility of Weld W9A after postirradiation annealing at 454°C or 399°C (UBR-62)

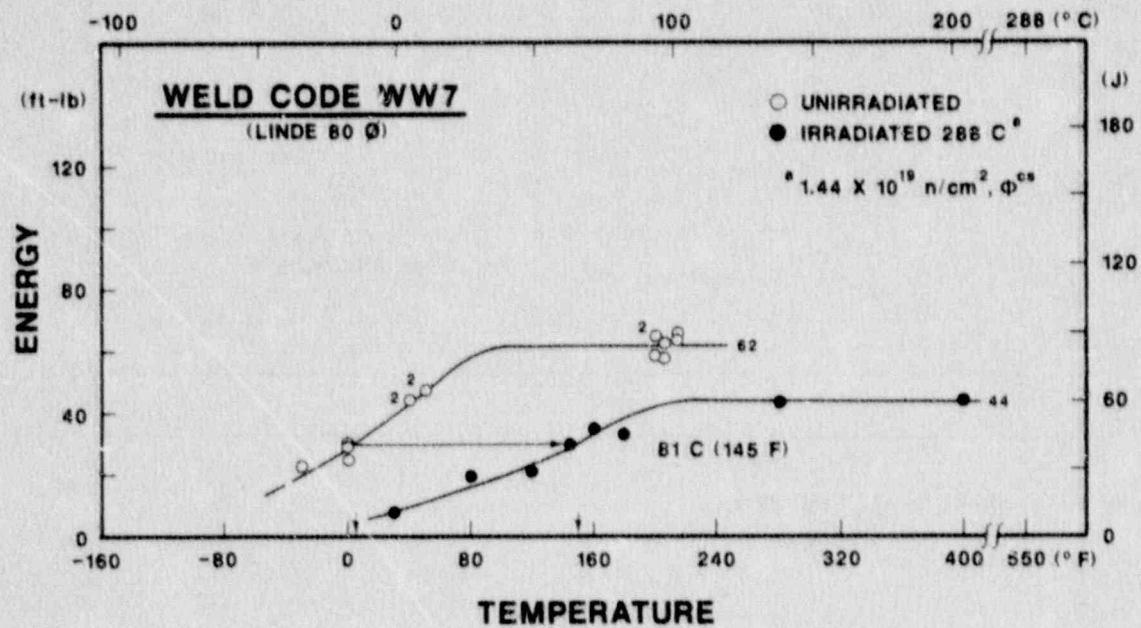


Fig. D-4 C_v notch ductility of Weld WW7 after irradiation to $1.44 \times 10^{19} \text{ n/cm}^2$ (UBR-62)

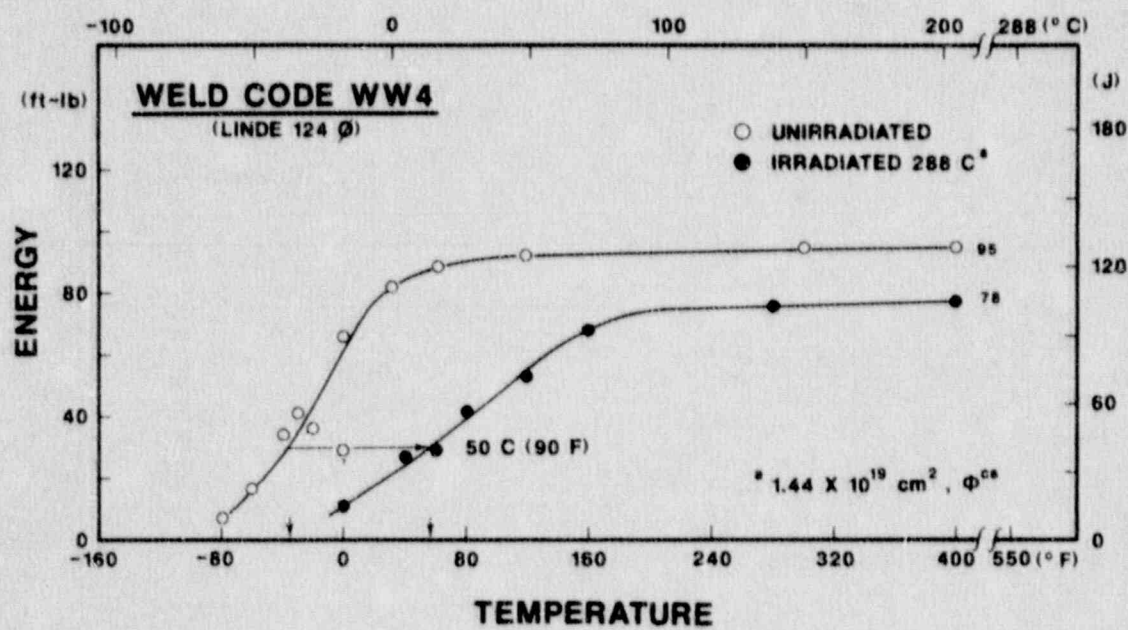


Fig. D-5 C_v notch ductility of Weld WW4 after irradiation to $1.44 \times 10^{19} \text{ n/cm}^2$ (UBR-62)

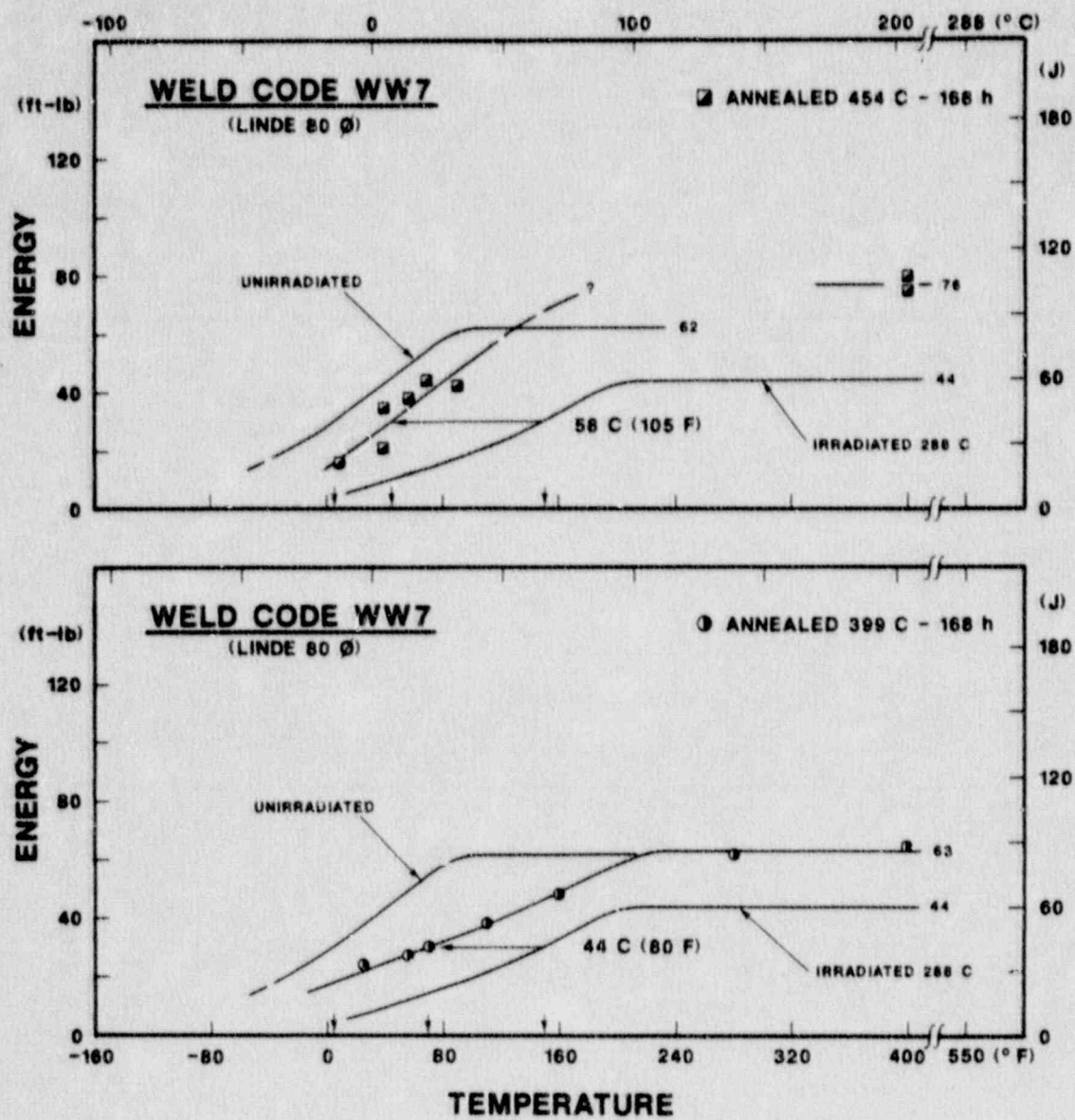


Fig. D-6 C_V notch ductility of Weld WW7 after postirradiation annealing at 454°C or 399°C (UBR-62)

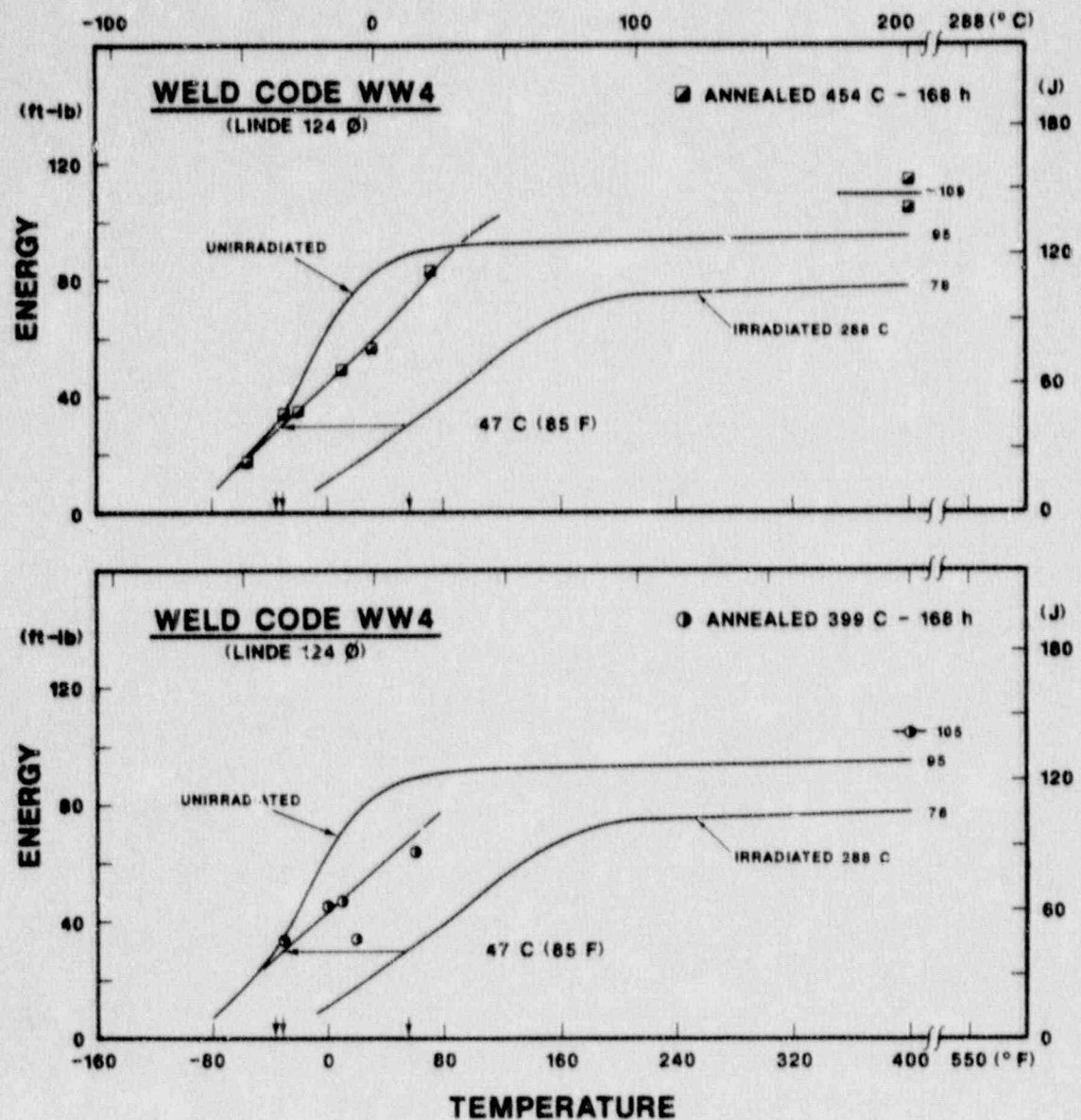


Fig. D-7 C_V notch ductility of Weld WW4 after postirradiation annealing at 454°C or 399°C (UBR-62)

Charpy-V Data from Irradiation Assembly UBR-70

(IAR Condition 1)

Code W8A (UBR-70, Capsule A, 399 C Annealed & Reirrad.)

No.	Specimen Number	Layer	Capsule	Test Temp. (°C)	Test Temp. (°F)	Energy (J)	Energy (ft-lb)	Lat. Exp. (mm)	Lat. Exp. (mils)	Shear (%)
1	441	9	70A	38	100	24.4	18.0	0.51	20	<100
2	439	7	70A	49	120	35.3	26.0	0.58	23	<100
3	436	4	70A	66	150	27.1	20.0	0.48	19	<100
4	434	2	70A	82	180	32.5	24.0	0.71	28	<100
5	444	12	70A	93	200	36.6	27.0	0.69	27	<100
6	517	1	70A	99	210	43.4	32.0	0.79	31	<100
7	440	8	70A	104	220	59.7	44.0	1.07	42	98
8	433	1	70A	116	240	54.2	40.0	0.94	37	<100
9	443	11	70A	149	300	59.7	44.0	0.86	34	100
10	438	6	70A	204	400	66.4	49.0	1.22	48	100
11	442	10	70A	204	400	56.9	42.0	1.09	43	100

Code W8A (UBR-70, Capsule B, 454 C Annealed & Reirrad.)

No.	Specimen Number	Layer	Capsule	Test Temp. (°C)	Test Temp. (°F)	Energy (J)	Energy (ft-lb)	Lat. Exp. (mm)	Lat. Exp. (mils)	Shear (%)
1	453	9	70B	-18	0	9.5	7.0	0.20	8	<100
2	34	10	70B	4	40	19.0	14.0	0.46	18	<100
3	520	4	70B	27	80	32.5	24.0	0.61	24	<100
4	47	11	70B	29	85	38.0	28.0	0.69	27	<100
5	454	10	70B	32	90	17.6	13.0	0.48	19	<100
6	451	7	70B	38	100	59.7	44.0	1.07	42	<100
7	450	6	70B	49	120	66.4	49.0	1.22	48	98
8	456	12	70B	49	120	46.1	34.0	0.97	38	<100
9	445	1	70B	57	135	52.9	39.0	1.19	47	<100
10	452	8	70B	66	150	70.5	52.0	1.50	59	<100
11	446	2	70B	82	180	59.7	44.0	1.14	45	<100
12	455	11	70B	204	400	71.9	53.0	1.52	60	100
13	448	4	70B	204	400	75.9	56.0	1.40	55	100

Code W9A (UBR-70, Capsule A, 399 C Annealed & Reirrad.)

No.	Specimen Number	Layer	Capsule	Test Temp. (°C)	Test Temp. (°F)	Energy (J)	Energy (ft-lb)	Lat. Exp. (mm)	Lat. Exp. (mils)	Shear (%)
1	361	1	70A	-18	0	25.8	19.0	0.36	14	----
2	366	6	70A	-7	20	32.5	24.0	0.51	20	<100
3	362	2	70A	4	40	31.2	23.0	0.58	23	<100
4	V18	---	70A	16	60	43.4	32.0	0.71	28	<100
5	367	7	70A	16	60	50.2	37.0	0.84	33	<100
6	372	12	70A	27	80	56.9	42.0	0.84	33	<100
7	368	8	70A	49	120	85.4	63.0	(ND)	(ND)	<100
8	369	9	70A	71	160	112.5	83.0	2.01	79	<100
9	371	11	70A	116	240	115.2	85.0	1.75	69	<100
10	364	4	70A	204	400	118.0	87.0	1.91	75	100
11	370	10	70A	204	400	119.3	88.0	1.60	63	100

Code W9A (UBR-70, Capsule B, 454 C Annealed & Reirrad.)

No.	Specimen Number	Layer	Capsule	Test Temp. (°C)	Test Temp. (°F)	Energy (J)	Energy (ft-lb)	Lat. Exp. (mm)	Lat. Exp. (mils)	Shear (%)
1	V21	---	70B	-40	-40	19.0	14.0	0.30	12	<100
2	383	11	70B	-18	0	43.4	32.0	0.66	26	<100
3	374	2	70B	-18	0	51.5	38.0	(ND)	(ND)	<100
4	23	11	70B	-18	0	48.8	36.0	0.74	29	<100
5	381	9	70B	-7	20	67.8	50.0	1.02	40	<100
6	373	1	70B	4	40	44.7	33.0	0.74	29	<100
7	382	10	70B	4	40	59.7	44.0	1.04	41	<100
8	378	6	70B	16	60	86.8	64.0	1.37	54	<100
9	384	12	70B	27	80	86.8	64.0	1.40	55	<100
10	379	7	70B	49	120	132.9	98.0	2.41	95	<100
11	380	8	70B	204	400	151.9	112.0	2.01	79	100
12	376	4	70B	204	400	154.6	114.0	1.57	62	100

Code WW7 (UBR-70, Capsule A, 399 C Annealed & Reirrad.)

No.	Specimen Number	Layer	Capsule	Test Temp. (°C)	Test Temp. (°F)	Energy (J)	Energy (ft-lb)	Lat. Exp. (mm)	Lat. Exp. (mils)	Shear (%)
1	77	12	70A	-18	0	16.3	12.0	0.28	11	<100
2	74	9	70A	4	40	19.0	14.0	0.28	11	<100
3	70	5	70A	27	80	29.8	22.0	0.53	21	<100
4	66	1	70A	32	90	27.1	20.0	0.53	21	---
5	67	2	70A	49	120	43.4	32.0	0.74	29	<100
6	71	6	70A	60	140	43.4	32.0	0.74	29	<100
7	78	13	70A	71	160	48.8	36.0	0.84	33	<100
8	73	8	70A	93	200	51.5	38.0	0.94	37	<100
9	69	4	70A	138	280	63.7	47.0	1.27	50	97
10	75	10	70A	204	400	70.5	52.0	1.37	54	100
11	72	7	70A	204	400	66.4	49.0	1.45	57	100

Code WW7 (UBR-70, Capsule B, 454 C Annealed & Reirrad.)

No.	Specimen Number	Layer	Capsule	Test Temp. (°C)	Test Temp. (°F)	Energy (J)	Energy (ft-lb)	Lat. Exp. (mm)	Lat. Exp. (mils)	Shear (%)
1	84	6	70B	-34	-30	8.1	6.0	0.15	6	<100
2	24	11	70B	-18	0	21.7	16.0	0.38	15	<100
3	86	8	70B	4	40	24.4	18.0	0.41	16	<100
4	91	13	70B	16	60	28.5	21.0	0.64	25	<100
5	82	4	70B	27	80	40.7	30.0	0.74	29	<100
6	87	9	70B	38	100	50.2	37.0	0.89	35	<100
7	80	2	70B	49	120	56.9	42.0	1.07	42	<100
8	83	5	70B	60	140	56.9	42.0	0.99	39	<100
9	90	12	70B	71	160	59.7	44.0	1.14	45	<100
10	20	7	70B	93	200	75.9	56.0	1.30	51	98
11	79	1	70B	138	280	73.2	54.0	1.35	53	98
12	85	7	70B	204	400	84.1	62.0	1.52	60	100
13	88	10	70B	204	400	85.4	63.0	1.55	61	100

Code WW4 (UBR-70, Capsule A, 399 C Annealed & Reirrad.)

No.	Specimen Number	Layer	Capsule	Test Temp. (°C)	Test Temp. (°F)	Energy (J)	Energy (ft-lb)	Lat. Exp. (mm)	Lat. Exp. (mils)	Shear (%)
1	86	2	70A	-18	0	23.0	17.0	0.53	21	<100
2	91	7	70A	-7	20	31.2	23.0	0.53	21	<100
3	88	4	70A	4	40	43.4	32.0	0.71	28	<100
4	90	6	70A	4	40	44.7	33.0	0.71	28	<100
5	153	5	70A	27	80	58.3	43.0	0.97	38	<100
6	159	3	70A	38	100	73.2	54.0	1.24	49	<100
7	156	8	70A	49	120	84.1	62.0	1.40	55	<100
8	85	1	70A	104	220	97.6	72.0	1.73	68	99
9	92	8	70A	149	300	120.7	89.0	2.18	86	100
10	149	1	70A	182	360	119.3	88.0	1.91	75	100
11	162	6	70A	182	360	111.2	82.0	2.24	88	100

Code WW4 (UBR-70, Capsule B, 454 C Annealed & Reirrad.)

No.	Specimen Number	Layer	Capsule	Test Temp. (°C)	Test Temp. (°F)	Energy (J)	Energy (ft-lb)	Lat. Exp. (mm)	Lat. Exp. (mils)	Shear (%)
1	99	7	70B	-40	-40	8.1	6.0	0.20	8	<100
2	161	5	70B	-23	-10	24.4	18.0	0.46	18	----
3	154	6	70B	-18	0	32.5	24.0	0.61	24	<100
4	151	3	70B	-7	20	50.2	37.0	0.89	35	<100
5	93	1	70B	4	40	48.8	36.0	0.94	37	<100
6	94	2	70B	16	60	62.4	46.0	1.07	42	<100
7	96	4	70B	27	80	71.9	53.0	1.12	44	<100
8	100	8	70B	49	120	107.1	79.0	1.73	68	<100
9	98	6	70B	104	220	120.7	89.0	2.06	81	<100
10	163	7	70B	182	360	127.4	94.0	2.08	82	100
11	157	1	70B	182	360	132.9	98.0	2.36	93	100

Charpy-V Data from Irradiation Assembly UBR-71

(IAR Condition 2)

Code WBA (UBR-71, Capsule A, 399 C Annealed & Reirrad.)

No.	Specimen Number	Layer	Capsule	Test Temp. (°C)	Test Temp. (°F)	Energy (J)	Energy (ft-lb)	Lat. Exp. (mm)	Lat. Exp. (mils)	Shear (%)
1	469	1	71A	38	100	24.4	18.0	0.46	18	<100
2	477	9	71A	54	130	33.9	25.0	0.61	24	<100
3	523	7	71A	77	170	46.1	34.0	0.81	32	<100
4	478	10	71A	88	190	27.1	20.0	0.58	23	<100
5	472	4	71A	93	200	32.5	24.0	0.64	25	<100
6	476	8	71A	104	220	59.7	44.0	0.99	39	<100
7	475	7	71A	104	220	56.9	42.0	1.27	50	100
8	470	2	71A	121	250	54.2	40.0	1.04	41	<100
9	480	12	71A	160	320	58.3	43.0	1.52	60	100
10	474	6	71A	204	400	61.0	45.0	1.24	49	100

Code WBA (UBR-71, Capsule B, 454 C Annealed & Reirrad.)

No.	Specimen Number	Layer	Capsule	Test Temp. (°C)	Test Temp. (°F)	Energy (J)	Energy (ft-lb)	Lat. Exp. (mm)	Lat. Exp. (mils)	Shear (%)
1	35	11	71B	-9	15	12.2	9.0	0.25	10	<100
2	489	9	71B	4	40	14.9	11.0	0.30	12	<100
3	490	10	71B	16	60	25.8	19.0	0.56	22	<100
4	487	7	71B	27	80	42.0	31.0	0.79	31	<100
5	48	12	71B	38	100	23.0	17.0	0.56	22	<100
6	482	2	71B	49	120	43.4	32.0	0.74	29	<100
7	524	8	71B	49	120	54.2	40.0	0.91	36	<100
8	492	12	71B	66	150	52.9	39.0	1.12	44	<100
9	486	6	71B	77	170	69.1	51.0	1.32	52	97
10	488	8	71B	104	220	78.6	58.0	1.22	48	99
11	484	4	71B	149	300	70.5	52.0	1.09	43	99
12	491	11	71B	204	400	78.6	58.0	1.12	44	100

Code W9A (UBR-71, Capsule A, 399 C Annealed & Reirrad.)

No.	Specimen Number	Layer	Capsule	Test Temp. (°C)	Test Temp. (°F)	Energy (J)	Energy (ft-lb)	Lat. Exp. (mm)	Lat. Exp. (mils)	Shear (%)
1	485	9	71A	-18	0	16.3	12.0	0.28	11	<100
2	488	4	71A	10	50	32.5	24.0	0.51	20	<100
3	486	10	71A	21	70	35.3	26.0	0.56	22	<100
4	398	2	71A	27	80	54.2	40.0	0.81	32	<100
5	484	8	71A	38	100	69.1	51.0	1.09	43	<100
6	482	6	71A	49	120	93.6	69.0	1.45	57	<100
7	V27	---	71A	66	150	88.1	65.0	1.32	52	<100
8	488	12	71A	88	190	92.2	68.0	1.80	71	<100
9	487	11	71A	160	320	119.3	88.0	1.75	69	100
10	397	1	71A	204	400	113.9	84.0	1.88	74	100
11	483	7	71A	204	400	139.6	103.0	2.24	88	100

Code W9A (UBR-71, Capsule B, 454 C Annealed & Reirrad.)

No.	Specimen Number	Layer	Capsule	Test Temp. (°C)	Test Temp. (°F)	Energy (J)	Energy (ft-lb)	Lat. Exp. (mm)	Lat. Exp. (mils)	Shear (%)
1	438	10	71B	-32	-25	24.4	18.0	0.38	15	<100
2	428	6	71B	-18	0	55.6	41.0	0.84	33	<100
3	422	2	71B	-12	10	47.5	35.0	0.71	28	<100
4	429	9	71B	-7	20	73.2	54.0	1.17	46	<100
5	431	11	71B	4	40	51.5	38.0	0.76	38	<100
6	427	7	71B	10	50	99.0	73.0	1.42	56	<100
7	424	4	71B	18	65	89.5	66.0	1.42	56	<100
8	432	12	71B	38	100	120.7	89.0	1.24	49	<100
9	V33	---	71B	66	150	124.7	92.0	1.83	72	100
10	155	11	71B	160	320	135.6	100.0	2.01	79	100
11	421	1	71B	204	400	151.9	112.0	2.39	94	100
12	426	6	71B	204	400	155.9	115.0	2.54	100	100

Code WW7 (UBR-71, Capsule A, 399 C Annealed & Reirrad.)

No.	Specimen Number	Layer	Capsule	Test Temp. (°C)	Test Temp. (°F)	Energy (J)	Energy (ft-lb)	Lat. Exp. (mm)	Lat. Exp. (mils)	Shear (%)
1	184	11	71A	2	35	20.3	15.0	0.38	15	<100
2	96	4	71A	27	80	29.8	22.0	0.48	19	<100
3	95	3	71A	41	105	33.9	25.0	0.56	22	<100
4	183	10	71A	49	120	29.8	22.0	0.56	22	<100
5	92	1	71A	57	135	38.0	28.0	0.76	30	<100
6	93	2	71A	66	150	51.5	38.0	0.84	33	<100
7	97	5	71A	74	165	54.2	40.0	0.94	37	<100
8	180	8	71A	88	190	51.5	38.0	0.91	36	<100
9	99	7	71A	127	260	70.5	52.0	1.14	45	99
10	181	9	71A	160	320	77.3	57.0	1.02	48	100
11	98	6	71A	204	400	73.2	54.0	1.04	41	100

Code WW7 (UBR-71, Capsule B, 454 C Annealed & Reirrad.)

No.	Specimen Number	Layer	Capsule	Test Temp. (°C)	Test Temp. (°F)	Energy (J)	Energy (ft-lb)	Lat. Exp. (mm)	Lat. Exp. (mils)	Shear (%)
1	26	13	71B	-18	0	19.0	14.0	0.53	21	<100
2	114	9	71B	10	50	31.2	23.0	0.74	29	<100
3	116	10	71B	27	80	33.9	25.0	0.64	25	<100
4	109	4	71B	27	80	28.5	21.0	0.53	21	<100
5	105	1	71B	43	110	40.7	30.0	0.69	27	<100
6	106	2	71B	49	120	56.9	42.0	1.02	40	<100
7	117	11	71B	54	130	55.6	41.0	0.97	38	----
8	108	3	71B	66	150	58.3	43.0	0.99	39	<100
9	113	8	71B	104	220	71.9	53.0	1.27	50	<100
10	112	7	71B	121	250	74.6	55.0	1.35	53	<100
11	22	9	71B	160	320	86.8	64.0	1.75	69	100
12	111	6	71B	204	400	96.3	71.0	1.91	75	<100
13	110	5	71B	204	400	81.3	60.0	1.42	56	100

Code WW4 (UBR-71, Capsule A, 399 C Annealed & Reirrad.)

No.	Specimen Number	Layer	Capsule	Test Temp. (°C)	Test Temp. (°F)	Energy (J)	Energy (ft-lb)	Lat. Exp. (mm)	Lat. Exp. (mils)	Shear (%)
1	138	6	71A	-12	10	38.0	28.0	0.81	32	<100
2	101	1	71A	10	50	32.5	24.0	0.56	22	<100
3	104	4	71A	10	50	38.0	28.0	0.61	24	<100
4	13	1	71A	27	80	48.8	36.0	0.76	30	<100
5	164	8	71A	32	90	59.7	44.0	0.99	39	<100
6	108	8	71A	49	120	78.6	58.0	1.27	50	<100
7	102	2	71A	60	140	70.5	52.0	1.17	46	<100
8	152	4	71A	71	160	88.1	65.0	1.45	57	<100
9	139	7	71A	160	320	115.2	85.0	1.88	74	100
10	6	6	71A	182	360	111.2	82.0	1.96	77	100
11	158	2	71A	204	400	104.4	77.0	1.70	67	100

Code WW4 (UBR-71, Capsule B, 454 C Annealed & Reirrad.)

No.	Specimen Number	Layer	Capsule	Test Temp. (°C)	Test Temp. (°F)	Energy (J)	Energy (ft-lb)	Lat. Exp. (mm)	Lat. Exp. (mils)	Shear (%)
1	132	8	71B	-9	15	44.7	33.0	0.74	29	<100
2	128	4	71B	-7	20	43.4	32.0	0.64	25	<100
3	155	7	71B	4	40	39.3	29.0	0.74	29	<100
4	26	2	71B	16	60	31.2	23.0	0.58	23	<100
5	130	6	71B	27	80	67.8	50.0	1.12	44	<100
6	37	1	71B	29	85	56.9	42.0	0.91	36	<100
7	160	4	71B	38	100	77.3	57.0	1.83	72	<100
8	125	1	71B	66	150	70.5	52.0	1.30	51	<100
9	126	2	71B	71	160	81.3	60.0	1.42	56	<100
10	131	7	71B	160	320	138.3	102.0	1.73	68	100
11	150	2	71B	204	400	122.0	90.0	1.93	76	<100

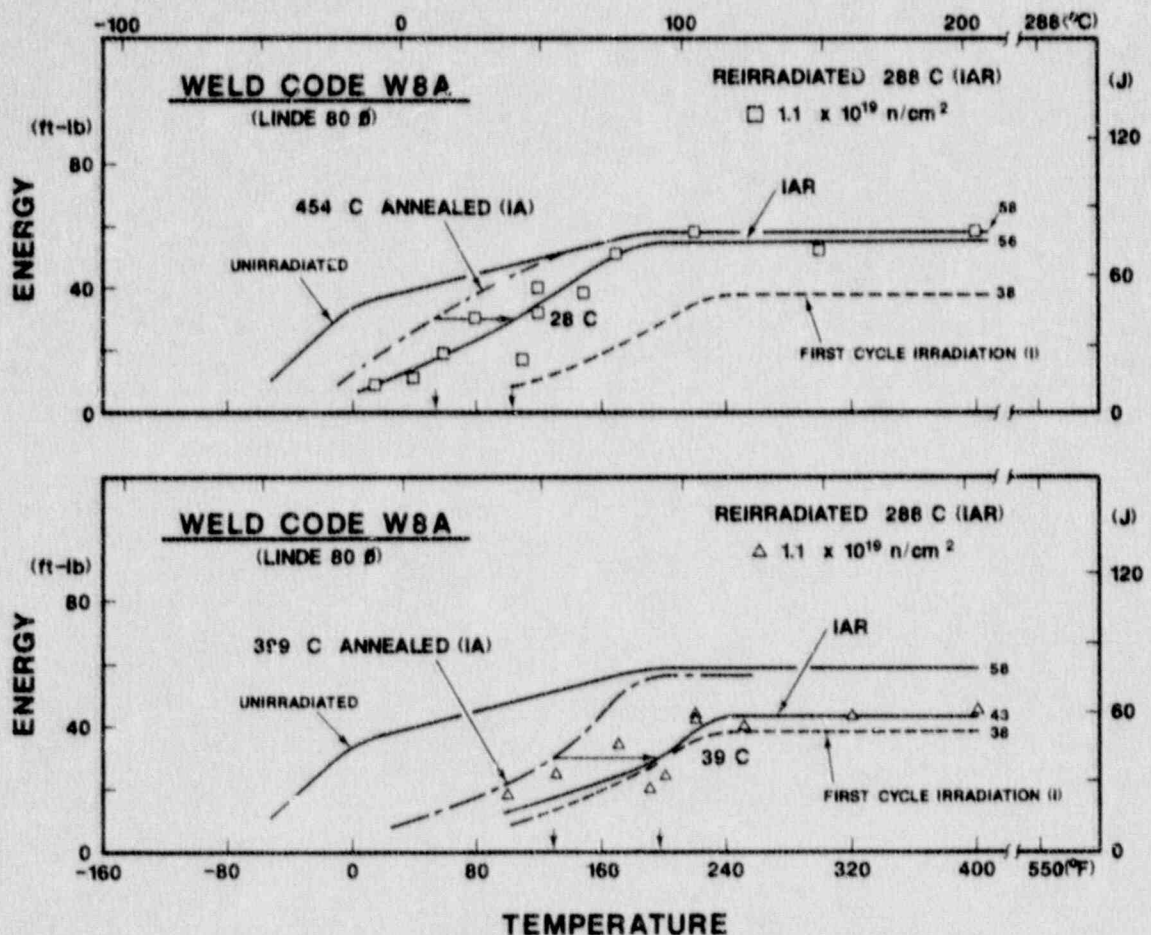


Fig. D-8 C_v notch ductility of Weld W8A after reirradiation by $1.1 \times 10^{19} \text{ n/cm}^2$ following a 454°C or 399°C intermediate anneal (UBR-71)

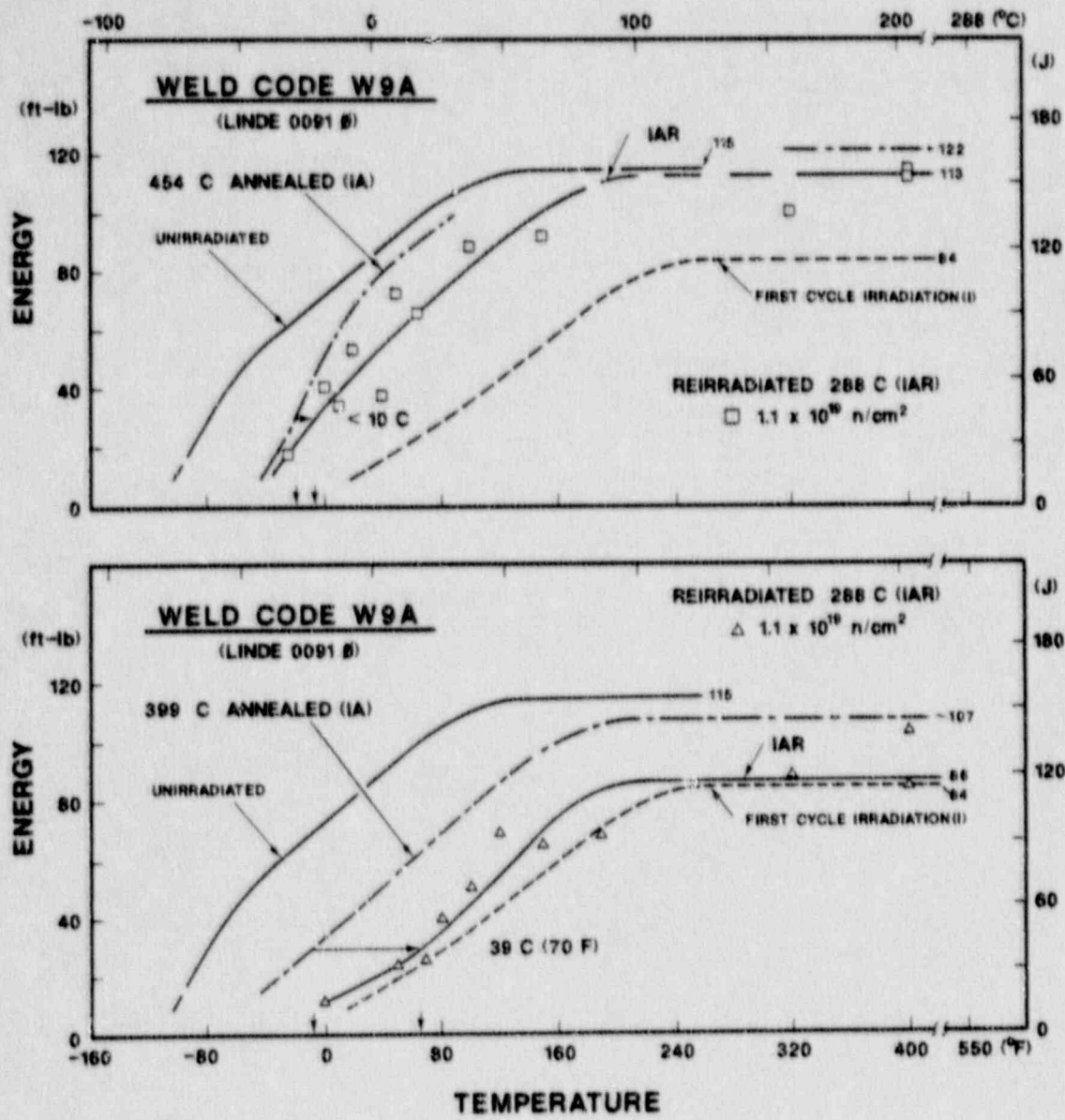


Fig. D-9 C_V notch ductility of Weld W9A after reirradiation by $1.1 \times 10^{19} \text{ n/cm}^2$ following a 454°C or 399°C intermediate anneal (UBR-71)

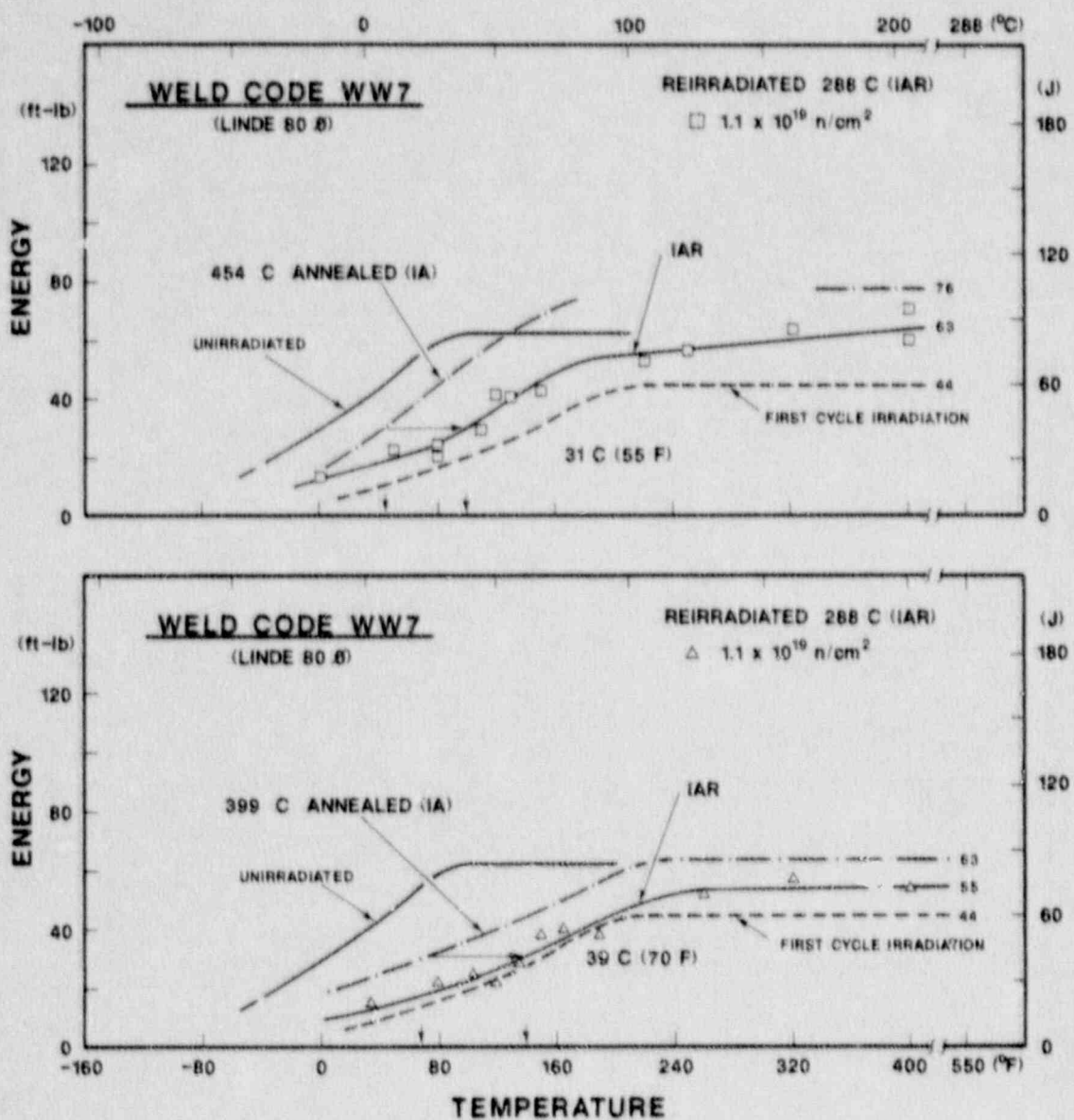


Fig. D-10 C_V notch ductility of Weld WW7 after reirradiation by $1.1 \times 10^{19} \text{ n/cm}^2$ following a 454°C or 399°C intermediate anneal (UBR-71)

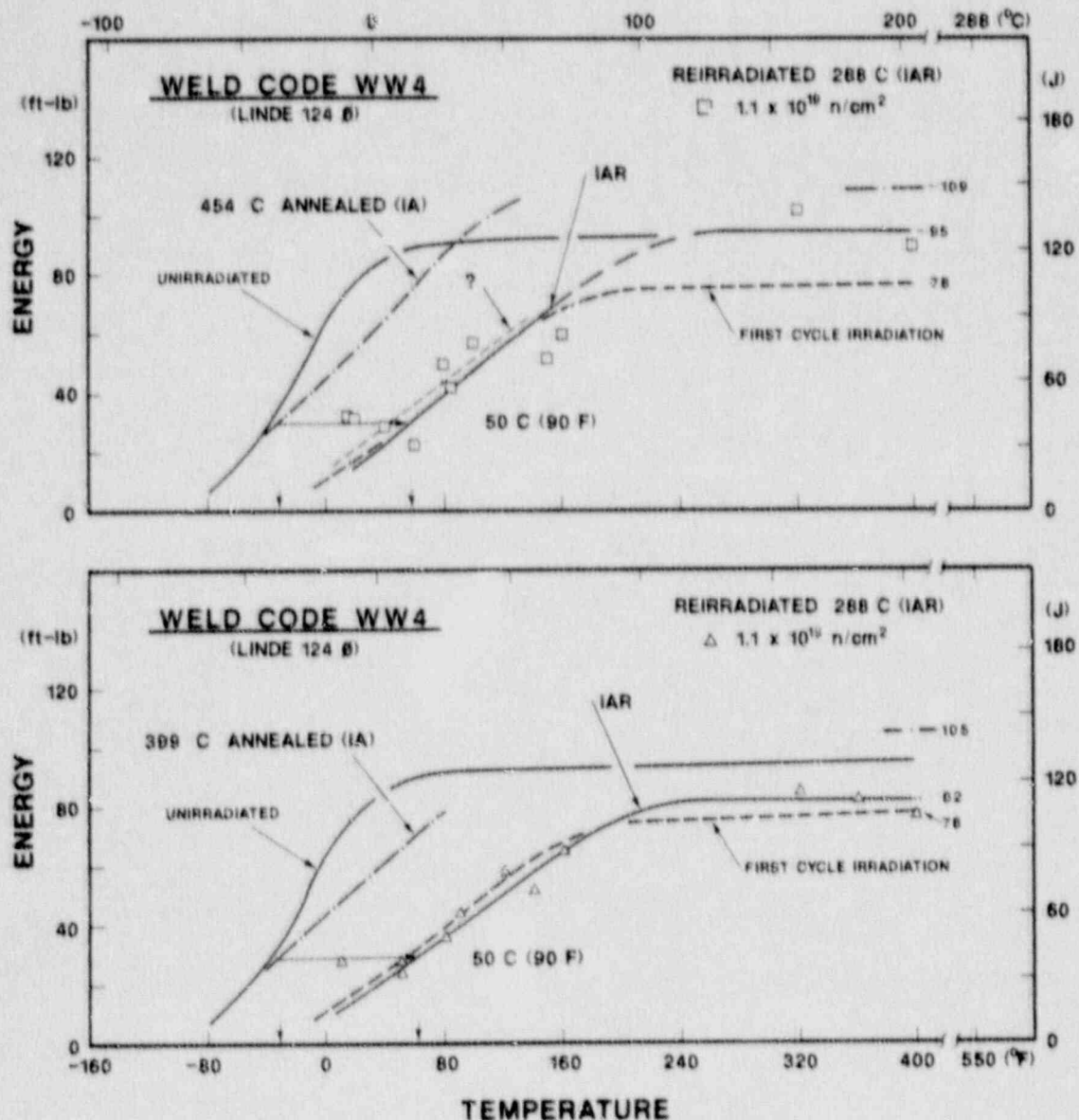


Fig. D-11 G_V notch ductility of Weld WW4 after reirradiation by $1.1 \times 10^{19} \text{ n/cm}^2$ following a 454°C or 399°C intermediate anneal (UBR-71)

Charpy-V Data from Irradiation Assembly UBR-72

(As-Irradiated Condition)

Code W8A (UBR-72, Capsule A, As-Irradiated)

No.	Specimen Number	Layer	Capsule	Test Temp. (°C)	Test Temp. (°F)	Energy (J)	Energy (ft-lb)	Lat. Exp. (mm)	Lat. Exp. (mils)	Shear (%)
1	513	9	72A	27	80	16.3	12.0	0.33	13	<100
2	*515	11	72A	27	80	43.4	32.0	0.84	33	<100
3	510	6	72A	49	120	31.2	23.0	0.48	19	<100
4	506	2	72A	60	140	24.4	18.0	0.48	19	<100
5	516	12	72A	71	160	31.2	23.0	0.53	21	<100
6	588	5	72A	82	180	32.5	24.0	0.64	25	<100
7	512	8	72A	93	200	43.4	32.0	0.86	34	<100
8	511	?	72A	104	220	52.9	39.0	0.97	38	<100
9	514	10	72A	121	250	47.5	35.0	0.81	32	99
10	505	1	72A	204	400	54.2	40.0	1.14	45	100
11	527	11	72A	204	400	51.5	38.0	1.12	44	100

* Post Irradiation Annealed at 454°C (-168 hr)

Code W9A (UBR-72, Capsule A, As-Irradiated)

No.	Specimen Number	Layer	Capsule	Test Temp. (°C)	Test Temp. (°F)	Energy (J)	Energy (ft-lb)	Lat. Exp. (mm)	Lat. Exp. (mils)	Shear (%)
1	*352	4	72A	-34	-30	23.0	17.0	0.36	14	<100
2	*357	9	72A	-29	-20	63.7	47.0	0.91	36	<100
3	356	8	72A	-23	-10	13.6	10.0	0.13	5	<100
4	360	12	72A	4	40	16.3	12.0	0.15	6	<100
5	354	6	72A	27	80	43.4	32.0	0.74	29	<100
6	358	10	72A	32	90	38.0	28.0	0.61	24	<100
7	350	4	72A	54	130	67.8	50.0	1.07	42	<100
8	349	1	72A	77	170	86.8	64.0	1.17	46	<100
9	V15	---	72A	121	250	111.2	82.0	2.11	83	<100
10	359	11	72A	204	400	116.6	86.0	1.42	56	100
11	355	7	72A	204	400	116.6	86.0	1.78	70	99

* Post Irradiation Annealed at 454°C (-168 hr)

Code WW4 (UBR-72, Capsule A, As-Irradiated)

No.	Specimen Number	Layer	Capsule	Test Temp. (°C)	Test Temp. (°F)	Energy (J)	Energy (ft-lb)	Lat. Exp. (mm)	Lat. Exp. (mils)	Shear (%)
1	136	4	72A	-18	0	24.4	18.0	0.41	16	<100
2	52	4	72A	-7	20	33.9	25.0	0.69	27	<100
3	134	2	72A	4	40	42.0	31.0	0.79	31	<100
4	50	2	72A	21	70	39.3	29.0	0.66	26	<100
5	133	1	72A	27	80	54.2	40.0	0.94	37	<100
6	106	6	72A	32	90	66.4	49.0	1.14	45	<100
7	140	8	72A	49	120	88.1	65.0	1.47	58	<100
8	19	7	72A	93	200	107.1	79.0	1.70	67	100
9	107	7	72A	204	400	113.9	84.0	2.18	86	100
10	39	3	72A	204	400	101.7	75.0	2.01	79	99

Code WW7 (UBR-72, Capsule A, As-Irradiated)

No.	Specimen Number	Layer	Capsule	Test Temp. (°C)	Test Temp. (°F)	Energy (J)	Energy (ft-lb)	Lat. Exp. (mm)	Lat. Exp. (mils)	Shear (%)
1	118	1	72A	-18	0	5.4	4.0	0.08	3	<100
2	*121	4	72A	-7	20	29.8	22.0	0.51	20	<100
3	*130	13	72A	10	50	46.1	34.0	0.91	36	<100
4	119	2	72A	27	80	24.4	18.0	(ND)	(ND)	<100
5	126	9	72A	49	120	31.2	23.0	0.66	26	<100
6	123	6	72A	66	150	47.5	35.0	(ND)	(ND)	<100
7	129	12	72A	77	170	48.8	36.0	0.94	37	<100
8	125	8	72A	121	250	59.7	44.0	1.04	41	<100
9	127	10	72A	204	400	67.8	50.0	1.24	49	100
10	124	7	72A	204	400	69.1	51.0	1.45	57	99

* Post Irradiation Annealed at 454°C (-168 hr)

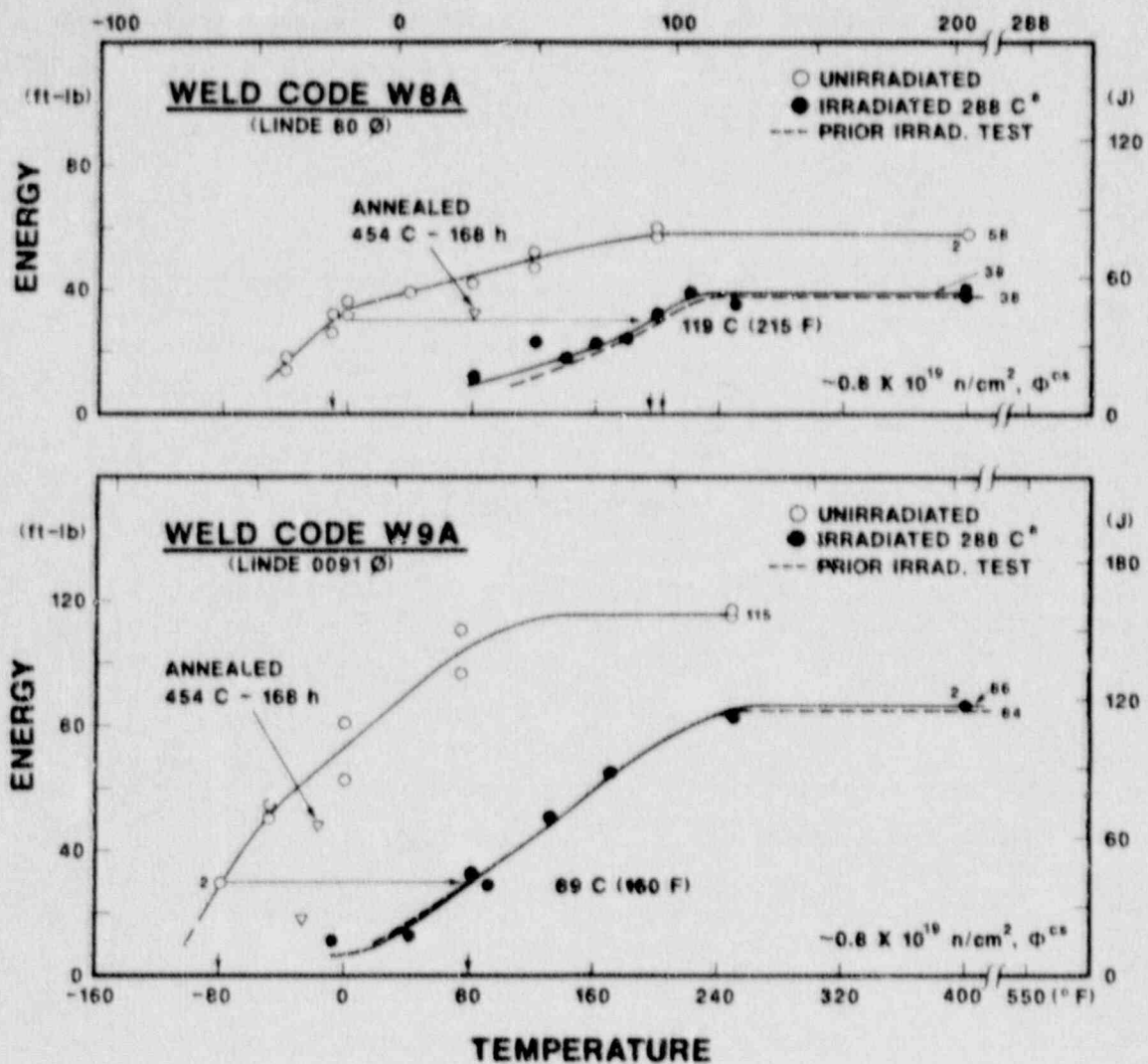


Fig. D-12 C_v notch ductility of Weld W8A and Weld W9A after irradiation to $1.06 \times 10^{19} \text{ n/cm}^2$ (UBR-72)

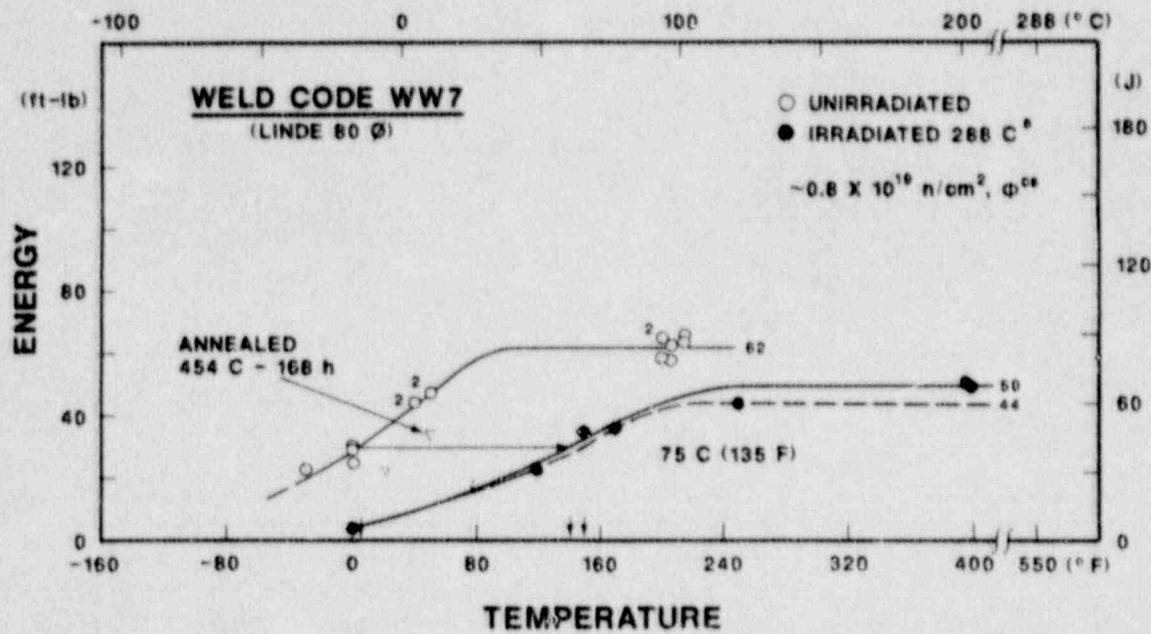


Fig. D-13 C_V notch ductility of Weld WW7 after irradiation to $1.06 \times 10^{19} \text{ n/cm}^2$ (UBR-72)

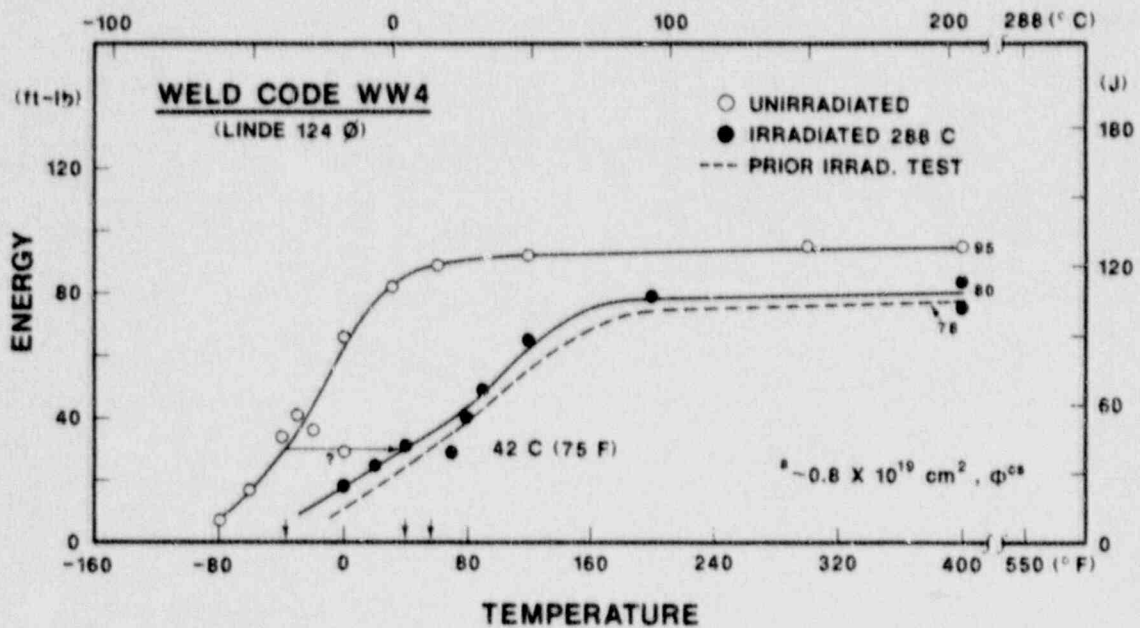


Fig. D-14 C_V notch ductility of Weld WW4 after irradiation to $1.06 \times 10^{19} \text{ n/cm}^2$ (UBR-72)

APPENDIX E

Computer Curve Fittings of Charpy-V Test Results
(Specimen Energy Absorption vs. Temperature)

OVERVIEW

The data curve fitting procedure employed the hyperbolic tangent (Tanh) curve fitting method as given by:

$$C_v = A + B \tanh \frac{T - T_0}{C}$$

Parameters A, B, C and T_0 are determined from non-linear regression analysis.

The quality of the fit to each data set generally depends upon the number of specimens tested and the availability of data defining the upper shelf and lower shelf for the data set. For many of the present data sets, both requirements are satisfied and an acceptable curve fit results. In other cases, either few tests were conducted or the data did not adequately define the lower shelf for the data set. For such cases, the lower shelf from a standard Tanh fit gives a lower shelf which is either above 27 J (20 ft-lb) or negative. Since such results are not satisfactory from either engineering or aesthetic standpoints, two modified curve fits can be applied. One (Case A) is illustrated for certain data sets of the plate Code 68B, 5C and 6A materials.

Case A is the result obtained when four fictitious data points with 7 J (5 ft-lb) of energy absorption are added at a temperature that is 28°C (50°F) below the intercept with the abscissa, of a line representing a linearized transition region. The line in this case is an eyeball fit to the data; the choice of a larger temperature shift (up to 56°C or 100°F) was found not to influence the result appreciably. Case B represents use of a fixed lower shelf of 7 J (5 ft-lb); this lower shelf is attained at a temperature of $-\infty$.

The use of the modified curve fits serve to force the curves to a reasonably low, positive value in the lower shelf region. This device is particularly useful for those cases where data are lacking in the lower shelf region for guiding the computer in its setting of bounding conditions. It should be noted that the American Society for Testing and Materials has not issued a standard method or a standard guide for curve-fitting C_v data for the irradiated condition.

Within this appendix, the curvefit sheet immediately following the data table represents a standard evaluation using the Tanh equation. The second curvefit sheet if present, gives the Case A results. For Case A, the fictitious data points are denoted by "O" on the graph and "*" in the data tabulation on the curvefit sheet. Table E-1 compares the 41-J temperatures indicated by the hand-drawn curves from Table 4. (See main text.)

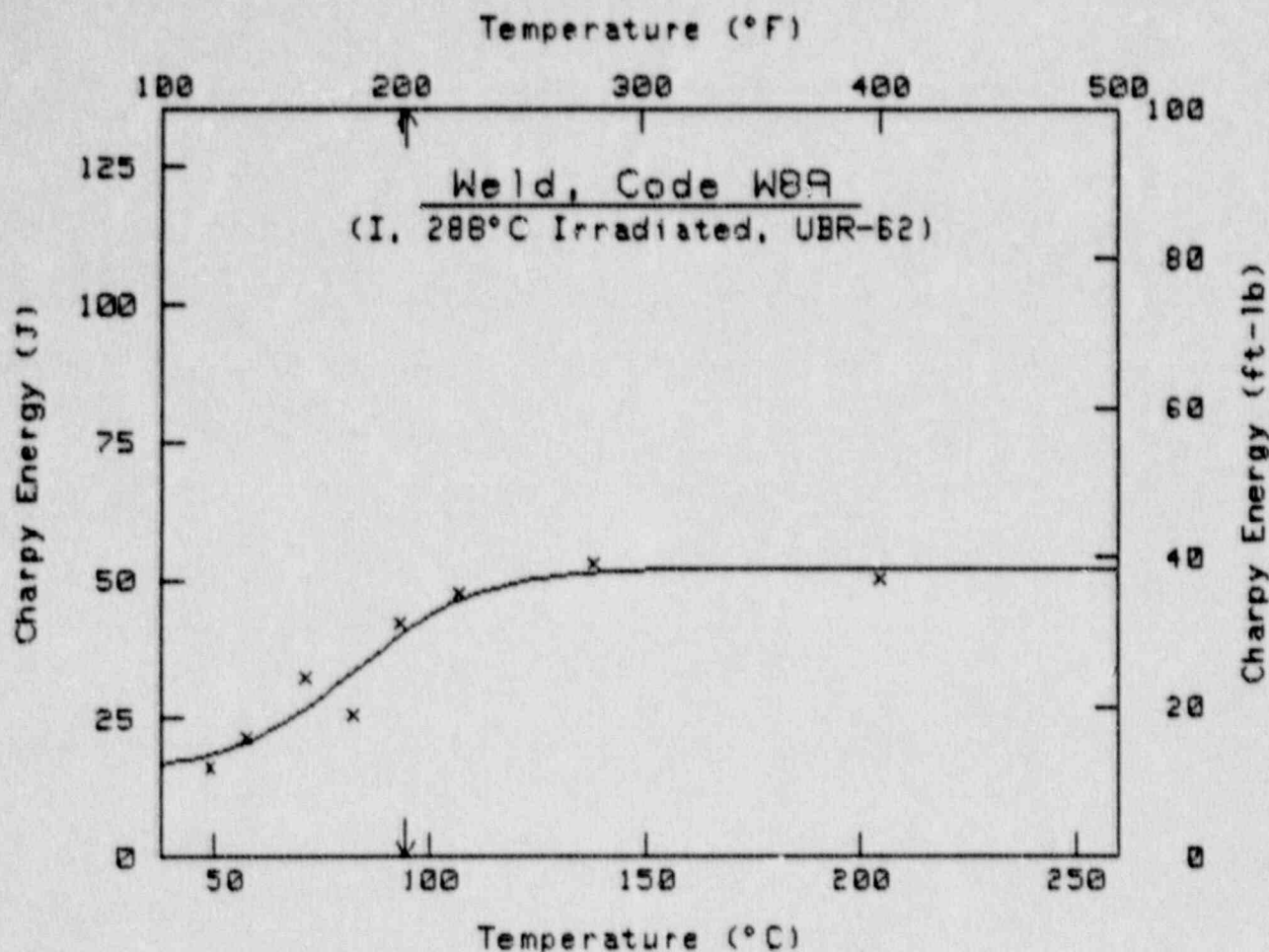
Table E-1 Comparison of Charpy-V Transition Temperature Indications From Two Data Curve Fitting Methods

Weld	Test Condition	C _V 41-J Transition Temperature (°C)			
		Hand-Drawn Curve (a)	Computer-Fit Curve (b)	Difference (a-b)	
W8A	I ₂	91	90.7 (92.4) ^a	0.3	(-1.4) ^a
	I ₁	96	94.6	1.4	
	IAR ₁ (399)	93	96.8 (84.7)	-3.8	(1.3)
	IAR ₂ (399)	~93	..(b) (80.5)	..(b)	(12.5)
	IAR ₁ (454)	35	35.0	0.0	
	IAR ₂ (454)	41	41.5	-0.5	
W9A	I ₂	27	30.5 (29.2)	+3.5	(-2.2)
	I ₁	27	20.8	6.2	
	IAR ₁ (399)	10	11.4	-1.4	
	IAR ₂ (399)	18	14.2	3.8	
	IAR ₁ (454)	-23	-20.6	+2.4	
	IAR ₂ (454)	-21	-22.2	1.2	
WW7	I ₂	60	47.9	12.1	
	I ₁	66	64.4	1.6	
	IAR ₁ (399)	54	54.2	-0.2	
	IAR ₂ (399)	60	57.2	2.8	
	IAR ₁ (454)	27	27.6	-0.6	
	IAR ₂ (454)	38	34.8	3.2	
WW4	I ₂	4	15.0 (8.7)	-11.0	(-4.7)
	I ₁	13	1.1	11.9	
	IAR ₁ (399)	2	1.5	0.5	
	IAR ₂ (399)	16	11.0 (10.7)	5.0	(5.3)
	IAR ₁ (454)	-7	-7.4	-0.4	
	IAR ₂ (454)	16	-10.7 (0.2)	26.7	(15.8)

^a Value using computer force-fitting procedure.

^b Not established.

Computer Curve Fittings of Data from Irradiation Assembly UBR-62



$$Cv = A + B \tanh[(T - T_0)/C]$$

	English	Metric
A	24.85 ft-lb	33.69 J
B	13.67 ft-lb	18.53 J
C	53.08 $^{\circ}$ F	29.49 $^{\circ}$ C
T ₀	181.30 $^{\circ}$ F	82.94 $^{\circ}$ C

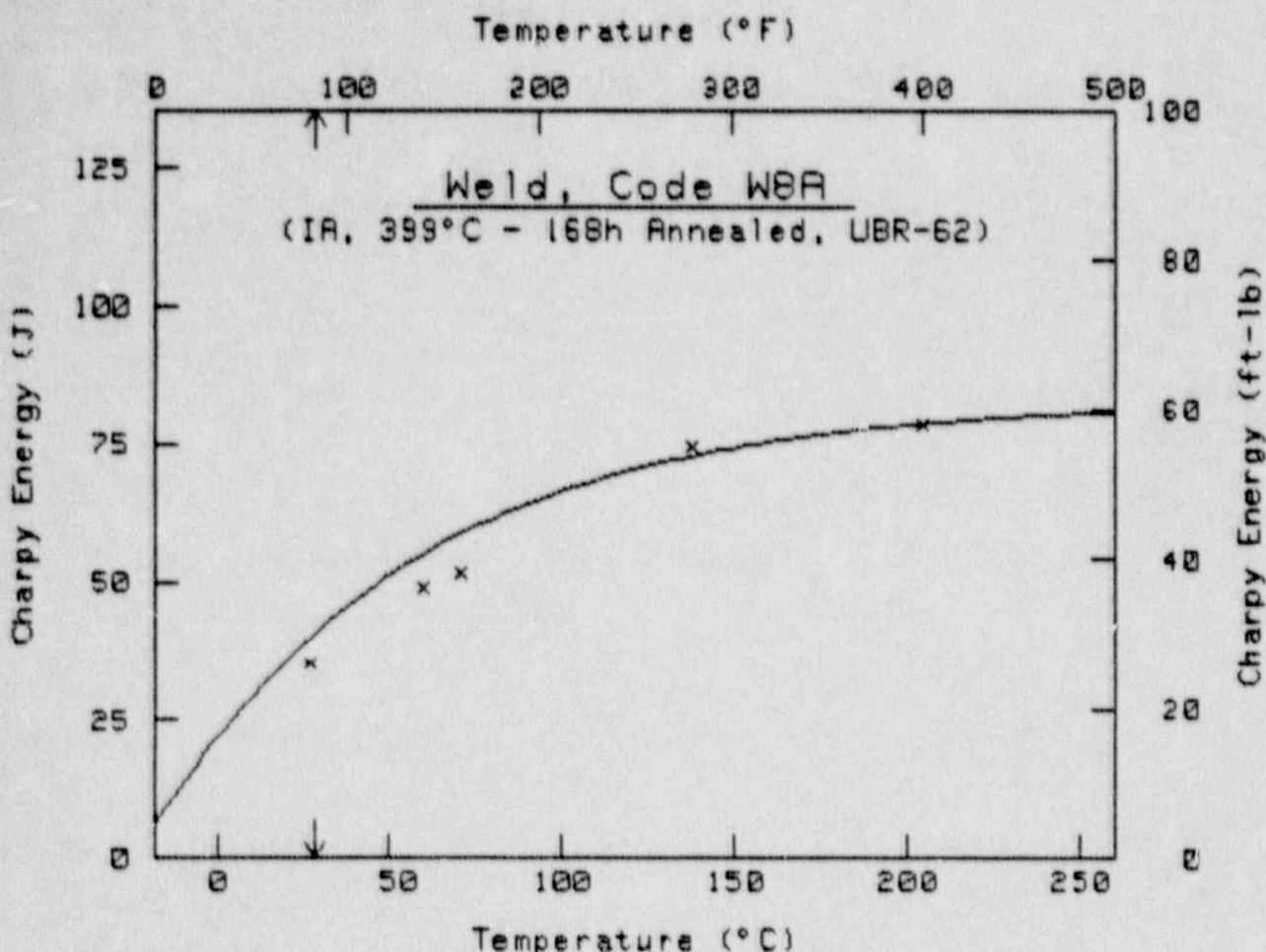
$$Cv = 30 \text{ ft-lb (41 J)} \text{ at } T = 202.3 \text{ }^{\circ}\text{F} \quad 94.6 \text{ }^{\circ}\text{C}$$

Upper Shelf Energy = 38.5 ft-lb 52.2 J

PT #	Temp ($^{\circ}$ F)	Energy (ft-lb)
1	120	12.0
2	135	16.0
3	160	24.0
4	180	19.0
5	200	31.0
6	225	35.0
7	280	39.0
8	400	37.0

O = Fictitious Point Added

* = Test Point Not Included



$$Cu = A + B \tanh[(T - T_0)/C]$$

	English	Metric
A	-771.73 ft-lb	-1046.32 J
B	832.87 ft-lb	1129.22 J
C	$272.15 \text{ }^{\circ}\text{F}$	$151.20 \text{ }^{\circ}\text{C}$
T_0	$-455.61 \text{ }^{\circ}\text{F}$	$-270.89 \text{ }^{\circ}\text{C}$

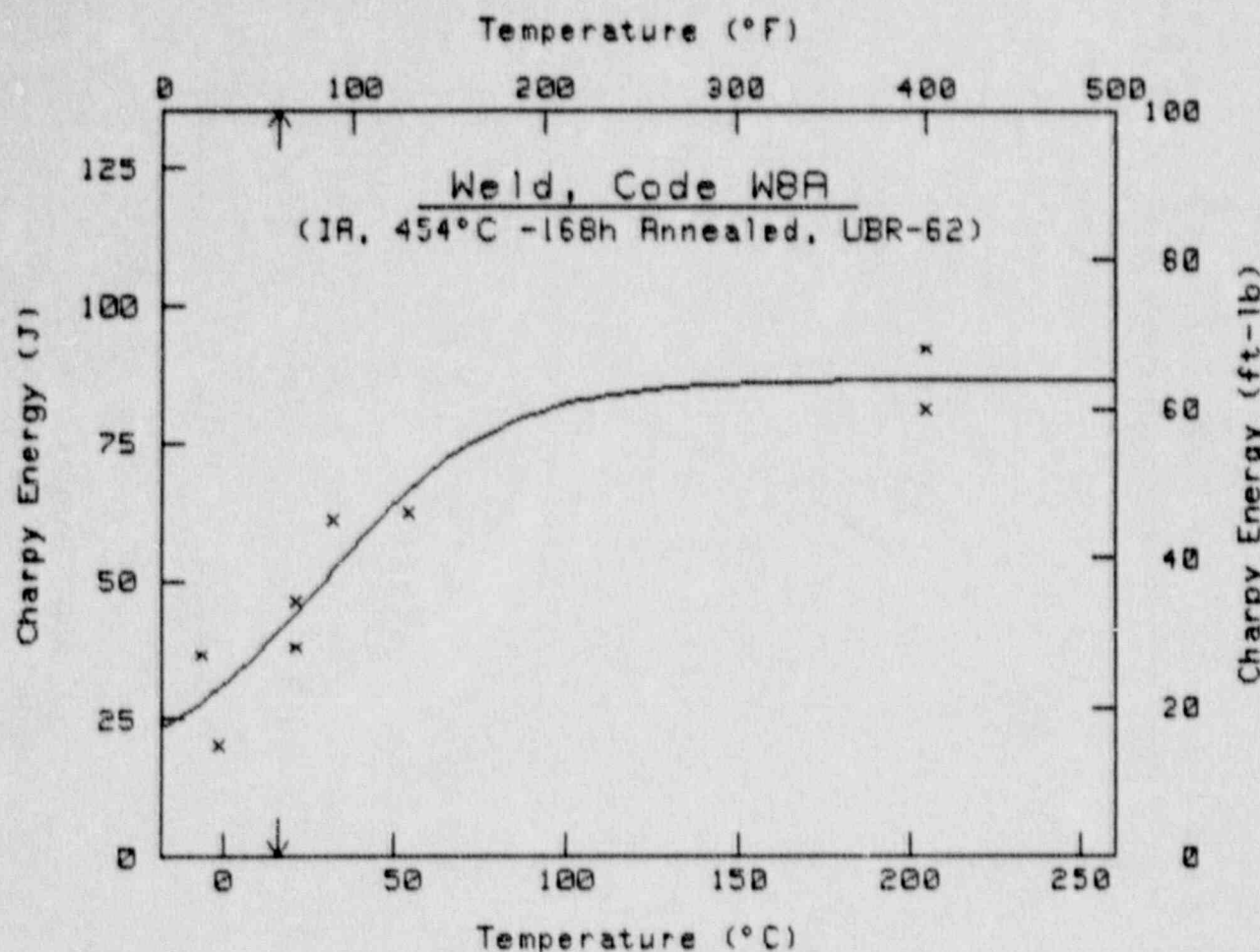
$$Cu = 30 \text{ ft-lb (41 J) at } T = \quad 83.3 \text{ }^{\circ}\text{F} \quad 28.5 \text{ }^{\circ}\text{C}$$

Upper Shelf Energy = 61.1 ft-lb 82.9 J

PT #	Temp ($^{\circ}\text{F}$)	Energy (ft-lb)
1	80	26.0
2	120	49.0
3	140	36.0
4	160	38.0
5	280	55.0
6	400	58.0

0 = fictitious Point Added

* = Test Point Not Included



$$C_U = A + B \tanh[(T - T_0)/C]$$

	English	Metric
A	36.78 ft-lb	49.87 J
B	27.06 ft-lb	36.69 J
C	93.15 $^{\circ}$ F	51.75 $^{\circ}$ C
T ₀	84.71 $^{\circ}$ F	29.28 $^{\circ}$ C

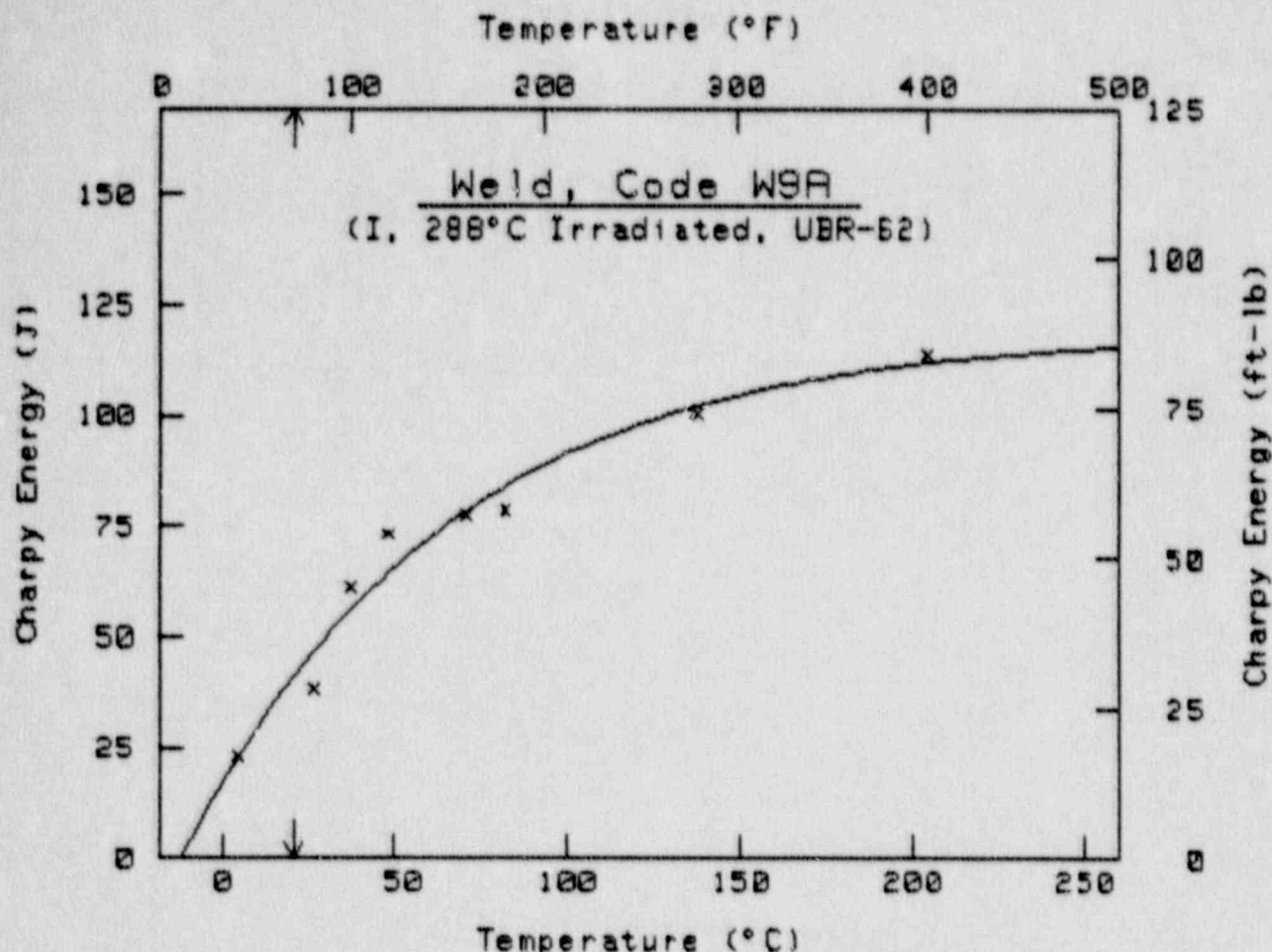
$$C_U = 38 \text{ ft-lb (41 J)} \text{ at } T = 68.8 \text{ }^{\circ}\text{F} \quad 16.0 \text{ }^{\circ}\text{C}$$

Upper Shelf Energy = 63.8 ft-lb 86.6 J

PT #	Temp ($^{\circ}$ F)	Energy (ft-lb)
1	20	27.8
2	30	15.0
3	70	34.0
4	70	28.0
5	90	45.0
6	130	46.0
7	400	68.0
8	400	68.0

0 = Fictitious Point Added

* = Test Point Not Included



$$C_U = A + B \tanh[(T - T_0)/C]$$

	English	Metric
A	-546.18 ft-lb	-740.41 J
B	633.72 ft-lb	859.21 J
C	266.95 $^{\circ}$ F	148.31 $^{\circ}$ C
T ₀	-336.88 $^{\circ}$ F	-204.93 $^{\circ}$ C

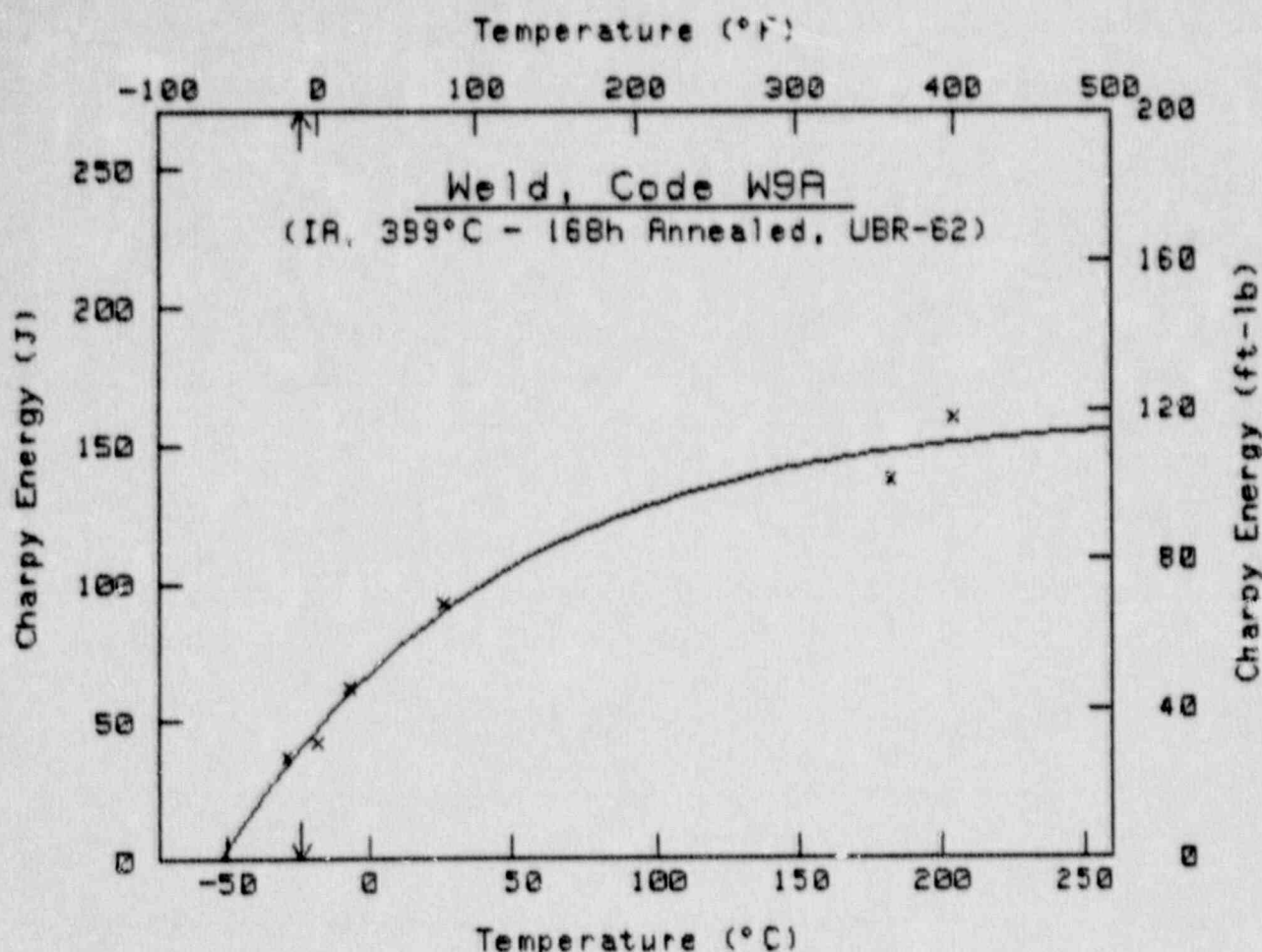
$$C_U = 38 \text{ ft-lb (41 J)} \text{ at } T = 69.5 \text{ }^{\circ}\text{F} \quad 20.8 \text{ }^{\circ}\text{C}$$

Upper Shelf Energy = 87.6 ft-lb 118.8 J

PT #	Temp ($^{\circ}$ F)	Energy (ft-lb)
1	40	17.0
2	80	28.0
3	100	45.0
4	120	54.0
5	160	57.0
6	180	58.0
7	280	74.0
8	400	84.0

0 = Fictitious Point Added

* = Test Point Not Included



$$Cu = A + B \tanh[(T - T_0)/C]$$

	English	Metric
A	-600.19 ft-lb	-813.74 J
B	718.93 ft-lb	974.74 J
C	329.82 $^{\circ}$ F	182.79 $^{\circ}$ C
T ₀	-458.47 $^{\circ}$ F	-272.48 $^{\circ}$ C

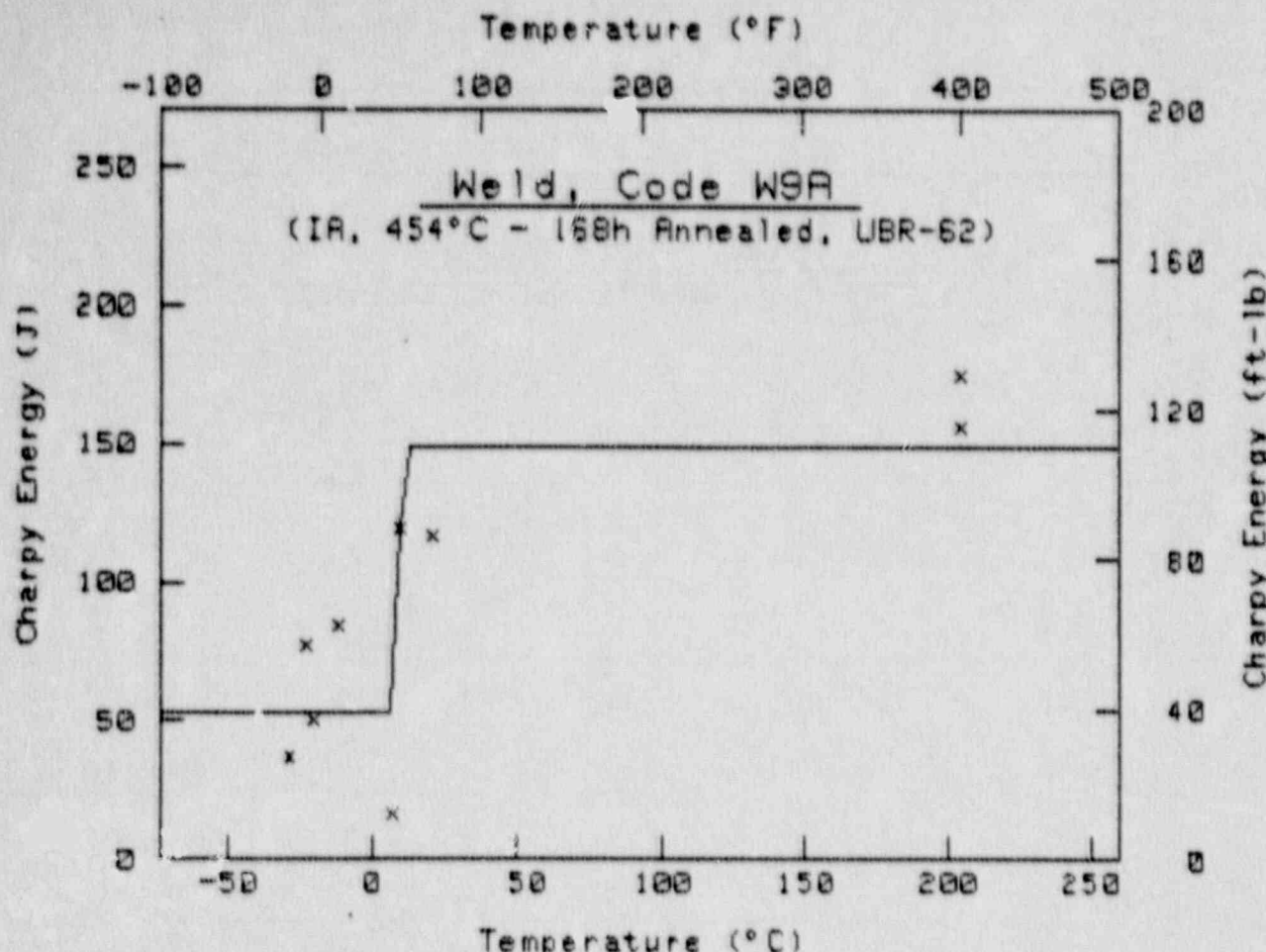
$$Cu = 38 \text{ ft-lb (41 J)} \text{ at } T = -10.8 \text{ }^{\circ}\text{F} \quad -23.8 \text{ }^{\circ}\text{C}$$

Upper Shelf Energy = 118.7 ft-lb 161.0 J

PT #	Temp ($^{\circ}$ F)	Energy (ft-lb)
1	-20	27.0
2	0	31.0
3	20	46.0
4	80	68.0
5	360	101.0
6	400	118.0

0 = Fictitious Point Added

* = Test Point Not Included



$$Cv = A + B \tanh[(T - T_0)/C]$$

	English	Metric
A	74.50 ft-lb	101.01 J
B	35.50 ft-lb	48.13 J
C	.45 $^{\circ}$ F	.25 $^{\circ}$ C
T ₀	49.82 $^{\circ}$ F	9.90 $^{\circ}$ C

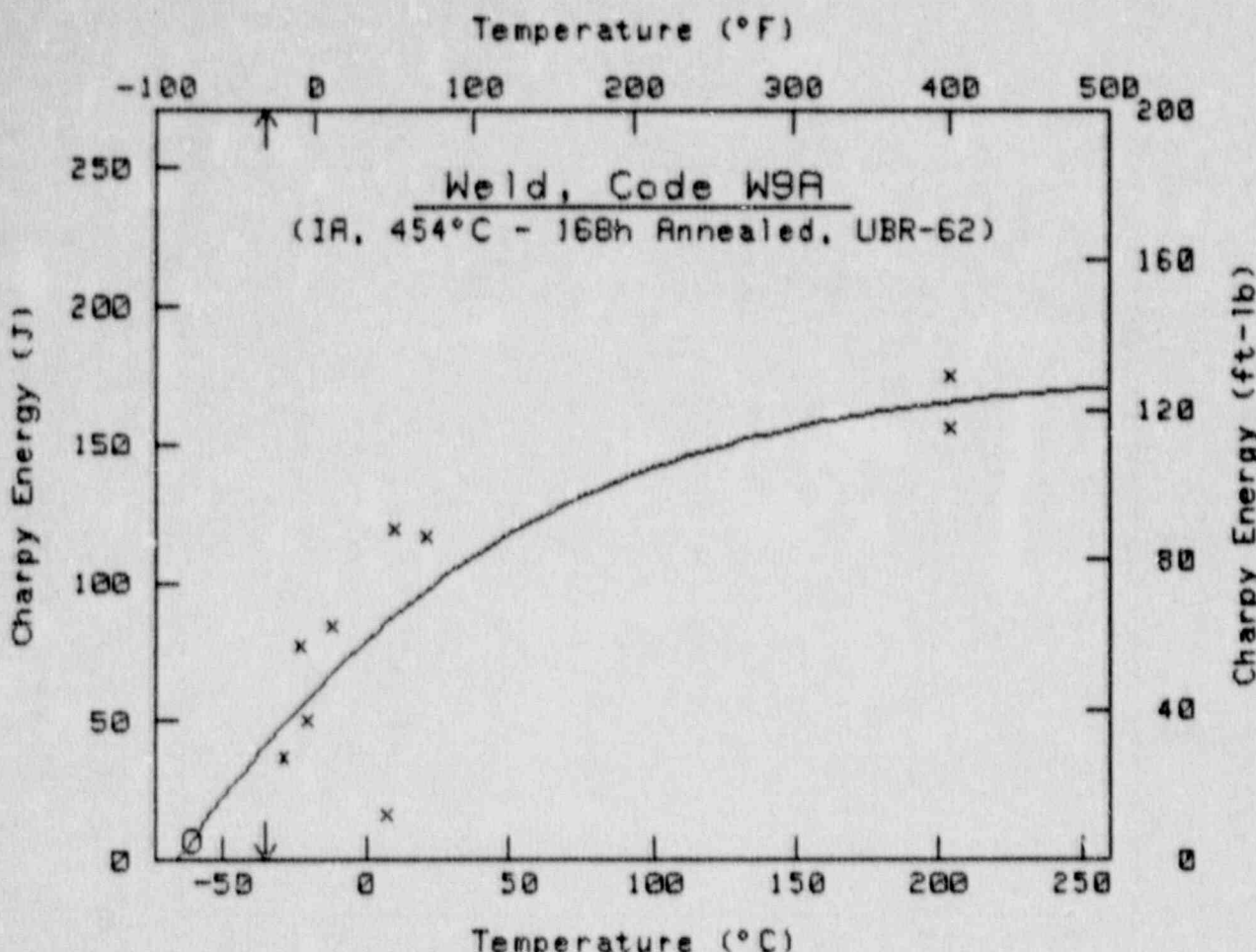
$Cv = 38$ ft-lb (41 J) at $T =$
 $-9.0000000000E+99$ 4D.D
 $^{\circ}$ F
 $-5.0000000000E+99$ 4D.D
 $^{\circ}$ C

Upper Shelf Energy = 110.0 ft-lb 149.1 J

PT #	Temp ($^{\circ}$ F)	Energy (ft-lb)
1	-20	27.0
2	-10	57.0
3	-5	37.0
4	10	62.0
5	45	12.0
6	50	88.0
7	70	86.0
8	400	115.0
9	400	129.0

0 = Fictitious Point Added

* = Test Point Not Included



$$CV = A + B \tanh[(T - T_0)/C]$$

	English	Metric
A	-122.72 ft-lb	-166.38 J
B	253.40 ft-lb	343.56 J
C	$323.65 \text{ }^{\circ}\text{F}$	$179.81 \text{ }^{\circ}\text{C}$
T ₀	$-257.78 \text{ }^{\circ}\text{F}$	$-160.99 \text{ }^{\circ}\text{C}$

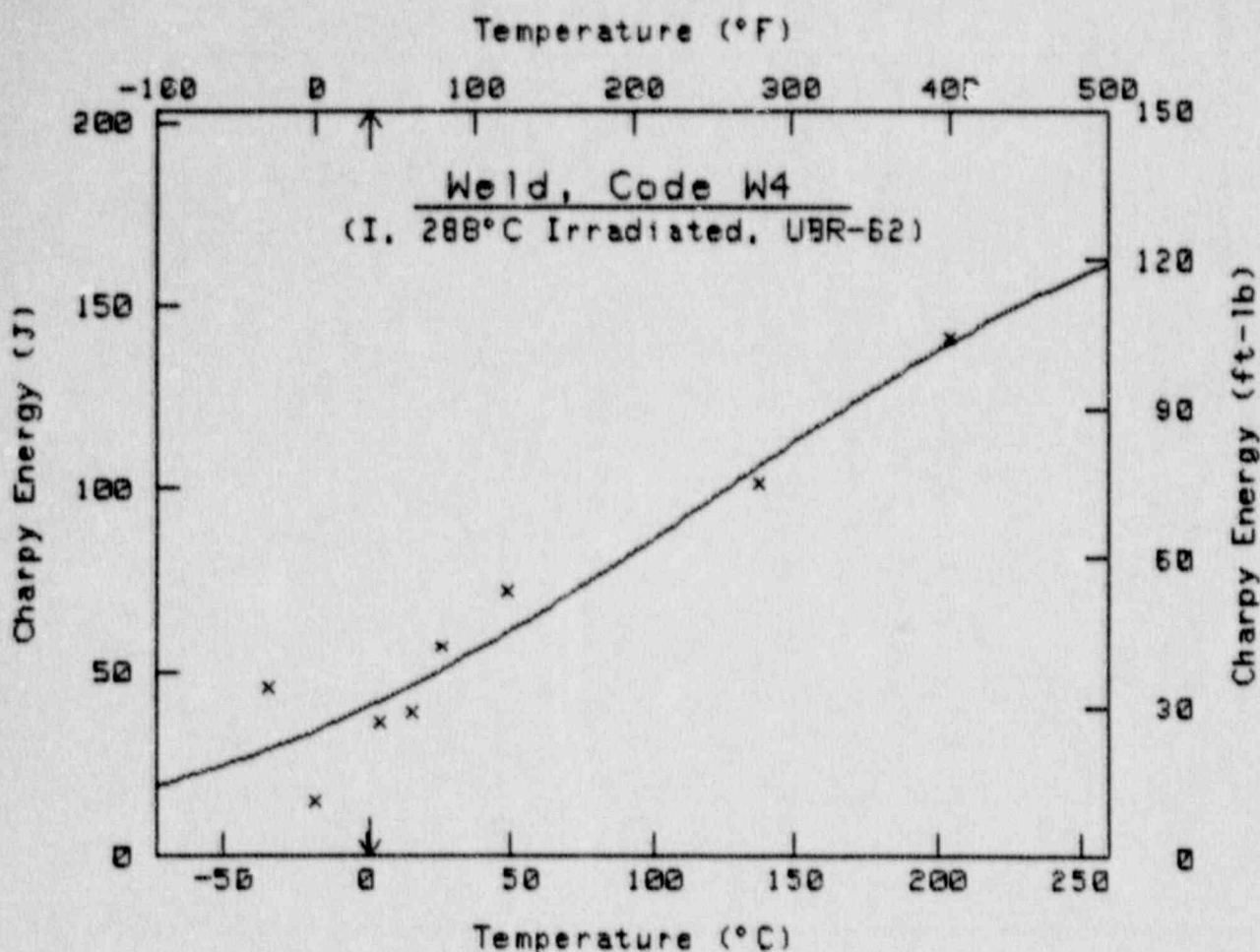
$$CV = 30 \text{ ft-lb (41 J) at } T = -32.1 \text{ }^{\circ}\text{F} \quad -35.6 \text{ }^{\circ}\text{C}$$

Upper Shelf Energy = 130.7 ft-lb 177.2 J

PT #	Temp ($^{\circ}$ F)	Energy (ft-lb)
1	-20	27.0
2	-10	57.0
3	-5	37.0
4	10	62.0
5	45	12.0
6	50	88.0
7	70	86.0
8	400	115.0
9	400	129.0
10	0	5.0
11	0	5.0
12	0	5.0
13	0	5.0

0 = Fictitious Point Added

* = Test Point Not Included



$$C_U = A + B \tanh[(T - T_0)/C]$$

	English	Metric
A	72.59 ft-lb	98.42 J
B	76.10 ft-lb	103.18 J
C	346.86 $^{\circ}$ F	192.78 $^{\circ}$ C
T ₀	253.39 $^{\circ}$ F	122.99 $^{\circ}$ C

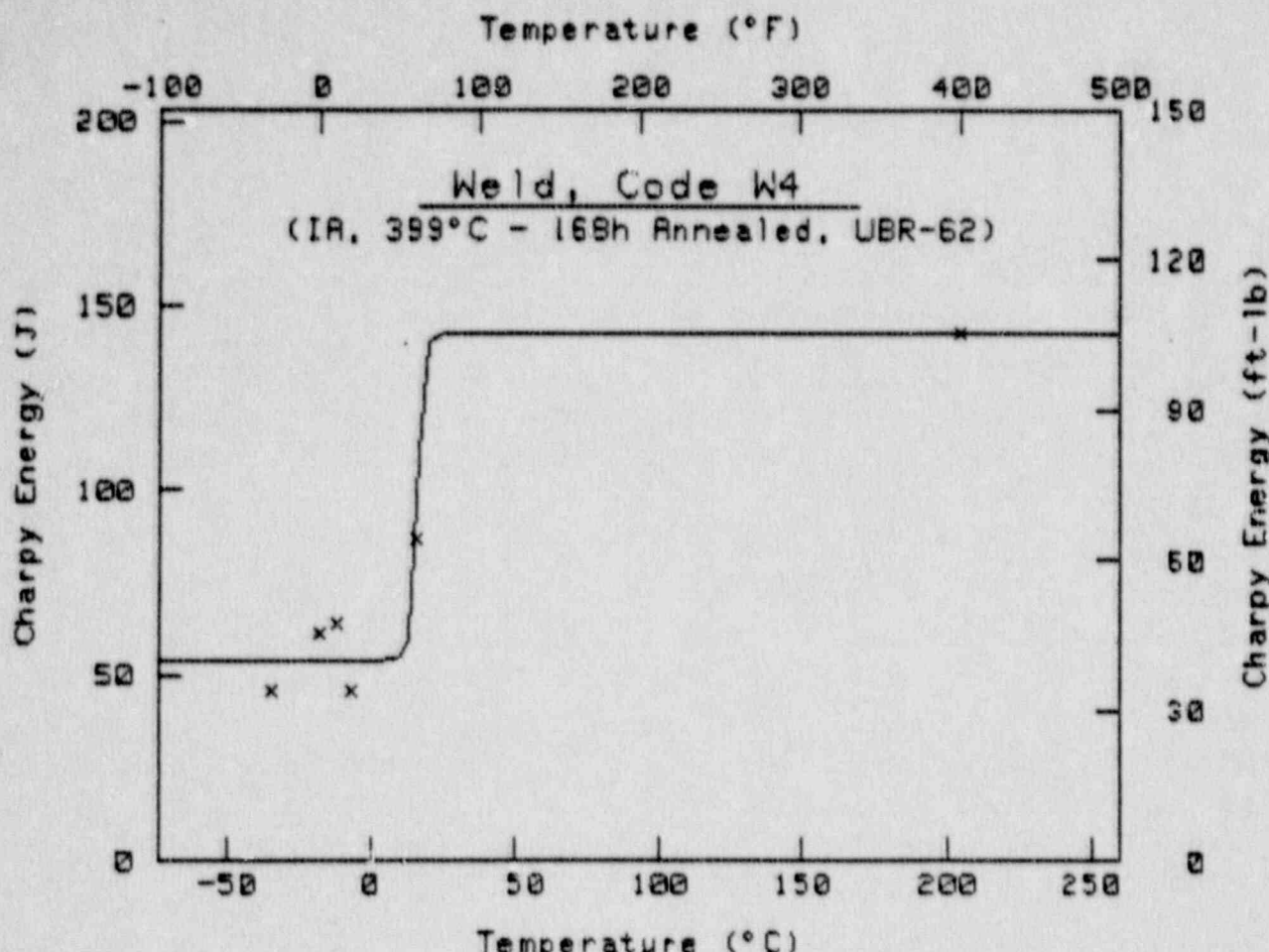
$$C_U = 30 \text{ ft-lb (41 J)} \text{ at } T = 34.0 \text{ }^{\circ}\text{F} \quad 1.1 \text{ }^{\circ}\text{C}$$

Upper Shelf Energy = 148.7 ft-lb 201.6 J

PT #	Temp ($^{\circ}$ F)	Energy (ft-lb)
1	-30	34.0
2	0	11.0
3	40	27.0
4	60	29.0
5	80	42.0
6	120	53.0
7	280	75.0
8	400	104.0

0 = Fictitious Point Added

* = Test Point Not Included



$$C_U = A + B \tanh[(T - T_0)/C]$$

	English	Metric
A	72.50 ft-lb	98.38 J
B	32.50 ft-lb	44.06 J
C	3.79 $^{\circ}$ F	2.11 $^{\circ}$ C
T ₀	61.02 $^{\circ}$ F	16.12 $^{\circ}$ C

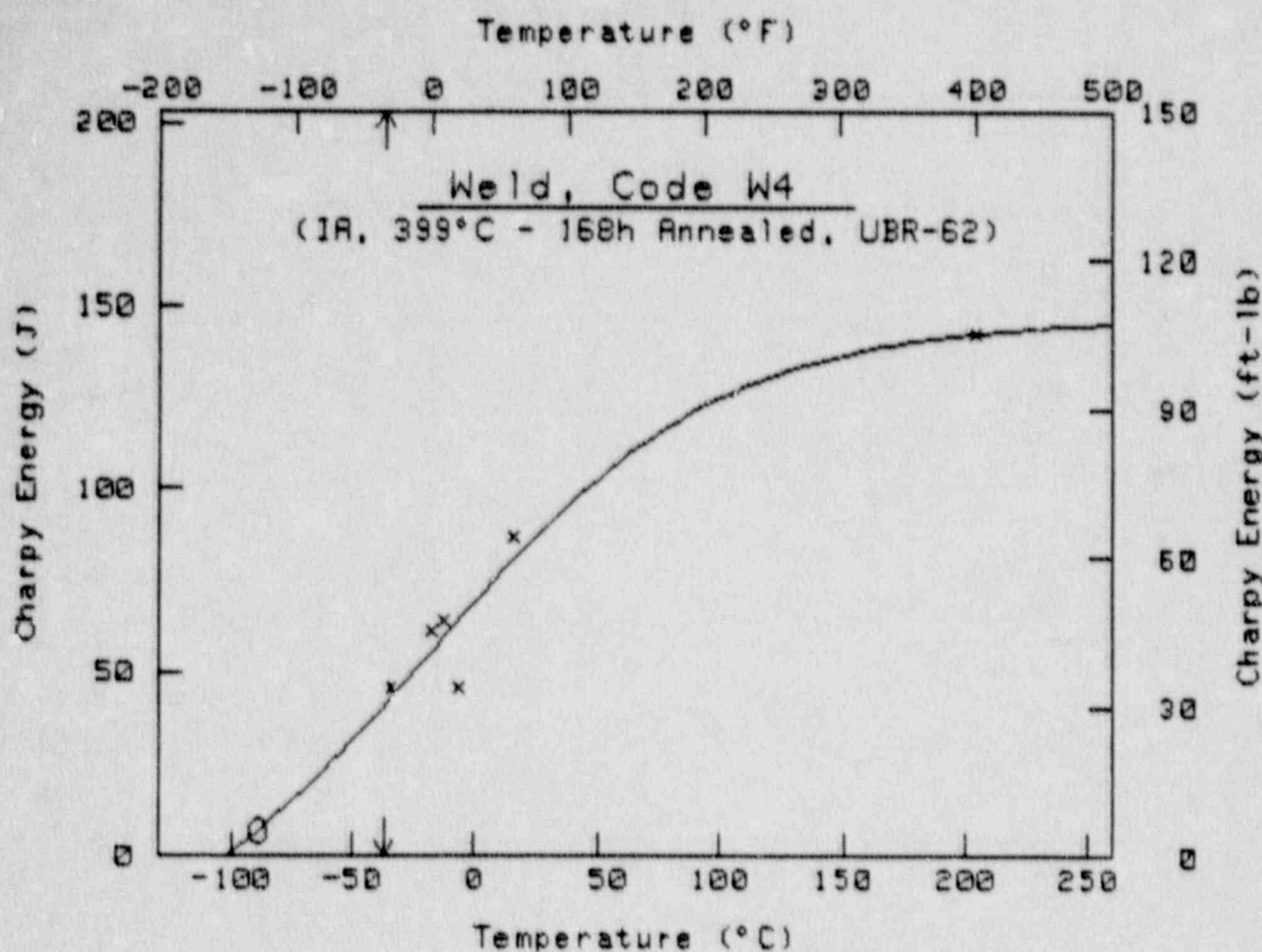
$C_U = 30$ ft-lb (41 J) at $T =$
 $-9.0000000000E+99$ 4D.D
 $^{\circ}$ F
 $-5.0000000000E+99$ 4D.D
 $^{\circ}$ C

Upper Shelf Energy = 105.0 ft-lb 142.4 J

PT #	Temp ($^{\circ}$ F)	Energy (ft-lb)
1	-30	34.0
2	0	45.0
3	10	47.0
4	20	34.0
5	60	64.0
6	400	105.0

0 = Fictitious Point Added

* = Test Point Not Included



$$Cv = A + B \tanh[(T - T_0)/C]$$

	English	Metric
A	41.31 ft-lb	56.81 J
B	66.94 ft-lb	90.76 J
C	213.43 $^{\circ}$ F	118.57 $^{\circ}$ C
T ₀	1.05 $^{\circ}$ F	-17.19 $^{\circ}$ C

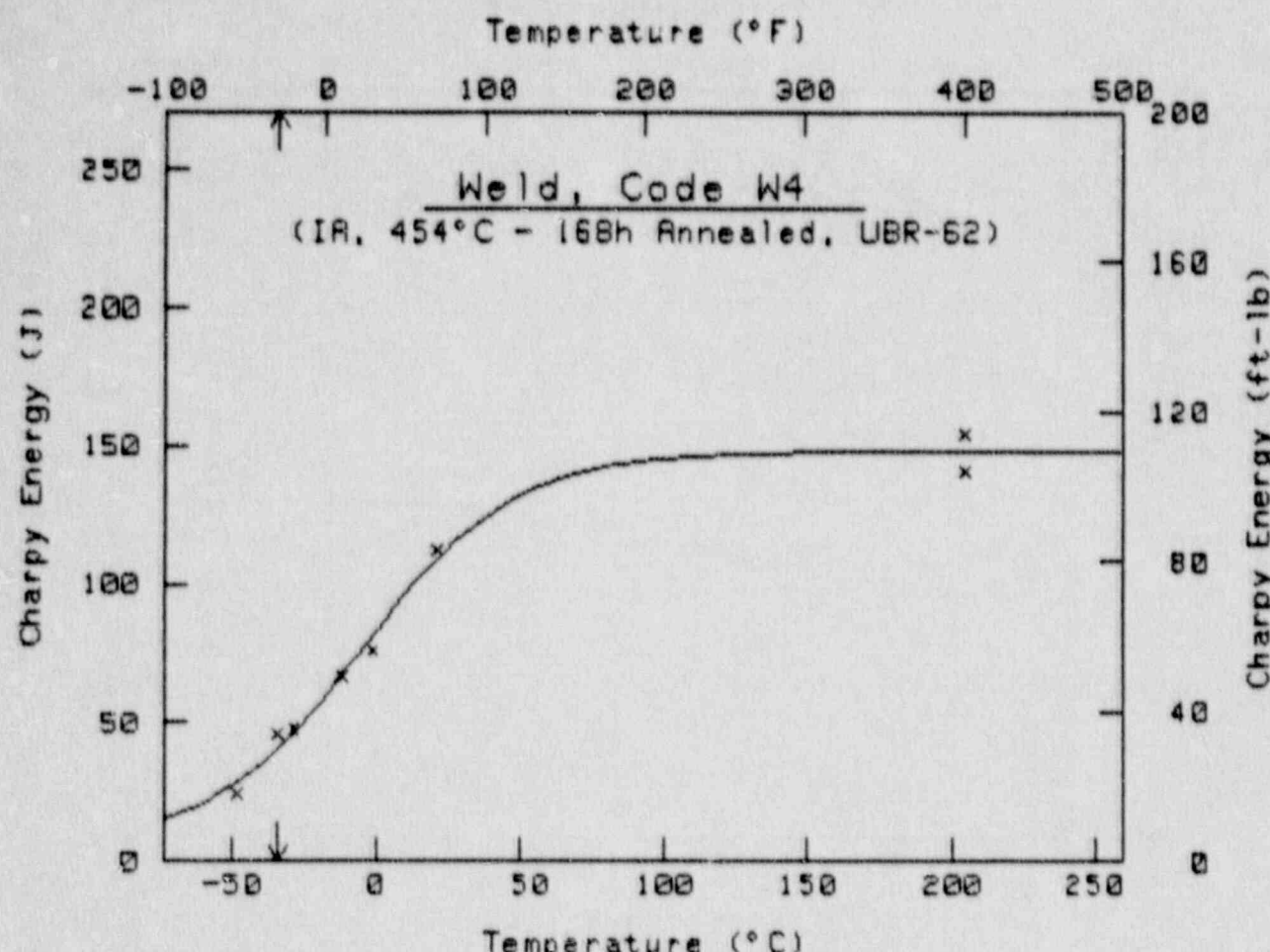
$$Cv = 38 \text{ ft-lb (41 J) at } T = -35.4 \text{ }^{\circ}\text{F} \quad -27.4 \text{ }^{\circ}\text{C}$$

Upper Shelf Energy = 108.3 ft-lb 146.8 J

PT #	Temp ($^{\circ}$ F)	Energy (ft-lb)
1	-30	34.0
2	0	45.0
3	10	47.0
4	20	34.0
5	60	64.0
6	400	105.0
7 O	-128	5.0
8 O	-128	5.0
9 O	-128	5.0
10 O	-128	5.0

O = Fictitious Point Added

* = Test Point Not Included



$$Cv = A + B \tanh[(T - T_0)/C]$$

	English	Metric
A	56.55 ft-lb	76.66 J
B	52.70 ft-lb	71.45 J
C	95.55 $^{\circ}$ F	53.08 $^{\circ}$ C
T ₀	23.43 $^{\circ}$ F	-4.76 $^{\circ}$ C

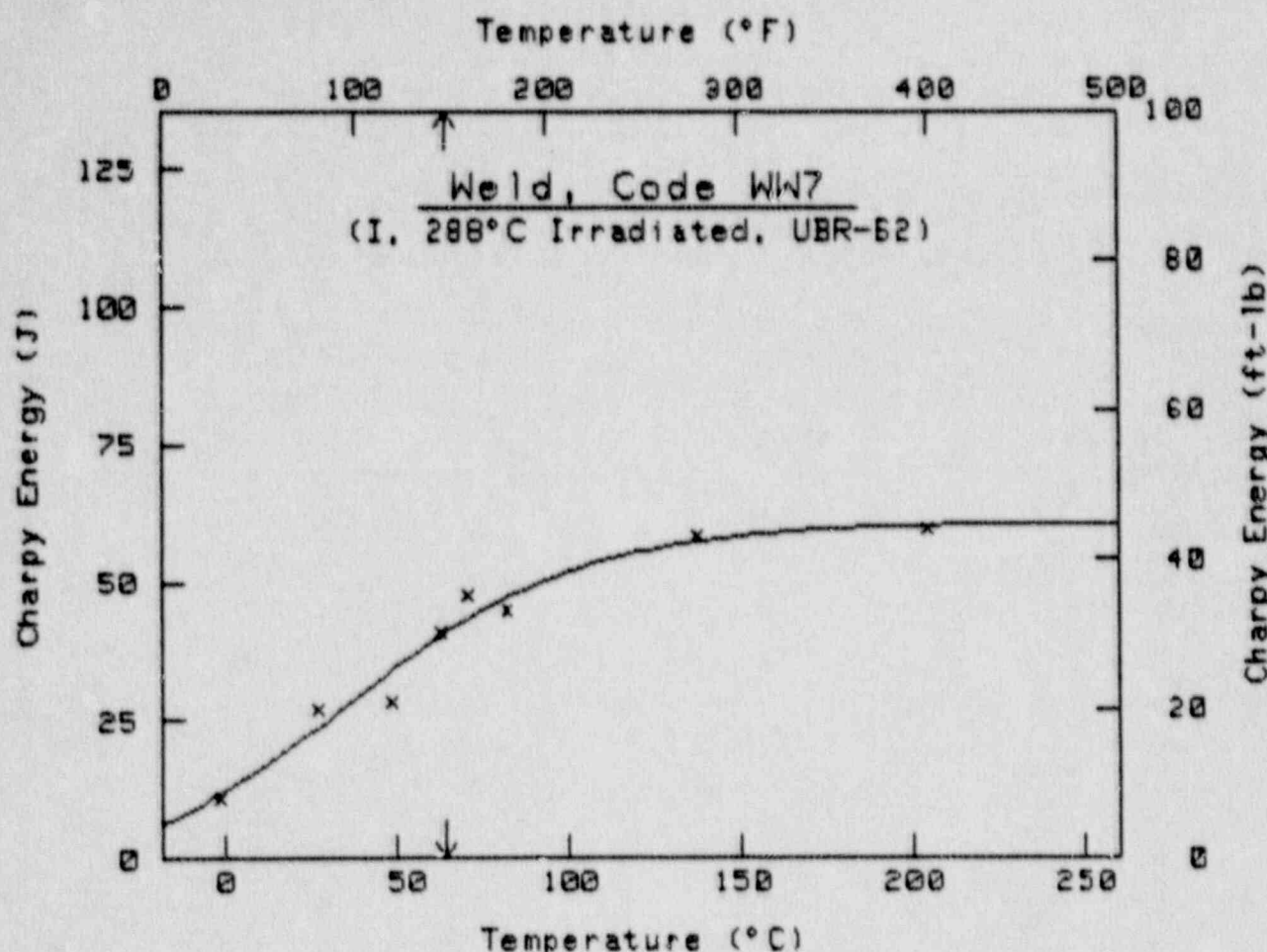
$$Cv = 30 \text{ ft-lb (41 J)} \text{ at } T = -29.5 \text{ }^{\circ}\text{F} \quad -34.2 \text{ }^{\circ}\text{C}$$

Upper Shelf Energy = 109.2 ft-lb 148.1 J

PT #	Temp ($^{\circ}$ F)	Energy (ft-lb)
1	-55	18.0
2	-30	34.0
3	-20	35.0
4	10	49.0
5	30	56.0
6	70	83.0
7	400	114.0
8	400	104.0

0 = Fictitious Point Added

* = Test Point Not Included



$$C_U = A + B \tanh[(T - T_0)/C]$$

	English	Metric
A	20.10 ft-lb	27.25 J
B	24.79 ft-lb	33.62 J
C	127.75 $^{\circ}$ F	70.97 $^{\circ}$ C
T ₀	93.92 $^{\circ}$ F	34.40 $^{\circ}$ C

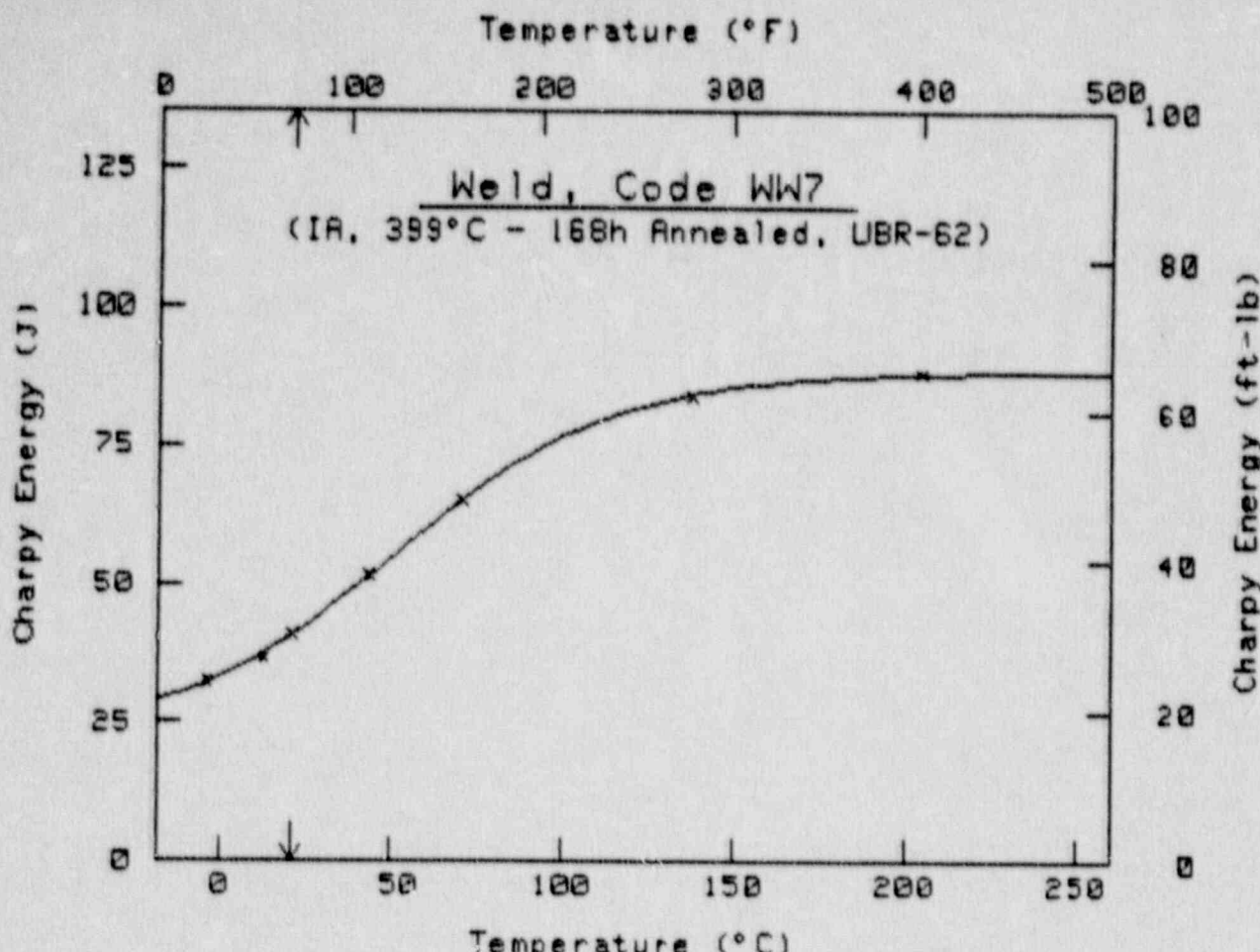
$$C_U = 30 \text{ ft-lb (41 J)} \text{ at } T = 148.0 \text{ }^{\circ}\text{F} \quad 64.4 \text{ }^{\circ}\text{C}$$

Upper Shelf Energy = 44.9 ft-lb 60.9 J

PT #	Temp ($^{\circ}$ F)	Energy (ft-lb)
1	30	8.0
2	80	20.0
3	120	21.0
4	145	30.0
5	160	35.0
6	180	33.0
7	280	43.0
8	400	44.0

0 = Fictitious Point Added

* = Test Point Not Included



 $C_U = A + B \tanh[(T - T_0)/C]$

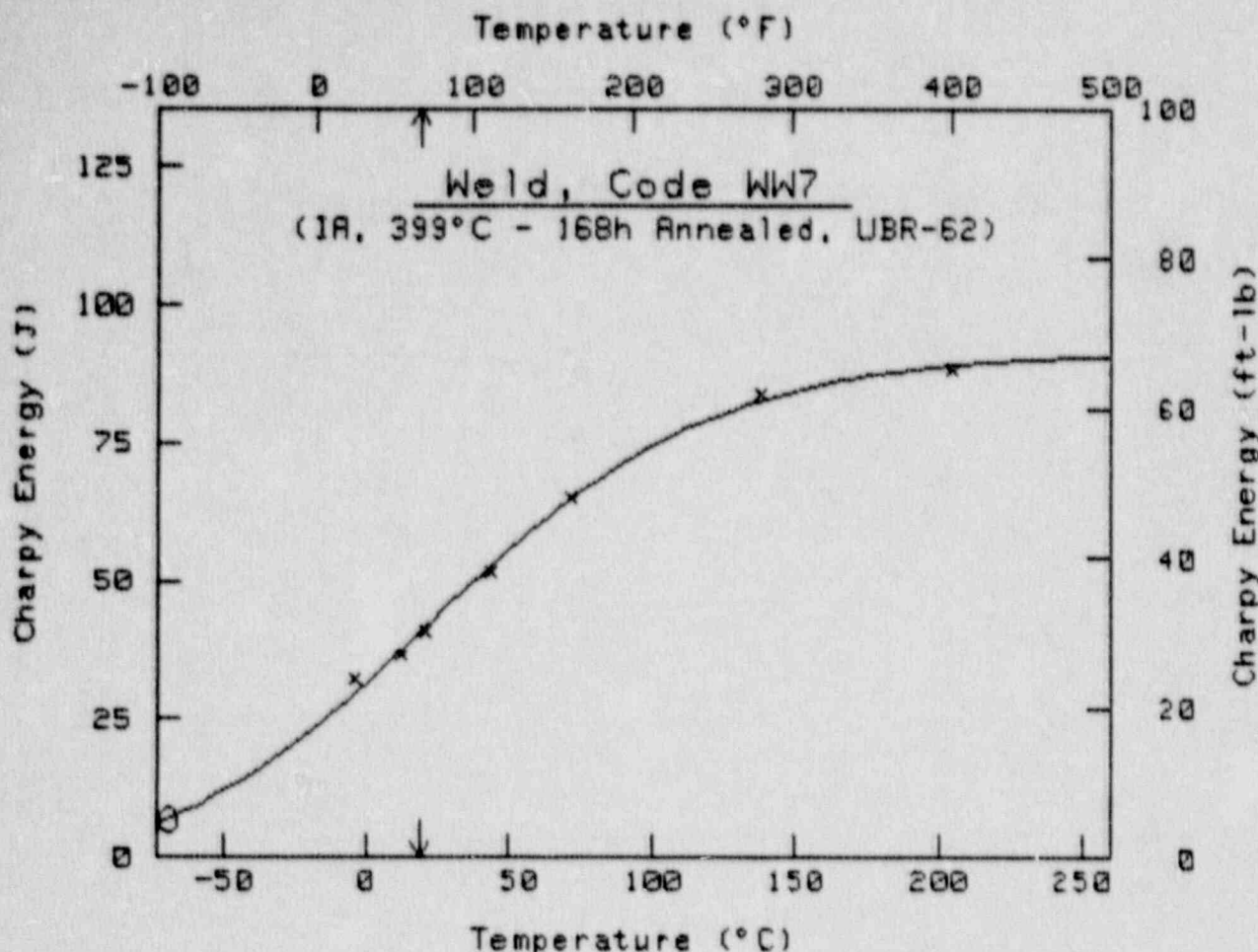
	<u>English</u>	<u>Metric</u>
A	40.74 ft-lb	55.23 J
B	24.56 ft-lb	33.29 J
C	115.89 $^{\circ}$ F	64.39 $^{\circ}$ C
T ₀	124.42 $^{\circ}$ F	51.34 $^{\circ}$ C

$C_U = 38$ ft-lb (41 J) at $T = 70.1$ $^{\circ}$ F 21.2 $^{\circ}$ C
 Upper Shelf Energy = 65.3 ft-lb 88.5 J

PT #	Temp ($^{\circ}$ F)	Energy (ft-lb)
1	25	24.0
2	55	27.0
3	70	30.0
4	110	38.0
5	160	48.0
6	280	62.0
7	400	65.0

0 = Fictitious Point Added

* = Test Point Not Included



$$C_v = A + B \tanh[(T - T_0)/C]$$

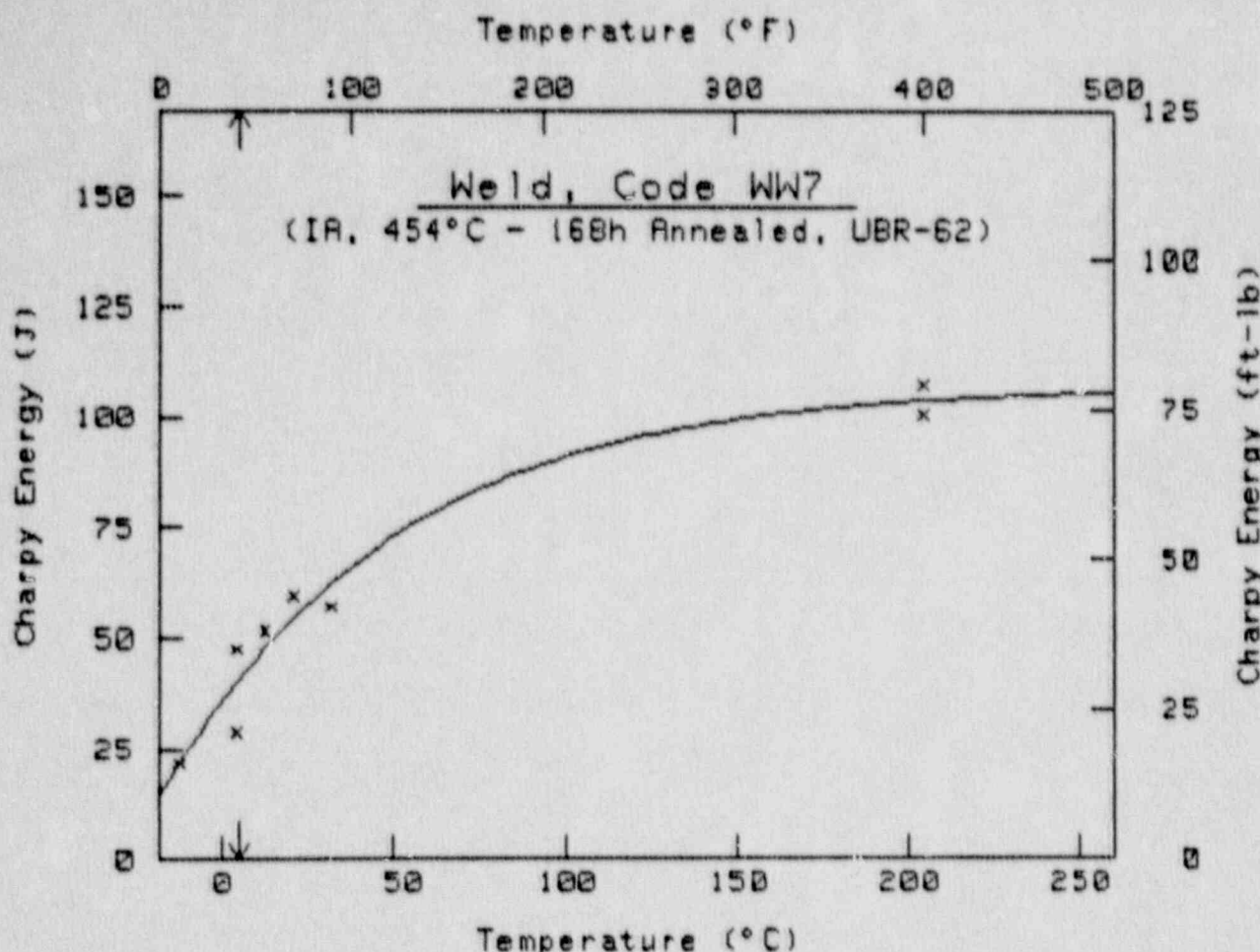
	English	Metric
A	31.41 ft-lb	42.59 J
B	36.16 ft-lb	49.02 J
C	179.77 $^{\circ}$ F	99.87 $^{\circ}$ C
T ₀	73.11 $^{\circ}$ F	22.84 $^{\circ}$ C

$$C_v = 30 \text{ ft-lb (41 J)} \text{ at } T = \begin{array}{ll} 66.1 \text{ }^{\circ}\text{F} & 18.9 \text{ }^{\circ}\text{C} \\ \text{Upper Shelf Energy} & 67.6 \text{ ft-lb} \quad 91.6 \text{ J} \end{array}$$

PT #	Temp ($^{\circ}$ F)	Energy (ft-lb)
1	25	24.0
2	55	27.0
3	70	30.0
4	110	38.0
5	160	48.0
6	280	62.0
7	400	65.0
8 0	-93	5.0
9 0	-93	5.0
10 0	-93	5.0
11 0	-93	5.0

0 = Fictitious Point Added

* = Test Point Not Included



$$C_U = A + B \tanh[(T - T_0)/C]$$

	English	Metric
A	-365.47 ft-lb	-495.51 J
B	444.28 ft-lb	602.36 J
C	$233.88 \text{ }^{\circ}\text{F}$	$129.93 \text{ }^{\circ}\text{C}$
T ₀	$-291.33 \text{ }^{\circ}\text{F}$	$-179.63 \text{ }^{\circ}\text{C}$

$$C_U = 38 \text{ ft-lb (41 J) at } T = 41.4 \text{ }^{\circ}\text{F} \quad 5.2 \text{ }^{\circ}\text{C}$$

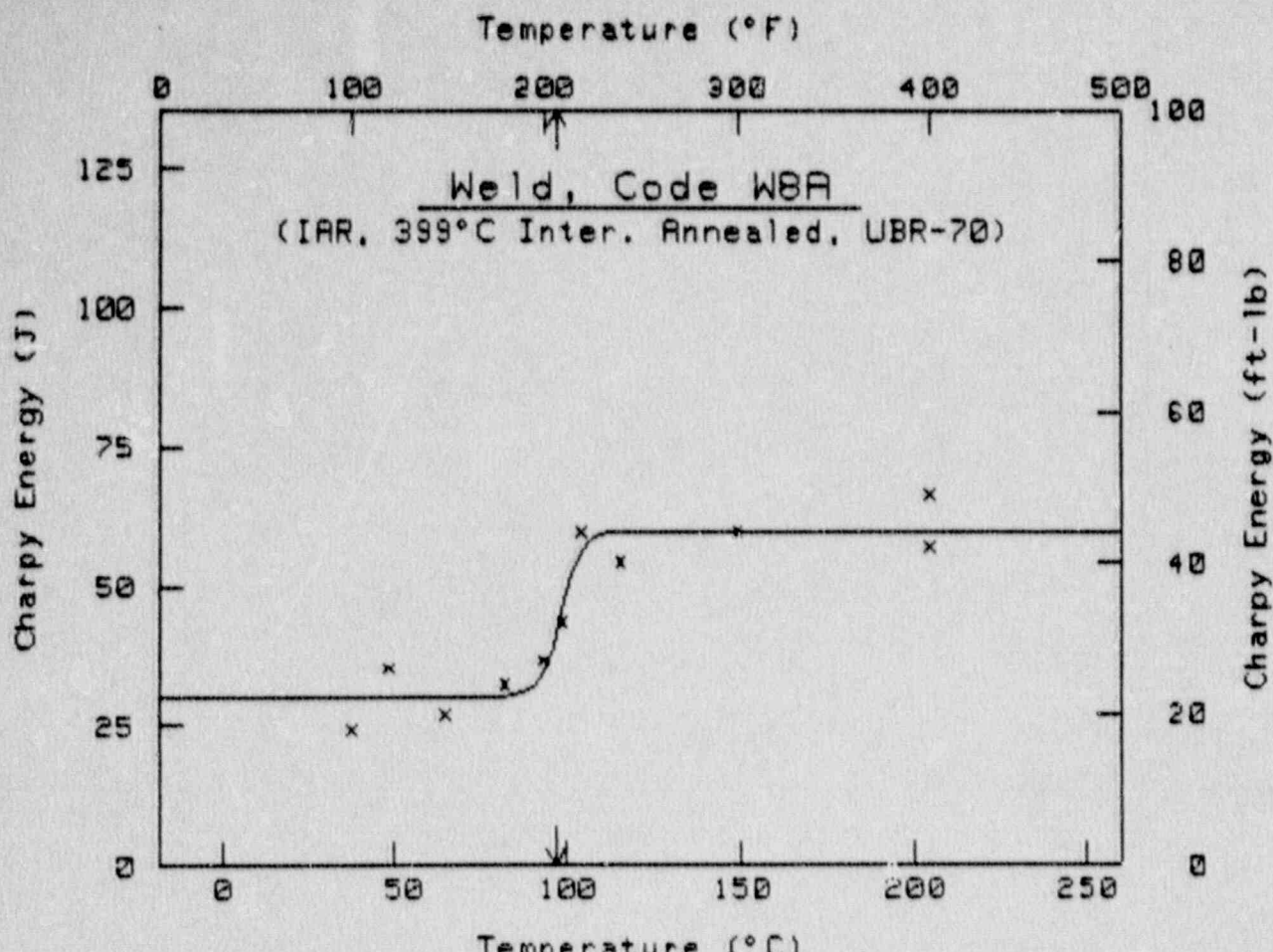
Upper Shelf Energy = 78.8 ft-lb 106.9 J

PT #	Temp ($^{\circ}$ F)	Energy (ft-lb)
1	10	16.0
2	40	21.0
3	40	35.0
4	55	38.0
5	70	44.0
6	90	42.0
7	400	79.0
8	400	74.0

0 = Fictitious Point Added

* = Test Point Not Included

Computer Curve Fittings of Data from Irradiation Assembly UBR-70



*****: *****: *****: *****: *****: *****: *****:
 $C_v = A + B \tanh[(T - T_0)/C]$

	English	Metric
A =	33.15 ft-lb	44.94 J
B =	10.99 ft-lb	14.98 J
C =	10.71 $^{\circ}$ F	5.95 $^{\circ}$ C
T ₀ =	209.32 $^{\circ}$ F	98.51 $^{\circ}$ C

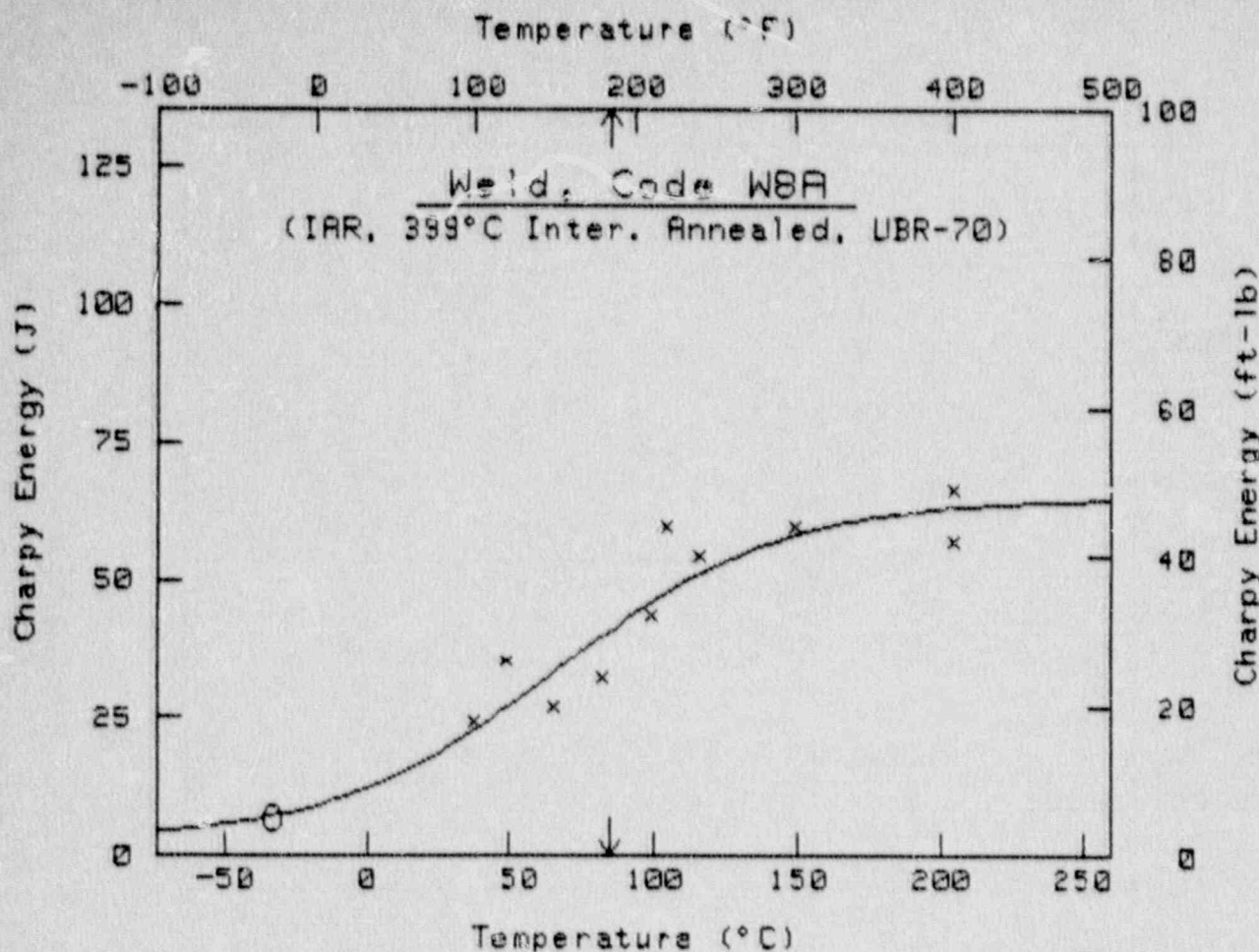
$C_v = 30$ ft-lb (41 J) at $T = 206.2$ $^{\circ}$ F 96.8 $^{\circ}$ C
 Upper Shelf Energy = 44.1 ft-lb 59.8 J

*****: *****: *****: *****: *****: *****: *****:

PT #	Temp ($^{\circ}$ F)	Energy (ft-lb)
1	100	18.0
2	120	26.0
3	150	20.0
4	180	24.0
5	200	27.0
6	210	32.0
7	220	44.0
8	240	40.0
9	300	44.0
10	400	49.0
11	400	42.0

0 = Fictitious Point Added

* = Test Point Not Included



$$Cu = A + B \tanh[(T - T_0)/C]$$

	English	Metric
A	24.96 ft-lb	33.84 J
B	22.93 ft-lb	31.09 J
C	140.96 $^{\circ}$ F	78.31 $^{\circ}$ C
T ₀	152.99 $^{\circ}$ F	67.22 $^{\circ}$ C

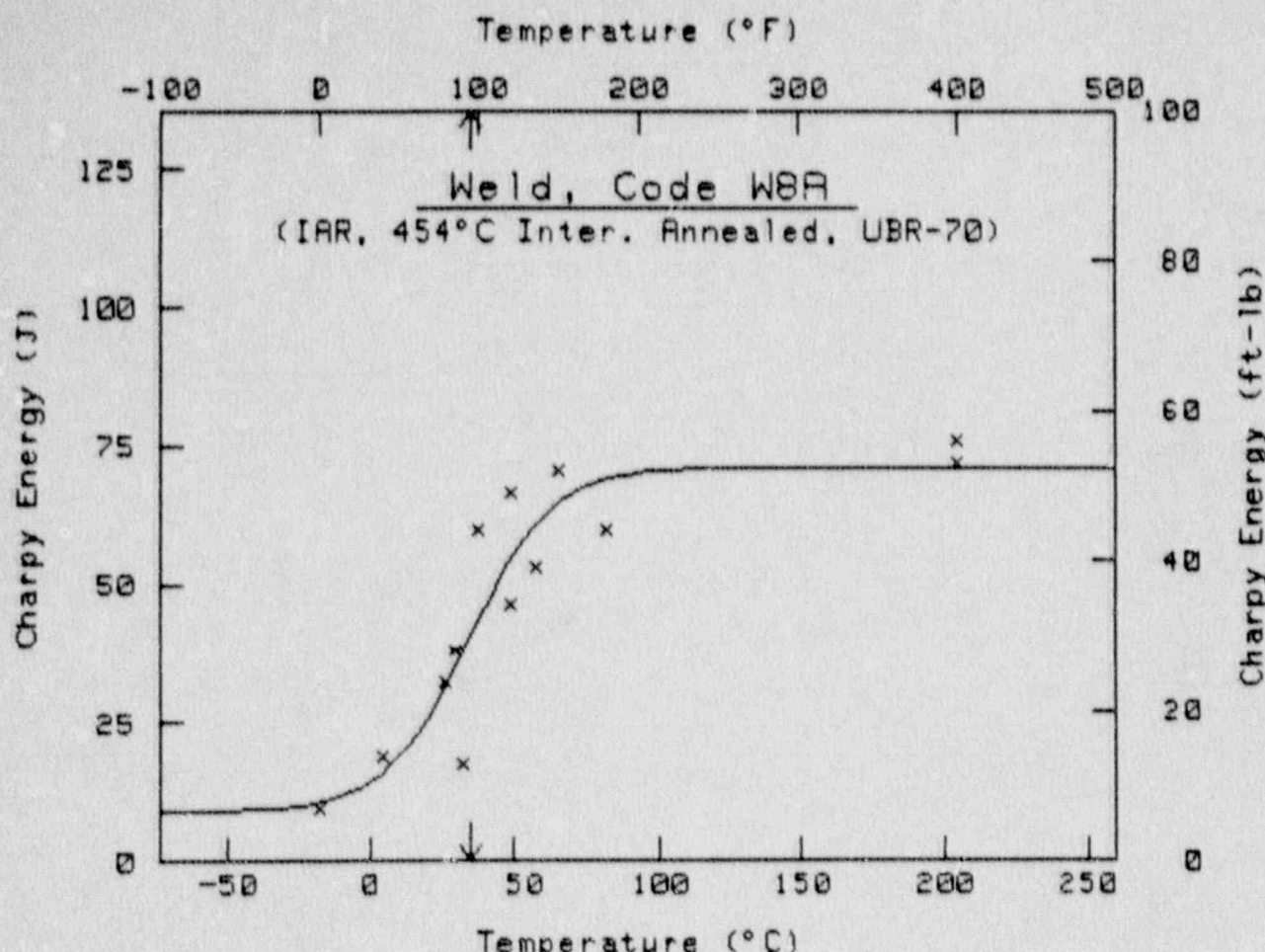
$$Cu = 30 \text{ ft-lb (41 J)} \text{ at } T = 184.5 \text{ }^{\circ}\text{F} \quad 84.7 \text{ }^{\circ}\text{C}$$

Upper Shelf Energy = 47.9 ft-lb 64.9 J

PT #	Temp ($^{\circ}$ F)	Energy (ft-lb)
1	100	18.0
2	120	26.0
3	150	20.0
4	180	24.0
5	200	27.0
6	210	32.0
7	220	44.0
8	240	40.0
9	300	44.0
10	400	49.0
11	400	42.0
12*	-28	5.0
13*	-28	5.0
14*	-28	5.0
15*	-28	5.0

* = Fictitious Point Added

* = Test Point Not Included



$$C_U = A + B \tanh[(T - T_0)/C]$$

	English	Metric
A =	29.52 ft-lb	40.02 J
B =	22.88 ft-lb	31.02 J
C =	52.10 $^{\circ}$ F	28.94 $^{\circ}$ C
T ₀ =	93.84 $^{\circ}$ F	34.35 $^{\circ}$ C

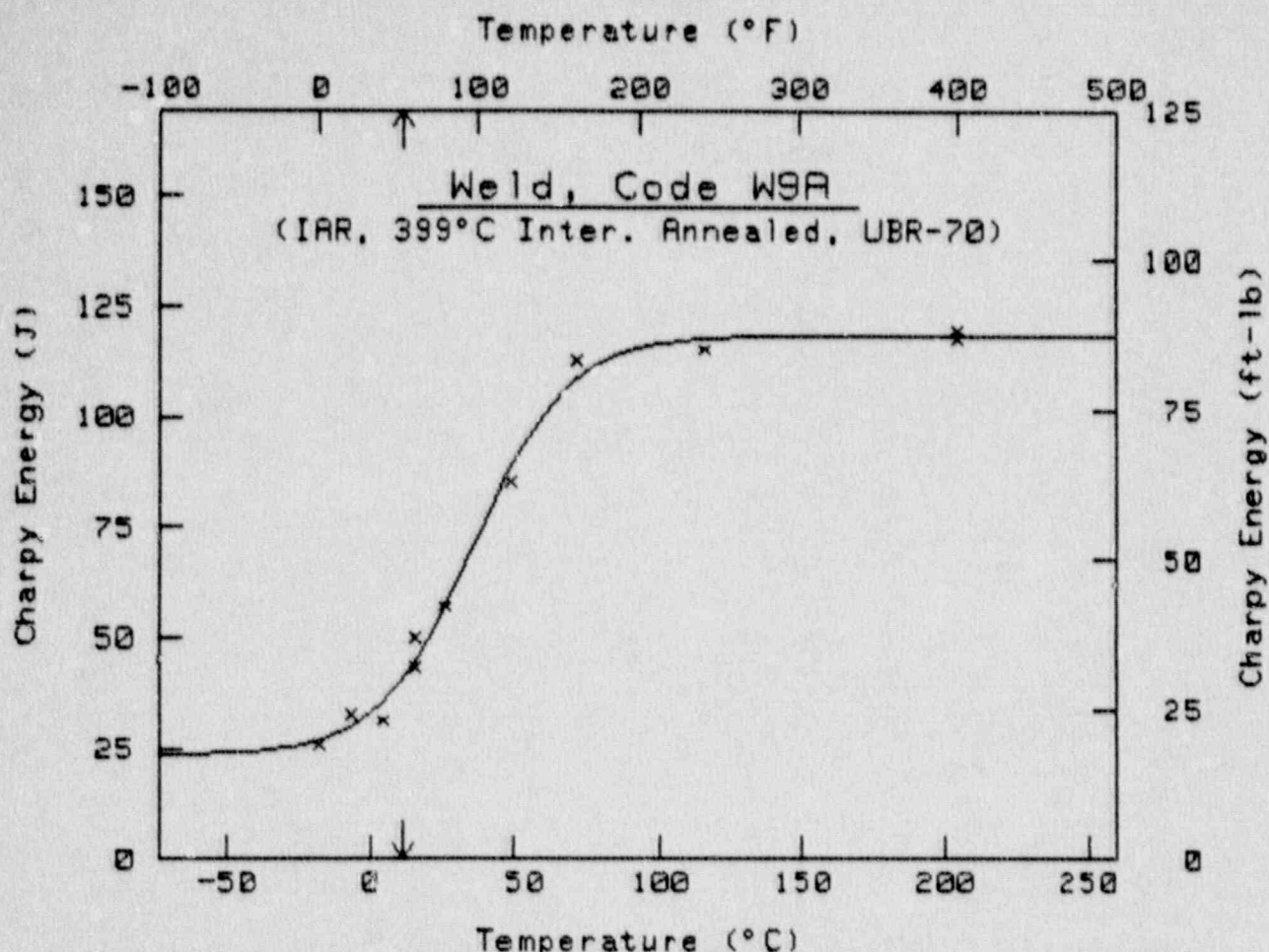
$$C_U = 30 \text{ ft-lb (41 J) at } T = 94.9 \text{ }^{\circ}\text{F} \quad 35.0 \text{ }^{\circ}\text{C}$$

Upper Shelf Energy = 52.4 ft-lb 71.0 J

PT #	Temp ($^{\circ}$ F)	Energy (ft-lb)
1	0	7.0
2	40	14.0
3	80	24.0
4	85	28.0
5	90	13.0
6	100	44.0
7	120	49.0
8	120	34.0
9	135	39.0
10	150	52.0
11	180	44.0
12	400	53.0
13	400	56.0

0 = Fictitious Point Added

* = Test Point Not Included



$$Cv = A + B \tanh[(T - T_0)/C]$$

	English	Metric
A	52.36 ft-lb	70.99 J
B	35.00 ft-lb	47.45 J
C	59.07 $^{\circ}$ F	32.81 $^{\circ}$ C
T ₀	97.19 $^{\circ}$ F	36.22 $^{\circ}$ C

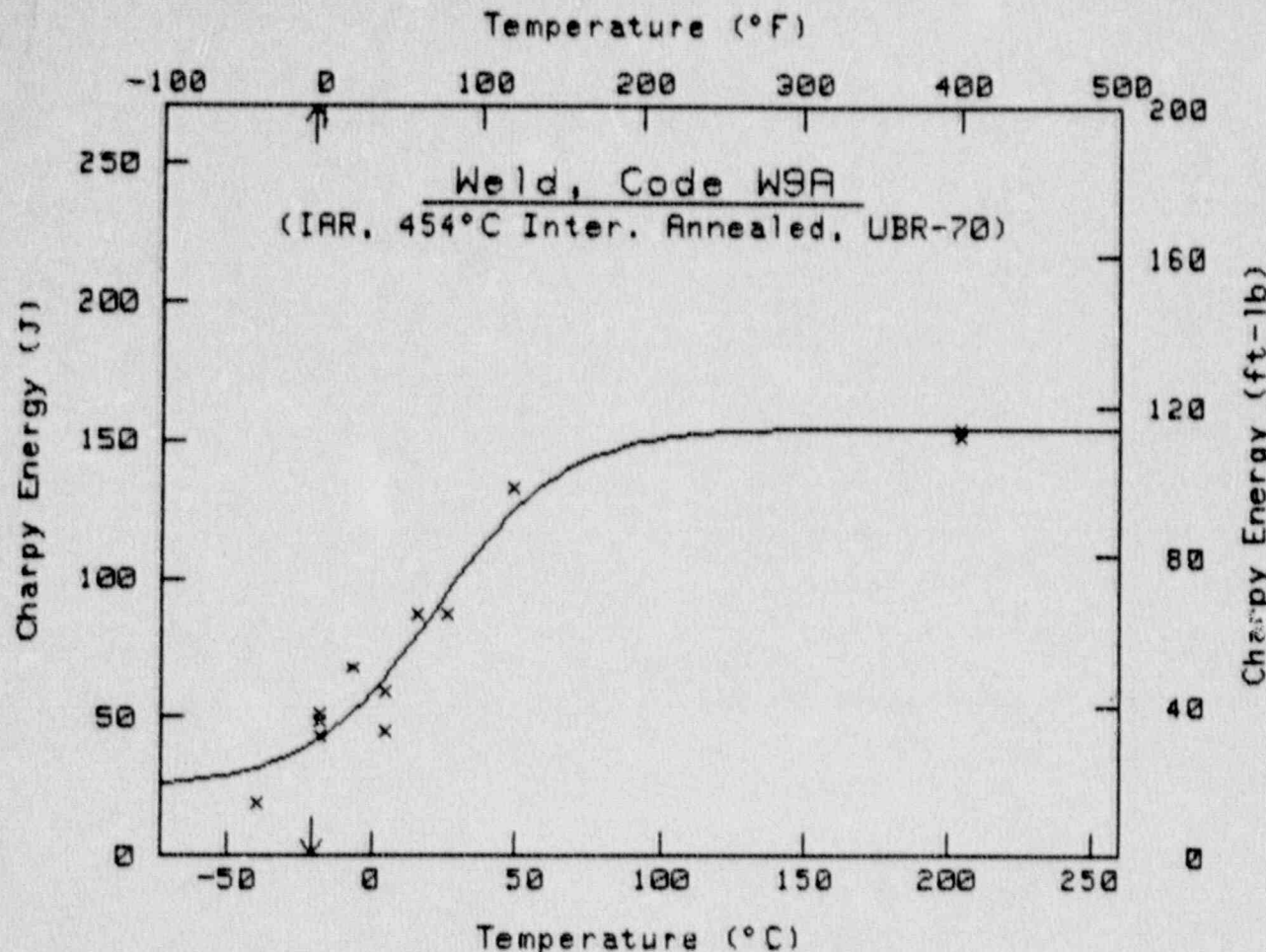
$$Cv = 38 \text{ ft-lb (41 J)} \text{ at } T = 52.5 \text{ }^{\circ}\text{F} \quad 11.4 \text{ }^{\circ}\text{C}$$

Upper Shelf Energy = 87.4 ft-lb 118.4 J

PT #	Temp ($^{\circ}$ F)	Energy (ft-lb)
1	0	19.0
2	20	24.0
3	40	23.0
4	60	32.0
5	60	37.0
6	80	42.0
7	120	63.0
8	160	83.0
9	240	85.0
10	400	87.0
11	400	88.0

O = Fictitious Point Added

* = Test Point Not Included



 $Cv = A + B \tanh[(T - T_0)/C]$

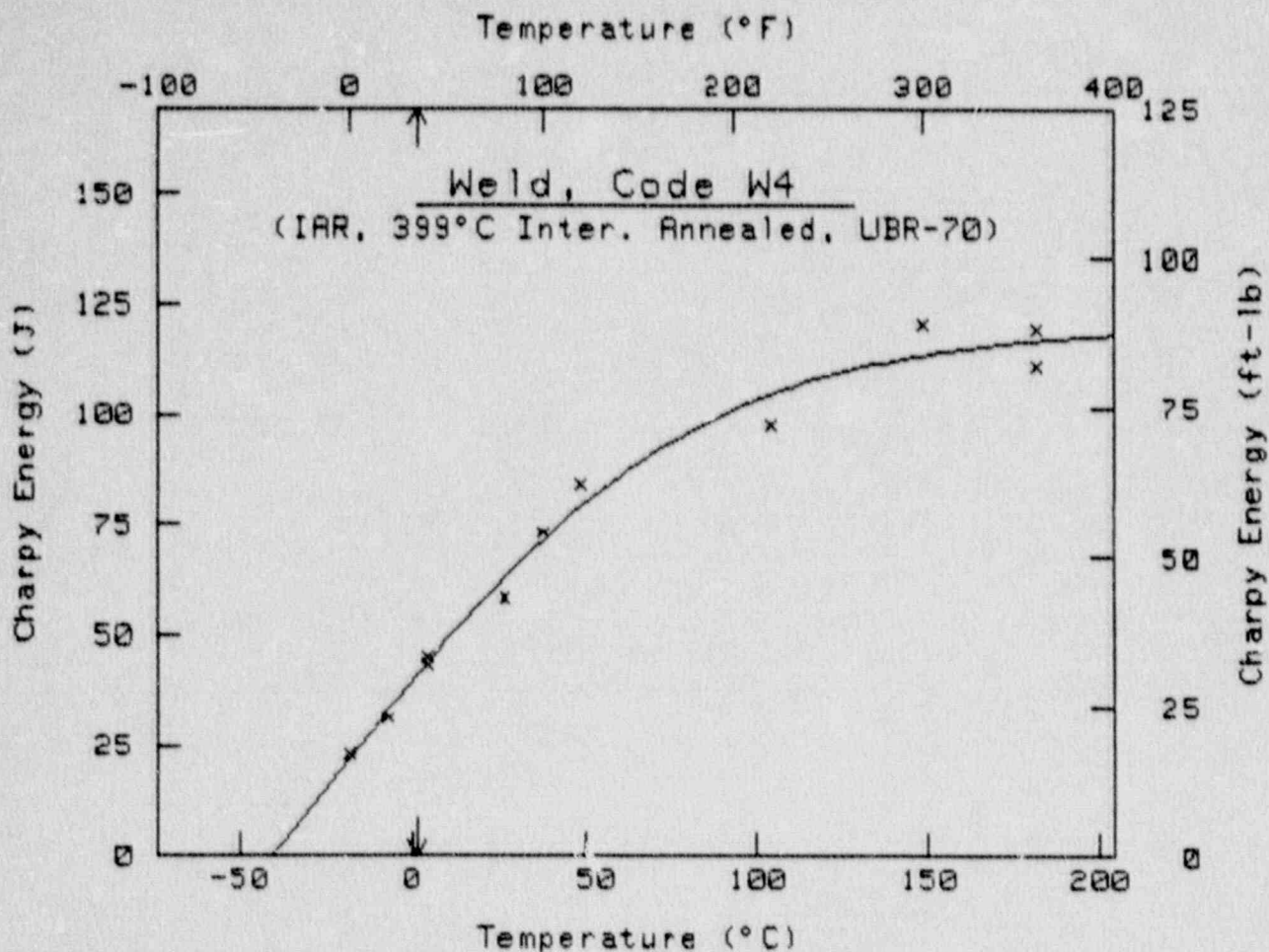
	English	Metric
A	66.03 ft-lb	89.53 J
B	47.96 ft-lb	65.02 J
C	79.71°F	44.28°C
T_0	72.71°F	22.61°C

$Cv = 38 \text{ ft-lb (41 J)} \text{ at } T = -5.1^{\circ}\text{F} \quad -20.6^{\circ}\text{C}$
 Upper Shelf Energy = $114.0 \text{ ft-lb} \quad 154.5 \text{ J}$

PT #	Temp ($^{\circ}\text{F}$)	Energy (ft-lb)
1	-40	14.0
2	0	32.0
3	0	38.0
4	0	36.0
5	20	50.0
6	40	33.0
7	40	44.0
8	60	64.0
9	80	64.0
10	120	98.0
11	400	112.0
12	400	114.0

0 = Fictitious Point Added

* = Test Point Not Included



$$Cv = A + B \tanh[(T - T_0)/C]$$

	English	Metric
A	15.71 ft-lb	21.31 J
B	73.08 ft-lb	99.09 J
C	181.72 $^{\circ}$ F	100.95 $^{\circ}$ C
T ₀	-1.33 $^{\circ}$ F	-18.51 $^{\circ}$ C

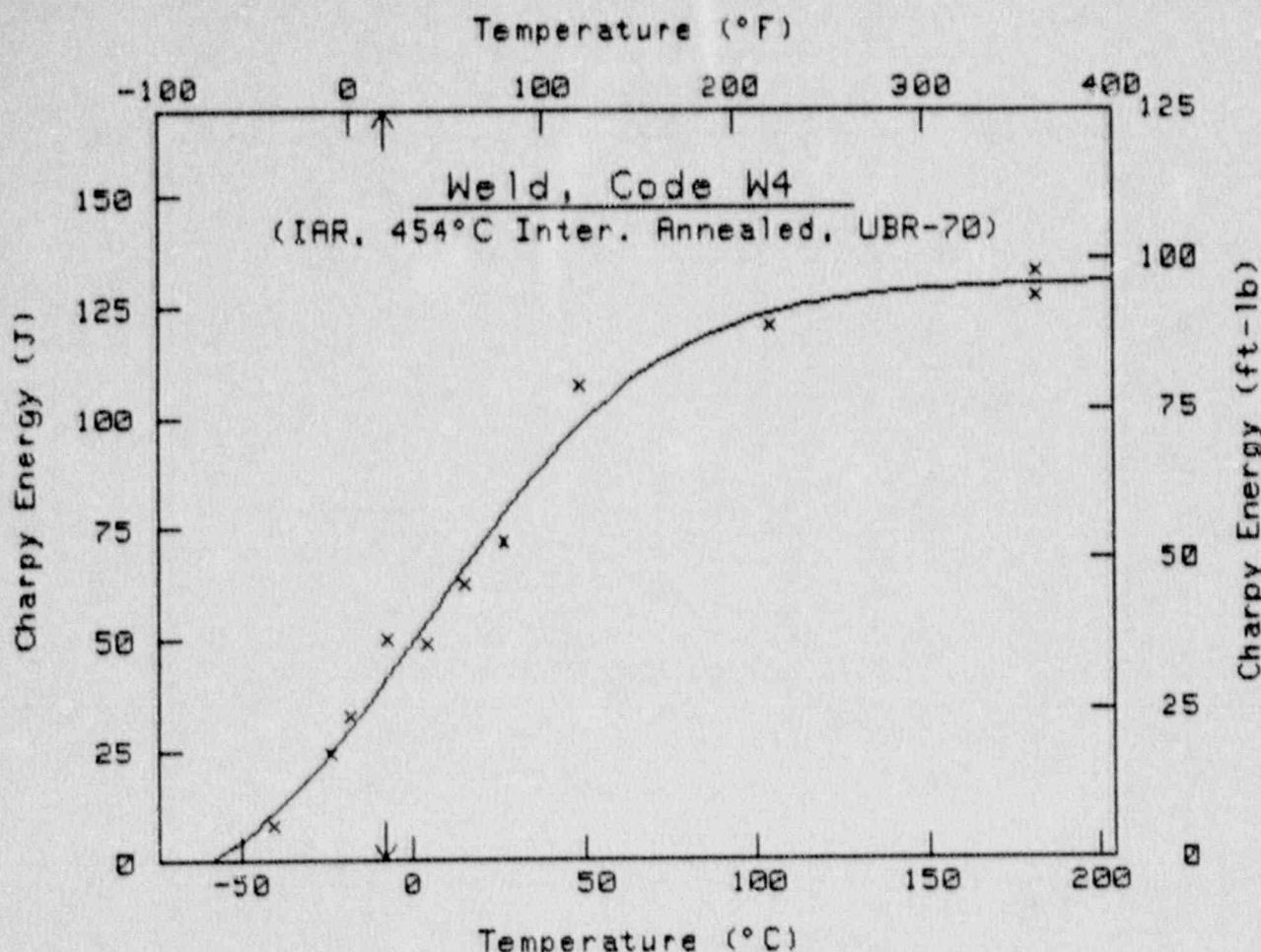
$$Cv = 30 \text{ ft-lb (41 J)} \text{ at } T = 34.7 \text{ }^{\circ}\text{F} \quad 1.5 \text{ }^{\circ}\text{C}$$

Upper Shelf Energy = 88.8 ft-lb 120.4 J

PT #	Temp ($^{\circ}$ F)	Energy (ft-lb)
1	0	17.0
2	20	23.0
3	40	32.0
4	40	33.0
5	80	43.0
6	100	54.0
7	120	62.0
8	220	72.0
9	300	89.0
10	360	88.0
11	360	82.0

0 = Fictitious Point Added

* = Test Point Not Included



 $C_U = A + B \tanh[(T - T_0)/C]$

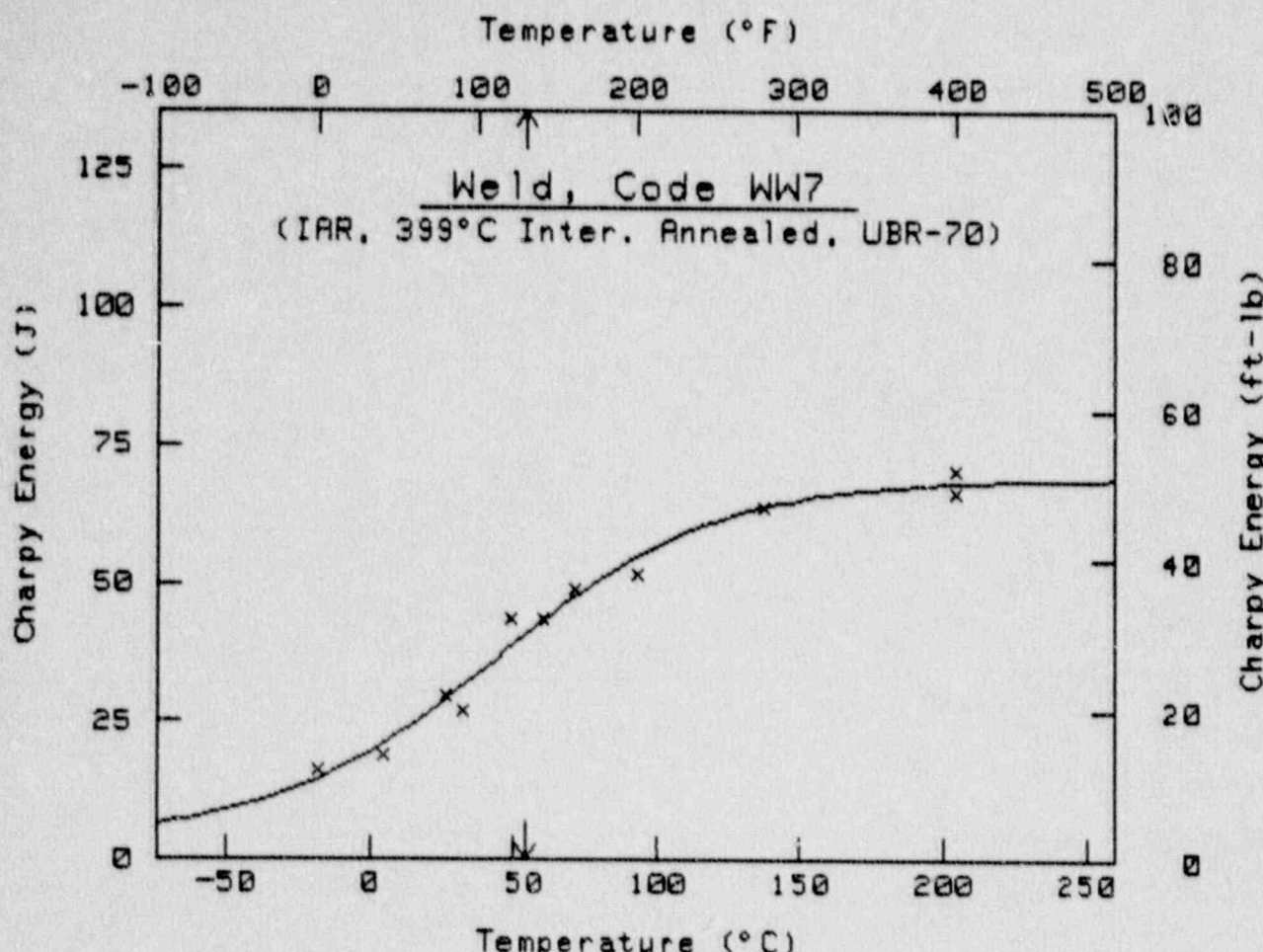
	English	Metric
A	41.19 ft-lb	55.84 J
B	55.29 ft-lb	74.96 J
C	120.29 $^{\circ}$ F	66.83 $^{\circ}$ C
T ₀	43.31 $^{\circ}$ F	6.28 $^{\circ}$ C

$C_U = 30 \text{ ft-lb (41 J)} \text{ at } T = 18.6 \text{ }^{\circ}\text{F} \quad -7.4 \text{ }^{\circ}\text{C}$
 Upper Shelf Energy = 96.5 ft-lb 130.8 J

PT #	Temp ($^{\circ}$ F)	Energy (ft-lb)
1	-40	6.0
2	-10	18.0
3	0	24.0
4	20	37.0
5	40	36.0
6	60	46.0
7	80	53.0
8	120	79.0
9	220	89.0
10	360	94.0
11	360	98.0

0 = Fictitious Point Added

* = Test Point Not Included



$$Cv = A + B \tanh[(T - T_0)/C]$$

	English	Metric
A	26.80 ft-lb	36.34 J
B	24.18 ft-lb	32.79 J
C	139.42°F	77.46°C
T ₀	110.97°F	43.87°C

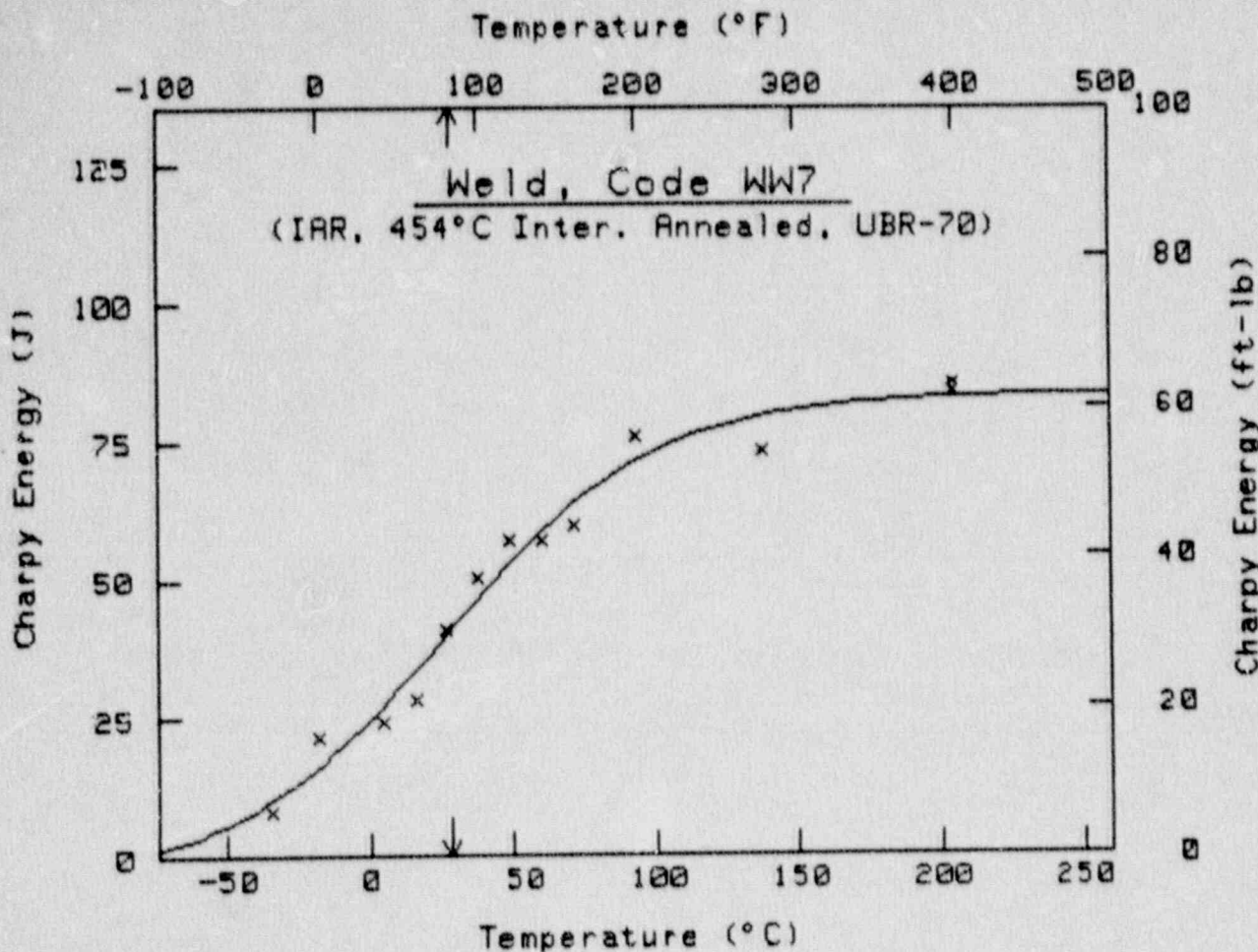
$$Cv = 30 \text{ ft-lb (41 J)} \text{ at } T = 129.5^{\circ}\text{F} \quad 54.2^{\circ}\text{C}$$

Upper Shelf Energy = 51.0 ft-lb 69.1 J

PT #	Temp ($^{\circ}$ F)	Energy (ft-lb)
1	0	12.0
2	40	14.0
3	80	22.0
4	90	28.0
5	120	32.0
6	140	32.0
7	150	36.0
8	200	38.0
9	280	47.0
10	400	52.0
11	400	49.0

0 = Fictitious Point Added

* = Test Point Not Included



$$Cv = A + B \tanh[(T - T_0)/C]$$

	English	Metric
A	29.19 ft-lb	39.57 J
B	32.50 ft-lb	44.06 J
C	133.50 $^{\circ}$ F	74.17 $^{\circ}$ C
T ₀	78.37 $^{\circ}$ F	25.76 $^{\circ}$ C

$$Cv = 38 \text{ ft-lb (41 J)} \text{ at } T = 81.7 \text{ }^{\circ}\text{F} \quad 27.6 \text{ }^{\circ}\text{C}$$

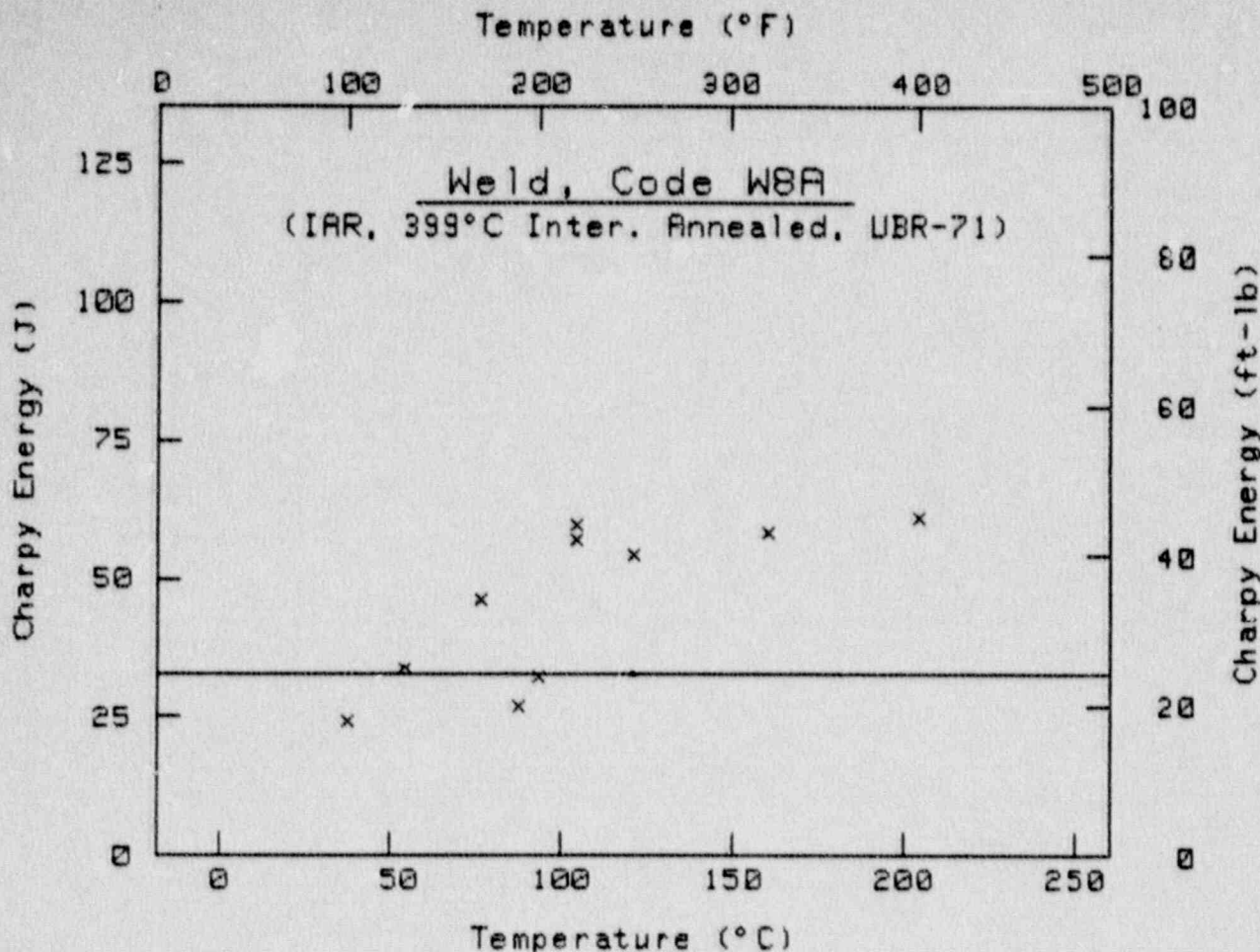
Upper Shelf Energy = 61.7 ft-lb 83.6 J

PT #	Temp ($^{\circ}$ F)	Energy (ft-lb)
1	-30	6.0
2	0	16.0
3	40	18.0
4	60	21.0
5	80	30.0
6	100	37.0
7	120	42.0
8	140	42.0
9	160	44.0
10	200	56.0
11	280	54.0
12	400	62.0
13	400	63.0

0 = Fictitious Point Added

* = Test Point Not Included

Computer Curve Fittings of Data from Irradiation Assembly UBR-71



 $C_U = A + B \tanh[(T - T_0)/C]$

	English	Metric
A	33.43 ft-lb	45.33 J
B	9.23 ft-lb	12.52 J
C	= -1053.43 $^{\circ}$ F	= -585.24 $^{\circ}$ C
T ₀		

-16381.7929586 M4D.DD
 $^{\circ}$ F -9118.77 $^{\circ}$ C

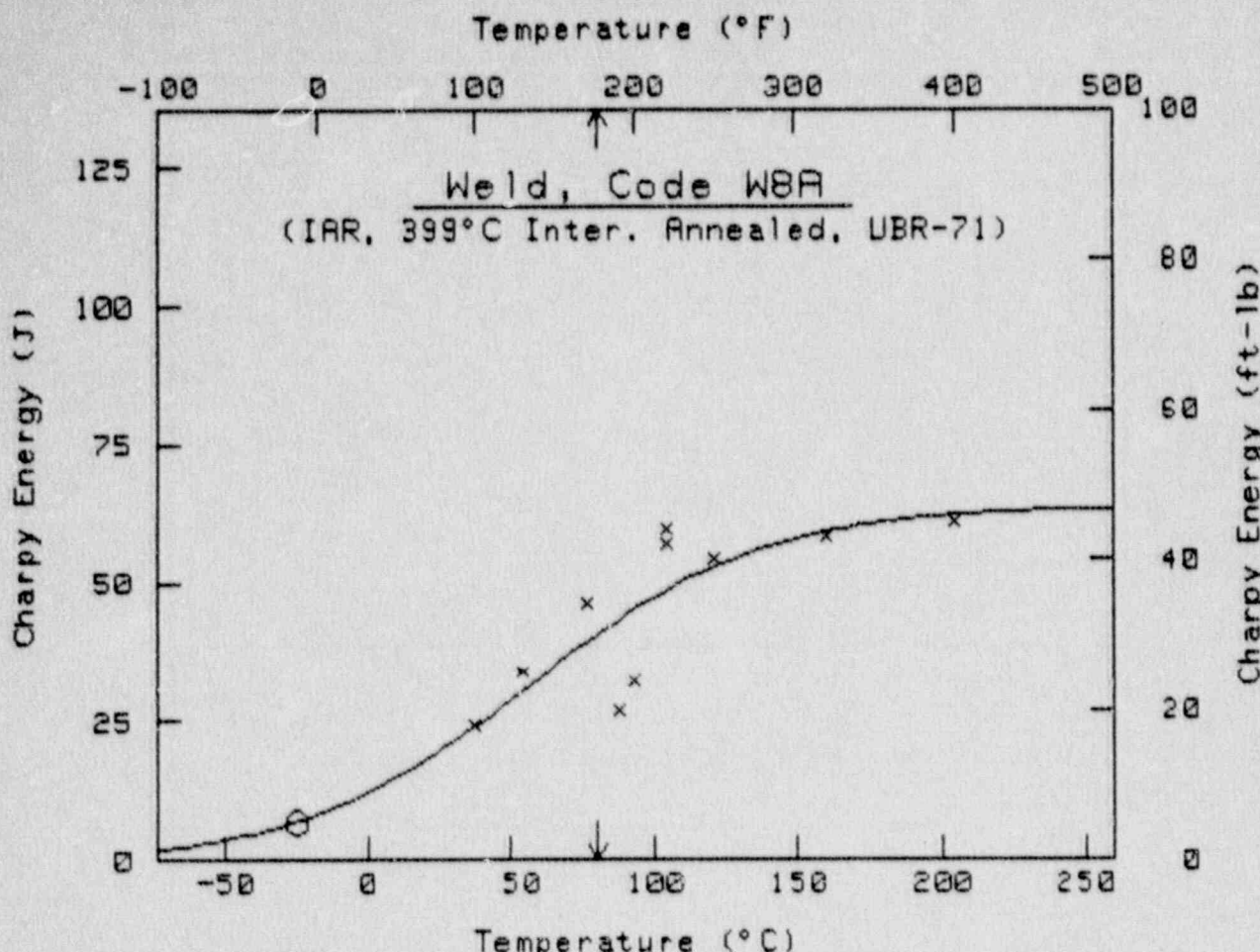
$C_U = 30$ ft-lb (41 J) at $T =$
-15970.1808453 4D.D
 $^{\circ}$ F
-8890.10046961 4D.D
 $^{\circ}$ C

Upper Shelf Energy = 42.7 ft-lb 57.8 J

PT #	Temp ($^{\circ}$ F)	Energy (ft-lb)
1	100	18.0
2	130	25.0
3	170	34.0
4	190	20.0
5	200	24.0
6	220	44.0
7	220	42.0
8	250	40.0
9	320	43.0
10	400	45.0

O = Fictitious Point Added

* = Test Point Not Included



$$C_U = A + B \tanh[(T - T_0)/C]$$

	English	Metric
A	23.35 ft-lb	31.66 J
B	23.78 ft-lb	32.25 J
C	146.03 $^{\circ}$ F	81.13 $^{\circ}$ C
T ₀	135.00 $^{\circ}$ F	57.22 $^{\circ}$ C

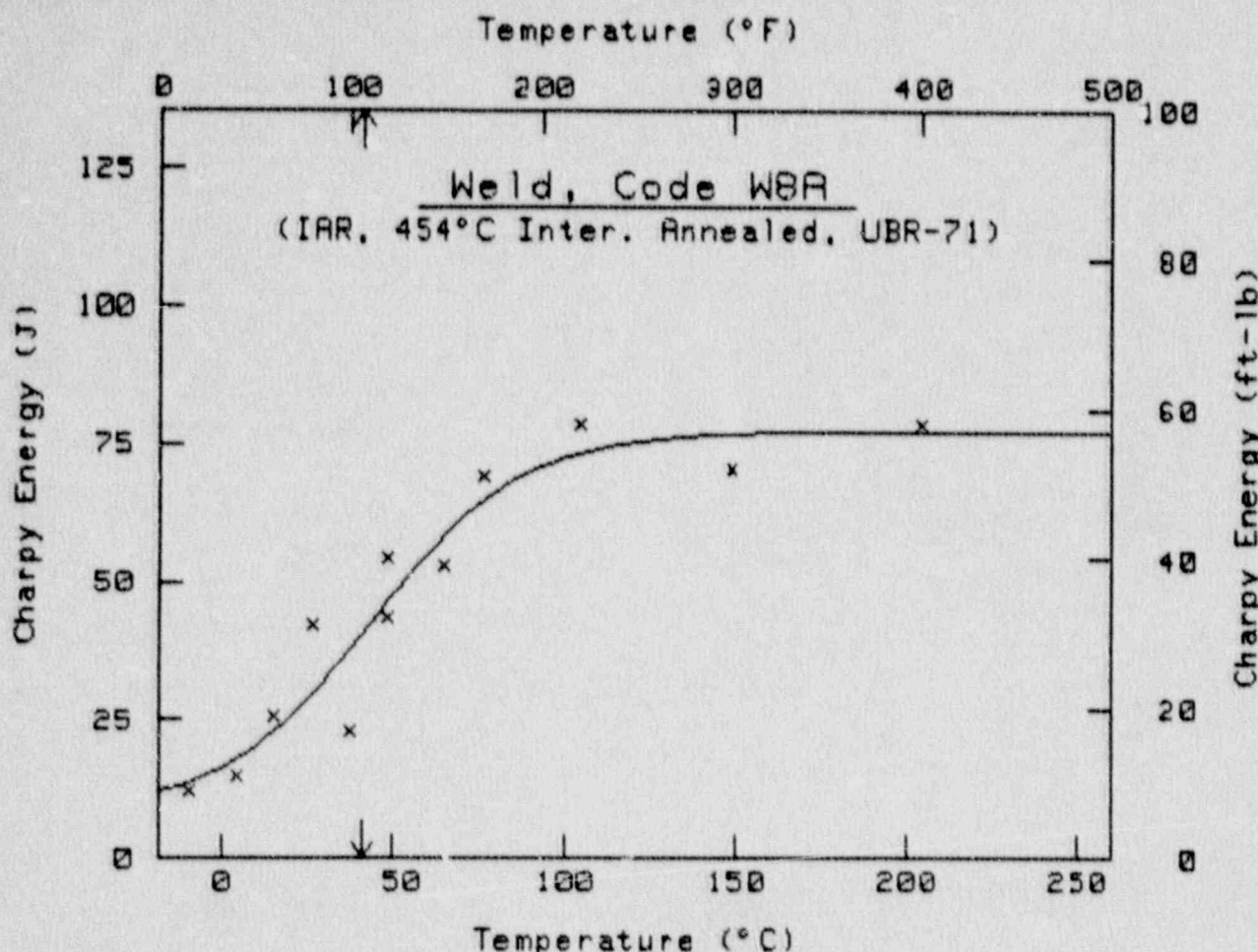
$$C_U = 30 \text{ ft-lb (41 J)} \text{ at } T = 176.9 \text{ }^{\circ}\text{F} \quad 80.5 \text{ }^{\circ}\text{C}$$

Upper Shelf Energy = 47.1 ft-lb 63.9 J

PT #	Temp ($^{\circ}$ F)	Energy (ft-lb)
1	100	18.0
2	130	25.0
3	170	34.0
4	190	28.0
5	200	24.0
6	220	44.0
7	220	42.0
8	250	40.0
9	320	43.0
10	400	45.0
11 0	-13	5.0
12 0	-13	5.0
13 0	-13	5.0
14 0	-13	5.0

O = Fictitious Point Added

* = Test Point Not Included



$$Cv = A + B \tanh[(T - T_0)/C]$$

	English	Metric
A	31.54 ft-lb	42.77 J
B	25.50 ft-lb	34.57 J
C	78.77 $^{\circ}$ F	43.76 $^{\circ}$ C
T ₀	111.42 $^{\circ}$ F	44.12 $^{\circ}$ C

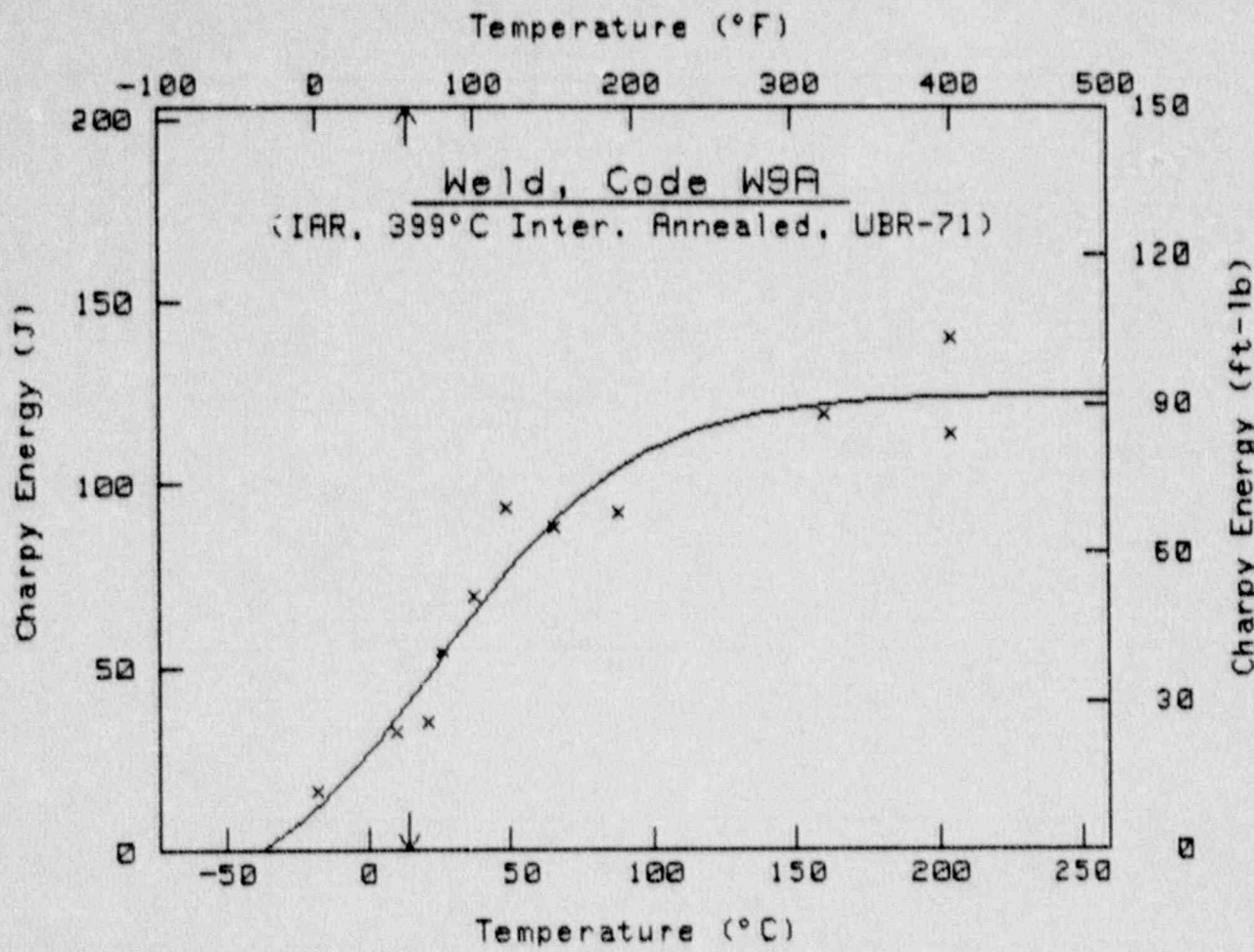
$$Cv = 30 \text{ ft-lb (41 J) at } T = 106.6 \text{ }^{\circ}\text{F} \quad 41.5 \text{ }^{\circ}\text{C}$$

$$\text{Upper Shelf Energy} = 57.0 \text{ ft-lb} \quad 77.3 \text{ J}$$

PT #	Temp ($^{\circ}$ F)	Energy (ft-lb)
1	15	9.0
2	40	11.0
3	60	19.0
4	80	31.0
5	100	17.0
6	120	32.0
7	120	40.0
8	150	39.0
9	170	51.0
10	220	58.0
11	300	52.0
12	400	58.0

0 = Fictitious Point Added

* = Test Point Not Included



$$Cv = A + B \tanh[(T - T_0)/C]$$

	English	Metric
A	38.27 ft-lb	51.89 J
B	53.73 ft-lb	72.65 J
C	126.01 $^{\circ}$ F	70.00 $^{\circ}$ C
T ₀	77.05 $^{\circ}$ F	25.03 $^{\circ}$ C

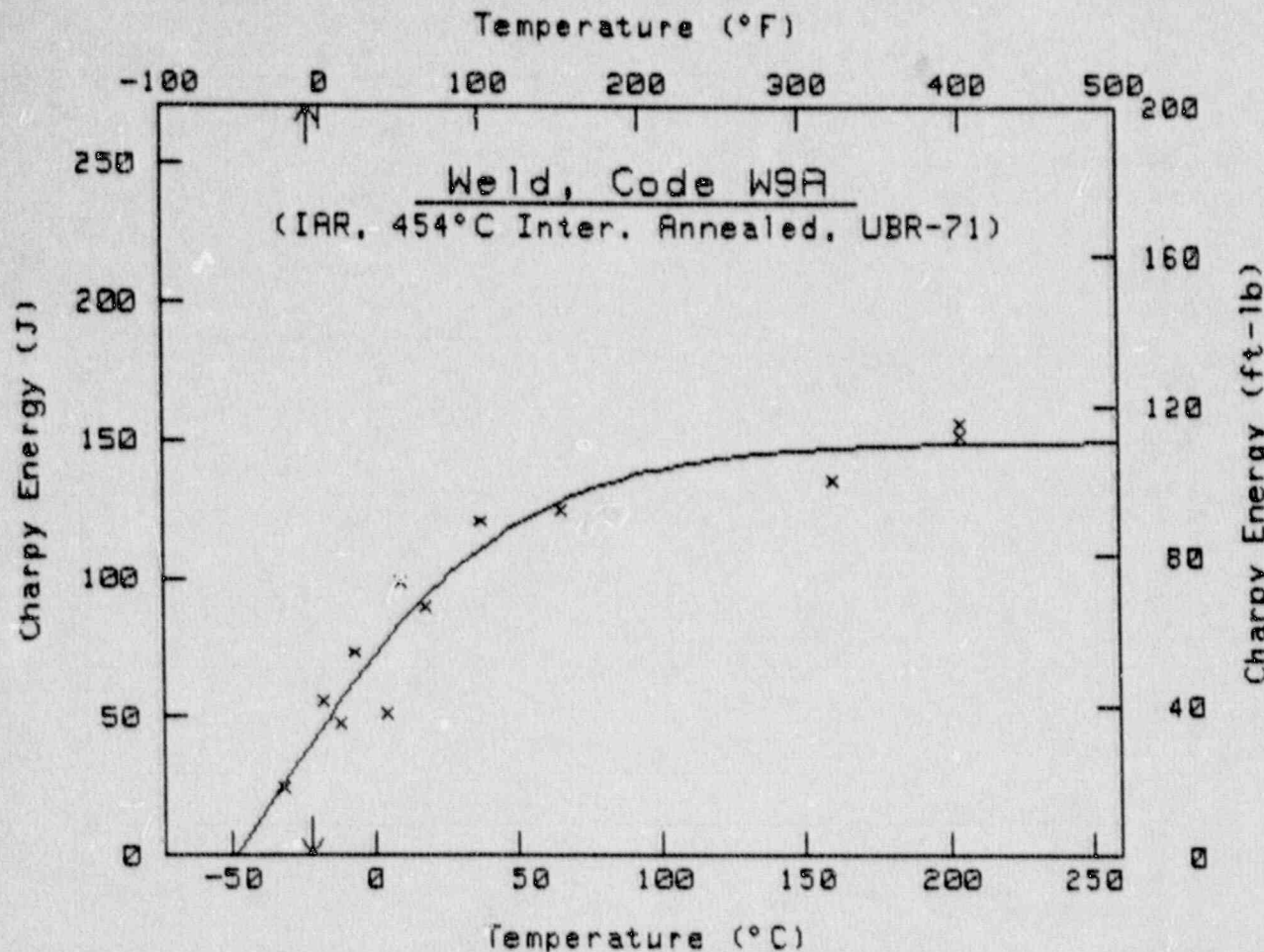
$$Cv = 30 \text{ ft-lb (41 J)} \text{ at } T = 57.5 \text{ }^{\circ}\text{F} \quad 14.2 \text{ }^{\circ}\text{C}$$

Upper Shelf Energy = 92.0 ft-lb 124.7 J

PT #	Temp ($^{\circ}$ F)	Energy (ft-lb)
1	0	12.0
2	50	24.0
3	70	26.0
4	80	40.0
5	100	51.0
6	120	69.0
7	150	65.0
8	190	68.0
9	320	88.0
10	400	84.0
11	400	103.0

0 = Fictitious Point Added

* = Test Point Not Included



$$Cv = A + B \tanh[(T - T_0)/C]$$

	English	Metric
A	12.78 ft-lb	17.33 J
B	97.65 ft-lb	132.39 J
C	153.99 $^{\circ}$ F	85.55 $^{\circ}$ C
T ₀	-35.33 $^{\circ}$ F	-37.41 $^{\circ}$ C

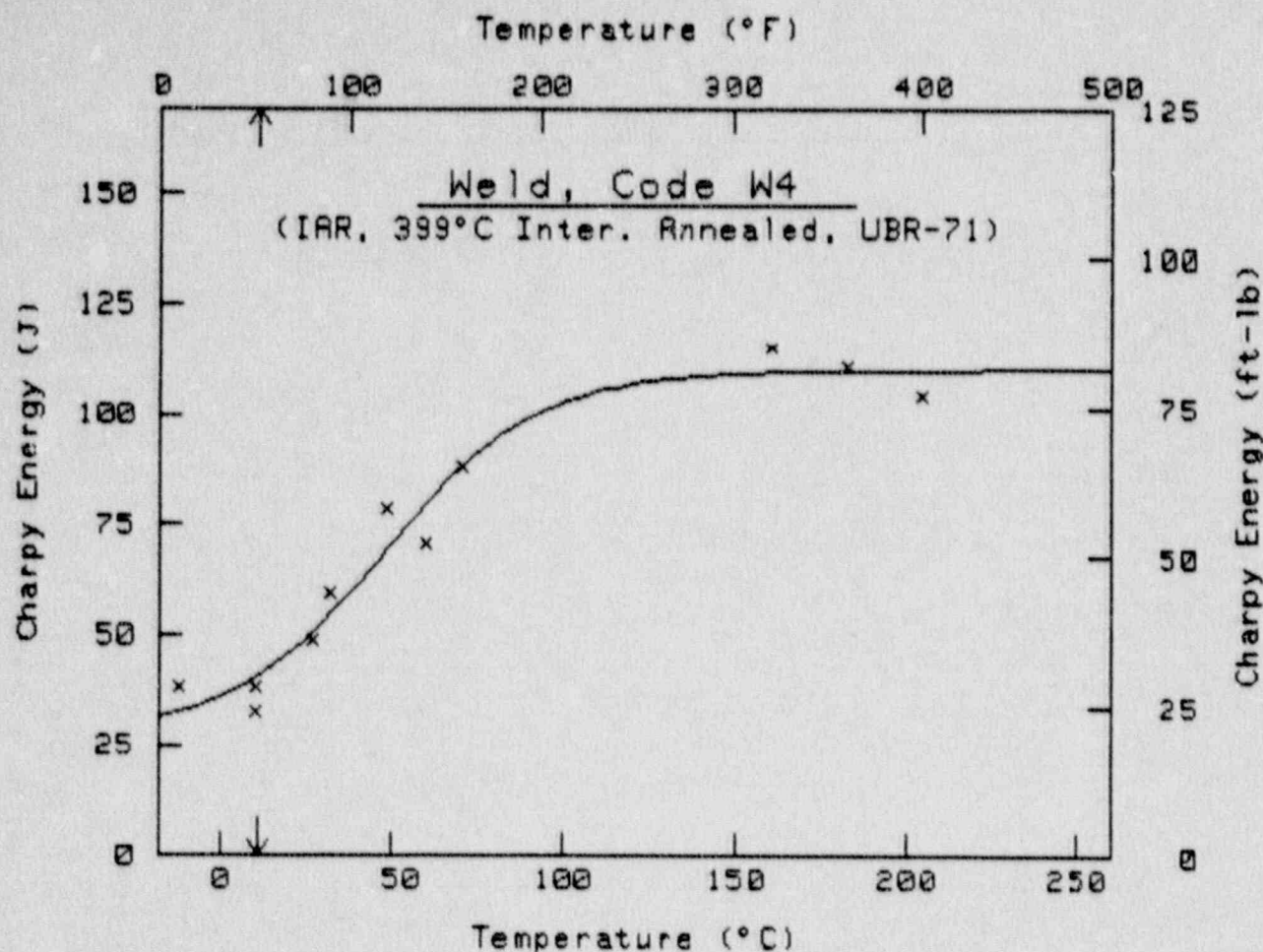
$$Cv = 30 \text{ ft-lb (41 J)} \text{ at } T = -7.9 \text{ }^{\circ}\text{F} \quad -22.2 \text{ }^{\circ}\text{C}$$

Upper Shelf Energy = 110.4 ft-lb 149.7 J

PT #	Temp ($^{\circ}$ F)	Energy (ft-lb)
1	-25	18.0
2	0	41.0
3	10	35.0
4	20	54.0
5	40	38.0
6	50	73.0
7	65	66.0
8	100	89.0
9	150	92.0
10	320	100.0
11	400	112.0
12	400	115.0

0 = Fictitious Point Added

* = Test Point Not Included



 $C_v = A + B \tanh[(T - T_0)/C]$

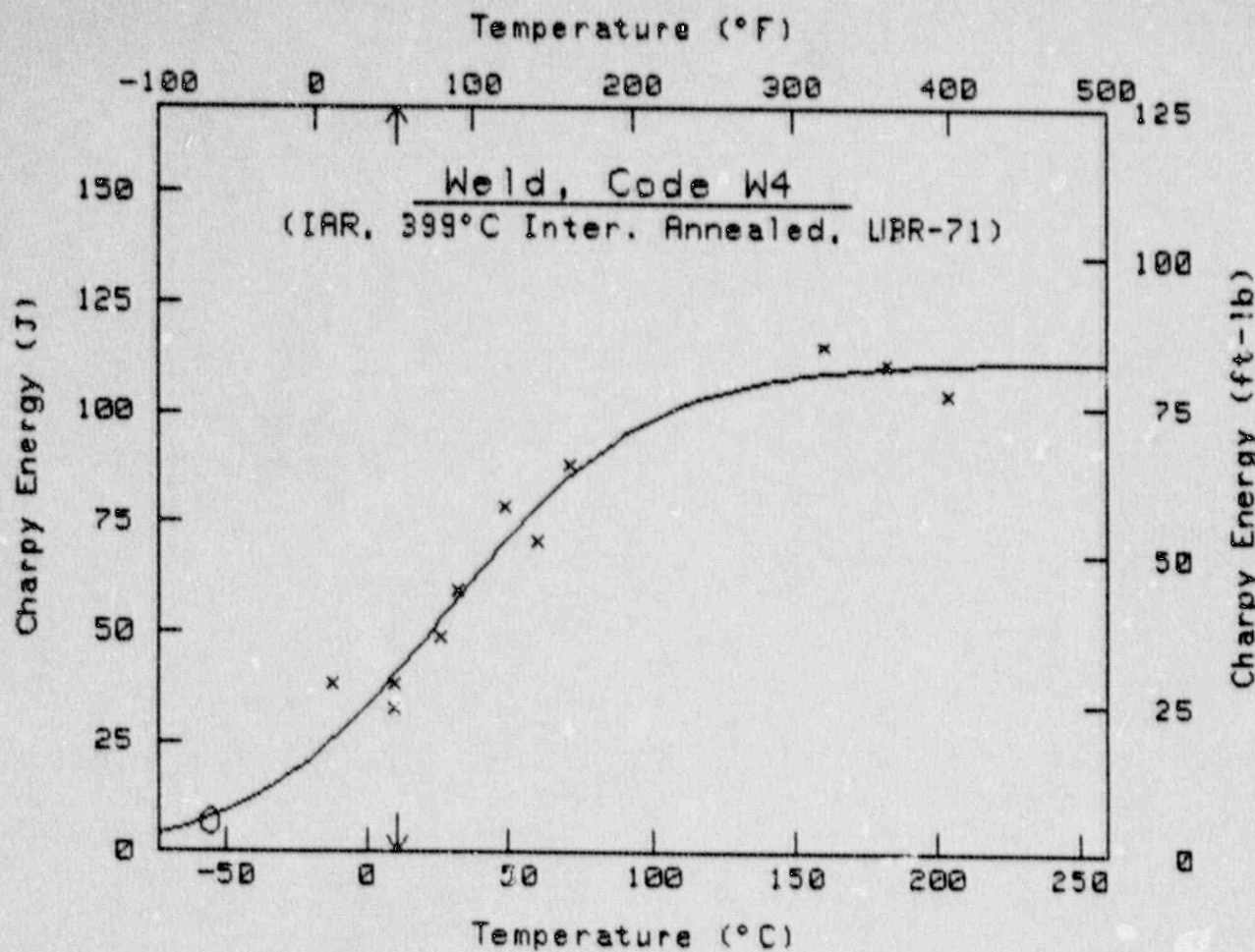
	English	Metric
A	50.64 ft-lb	68.65 J
B	30.64 ft-lb	41.54 J
C	81.48 $^{\circ}$ F	45.27 $^{\circ}$ C
T ₀	118.33 $^{\circ}$ F	47.96 $^{\circ}$ C

$C_v = 30$ ft-lb (41 J) at $T = 51.7$ $^{\circ}$ F 11.0 $^{\circ}$ C
 Upper Shelf Energy = 81.3 ft-lb 110.2 J

PT #	Temp ($^{\circ}$ F)	Energy (ft-lb)
1	10	28.0
2	50	24.0
3	56	28.0
4	80	36.0
5	90	44.0
6	120	58.0
7	140	52.0
8	160	65.0
9	320	85.0
10	360	82.0
11	400	77.0

0 = Fictitious Point Added

* = Test Point Not Included



$$C_v = A + B \tanh[(T - T_0)/C]$$

	English	Metric
A	40.55 ft-lb	54.97 J
B	41.99 ft-lb	56.93 J
C	128.22 $^{\circ}$ F	71.23 $^{\circ}$ C
T ₀	84.08 $^{\circ}$ F	28.93 $^{\circ}$ C

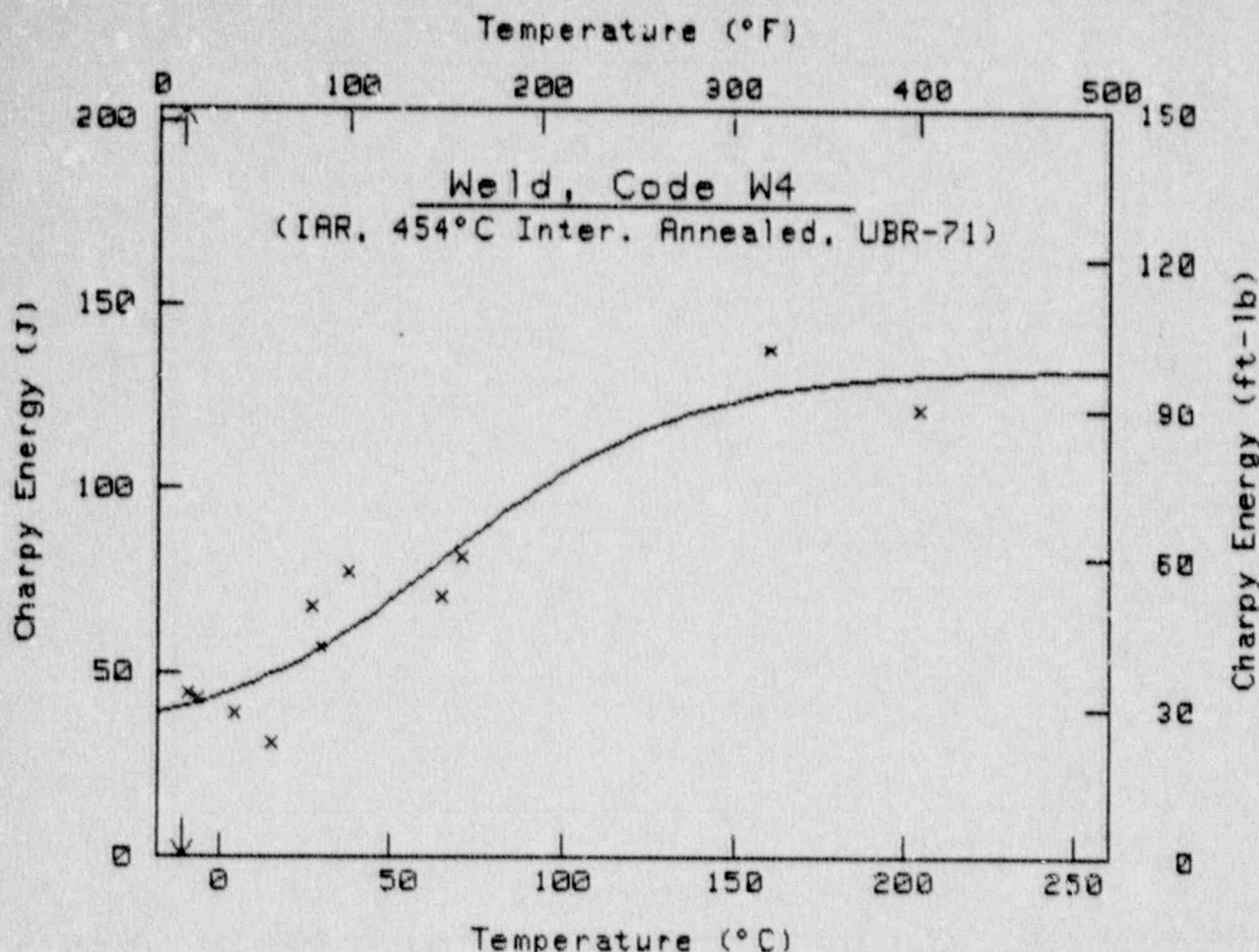
$$C_v = 30 \text{ ft-lb (41 J) at } T = 51.2 \text{ }^{\circ}\text{F} \quad 10.7 \text{ }^{\circ}\text{C}$$

Upper Shelf Energy = 82.5 ft-lb 111.9 J

PT #	Temp ($^{\circ}$ F)	Energy (ft-lb)
1	10	28.0
2	50	24.0
3	50	28.0
4	80	36.0
5	90	44.0
6	120	58.0
7	140	52.0
8	160	65.0
9	320	85.0
10	360	82.0
11	400	77.0
12	0 -68	5.0
13	0 -68	5.0
14	0 -68	5.0
15	0 -68	5.0

0 = Fictitious Point Added

* = Test Point Not Included



$$C_U = A + B \tanh[(T - T_0)/C]$$

	English	Metric
A	60.47 ft-lb	81.99 J
B	37.54 ft-lb	50.90 J
C	124.31 $^{\circ}$ F	69.06 $^{\circ}$ C
T ₀	153.52 $^{\circ}$ F	67.51 $^{\circ}$ C

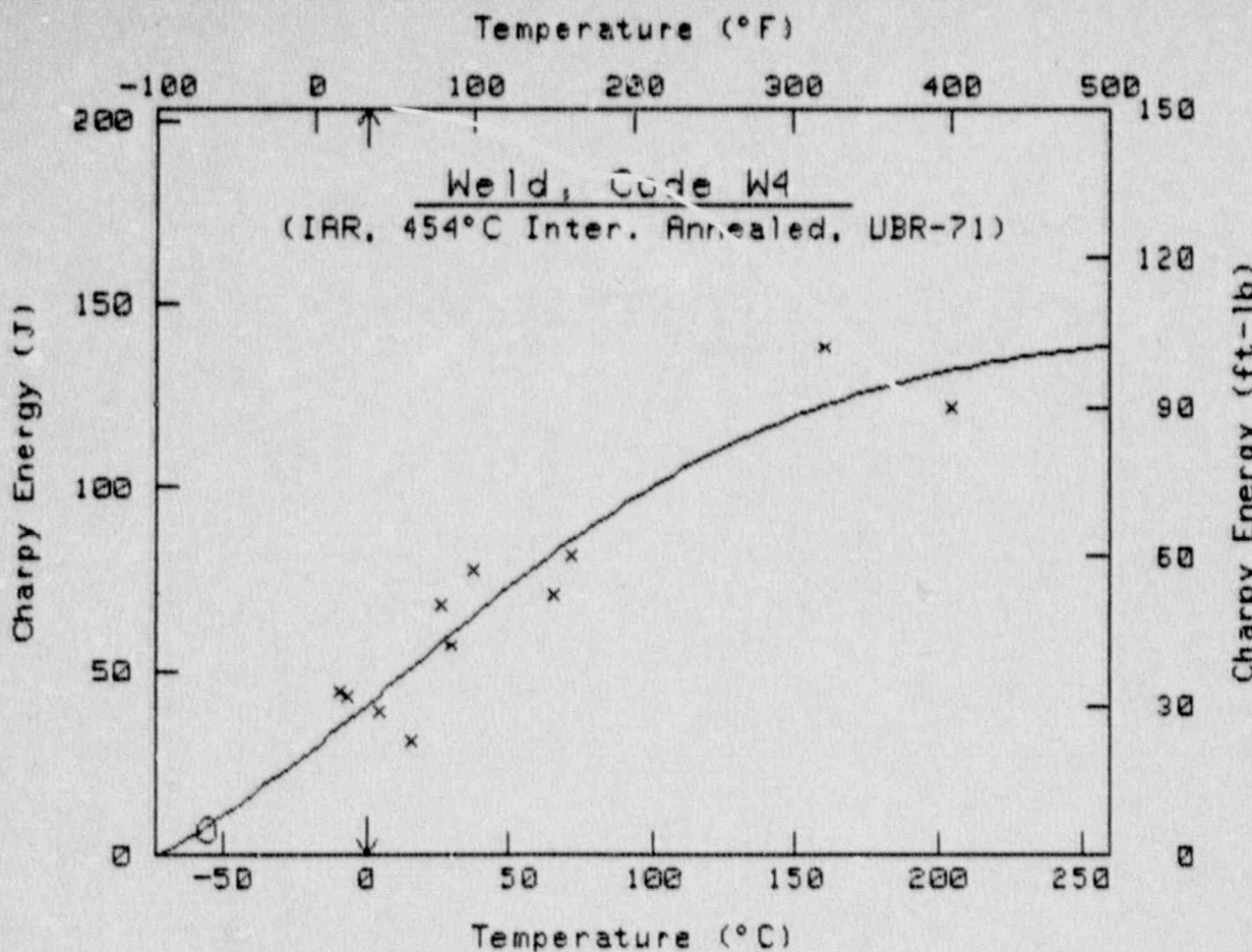
$$C_U = 38 \text{ ft-lb (41 J)} \text{ at } T = 12.8 \text{ }^{\circ}\text{F} \quad -10.7 \text{ }^{\circ}\text{C}$$

Upper Shelf Energy = 98.0 ft-lb 102.9 J

PT #	Temp ($^{\circ}$ F)	Energy (ft-lb)
1	15	33.0
2	20	32.0
3	40	29.0
4	60	23.0
5	80	50.0
6	85	42.0
7	100	57.0
8	150	52.0
9	160	60.0
10	320	102.0
11	400	90.0

0 = Fictitious Point Added

* = Test Point Not Included



$$Cu = A + B \tanh[(T - T_0)/C]$$

	English	Metric
A	37.44 ft-lb	50.77 J
B	69.35 ft-lb	94.03 J
C	259.85 $^{\circ}$ F	144.36 $^{\circ}$ C
T ₀	60.35 $^{\circ}$ F	15.75 $^{\circ}$ C

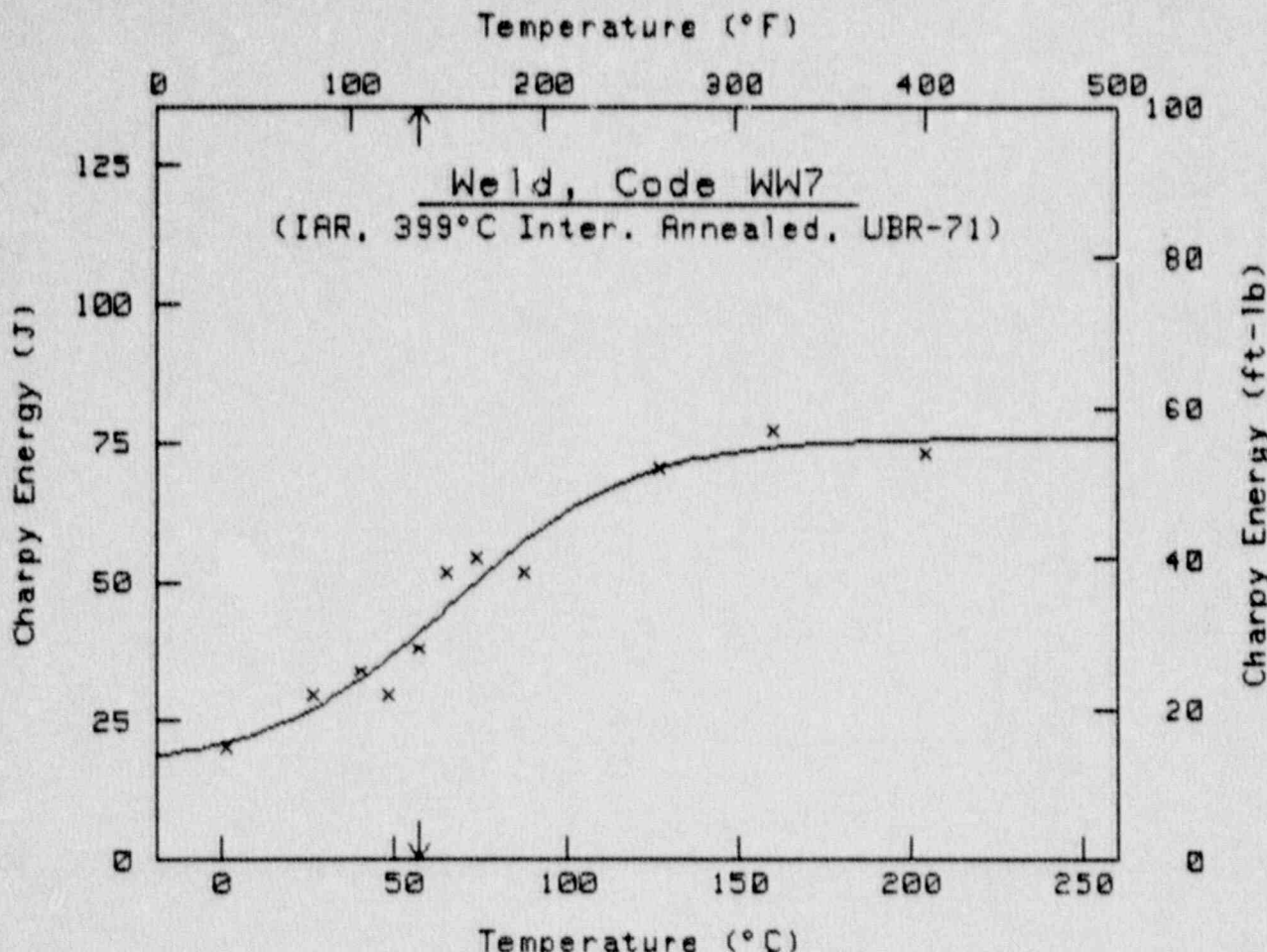
$$Cu = 30 \text{ ft-lb (41 J) at } T = 32.3 \text{ }^{\circ}\text{F} \quad .2 \text{ }^{\circ}\text{C}$$

Upper Shelf Energy = 106.8 ft-lb 144.8 J

PT #	Temp ($^{\circ}$ F)	Energy (ft-lb)
1	15	33.0
2	20	32.0
3	40	29.0
4	60	23.0
5	80	50.0
6	85	42.0
7	100	57.0
8	150	52.0
9	160	60.0
10	320	102.0
11	400	90.0
12 0	-68	5.0
13 0	-68	5.0
14 0	-68	5.0
15 0	-68	5.0

0 = Fictitious Point Added

* = Test Point Not Included



$$C_U = A + B \tanh[(T - T_0)/C]$$

	English	Metric
A	34.10 ft-lb	46.23 J
B	21.87 ft-lb	29.65 J
C	95.11° F	52.84° C
T ₀	152.99° F	67.22° C

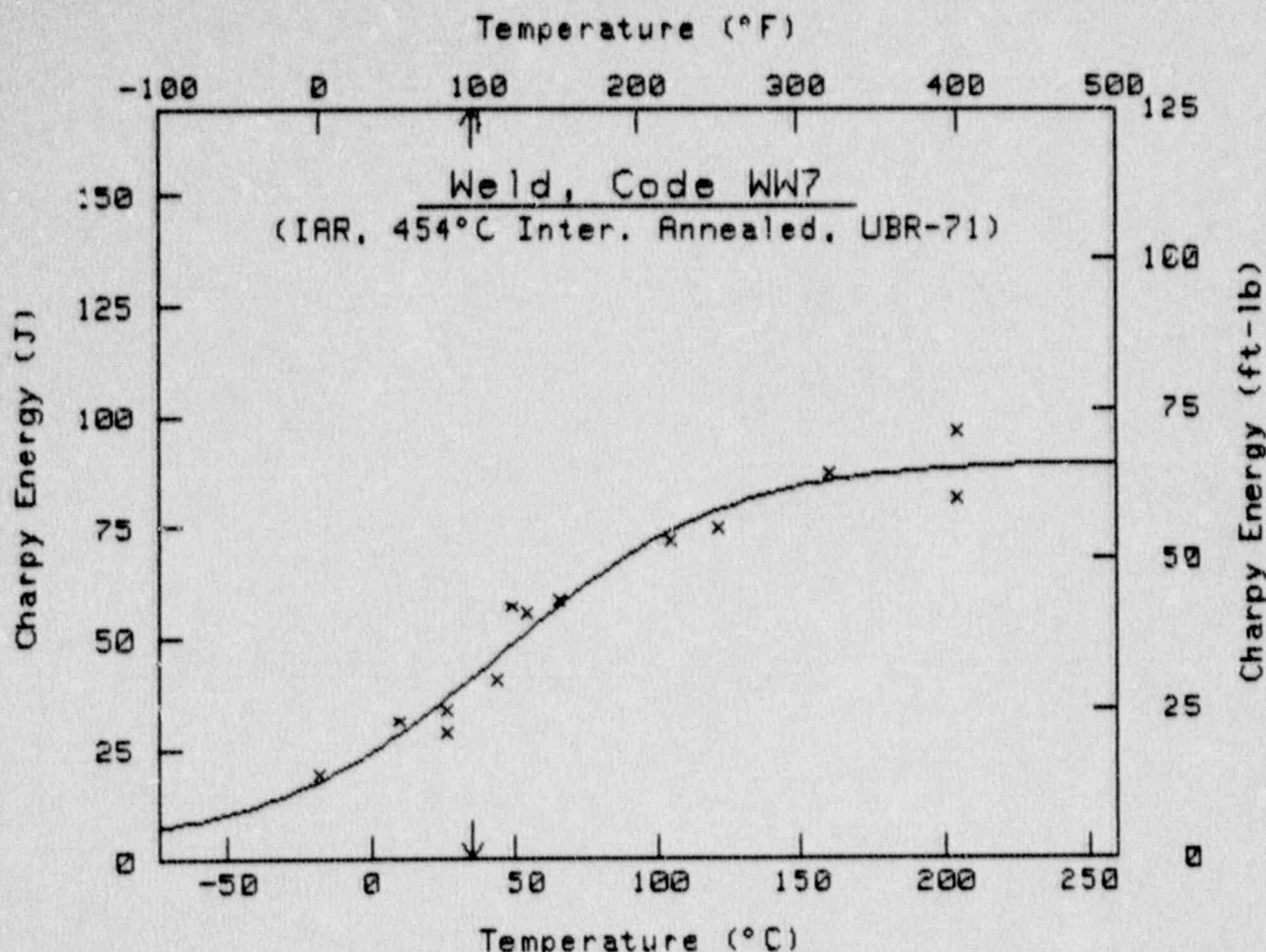
$$C_U = 30 \text{ ft-lb } (41 \text{ J}) \text{ at } T = 135.0^{\circ}\text{F} \quad 57.2^{\circ}\text{C}$$

Upper Shelf Energy = 56.0 ft-lb 75.9 J

PT #	Temp ($^{\circ}$ F)	Energy (ft-lb)
1	35	15.0
2	80	22.0
3	105	25.0
4	120	22.0
5	135	28.0
6	150	38.0
7	165	48.0
8	190	38.0
9	260	52.0
10	320	57.0
11	400	54.0

O = Fictitious Point Added

* = Test Point Not Included



$$Cv = A + B \tanh[(T - T_0)/C]$$

	English	Metric
A	34.26 ft-lb	46.45 J
B	31.96 ft-lb	43.34 J
C	142.95 $^{\circ}$ F	79.42 $^{\circ}$ C
T ₀	113.85 $^{\circ}$ F	45.47 $^{\circ}$ C

$$Cv = 30 \text{ ft-lb (41 J)} \text{ at } T = 94.7 \text{ }^{\circ}\text{F} \quad 34.8 \text{ }^{\circ}\text{C}$$

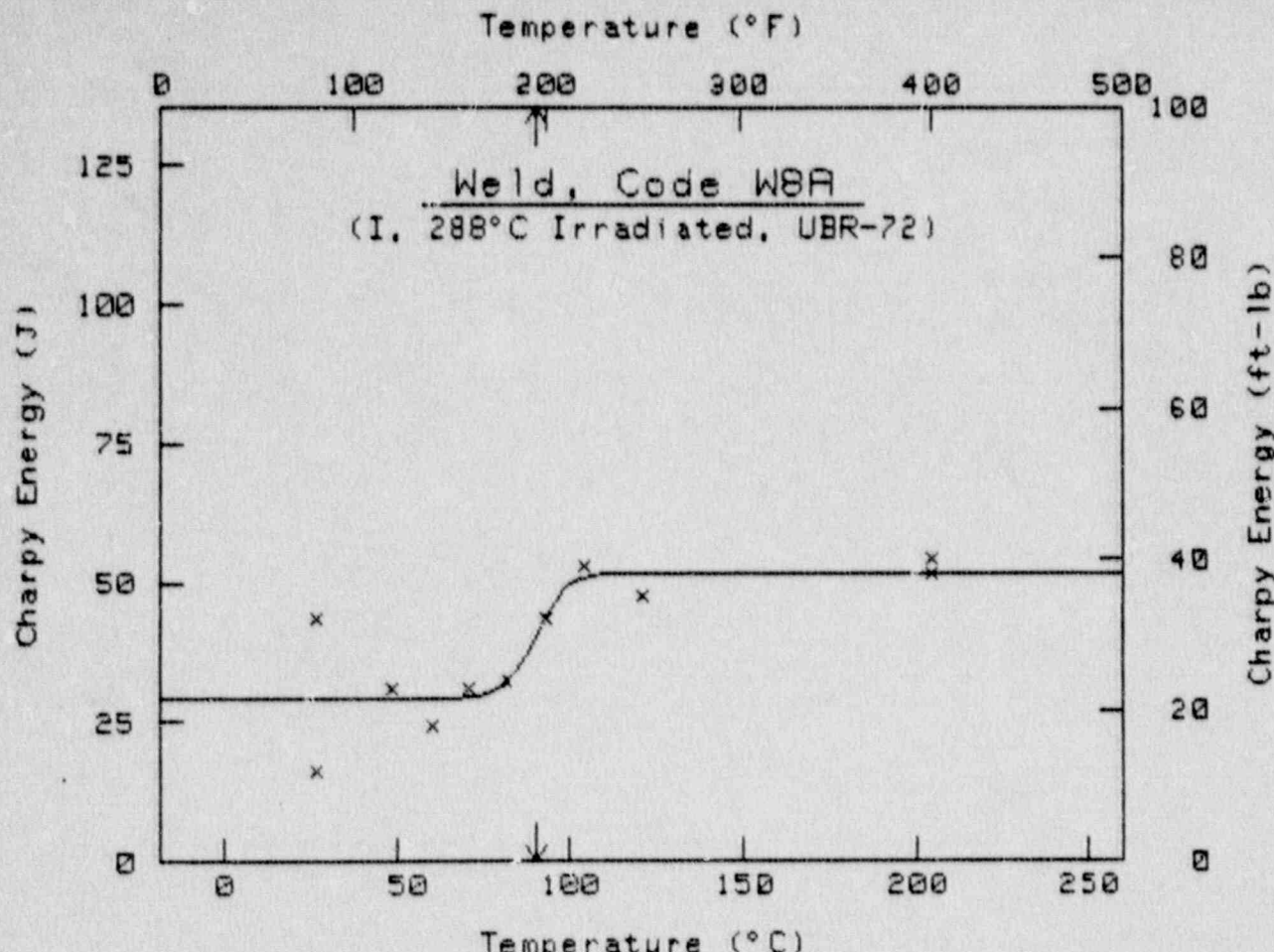
Upper Shelf Energy = 66.2 ft-lb 89.8 J

PT #	Temp ($^{\circ}$ F)	Energy (ft-lb)
1	0	14.0
2	50	23.0
3	80	25.0
4	80	21.0
5	110	30.0
6	120	42.0
7	130	41.0
8	150	43.0
9	220	53.0
10	250	55.0
11	320	64.0
12	400	71.0
13	400	60.0

0 = Fictitious Point Added

* = Test Point Not Included

Computer Curve Fittings of Data from Irradiation Assembly UBR-72



 $Cv = A + B \tanh[(T - T_0)/C]$

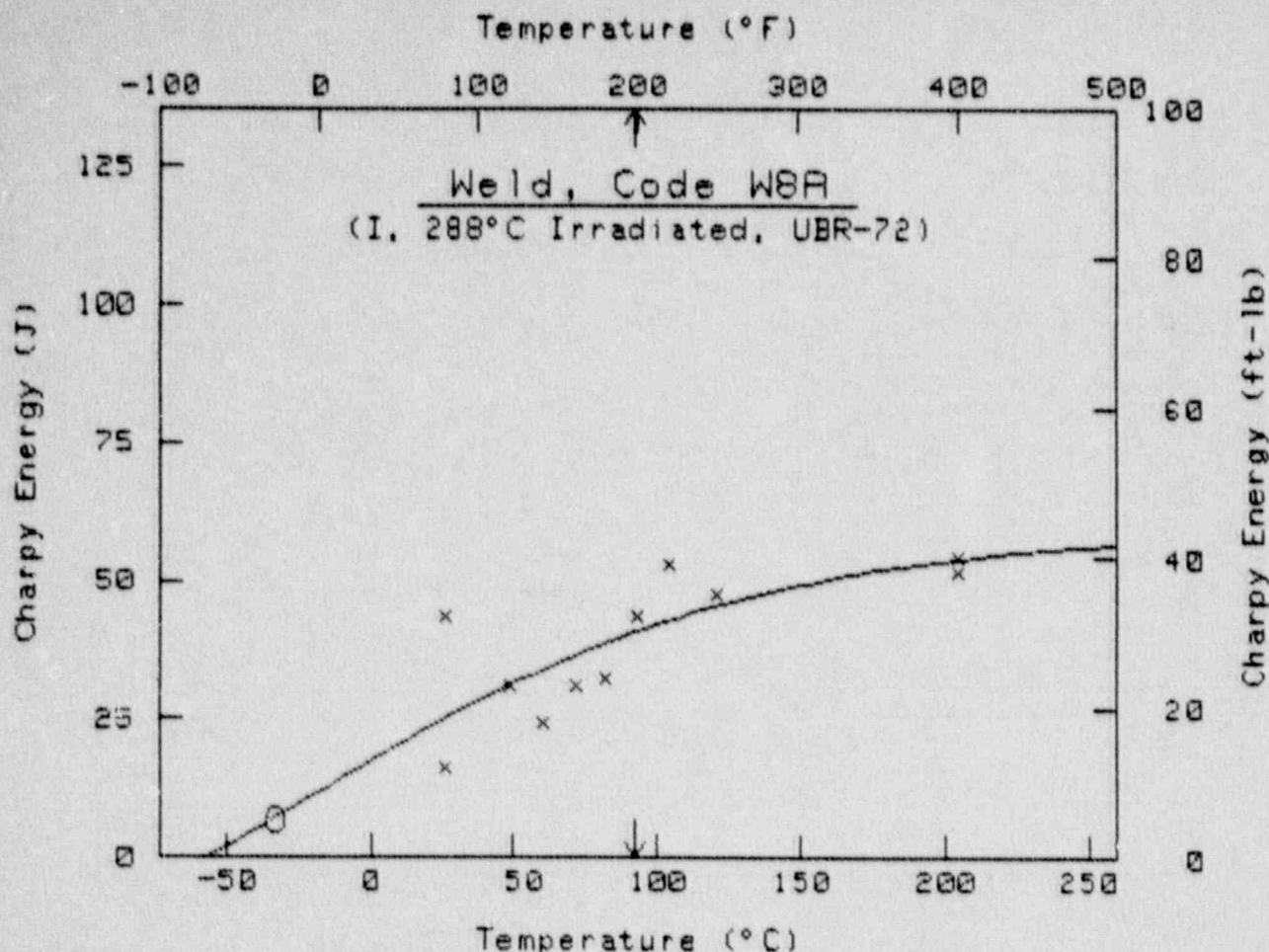
	English	Metric
A	29.84 ft-lb	40.46 J
B	8.25 ft-lb	11.18 J
C	15.57 $^{\circ}$ F	8.65 $^{\circ}$ C
T ₀	194.92 $^{\circ}$ F	90.51 $^{\circ}$ C

$Cv = 30 \text{ ft-lb (41 J) at } T = 195.2 \text{ }^{\circ}\text{F} \quad 90.7 \text{ }^{\circ}\text{C}$
 Upper Shelf Energy = $38.1 \text{ ft-lb} \quad 51.6 \text{ J}$

PT #	Temp ($^{\circ}$ F)	Energy (ft-lb)
1	80	12.0
2	80	32.0
3	120	23.0
4	140	18.0
5	160	23.0
6	180	24.0
7	200	32.0
8	220	39.0
9	250	35.0
10	400	40.0
11	400	38.0

0 = Fictitious Point Added

* = Test Point Not Included



$$C_U = A + B \tanh[(T - T_0)/C]$$

	English	Metric
A	6.75 ft-lb	9.16 J
B	36.99 ft-lb	50.16 J
C	290.27°F	161.26°C
T ₀	-16.04°F	-26.69°C

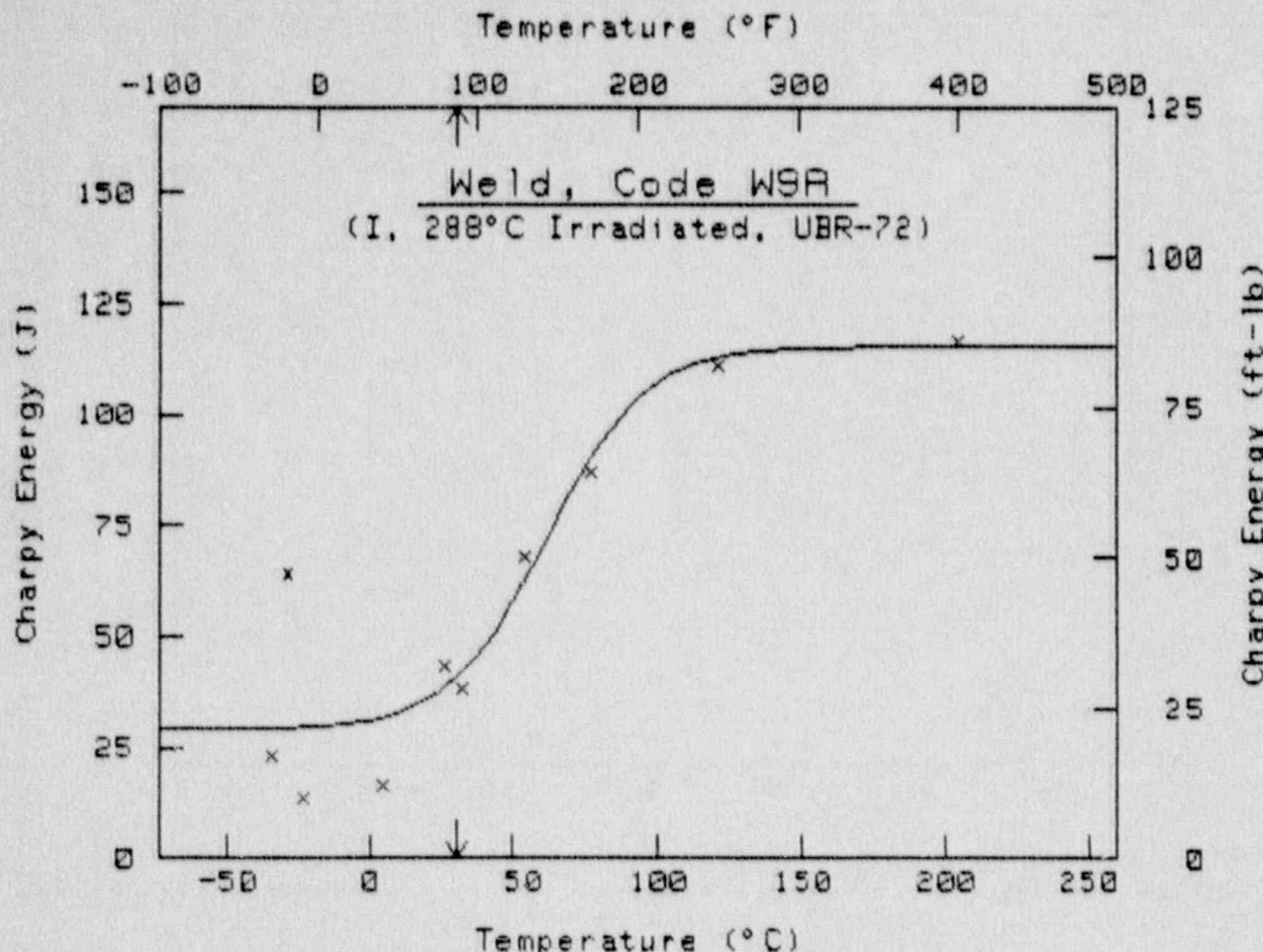
$$C_U = 30 \text{ ft-lb (41 J)} \text{ at } T = 198.4^{\circ}\text{F} \quad 92.4^{\circ}\text{C}$$

Upper Shelf Energy = 43.7 ft-lb 59.3 J

PT #	Temp ($^{\circ}$ F)	Energy (ft-lb)
1	80	12.0
2	80	32.0
3	120	23.0
4	140	18.0
5	160	23.0
6	180	24.0
7	200	32.0
8	220	39.0
9	250	35.0
10	400	40.0
11	400	38.0
12	-28	5.0
13	-28	5.0
14	-28	5.0
15	-28	5.0

O = Fictitious Point Added

* = Test Point Not Included



 $Cv = A + B \tanh[(T - T_0)/C]$

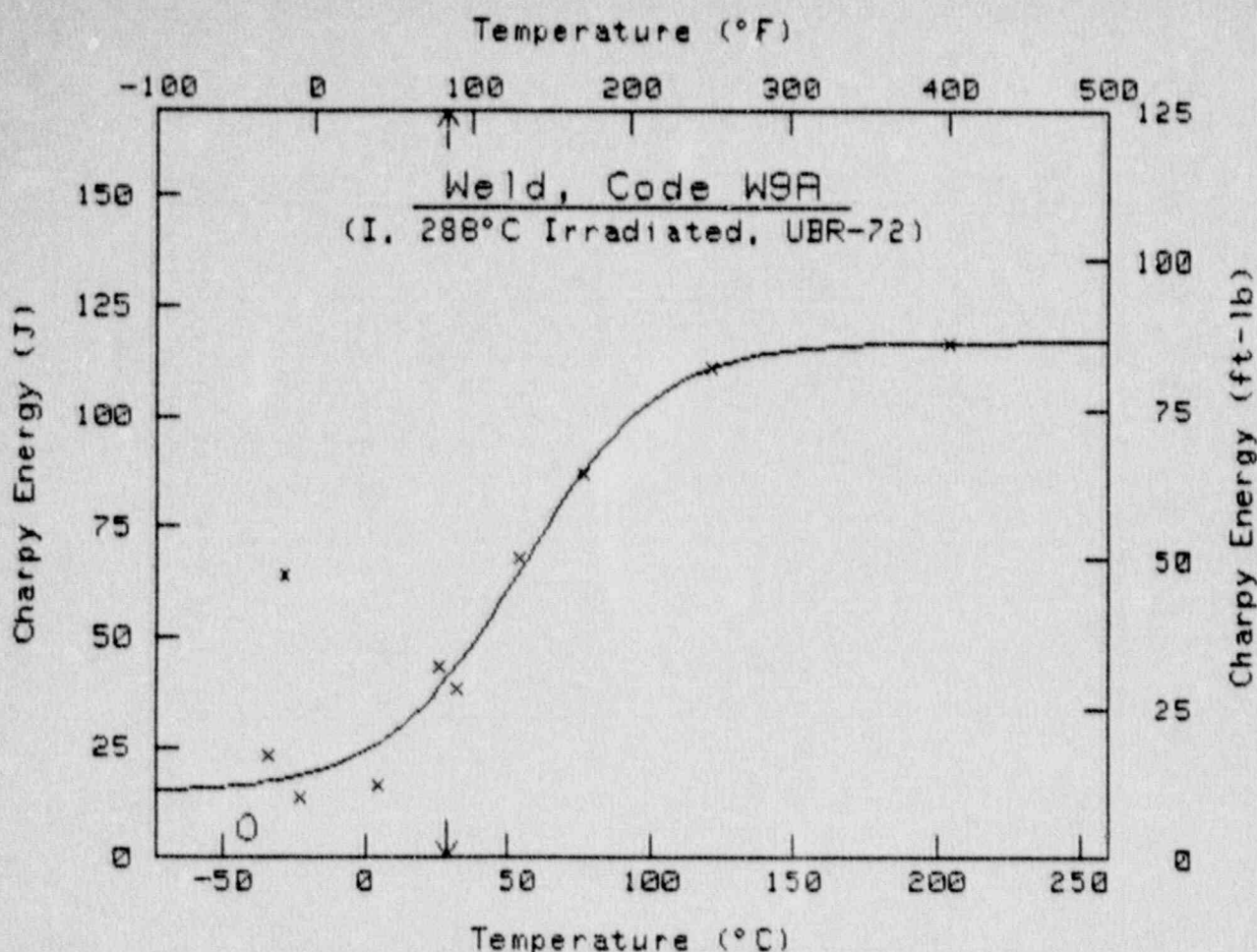
	English	Metric
A	53.24 ft-lb	72.19 J
B	31.84 ft-lb	43.17 J
C	60.76°F	33.76°C
T_0	143.29°F	61.83°C

$Cv = 30 \text{ ft-lb (41 J)} \text{ at } T = 86.9^{\circ}\text{F} \quad 30.5^{\circ}\text{C}$
 Upper Shelf Energy = $85.1 \text{ ft-lb} \quad 115.4 \text{ J}$

PT #	Temp ($^{\circ}\text{F}$)	Energy (ft-lb)
1	-30	17.0
2	-20	47.0
3	-10	10.0
4	40	12.0
5	80	32.0
6	90	28.0
7	130	50.0
8	170	64.0
9	250	82.0
10	400	86.0
11	400	86.0

0 = Fictitious Point Added

* = Test Point Not Included



$$Cv = A + B \tanh[(T - T_0)/C]$$

	English	Metric
A	48.56 ft-lb	65.84 J
B	37.70 ft-lb	51.12 J
C	86.27°F	47.93°C
T ₀	131.06°F	55.03°C

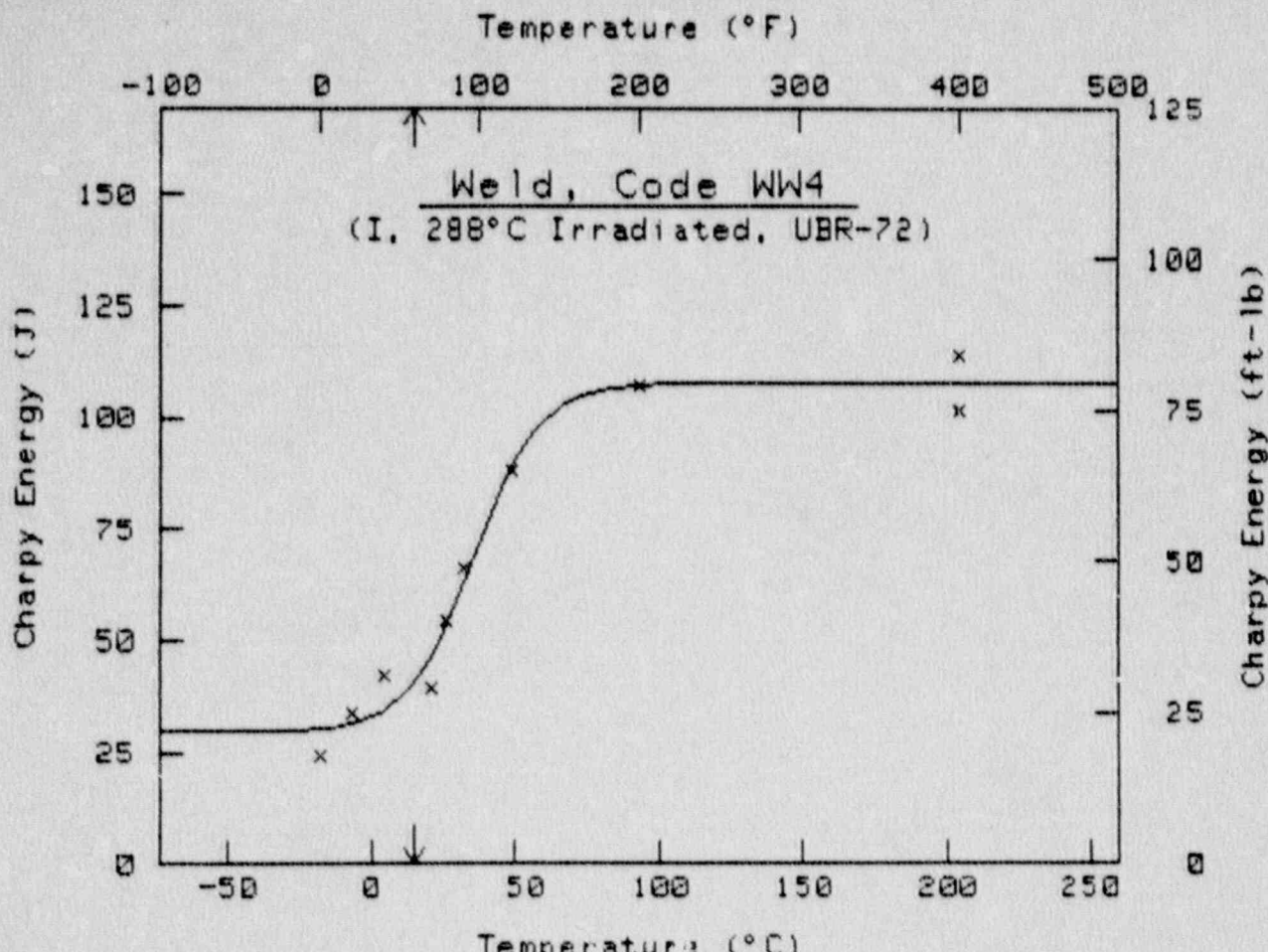
$$Cv = 30 \text{ ft-lb (41 J) at } T = 84.5^{\circ}\text{F} \quad 29.2^{\circ}\text{C}$$

Upper Shelf Energy = 86.3 ft-lb 117.0 J

PT #	Temp ($^{\circ}$ F)	Energy (ft-lb)
1	-30	17.0
2	-20	47.0
3	-10	10.0
4	40	12.0
5	80	32.0
6	90	28.0
7	130	50.0
8	170	64.0
9	250	82.0
10	400	86.0
11	400	86.0
12 0	-43	5.0
13 0	-43	5.0
14 0	-43	5.0
15 0	-43	5.0

O = Fictitious Point Added

* = Test Point Not Included



 $C_U = A + B \tanh[(T - T_0)/C]$

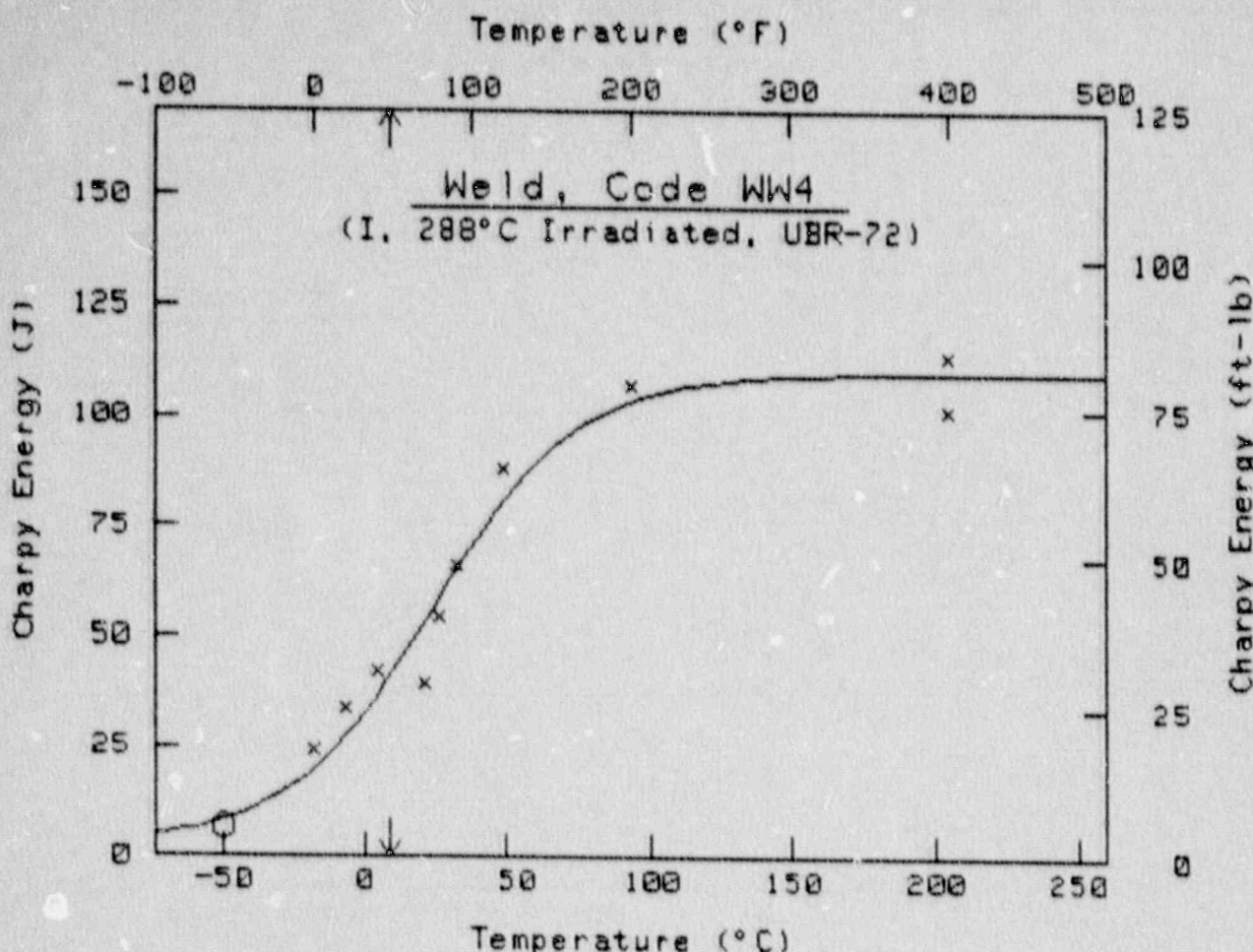
	English	Metric
A	50.62 ft-lb	68.63 J
B	28.84 ft-lb	39.11 J
C	41.60°F	23.11°C
T ₀	96.31°F	35.73°C

$C_U = 30 \text{ ft-lb (41 J)} \text{ at } T = 59.0^{\circ}\text{F} \quad 15.0^{\circ}\text{C}$
 Upper Shelf Energy = $79.5 \text{ ft-lb} \quad 107.7 \text{ J}$

PT #	Temp ($^{\circ}\text{F}$)	Energy (ft-lb)
1	0	18.0
2	20	25.0
3	40	31.0
4	70	29.0
5	80	40.0
6	90	49.0
7	120	65.0
8	200	79.0
9	400	84.0
10	400	75.0

O = Fictitious Point Added

* = Test Point Not Included



 $C_U = A + B \tanh[(T - T_0)/C]$

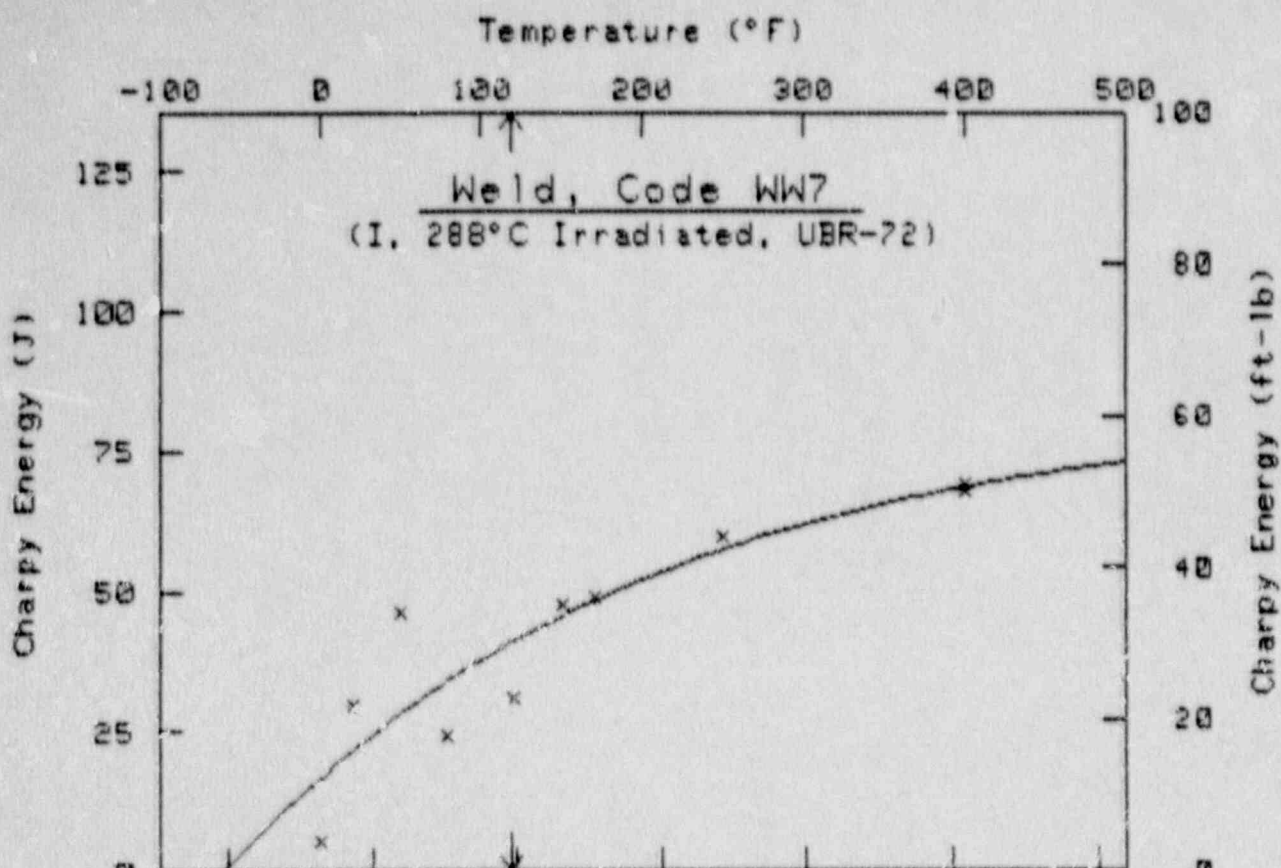
	English	Metric
A	41.58 ft-lb	56.37 J
B	39.58 ft-lb	53.66 J
C	91.62 $^{\circ}$ F	50.90 $^{\circ}$ C
T ₀	75.34 $^{\circ}$ F	24.08 $^{\circ}$ C

$C_U = 38$ ft-lb (41 J) at $T = 47.7$ $^{\circ}$ F 8.7 $^{\circ}$ C
 Upper Shelf Energy = 81.2 ft-lb 110.0 J

PT #	Temp ($^{\circ}$ F)	Energy (ft-lb)
1	0	18.0
2	20	25.0
3	40	31.0
4	70	29.0
5	80	40.0
6	90	49.0
7	120	65.0
8	200	79.0
9	400	84.0
10	400	75.0
11 0	-58	5.0
12 0	-58	5.0
13 0	-58	5.0
14 0	-58	5.0

O = Fictitious Point Added

* = Test Point Not Included



$$Cu = A + B \tanh[(T - T_0)/C]$$

	English	Metric
A	-349.25 ft-lb	-473.52 J
B	489.89 ft-lb	555.73 J
C	496.42 $^{\circ}$ F	275.79 $^{\circ}$ C
T ₀	-688.11 $^{\circ}$ F	-400.06 $^{\circ}$ C

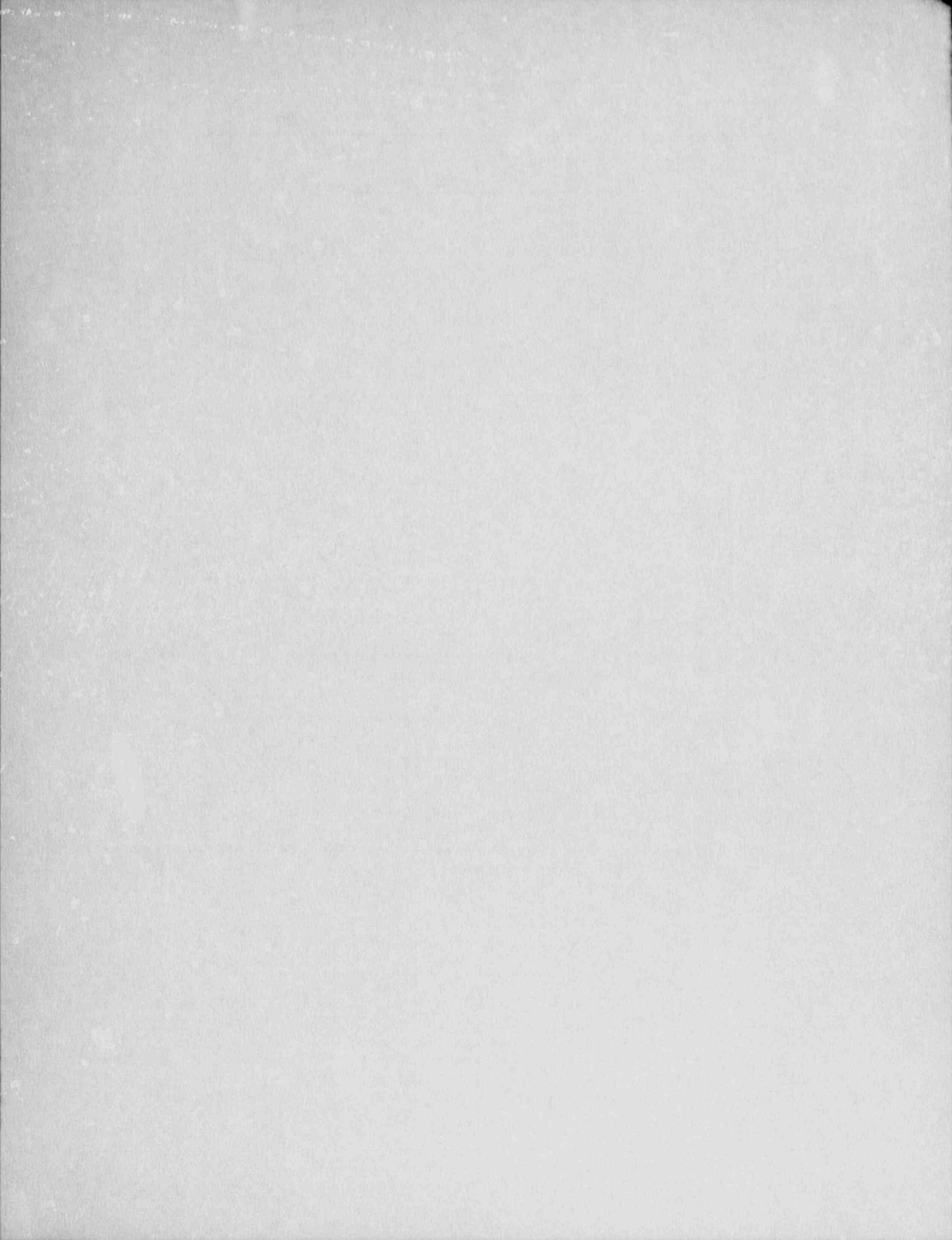
$$Cu = 38 \text{ ft-lb (41 J)} \text{ at } T = 118.2 \text{ }^{\circ}\text{F} \quad 47.9 \text{ }^{\circ}\text{C}$$

Upper Shelf Energy = 60.6 ft-lb 82.2 J

PT	Temp ($^{\circ}$ F)	Energy (ft-lb)
1	0	4.0
2	20	22.0
3	50	34.0
4	80	18.0
5	120	23.0
6	150	35.0
7	170	36.0
8	250	44.0
9	400	50.0
10	400	51.0

0 = Fictitious Point Added

* = Test Point Not Included



UNITED STATES
NUCLEAR REGULATORY COMMISSION
WASHINGTON, D.C. 20555

SPECIAL FOURTH-CLASS RATE
POSTAGE & FEES PAID
USNRC
PERMIT NO. G-67

OFFICIAL BUSINESS
PENALTY FOR PRIVATE USE. \$300

120555139531 1 1AN1RF1R5
US NRC • OADM
DIV FOIA & PUBLICATIONS SVCS
TPS PDR-NUREG
P-223
WASHINGTON DC 20555